NTNU

Norwegian University of
Science and Technology

Hydro Turbine and Governor Modelling

Electric - Hydraulic Interaction

Luz Alexandra Lucero Tenorio

Master of Science in Electric Power Engineering

Submission date: June 2010

Supervisor: Kjetil Uhlen, ELKRAFT

Co-supervisor: Trond Toftevaag, SINTEF Energy Research

Norwegian University of Science and Technology
Department of Electric Power Engineering

Problem Description

Traditionally, mathematical models for hydraulic power plants, normally found in relevant literature and power system analysis tools are often simplified models. Approaches based on approximate linear models assuming an ideal lossless turbine and ignoring the elasticity of the conduit system, are not suitable for the accurate study of the interaction between hydraulic system and power system. This implies that these models only reflect part of the real situations and as such could have a limited application.

Assignment given: 25. January 2010
Supervisor: Kjetil Uhlen, ELKRAFT

Abstract

This Master's Thesis work deals with the development of improved hydro turbine models for the evaluation of a hydraulic power generating system performance in response to small disturbances in power system analysis tool. These improved models must be able to reflect the possible interaction between the hydraulic system and power system in the computer simulations of a power plant equipped with Francis turbines.

The accuracy of a Hydraulic Power Generating System is studied by means of analysis of the dynamic behaviour of different models of the hydraulic machine and conduit system. The stability study of different models for Synchronous Machines and Turbine Governing System are beyond the scope of this work.

Appropriate representations of the hydraulic turbine and conduit system are developed in various models of varying degrees of detail. Firstly, nonlinear models for a simple turbine without surge tank considering the inelastic and elastic travelling wave effects have been developed. After that, nonlinear models considering the inelastic and elastic travelling wave effects for a turbine with surge tank for Hydropower Systems with long length penstocks are implemented. Finally, the nonlinear models for a turbine with long length penstocks are linearized at an operating point considering both the nonlinear turbine characteristics and the travelling wave effects.

The Master's Thesis work is divided into three parts. The first part, comprising Chapters 2 to 8, reviews the physical characteristics and mathematical models of the components of a hydraulic power generating system. The influence of each component of the power system by means of appropriate mathematical models is essential for the understanding of system stability. The second part, comprising Chapters 9 to 11, deals with the dynamic study of the system stability characteristics of the different hydraulic power generating system models implemented in SIMPOW and LVTrans. Finally, the third part, Chapter 12 and Chapter 13, presents the discussion of the simulation results of the hydroelectric power system models, and draws general conclusions on this work and suggests possibilities for the approach further work, respectively.

It was concluded that approaches based on nonlinear and linear models including the elasticity of the conduit system and the nonlinear turbine characteristics extracted from the Hill Charts, are the most accurate models for any acceptable study of the interaction between hydraulic system and power system.

The study of dynamic performance and interaction between the hydraulic system and power system of these extended linear and nonlinear models including the elastic water hammer effect and varying the nonlinear characteristics of the hydraulic turbine must be studied in detail.

Table of Contents

Page

ABSTRACT ..... **II**

TABLE OF CONTENTS ..... **III**

LIST OF FIGURES ..... **VI**

LIST OF TABLES ..... **IX**

PREFACE ..... **X**

LIST OF SYMBOLS ..... **XII**

1 INTRODUCTION **1**

1.1 Background information 1
1.2 Objective 1
1.3 Scope 1
1.4 Outline of the project 2

2 PRESSURE WATER CONDUIT SYSTEM **3**

2.1 Hydraulic Transients Fundamentals 3
2.1.1 Pressure wave velocity in conduits *4*
2.1.2 Wave propagation and reflections in the conduit *4*
2.1.3 Head losses due to Friction *5*
2.2 Closed-Conduit Systems 6
2.2.1 Basic Assumptions *6*
2.2.2 Basic Differential Equations for Transient Flow *6*
2.2.2.1 Equation of Continuity 7
2.2.2.2 Equation of Motion 9
2.2.2.3 General Remarks 10
2.2.3 Mathematical Model *11*
2.3 Pressure Control Systems 15
2.3.1 Governing Equations *15*
2.3.2 Surge Tank Mathematical Model *17*

3 HYDRAULIC TURBINES **18**

3.1 Hydraulic Turbines Overview 18
3.1.1 Impulse turbines *18*
3.1.2 Reaction Turbines *19*
3.2 General Technical Aspects 20
3.2.1 Neat Head, Power and Efficiency *20*
3.2.2 Turbine Hill Charts *21*
3.3 Hydraulic Turbine Modelling 22
3.3.1 Simplified Nonlinear Turbine model *23*
3.3.2 The linearized hydro turbine model *23*

4 SYNCHRONOUS MACHINE **26**

4.1 Synchronous Generator 26
4.2 Synchronous Generator Equations 27
4.3 Synchronous Generator Models 28
4.3.1 Synchronous Machine Represented by the Classical Model *29*

5 TURBINE GOVERNING SYSTEMS **30**

5.1 Governing System 30
5.2 Mechanical-hydraulic Governor 31
5.2.1 Mathematical Modelling *31*
5.3 Electro-Hydraulic Governing System 34
5.3.1 Mathematical Model *34*

6 HYDRAULIC POWER PLANT MODELS 36

6.1 HYDROPOWER PLANT MODELS 36
6.2 NONLINEAR TURBINE MODELS 38
6.2.1 Simplified Nonlinear Turbine Model 38
6.2.2 Nonlinear Model without Surge Tank assuming Inelastic Water Column 39
6.2.3 Nonlinear Model without surge tank including Elastic Water Column Effect 39
6.2.4 Nonlinear Model with Surge Tank assuming Inelastic Water Columns 40
6.2.5 Nonlinear Model with Surge Tank assuming Elastic Water Column in Penstock and Inelastic Water Column in Upstream Tunnel 41
6.3 HYDRO TURBINE LINEAR MODELS 43
6.3.1 Linear Turbine Model with Surge Tank assuming Inelastic Water Columns 43
6.3.2 Linear Turbine Model with Surge Tank assuming Elastic Water Column in Penstock 44

7 HYDROELECTRIC POWER PLANT MODELLING BY STRUCTURE MATRIX METHOD 46

7.1 DEFINITION OF THE METHOD 46
7.2 MATRIX REPRESENTATIONS OF THE BASIC ELEMENTS IN HYDRO POWER SYSTEMS 47
7.2.1 Pipes and Tunnels 47
7.2.2 Surge tanks or air accumulators 47
7.2.3 Local Losses 48
7.2.4 Hydro Turbine 49
7.2.4.1 Hydro Turbine Characteristics 49
7.2.4.2 Hydro Turbine Matrix Representation 50
7.2.5 The synchronous generator and the electric grid 52
7.2.6 Turbine Speed Governor 53
7.2.6.1 Traditional Governor 53
7.2.6.2 PID Governor 54
7.3 COMPOSITION OF THE GLOBAL STRUCTURE MATRIX 55
7.4 STRUCTURE MATRIX OF THE HYDRO TURBINE UNIT 55
7.5 HYDRO POWER PLANT STRUCTURE MATRIX 56
7.6 DYNAMIC ANALYSIS 58
7.6.1 Frequency Response Analysis 58
7.6.2 Free Vibration Analysis 58

8 POWER SYSTEM STABILITY ANALYSIS 59

8.1 POWER SYSTEM STABILITY 59
8.1.1 Small-Signal Stability Analysis 59
8.2 FUNDAMENTALS OF POWER SYSTEM STABILITY 60
8.3 EIGENVALUE ANALYSIS 61
8.3.1 Eigenvalues and Eigenvectors 61
8.3.2 Eigenvalue Analysis 61
8.3.3 Modal and Sensitivity Analysis 62
8.4 SMALL-SIGNAL STABILITY ANALYSIS OF A GENERATOR-INFINITE BUS SYSTEM 63
8.5 DYNAMIC ANALYSIS 64
8.5.1 Natural frequency analysis 64
8.5.2 Frequency Response Analysis 65

9 TEST SYSTEM MODEL 66

9.1 OVERVIEW OF THE TEST SYSTEM 66
9.2 MODELS OF THE DIFFERENT COMPONENTS 67
9.2.1 Power Plant Model 67
9.2.2 Hydraulic Turbine 68
9.2.3 Synchronous Generator 69
9.2.4 Governing Systems for Hydraulic Turbines 70
9.3 POWER FLOW ANALYSIS 70
9.4 POWER SYSTEM STABILITY ANALYSIS – THEORETICAL RESULTS 71
9.4.1 Eigenvalue Analysis 71
9.4.2 Natural frequency analysis 72

10 DYNAMIC SIMULATIONS IN SIMPOW 73

10.1 MODEL 1: SIMPLIFIED NONLINEAR TURBINE MODEL 74
10.1.1 Eigenvalue Analysis *74*
10.1.2 Dynamic Simulation Analysis *75*
10.1.3 Frequency Response Analysis *76*
10.2 MODEL 2: NONLINEAR TURBINE MODEL WITHOUT SURGE TANK ASSUMING INELASTIC WATER COLUMN 79
10.2.1 Eigenvalue Analysis *79*
10.2.2 Dynamic Response Analysis *80*
10.2.3 Frequency Response Analysis *81*
10.3 MODEL 3: NONLINEAR TURBINE MODEL WITHOUT SURGE TANK INCLUDING ELASTIC WATER COLUMN EFFECTS 84
10.3.1 Eigenvalue Analysis *84*
10.3.2 Dynamic Simulation Analysis *85*
10.3.3 Frequency Response Analysis *86*
10.4 MODEL 4: NONLINEAR TURBINE MODEL WITH SURGE TANK ASSUMING INELASTIC WATER COLUMNS 89
10.4.1 Eigenvalue Analysis *89*
10.4.2 Dynamic Simulation Analysis *90*
10.4.3 Frequency Response Analysis *91*
10.5 MODEL 5: NONLINEAR MODEL WITH SURGE TANK ASSUMING ELASTIC WATER COLUMN IN PENSTOCK AND INELASTIC WATER COLUMN IN TUNNEL 94
10.5.1 Eigenvalue Analysis *94*
10.5.2 Dynamic Simulation Analysis *95*
10.5.3 Frequency Response Analysis *96*
10.6 MODEL 6: LINEAR TURBINE MODEL WITH SURGE TANK ASSUMING INELASTIC WATER COLUMNS 99
10.6.1 Eigenvalue Analysis *99*
10.6.2 Dynamic Simulation Analysis *100*
10.6.3 Frequency Response Analysis *101*
10.7 MODEL 7: LINEAR TURBINE MODEL WITH SURGE TANK ASSUMING ELASTIC WATER COLUMN IN PENSTOCK 104
10.7.1 Eigenvalue Analysis *104*
10.7.2 Dynamic Simulation Analysis *105*
10.7.3 Frequency Response Analysis *106*

11 POWER SYSTEM MODELLED IN LVTRANS 109

11.1 DESCRIPTION OF LVTRANS 109
11.2 HYDRAULIC SYSTEM MODELLING 110
11.3 DYNAMIC SIMULATION 111
11.3.1 Frequency Response Analysis computed in LVTrans8_1.1.2 ..... *112*
11.3.2 Frequency Response Analysis computed in LVTrans86_1.3.1_T *114*
11.3.3 Comparison of the Frequency Response Analysis of the Hydraulic Power Plant computed in LVTrans8_1.1.2 and LVTrans86_1.3.1_T *114*

12 DISCUSSION 117

12.1 SUMMARY OF SIMULATION RESULTS OF THE MODELS COMPUTED IN SIMPOW 117
12.2 SUMMARY OF THE EIGENVALUE ANALYSIS COMPUTED IN SIMPOW 118
12.3 COMPARISON OF THE RESULTS OF THE MODELS IN SIMPOW 119
12.3.1 Comparison of Nonlinear Turbine Models without surge tank *119*
12.3.2 Comparison of Turbine Models with Surge Tank *122*
12.4 COMPARISON OF THE SIMULATION RESULTS COMPUTED IN SIMPOW AND LVTRANS 125

13 CONCLUSIONS 127

13.1 CONCLUSIONS 127
13.2 FURTHER WORK 129

14 REFERENCE BIBLIOGRAPHY 130

List of Figures

Figure 2-1: Control volume for the derivation of the equation of continuity 7
Figure 2-2: Control volume for the derivation of the equation of motion 9
Figure 2-3: Simple surge tank, [6] 16
Figure 3-1: Impulse Turbine 18
Figure 3-2: Francis Turbine 19
Figure 3-3: Schematic of Hydraulic Power Plant with a reaction turbine 20
Figure 3-4: Functional Block Diagram of the hydro turbine, [1, 28] 22
Figure 4-1: Equivalent circuit of the classical model of the generator 29
Figure 5-1: Schematic diagram of the Governing System, [48] 31
Figure 5-2: Mechanical-Hydraulic Governing System. [47] 31
Figure 5-3: Model of governor for hydraulic turbines, [2] 33
Figure 5-4: Typical PID Governor Controller, [2] 34
Figure 6-1: Functional Block Diagram of the Hydraulic Turbine Generating System 37
Figure 6-2: Simplified Nonlinear Turbine Model 38
Figure 6-3: Nonlinear Model without Surge Tank assuming Inelastic Water Column 39
Figure 6-4: Nonlinear Model without surge tank including Elastic Water Column Effect 40
Figure 6-5: Nonlinear Model with Surge Tank assuming Inelastic Water Columns 41
Figure 6-6: Nonlinear Model with surge tank assuming elastic water column in penstock and inelastic water column in upstream tunnel 42
Figure 6-7: Linear Model with Surge Tank assuming Inelastic Water Columns 44
Figure 6-8: Linear Model with Surge Tank assuming Elastic Water Column in Penstock 45
Figure 7-1: Layout of Hydro Power Plant for Structure Matrix Method Modelling 56
Figure 9-1: Single machine infinite bus power system 66
Figure 9-2: A general Layout of Hydro Power Plant, [19] 67
Figure 9-3: Circuit model of the test system 71
Figure 10-1: Fault simulation results: (a) angle, (b) speed, (c) mechanical torque, (d) gate position, (e) flow rate and (f) head pressure of Model 1 75
Figure 10-2: Frequency response of the transfer function from Gate position to Mechanical Power of model 1 76
Figure 10-3: Frequency response of the transfer function from Gate position to Mechanical Torque of Model 1 77
Figure 10-4: Frequency response of the transfer function of the conduit system of Model 1 77
Figure 10-5: Frequency response of the transfer function from gate position to electrical angle of Model 1 78
Figure 10-6: Frequency response of the transfer function of the mechanical-hydraulic governor of Model 1 78
Figure 10-7: Fault simulation Results: (a) Power angle, (b) Speed, (c) Mechanical Torque, (d) Gate Position, (e) Flow Rate and (f) Head Pressure of Model 2 80
Figure 10-8: Frequency response of the transfer function from Gate position to Mechanical Power of Model 2 81
Figure 10-9: Frequency response of the transfer function from Gate position to Mechanical Torque of Model 2 82
Figure 10-10: Frequency response of the transfer function of the conduit system of Model 2 82
Figure 10-11: Frequency response of the transfer function from Gate position to Electrical Angle of Model 2 83

Figure 10-12: Frequency Response of the transfer function of the mechanical-hydraulic governor of Model 2 83
Figure 10-13: Fault simulation results: (a) angle, (b) speed, (c) mechanical torque, (d) gate position, (e) flow rate and (f) water pressure of Model 3 85
Figure 10-14: Frequency response of the transfer function from Gate position to Mechanical Power of Model 3 86
Figure 10-15: Frequency response of the transfer function from Gate position to Mechanical Torque of Model 3 87
Figure 10-16: Frequency Response of the transfer function of the conduit system of Model 3 87
Figure 10-17: Frequency response of the transfer function from Gate position to Electrical Angle of Model 3 88
Figure 10-18: Frequency Response of the transfer function of the mechanical-hydraulic governor of Model 3 88
Figure 10-19: Fault simulation results: (a) angle, (b) Speed, (c) Mechanical Torque, (d) Gate Position, (e) Flow Rate and (f) Head Pressure of Model 4 90
Figure 10-20: Frequency response of the transfer function from Gate position to Mechanical Power of Model 4 91
Figure 10-21: Frequency response of the transfer function from Gate position to Mechanical Torque of Model 4 92
Figure 10-22: Frequency Response of the transfer function of the conduit system of Model 4 92
Figure 10-23: Frequency response of the transfer function from Gate position to Electrical Angle of Model 4 93
Figure 10-24: Frequency Response of the transfer function of the mechanical-hydraulic governor of Model 4 93
Figure 10-25: Fault simulation Results: (a) angle, (b) Speed, (c) mechanical torque, (d) gate position, (e) flow rate and (f) water pressure of Model 5 95
Figure 10-26: Frequency response of the transfer function from Gate position to Mechanical Power of Model 5 96
Figure 10-27: Frequency response of the transfer function from Gate position to Mechanical Torque of Model 5 97
Figure 10-28: Frequency Response of the transfer function of the conduit system of Model 5 97
Figure 10-29: Frequency response of the transfer function from Gate position to Electrical Angle of Model 5 98
Figure 10-30: Frequency Response of the transfer function of the mechanical-hydraulic governor of Model 5 98
Figure 10-31: Fault simulation Results: (a) angle, (b) speed, (c) mechanical torque, (d) gate position, (e) flow rate and (f) water pressure of Model 6 100
Figure 10-32: Frequency response of the transfer function from Gate position to Mechanical Power of Model 6 101
Figure 10-33: Frequency response of the transfer function from Gate position to Mechanical Torque of Model 6 102
Figure 10-34: Frequency Response of the transfer function of the conduit system of Model 6 102
Figure 10-35: Frequency response of the transfer function from Gate position to Electrical Angle of Model 6 103
Figure 10-36: Frequency Response of the transfer function of the mechanical-hydraulic governor of Model 6 103
Figure 10-37: Fault simulation Results: (a) Power angle, (b) Speed, (c) Mechanical Torque, (d) Gate Position, (e) Flow Rate and (f) Head Pressure of Model 7 105

Figure 10-38: Frequency response of the transfer function from Gate position to Mechanical Power of Model 7 106
Figure 10-39: Frequency response of the transfer function from Gate position to Mechanical Torque of Model 7 107
Figure 10-40: Frequency Response of the transfer function of the conduit system of Model 7 107
Figure 10-41: Frequency response of the transfer function from Gate position to Electrical Angle of Model 7 108
Figure 10-42: Frequency Response of the transfer function of the mechanical-hydraulic governor of Model 7 108
Figure 11-1: Block Diagram of the Hydraulic System Model 110
Figure 11-2: Simulation Results: (a) gate opening position, (b) Pressure Head of the Hydraulic Test Model in LVTrans86_1.3.1_T 111
Figure 11-3: Frequency Response of the transfer function from gate position to pressure head of the hydraulic power plant simulated without droop in LVTrans8_1.1.2 112
Figure 11-4: Frequency Response of the transfer function from gate position to pressure head of the hydraulic power plant simulated with droop in LVTrans8_1.1.2 112
Figure 11-5: Frequency Response of the transfer function from gate position to pressure head of the hydraulic power plant simulated without and with droop in LVTrans8_1.1.2 113
Figure 11-6: Frequency Response of the transfer function from gate position to pressure head of the hydraulic power plant simulated in LVTrans86_1.3.1_T 114
Figure 11-7: Comparison of the Frequency response of the hydraulic power generating system simulated without droop in LVTrans8_1.1.2 and computed in LVTrans86_1.3.1_T 115
Figure 11-8: Comparison of the Frequency Response of the hydraulic power generating system simulated with droop in LVTrans8_1.1.2 and computed in LVTrans86_1.3.1_T 115
Figure 12-1: Fault Simulation Results of hydraulic turbine represented by model 1, 2 and 3 119
Figure 12-2: Frequency response of the transfer functions from Gate position to Mechanical Power of a simple hydraulic turbine represented by Model 1, 2 and 3 120
Figure 12-3: Frequency response of the transfer function from Gate position to Mechanical Torque of a hydraulic turbine represented by Model 1, 2 and 3 121
Figure 12-4: Frequency response of the transfer functions of the conduit system of Model 1, 2 and 3 121
Figure 12-5: Fault Simulation Results of hydraulic turbine represented by Model 4, 5, 6 and 7 122
Figure 12-6: Frequency response of the transfer function from gate position to Mechanical Power of Model 4, 5, 6 and 7 123
Figure 12-7: Frequency Response of the transfer function from Gate position to Mechanical Torque of a simple hydraulic turbine represented by Model 4, 5, 6 and 7 123
Figure 12-8: Frequency response of the transfer function of the conduit system of Model 4, 5, 6 and 7 124
Figure 12-9: Frequency Responses of the transfer function of the conduit system of Hydraulic Power System Models implemented in SIMPOW and LVTrans (without droop) 125
Figure 12-10: Frequency Responses of the transfer function of the conduit system of Hydraulic Power System Models implemented in SIMPOW and LVTrans (with droop) 126

List of Tables

Table 2-1: Propagation of pressure waves caused by instantaneous closure of valve 5
Table 3-1: Turbine coefficients, [11, 37] 24
Table 3-2: Turbine Coefficients, [32] 25
Table 5-1: Typical values and range of Parameters, [47] 33
Table 9-1: System parameters and operating conditions 67
Table 9-2: Hydraulic Power Plant Model 68
Table 9-3: Hydraulic Turbine Parameters 68
Table 9-4: Hydraulic Turbine Models 69
Table 9-5: Synchronous machine Parameters 69
Table 9-6: Typical Values of parameters of turbine governing system 70
Table 9-7: Power Flow results 70
Table 9-8: Results of the Synchronous machine represented by Classical Model 72
Table 10-1: Eigenvalues and the state variable for a model 1 74
Table 10-2: Participation matrix for a model 1 75
Table 10-3: Eigenvalues and the state variable for Model 2 79
Table 10-4: Participation factors matrix of a turbine Model 2 80
Table 10-5: Eigenvalues and the state variable for the Turbine Model 3 84
Table 10-6: Participation factors matrix of a Turbine Model 3 85
Table 10-7: Eigenvalues and the state variable for the turbine Model 4 89
Table 10-8: Participation factors matrix of a hydraulic turbine Model 4 90
Table 10-9: Eigenvalues and state variables for Model 5 94
Table 10-10: Participation factors matrix for Model 5 95
Table 10-11: Eigenvalues and the state variable for Model 6 99
Table 10-12: Participation factors matrix of a Model 6 100
Table 10-13: Eigenvalues and the state variable for the Model 7 104
Table 10-14: Participation factors matrix of a Model 7 105
Table 12-1: Summary of the electromechanical oscillatory mode of the models of the models ... 118
Table 12-2: Error between the calculated eigenvalues and the computed eigenvalues 118

Preface

In January 2005, an internal project called "Turbine and hydropower modelling" was started at SINTEF Energy Research. That project was concerned about the study of dynamic performance and possible interaction between the hydraulic system and power system of a power plant equipped with Francis turbines. Traditionally, mathematical models for hydraulic power plants, normally found in relevant literature and power system analysis tools are often simplified models. Approaches based on approximate linear models assuming an ideal lossless turbine and ignoring the elasticity of the conduit system, are not suitable for the accurate study of the interaction between hydraulic system and power system. This implies that these models only reflect part of the real situations and as such could have a limited application.

The Master's Thesis work develops improved hydro turbine models of a typical hydraulic power generating system for their representation in dynamic studies of power systems in response to any small disturbance. These improved models must be able to reflect the possible interaction between the hydraulic system and power system in the computer simulations of a power plant equipped with Francis turbines.

The study of dynamic performance and interaction of hydraulic system and power system of a power plant equipped with Francis turbines in the Master's Thesis work is based on the textbook *Power System Stability and Control* by P. Kundur, and the paper "*Hydraulic Turbine and Turbine Control Models for System Dynamic Studies*" by IEEE Working Group.

The precision of the representation of a hydraulic power generating system in dynamic studies is examined by means of analysis of the dynamic behaviour of different models of the hydraulic machine and conduit system. The stability study of different models for Synchronous Machines and Turbine Governing System are beyond of the scope of this Master's Thesis work.

Appropriate representations of the hydraulic turbine and water conduit system are developed in models of varying degrees of detail. Firstly, nonlinear models for a simple turbine without surge tank considering the inelastic and elastic travelling wave effects have been developed. After that, nonlinear models considering the inelastic and elastic travelling wave effects for a turbine with surge tank for hydraulic power systems with long length penstocks are implemented. Finally, the nonlinear models for a turbine with long length penstocks are linearized at an operating point considering both the nonlinear turbine characteristics and the travelling wave effects.

The stability analysis of these implemented models contains power-flow calculation, linear analysis and time-domain simulation in the simulation software SIMPOW and the dynamic simulation tool LVTrans.

The Master's Thesis work is divided into three parts. The first part, comprising Chapters 2 to 8, reviews the physical characteristics and mathematical models of the components of a hydraulic power generating system. The influence of each component of the power system by means of appropriate mathematical models is essential for the understanding of system stability. The second part, comprising Chapters 9 to 11, deals with the dynamic study of the system stability characteristics of the different hydraulic power generating system models implemented in SIMPOW and LVTrans. Finally, the third part, Chapter 12 and Chapter 13, presents the discussion

of the simulation results of the hydroelectric power system models, and draws general conclusions on this work and suggests possibilities for the approach further work, respectively.

Chapter 2 to 5 present the physical description and the mathematical deduction of the equations describing appropriate models of the conduit systems and pressure control systems considering the water-hammer theory and friction head losses, hydraulic turbines, synchronous generators and turbine governing systems, respectively, for their representation in power system dynamic studies. Chapter 6 deals with the development of improved mathematical models of each component of a typical Hydraulic Power Generating System equipped with Francis turbines for their representation in power system dynamic studies. Chapter 7 shows an alternative method of Hydroelectric Power Plant modelling for stability studies. Chapter 8 describes fundamental aspects and analytical techniques in the study of small-signal stability of dynamic, and identifies factors influencing them.

Chapter 9 presents the physical characteristics and capability of the components of the test system. The general configuration of the test system consists of a single synchronous machine connected to a large power system through a transmission line. Chapter 10 deals with the study of the system stability characteristics of the different Hydraulic Turbine models within a typical Hydraulic Power Generating System implemented in the software SIMPOW. Chapter 11 studies the dynamic system characteristics of the Hydraulic System modelled in the dynamic simulation tool LVTrans.

The development of this work has the main contribution of Trond Toftevaag, Bjørnar Svingen, Kjetil Uhlen, and Lars Lindquist, STRI Sweden, who have assisted me in the dynamic study of the different models and their implementation in the simulation software SIMPOW® and the dynamic simulation tool LVTrans.

I would like to thank Trond Toftevaag, Bjørnar Svingen and Kjetil Uhlen for their continuous support in the project. A special thanks to Trond Toftevaag, who was always there to listen and to give advice. He showed me different ways to approach a research problem and the need to be persistent to accomplish any goal, and to ask me good questions to help me think through my problems (whether philosophical, analytical or computational).

Alexandra Lucero T.

Trondheim, June 15th 2010

List of Symbols

Notation

Upper case symbols normally denote physical values.
Lower case symbols normally denote per-unit values.
The suffix 0 denotes an initial steady-state value.
The prefix Δ denotes small deviations.

Symbols

a	Pressure wave velocity, [m/s]
A	Penstock cross-section area, [m^2]
A_s	Surge Tank cross-section area, [m^2]
A_t	constant proportionality factor, [-]
D	Pipe internal diameter, [m]
e	Pipe wall thickness, [m]
E	Young's modulus of elasticity, [N/m^2]
f	Darcy-Weisbach friction factor, [-]
g	Acceleration due to gravity, [m/s^2]
$H(x,t)$	Piezometric head (HGL) or water free surface level, [m]
H	Inertia Constant, [MWs/MVA]
H_f	Head losses due to friction effects in the conduit, [m]
i_d	Current flowing in the d-axis armature coil, [pu]
i_q	Current flowing in the q-axis armature coil, [pu]
K	Bulk modulus of elasticity, [N/m^2]
K_D	Damping-torque coefficient, [-]
K_d	Derivative gain, [s]
$K_{E'}$	Transient synchronizing power coefficient, [-]
K_i	Integral gain, [s^{-1}]
K_p	Proportional gain, [pu]
K_s	Servomotor gain, [-]
L	Length of the conduit, [m]
L_{ad}, L_{aq}	Mutual inductance between the stator and rotor windings
L_d	Self-Inductance of the d-axis armature windings
L_q	Self-Inductance of the q-axis armature windings
M_{11}	Hydraulic turbine Unit torque
M_e	Electromagnetic torque, [Nm]
M_m	Mechanical torque, [Nm]
$p(x,t)$	pressure, [Pa]
P_m	Mechanical power on the turbine shaft, [MW]
$Q(x,t)$	Flow discharge, [m^3/s]
Q_{11}	Hydraulic turbine unit flow rate
q_{NL}	water flow at zero electrical power, [-]
r	Pipe radius, [m]
R_a	Stator resistance, [pu]
R_e	Reynolds number, [-]
R_P	Permanent speed droop, [pu]
R_T	Temporary speed droop, [pu]
s	Laplace operator

S_N	Rated apparent power, [MVA]
t	Time, [s]
T_c	Gate closing time constant, [s]
T_{d0}', T_{d0}''	open-circuit d-axis transient and subtransient time constant, [s]
T_e	Wave travel time, [s]
T_g	Main Servomotor time constant [s]
T_M	Mechanical starting time $T_M=2H$, [s]
T_P	Pilot valve and servomotor time constant, [s]
T_{q0}''	Open-circuit q-axis subtransient time constant, [s]
T_R	Reset time or dashpot time constant, [s]
T_s	Surge Tank Filling Time, [s]
T_w	Water time constant or water starting time, [s]
$V(x,t)$	average Velocity, [m/s]
ν	Kinematics viscosity of the fluid, [m^2/s]
v_d, v_q	Voltage across the fictitious d- and q- axis armature coils, [pu]
V_g	Voltage at the generator terminals
V_S	Infinite bus bar voltage
x	Distance measured along the pipe axis, [m]
x_l	Stator leakage reactance, [pu]
X_d, X_d', X_d''	direct-axis synchronous, transient and subtransient reactance, [pu]
x_d, x_d', x_d''	Total direct-axis synchronous, transient and subtransient reactance between (and including) a generator and an infinite busbar, [pu]
X_q, X_q', X_q''	quadrature-axis synchronous, transient and subtransient reactance, [pu]
x_s	Internal reactance of an infinite busbar, [pu]
x_T	Series reactance of a transformer, [pu]
y	Turbine wicket gate position, [-]
z	Elevation of the pipe centreline, [m]
α	Slope of the pipe axis, [°]
δ	Power angle with respect to an infinite busbar
$\boldsymbol{\varepsilon}$	Internal pipe roughness, [m]
ζ	Damping ratio, [-]
η	Turbine efficiency
λ	Eigenvalue
ρ	Fluid mass density, [kg/m^3]
τ_0	Shear force between the fluid and the conduit walls, [N/m^2]
ϕ	Runner blade angle
ψ_D, ψ_Q	Total flux linkages of damper windings in d -axis and q-axis
ψ_d, ψ_q	Total d-axis and q-axis flux linkages
ψ_f	Total flux linkage of the field winding
ω_d	Damped natural frequency of rotor swings, [rad/s]
ω_N	Normalized velocity of the unit, [pu]
ω_{nat}	Undamped natural frequency of rotor swings for small oscillations, [rad/s]
ω	angular velocity of the generator, [electrical radians]
ω_s	Synchronous angular velocity (equal to $2\pi f$), [electrical radians]
$\boldsymbol{\epsilon}$	Conduit wall tensile strain

1 Introduction

1.1 Background information

In January 2005, an internal project called “Turbine and hydropower modelling” was started at SINTEF Energy Research. This project was concerned about the study of dynamic performance and possible interaction between the hydraulic system and power system of a power plant equipped with Francis turbines. Traditionally, mathematical models for hydraulic power plants, normally found in relevant literature and power system analysis tools are often simplified models. Approaches based on approximate linear models assuming an ideal lossless turbine and ignoring the elasticity of the conduit system, are not suitable for the accurate study of the interaction between hydraulic system and power system. This implies that these models only reflect part of the real situations and as such could have a limited application.

1.2 Objective

The purpose of this Master’s Thesis work is to develop improved hydraulic turbine models of a typical hydraulic power generating system for their representation in dynamic studies of power systems in response to any small disturbance. These improved models must be able to reflect the possible interaction between the hydraulic system and power system in the computer simulations of a power plant equipped with Francis turbines.

1.3 Scope

The precision of the representation of a Hydraulic Power Generating System in dynamic studies is examined by means of analysis of the dynamic behaviour of different models of the hydraulic machine and water conduit system. The stability study of different models for Synchronous Machines and Turbine Governing System are beyond of the scope of this Master’s Thesis work.

Appropriate representations of the hydraulic turbine and water conduit system are developed in models of varying degrees of detail. Firstly, nonlinear models for a simple turbine without surge tank considering the inelastic and elastic travelling wave effects have been developed. After that, nonlinear models considering the inelastic and elastic travelling wave effects for a turbine with surge tank for hydraulic power systems with long length penstocks are implemented. Finally, the nonlinear models for a turbine with long length penstocks are linearized at an operating point considering both the nonlinear turbine characteristics and the travelling wave effects.

The stability analysis of these implemented models contains power-flow calculation, linear analysis and time-domain simulation in the simulation software SIMPOW and the dynamic simulation tool LVTrans.

1.4 Outline of the project

Chapter 2 contains the mathematical deduction of the equations of continuity and momentum describing the transient state flows in closed-conduit systems and pressure control systems including travelling wave effects and friction losses.

Chapter 3, Chapter 4 and Chapter 5 presents the physical description and the mathematical deduction of the equations describing appropriate models of hydraulic turbines, synchronous generators and turbine governing systems, respectively, for their representation in power system dynamic studies. Standard models are normally found in considerable number of relevant literature related to hydraulic power generating system modelling. These chapters represent the basis for the dynamic modelling of the different configurations of the test system.

Chapter 6 deals with the development of improved mathematical models of each component of a typical hydraulic power generating system equipped with Francis turbines for their representation in power system dynamic studies.

Chapter 7 shows an alternative method of Hydroelectric Power Plant modelling for stability studies. The hydraulic turbine and hydroelectric power plant may be modelled by the Structure Matrix Method. This model covers a wide range of parameters such as influence of the turbine characteristics, frictional damping of oscillatory flow in elastic conduits, influence of the generator load and the analysis of the turbine governing system.

Chapter 8 describes fundamental aspects and analytical techniques in the study of small-signal stability of dynamic, and identifies factors influencing them. The stability of the generator-infinite busbar system following a small disturbance is discussed.

Chapter 9 presents the physical characteristics and capability of the components of the test system such as water upstream tunnel, surge tank, penstock, hydraulic turbine, speed governor, generator, and electrical network. The general configuration of the test system consists of a single synchronous machine connected to a large power system through a transmission line.

Chapter 10 deals with the study of the system stability characteristics of the different Hydraulic Turbine models within a typical Hydraulic Power Generating System implemented in the software SIMPOW. The objective of the dynamic modelling of the test system is to analyze the stability characteristics of the Hydro Power System about the steady-state operating condition following a three-phase fault to ground.

Chapter 11 studies the dynamic system characteristics of the Hydraulic System, described in Chapter 9, modelled in the dynamic simulation tool LVTrans. The dynamic behaviour of the Hydraulic Power System is analyzed in the program LVTrans version LVTrans8_1.1.2 and version LVTrans86_1.3.1_T.

Finally, Chapter 12 presents the discussion of the simulation results of the hydroelectric power system models implemented in SIMPOW and LVtrans, and Chapter 13 draws general conclusions on the Master's Thesis work and suggests possibilities for the approach and scope for further work.

2 Pressure Water Conduit System

Depending on the site, the conduit system is composed of a water-diverting structure; a canal to carry the water flow to the reservoir; a surge tank; a penstock pipe to convey the water to the powerhouse; and, a tailrace through which the water is released back to the river. Hydraulic transients in closed-conduits consist of pressure disturbances when the system undergoes a change from one operational steady-state condition to another. The disturbances in a hydroelectric plant are initiated by an adjustment in the setting of a control valve or the change in operation of the hydro turbines. The damping of pressure transients is achieved when the system energy loss occurs in the form of conduit friction or minor losses.

Hydroelectric power plants with long conduits may have severe water hammer and governing stability problems. The classical solution is to insert a surge tank upstream or/and downstream the power plant to minimize the hydraulic transient effects.

This chapter contains the mathematical deduction of the equations describing the transient state flows in the surge tank and closed-conduit systems including travelling wave effects and friction losses. These equations are usually referred to as equations of continuity and momentum. Hydraulic transient analysis is essential to good design and operation of conduit systems.

2.1 Hydraulic Transients Fundamentals

Hydraulic transient refers to the pressure fluctuations in the water caused during a change in mean flow conditions. The main components of the disturbances are pressure and flow changes at a rated point that causes propagation of pressure waves throughout the system. The pressure waves travel with the velocity of sound, which depends on the characteristics of the conduit system and on the water elasticity. When a closed conduit is filled with moving water, the law governing the changes of pressure and discharge depends upon the conditions under which the flow occurs. [3-7]

Any disturbance in the water caused during a change in mean flow conditions initiates a sequence of transient pressure. Typical events of the causes of transients in engineering systems include:

- Pump start-up or shutdown;
- Valve opening, closing or “chattering”;
- Changes in boundary pressures;
- Hydraulic turbine start-up, accepting or rejecting load;
- Vibrations of the vanes of a runner or an impeller;
- Sudden changes in the canal inflow or outflow by opening or closing the control gate;
- Dam failure or collapse;

2.1.1 Pressure wave velocity in conduits

The pressure wave velocity ***a*** depends upon the characteristics of the liquid, such as the Bulk modulus and density, the characteristics of the pipe material, including the conduit size, wall thickness and wall material; the external constraints include the type of supports and the freedom of conduit movement in the longitudinal direction. The wave velocity in a thin-walled elastic conduit with multiple joints is given by the classical Korteweg's equation. [1, 6, 8-9]

$$a = \sqrt{\frac{K}{\rho\left(1+\frac{DK}{eE}\right)}} \tag{2.1}$$

Expressions for ***a*** for different support conditions and for other conduit parameters are given in Section 22 of the textbook *"Davis' Handbook of Applied Hydraulics".* [9]

The wave velocity for a perfectly rigid pipe, where E is infinite, simplifies to

$$a = \sqrt{\frac{K}{\rho}} \tag{2.2}$$

Typical values for wave velocity are in the range of 1000 to 1200 m/s.

2.1.2 Wave propagation and reflections in the conduit

The wave transmission phenomenon due to the gate closure is characterized by the wave propagation and reflection along a pipeline until they are damped out by friction. According to the water hammer theory developed by Allievi in the early 1900's, pressure waves may arise in long penstocks propagating with wave velocity ***a***. [3, 6, 10-12]

The time taken for the pressure wave to travel the length of the penstock to the open surface is given by

$$T_e = \frac{L}{a} \tag{2.3}$$

Considering a pipeline in which the flow is initially steady. A sudden rise in the pipe adjacent gate will be produced when an instantaneous gate closure takes place at the lower end of the pipe. The wave transmission phenomenon due to the gate closure is analyzed thoroughly in the textbook *"Waterhammer Analysis"*. [3]

The theoretical period T_{th} for a conduit having constant diameter, constant wall thickness is given by

$$T_{th} = \frac{4L}{a} \tag{2.4}$$

The sequence of events following the valve closure is explained briefly below.

Table 2-1: Propagation of pressure waves caused by instantaneous closure of valve

Stage	Events
$0 < t \le L/a$	The flow velocity at the valve is reduced to zero, The pipe is expanded, The fluid density is increased
$L/a < t \le 2L/a$	The fluid starts to flow from the pipeline into the reservoir. A negative wave travels toward the valve.
$2L/a < t \le 3L/a$	The velocity is instantaneously changed due to the valve is completely closed. The pressure is reduced and the negative wave propagates in the upstream direction.
$3L/a < t \le 4L/a$	The fluid flows towards the valve and the pressure head is restored.

2.1.3 Head losses due to Friction

The head loss is a measure of the reduction in the total head of the fluid as it moves through a pipeline. Head losses are present due to the friction of the fluid against the pipe walls. The head losses are usually the result of boundary losses and form losses. Boundary losses are those arising from the effects associated with the cross-sectional shape that affect the ratio of the flow area to the wetted perimeter, and from shear forces between the fluid and the boundary materials. Form losses arise from recirculating eddies produced by the geometry of the containing vessel such as bends and either expanding or contracting transitions. [9-10, 13-14]

Head losses along the pipe wall are called friction losses or head losses due to friction. The head loss due to friction H_f in a given conduit for a given discharge is usually determined by the Darcy-Weisbach equation.

$$H_f = f \frac{L}{D} \frac{V^2}{2g} \tag{2.5}$$

The dimensionless friction factor *f* is a function of velocity, roughness, viscosity of the fluid and conduit diameter. The evaluation of the friction factor under these widely varying conditions has been made possible by the contribution of Reynolds. The Reynolds criterion relates the inertial forces per unit of volume to the viscous forces per unit of volume. The Reynolds number for full flowing circular pipes can be expressed as

$$R_e = \frac{VD}{v} \tag{2.6}$$

The friction factor *f* in a laminar regime is independent of the wall roughness and inversely proportional to the Reynolds number. The friction factor for a laminar flow is calculated from the Hagen-Poiseuille equation as

$$f = \frac{64}{R_e} \tag{2.7}$$

For turbulent flow ($R_e > 4000$), the friction factor *f* is a function of the Reynolds number R_e and the relative roughness height (ε / D). Colebrook-White equation relates the friction factor to the Reynolds number and relative roughness as

$$\frac{1}{\sqrt{f}} = -2\log_{10}\left(\frac{\varepsilon}{3.7D} + \frac{2.51}{R_e\sqrt{f}}\right) \tag{2.8}$$

2.2 Closed-Conduit Systems

2.2.1 Basic Assumptions

Hydraulic transients arise as a consequence of rapid variations in the flow conditions in pressure conduits. Due to the elasticity of the material and the compressibility of the fluid, such variations in the pressure and/or flow velocity propagate in the conduits at very high speeds.

In order to obtain the basic physical laws of the hydraulic transients in a closed conduit, it is assumed that:

- The pipe is uniform and flow is one-dimensional; for quasi-incompressible fluids, the velocity and pressure distributions are uniform in each cross section of the conduit.
- Pipe deformations are proportional to the stresses (Hooke's law) and the liquid compressibility effects can be characterized by a constant bulk modulus.
- No vaporization of the liquid occurs during the hydraulic transient.
- The formulas used for the calculation of head losses in steady state flow remains valid during transient conditions.
- No distributed lateral flows are considered.

The analysis of transients in closed conduit is subdivided in two types: distributed systems and lumped systems. In the former case, the transient phenomenon occurs in form of travelling waves. Any change in the flow condition is assumed to take place instantaneously throughout the system in a lumped system.

Mathematically, the transients in the distributed systems are represented by partial differential equations, whereas the transients in the lumped systems are described by ordinary differential equations. The system may be analyzed as a lumped system when $\omega L/a$ is much less than 1.

2.2.2 Basic Differential Equations for Transient Flow

Equations for the conservation of mass and momentum describe the transient state flows in closed conduits. The condition of dynamic equilibrium requires that Newton's second law of motion be satisfied. The condition of continuity for the element requires that all available space inside the boundaries of the conduit be occupied by water at all times. [3]

The partial differential equations of continuity and motion are expressed in terms of two dependent variables, the pressure *p(x,t)* and flow velocity *V(x,t)* and two independent variables time (*t*) and displacement (*x*).

2.2.2.1 Equation of Continuity

The continuity differential equation, which takes into account the water compressibility and the tube elasticity, is based in the conservation mass law for a control volume. The radial velocity due to radial expansion and contraction is not included in the analysis. The distance *x*, flow discharge *Q* and velocity *V* will be considered positive from the left (upstream) to right (downstream). Heads *H* are measured relatively to a horizontal datum to which will be also referred elevations *z* and slope *α* of the pipe axis. The slope is considered positive for a rising pipe in the positive direction of x, as shown in Figure 2-1**.** The pipe cross sectional area *A* and the liquid mass density ρ are both function of pressure *p(x,t).* [6, 8-9, 15-16]

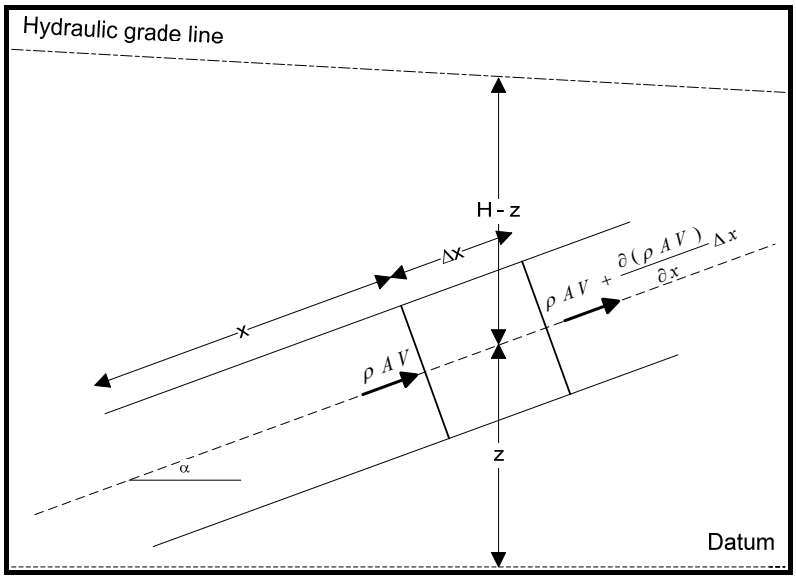

Figure 2-1: Control volume for the derivation of the equation of continuity

The equation of continuity of a control volume $\forall_c$ at an instant *t*, shown in Figure 2-1, yields

$$\rho AV = \rho AV + \frac{\partial}{\partial t}\rho AV\left(\Delta x\right) \tag{2.9}$$

Expanding Equation (2.9):

$$\frac{\partial}{\partial t}\left(\rho A\right)+\frac{\partial}{\partial x}\left(\rho AV\right)=A\frac{\partial \rho}{\partial t}+\rho\frac{\partial A}{\partial t}+\rho A\frac{\partial V}{\partial x}+\rho V\frac{\partial A}{\partial x}+AV\frac{\partial \rho}{\partial x} \tag{2.10}$$

Rearranging terms, using expressions for the total derivatives and dividing throughout by ρA, Equation (2.9) may be written as:

$$\frac{1}{A}\frac{dA}{dt}+\frac{1}{\rho}\frac{d\rho}{dt}+\frac{\partial V}{\partial x}=0 \tag{2.11}$$

For a circular conduit having radius *r*,

$$\frac{dA}{dt}=2\pi r\frac{dr}{dt} \tag{2.12}$$

In terms of the conduit wall tensile strain $\in$, Equation (2.12) can be written as

$$\frac{dA}{dt} = 2\pi r \frac{dr}{dt} = 2A \frac{d\in}{dt} \tag{2.13}$$

Assuming that the conduit walls area linearly elastic, then

$$\frac{d\in}{dt} = \frac{1}{E - \frac{pD}{2e}} \frac{D}{2e} \frac{dp}{dt} \tag{2.14}$$

The first term of Equation (2.11) refers to change in conduit are with time becomes

$$\frac{1}{A}\frac{dA}{dt} = \frac{1}{E - \frac{pD}{2e}} \frac{D}{e} \frac{dp}{dt} \tag{2.15}$$

The second term of Equation (2.11) refers to the rate of change of fluid density. The bulk modulus of elasticity of a fluid is by definition

$$K = \frac{dp}{\left(d\forall / \forall\right)} = \frac{dp}{\left(d\rho / \rho\right)} \tag{2.16}$$

and the second term of Equation (2.11) becomes

$$\frac{1}{\rho}\frac{d\rho}{dt} = \frac{1}{K}\frac{dp}{dt} \tag{2.17}$$

Substituting Equation (2.15) and (2.17) into Equation (2.11) gives

$$\left(\frac{1}{K} + \frac{1}{\frac{eE}{D} - \frac{p}{2}} \right) \frac{dp}{dt} + \frac{\partial V}{\partial x} = 0 \tag{2.18}$$

Since $p/2 \ll eE/D$ in most applications, Equation (2.18) gives

$$\frac{1}{K}\left(1 + \frac{1}{\frac{eE}{DK}} \right) \frac{dp}{dt} + \frac{\partial V}{\partial x} = 0 \tag{2.19}$$

Substituting Equation (2.1) and the expression for the total derivative into Equation (2.19) gives

$$\frac{\partial p}{\partial t} + V\frac{\partial p}{\partial x} + \rho a^2 \frac{\partial V}{\partial x} = 0 \tag{2.20}$$

2.2.2.2 Equation of Motion

The differential equation of motion for a transient flow is given applying the second Newton's law for a fluid element inside a tube. [17]

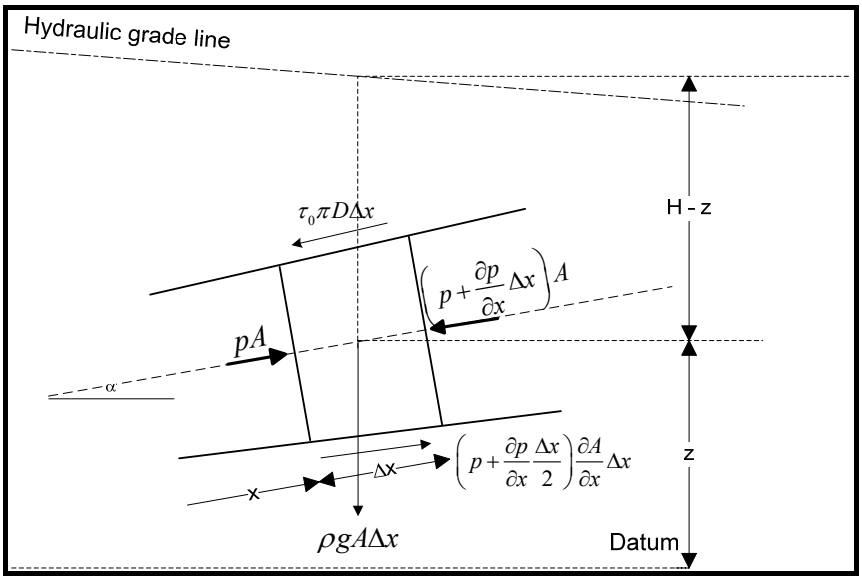

Figure 2-2: Control volume for the derivation of the equation of motion

The equation of motion for the control volume defined in Figure 2-2 at a given instant *t*, when the pipe is deformed due to transient forces

$$pA - \left(p - \frac{\partial p}{\partial x}\Delta x\right)A + \left(p + \frac{1}{2}\frac{\partial p}{\partial x}\Delta x\right)\frac{\partial A}{\partial x}\Delta x - \tau_0 \pi D \Delta x - \rho g A \Delta x \sin\alpha = \rho A \Delta x \frac{dV}{dt} \qquad (2.21)$$

Omitting Δx^2, Equation (2.21) yields

$$A\frac{\partial p}{\partial x} + \tau_0 \pi D + \rho g A \sin\alpha + \rho A \frac{dV}{dt} = 0 \qquad (2.22)$$

The force resulting from the shear stress τ_0 may be defined in terms of the Darcy-Weisbach expression for friction losses for a turbulent pipe flow.

$$\tau_0 = \frac{1}{8} f \rho V |V| \qquad (2.23)$$

Substituting Equation (2.23) into Equation (2.22) and dividing throughout ρA, yields

$$\frac{\partial V}{\partial t} + V\frac{\partial V}{\partial x} + \frac{1}{\rho}\frac{\partial p}{\partial x} + g\sin\alpha + \frac{fV}{2D}|V| = 0 \qquad (2.24)$$

2.2.2.3 General Remarks

In many engineering applications, the convective acceleration terms $V(\partial p/\partial x)$ and $V(\partial V/\partial x)$ are usually considered negligible in comparison with the remaining terms. The slope term is also possible neglect. The system parameters ρ and *D* remain constant with respect to time. Therefore, eliminating these terms from the general Equations (2.20) and (2.24) become

$$\frac{\partial p}{\partial t}+\rho a^2\frac{\partial V}{\partial x}=0 \tag{2.25}$$

$$\frac{\partial V}{\partial t}+\frac{1}{\rho}\frac{\partial p}{\partial x}+\frac{fV}{2D}|V|=0 \tag{2.26}$$

In the analysis of hydraulic transients, the pressures in the pipelines are usually expressed in terms of the piezometric head, *H*, above a specified datum. Additionally the flow velocity is replaced by the discharge, *Q.* The pressure and the flow velocity may be written as

$$p=\rho g(H-z) \tag{2.27}$$

$$Q=VA \tag{2.28}$$

Assuming the fluid is slightly compressible and the conduit walls are slightly deformable and neglecting the variation of ρ and flow area *A* due to variation of the inside pressure. The small variations of ρ and flow area *A* are indirectly taken into account by considering the wave speed *a* have a finite value. Substituting Equations (2.27) and (2.28) into Equations (2.25) and (2.26) give

$$\left(\frac{\partial H}{\partial t}-\frac{\partial z}{\partial t}\right)+\frac{a^2}{gA}\frac{\partial Q}{\partial x}=0 \tag{2.29}$$

$$\frac{1}{A}\frac{\partial Q}{\partial t}+g\left(\frac{\partial H}{\partial x}-\frac{\partial z}{\partial x}\right)+\frac{fQ}{2DA^2}|Q|=0 \tag{2.30}$$

If the pipe axis is fixed $\partial z/\partial t=0$ and $\partial z/\partial x=\sin\alpha$. It is possible to eliminate the tube inclination effect, $\partial z/\partial x=\sin\alpha=0$. Therefore, Equations (2.29) and (2.30) become

$$\frac{\partial Q}{\partial x}+\frac{gA}{a^2}\frac{dH}{dt}=0 \tag{2.31}$$

$$\frac{\partial H}{\partial x}+\frac{1}{gA}\frac{dQ}{dt}+\frac{fQ}{2gA^2D}|Q|=0 \tag{2.32}$$

Equations (2.31) and (2.32) can be normalized by substituting for the relative terms $h = H/H_0$ and $q = Q/Q_0$, giving

$$\frac{\partial q}{\partial x} + \frac{gA}{a^2}\frac{H_0}{Q_0}\frac{\partial h}{\partial t} = 0 \tag{2.33}$$

$$\frac{\partial h}{\partial x} + \frac{Q_0}{gAH_0}\frac{\partial q}{\partial t} + \frac{f}{2gA^2D}\frac{Q_0^2}{H_0}q|q| = 0 \tag{2.34}$$

The water time constant or water starting time, T_W, is associated with the acceleration time for water in the penstock between the turbine inlet and the reservoir or the surge tank, if one exists. The equation for water starting time is:

$$T_W = \frac{L}{gA}\frac{Q_0}{H_0} \tag{2.35}$$

Introducing the water time constant T_W in Equation (2.33) and (2.34)

$$\frac{\partial q}{\partial x} + \frac{1}{a^2}\frac{L}{T_W}\frac{\partial h}{\partial t} = 0 \tag{2.36}$$

$$\frac{\partial h}{\partial x} + \frac{T_W}{L}\frac{\partial q}{\partial t} + f\frac{T_W}{L}\frac{Q_0}{2AD}q|q| = 0 \tag{2.37}$$

2.2.3 Mathematical Model

The analysis of transients in hydroelectric systems is subdivided in mass-oscillation response and waterhammer response. Ordinary differential equations describe the mathematical model for mass-oscillation (or rigid water column) between the reservoir and the surge tank. Partial differential equations show the mathematical model for waterhammer along the penstock and draft tube. [15-20]

The mathematical model of the conduit system taking into account the waterhammer theory and considering the head losses is based on the linearized Equation (2.36) and (2.37), and on sinusoidal flow and pressure fluctuations.

Using the Laplace transform to express Equations (2.36) and (2.37) in the frequency domain

$$\frac{\partial q(s)}{\partial x} + \frac{1}{a^2}\frac{L}{T_W}\left(sh(s) - h\left(0^+\right)\right) = 0 \tag{2.38}$$

$$\frac{\partial h(s)}{\partial x} + \frac{T_W}{L}\left(sq(s) - q\left(0^+\right)\right) + f\frac{T_W}{L}\frac{Q_0}{2AD}q(s) = 0 \tag{2.39}$$

The third term in Equation (2.39) is related to the head losses due to friction. Assuming an initial steady state situation, $h\left(0^+\right)=0$ and $q\left(0^+\right)=0$, Equation (2.38) and (2.39) gives

$$\frac{\partial q(s)}{\partial x}+\frac{1}{a^2}\frac{L}{T_W}sh(s)=0 \tag{2.40}$$

$$\frac{\partial h(s)}{\partial x}+\frac{T_W}{L}\left(s+f\frac{Q_0}{2AD}\right)q(s)=0 \tag{2.41}$$

Differentiating Equation (2.41) with respect to *x* yields

$$\frac{\partial^2 h(s)}{\partial x^2}=\frac{T_W}{L}\left(s+f\frac{Q_0}{2AD}\right)\frac{\partial q(s)}{\partial x} \tag{2.42}$$

Substituting $\partial q(s)/\partial x$ by Equation (2.40) into Equation (2.42)

$$\frac{\partial^2 h(s)}{\partial x^2}=\frac{1}{a^2}\left(s^2+f\frac{Q_0}{2AD}s\right)h(s) \tag{2.43}$$

Introducing the variable *z*

$$z^2=s^2+\frac{fQ_0}{2DA}s \tag{2.44}$$

The general solution for the second order homogeneous Equation (2.43) is

$$h(s)=C_1e^{\frac{z}{a}x}+C_2e^{-\frac{z}{a}x} \tag{2.45}$$

By differentiating equation (2.45) with respect to *x* yields

$$\frac{\partial h(s)}{\partial x}=C_1\frac{z}{a}e^{\frac{z}{a}x}-C_2\frac{z}{a}e^{-\frac{z}{a}x} \tag{2.46}$$

Substituting $\partial h(s)/\partial x$ by equation (2.46) into equation (2.41) gives

$$q(s)=\frac{L}{aT_W}\frac{s}{z}\left(C_1e^{\frac{z}{a}x}-C_2e^{-\frac{z}{a}x}\right) \tag{2.47}$$

The water pressure and the flow rate of upstream inlet of the tube at *x=0* is

$$h_U(s) = C_1 + C_2 \tag{2.48}$$

$$q_U(s) = \frac{L}{aT_W}\frac{s}{z}(C_1 - C_2) \tag{2.49}$$

The water pressure and the flow rate of downstream outlet of the tube at *x=L* is

$$h_D(s) = C_1 e^{\frac{z}{a}L} + C_2 e^{-\frac{z}{a}L} \tag{2.50}$$

$$q_D(s) = \frac{L}{aT_W}\frac{s}{z}\left(C_1 e^{\frac{z}{a}L} - C_2 e^{-\frac{z}{a}L}\right) \tag{2.51}$$

Hence, it follows from Equation (2.50) and (2.51) that

$$C_1 = \frac{1}{2}e^{-\frac{z}{a}L}h_D(s) + \frac{1}{2}\frac{aT_W}{L}\frac{z}{s}e^{-\frac{z}{a}L}q_D(s) \tag{2.52}$$

$$C_2 = \frac{1}{2}e^{\frac{z}{a}L}h_D(s) - \frac{1}{2}\frac{aT_W}{L}\frac{z}{s}e^{\frac{z}{a}L}q_D(s) \tag{2.53}$$

The substitution of the values of T_e, C_1 and C_2 from Equations (2.3), (2.52) and (2.53) into Equations (2.48) and (2.49) yield

$$h_U(s) = \frac{1}{2}\left(e^{-zT_e} + e^{zT_e}\right)h_D(s) + \frac{1}{2}\frac{T_W}{T_e}\frac{z}{s}\left(e^{-zT_e} - e^{zT_e}\right)q_D(s) \tag{2.54}$$

$$q_U(s) = \frac{1}{2}\frac{T_e}{T_W}\frac{s}{z}\left(e^{-zT_e} - e^{zT_e}\right)h_D(s) + \frac{1}{2}\left(e^{-zT_e} + e^{zT_e}\right)q_D(s) \tag{2.55}$$

The transfer function of flow rate and water pressure of upstream inlet and downstream outlet of the tube, expressed in the matrix notation, is

$$\begin{bmatrix} h_U(s) \\ q_U(s) \end{bmatrix} = \begin{bmatrix} \cosh(zT_e) & -Z_c \sinh(zT_e) \\ -\frac{1}{Z_c}\sinh(zT_e) & \cosh(zT_e) \end{bmatrix} \begin{bmatrix} h_D(s) \\ q_D(s) \end{bmatrix} \tag{2.56}$$

In which the ***characteristic impedance*** for the pipe is

$$Z_c = \frac{T_W}{T_e}\frac{z}{s} \tag{2.57}$$

The classical wave solution given by an analysis of the partial differential equations in time and space defining pressure and flow rate at each point in the conduit taking into account the elastic water hammer theory and considering hydraulic loss as a hyperbolic tangent function is

$$\frac{h(s)}{q(s)} = -\frac{T_W}{T_e}\left(1+\frac{fQ_0}{2DAs}\right)^{1/2} \tanh\left(\left(s^2 + s\frac{fQ_0}{2DA}\right)^{1/2} T_e\right) \tag{2.58}$$

Neglecting the hydraulic friction losses, Equation (2.58) can be simplified as

$$\frac{h(s)}{q(s)} = -\frac{T_W}{T_e}\tanh(sT_e) \tag{2.59}$$

The penstock is modelled assuming an incompressible fluid and a rigid conduit for hydroelectric power plants with short or medium penstock where the travelling pressure wave effects are relatively insignificant. With the assumption of an inelastic water column effect, $\tanh(sT_e) \approx sT_e$, Equation (2.58) for small variations around an operating point can be simplified as

$$\frac{h(s)}{q(s)} = -T_W s - H_f \tag{2.60}$$

Neglecting the hydraulic friction losses, Equation (2.60) yields

$$\frac{h(s)}{q(s)} = -T_W s \tag{2.61}$$

2.3 Pressure Control Systems

Hydroelectric power plants with long conduits may have severe water hammer and governing stability problems. In a reaction turbine having long pressure tunnels, the dynamic response of both upstream and downstream water columns must be studied in order to avoid excessive pressure or over speed problems. Pressure transients will only be produced at upstream side in an action turbine; at downstream there will be a canal with a transient free surface flow. The classical solution is to insert a surge tank upstream or/and downstream the power plant to minimize the hydraulic transient effects. However, the surge tank may be very costly structure or cause some environmental problems. [6, 8]

A surge tank is an open standpipe connected to the conduits of the hydroelectric power plant. The main functions of a surge tank are reduce the amplitude of pressure fluctuations by reflecting the incoming pressure waves; improve the regulating characteristics of a hydraulic turbine; and, store or provide water.

Depending upon the requirement of the hydroelectric plants, the surge tank can be placed at upstream and/or downstream side of the powerhouse.

Depending upon its configuration, a surge tank may be classified as:

- *Simple Surge Tank* is a tank or an open shaft directly connected to the pipeline, and there is very little head loss between the tank and the pipeline.
- An *Orifice Surge Tank* that is a simple surge tank with the entrance restricted by means of an orifice.
- A *Differential Surge Tank* is an orifice tank having a riser.
- In a *One-way Tank;* the liquid flows from the tank into the pipeline only when the pressure in the pipeline drop below the liquid level in the surge tank.
- A *Closed Surge Tank* has the top of the tank closed and there is compressed air between the water surface and the top of the tank.

2.3.1 Governing Equations

To simplify the derivation of the dynamic and continuity equations that describe the oscillations of the water level in the tank the following assumptions are made; [6]

- The conduit walls are rigid and the liquid is compressible. This means that a flow change at any point in the system is transmitted instantaneously throughout the system, and the liquid moves like a solid slug
- The inertia of the liquid in the surge tank is small compared to that of the liquid in the tunnel and can therefore be neglected.
- The heads losses in the system during the transient state can be computed by using the steady-state formulas for the corresponding flow velocities.

Figure 2-3 depicted a typical simple surge tank system. In a simple tank, the tank is directly connected to the pipeline. A flow variation results in the oscillation of the liquid level in the surge tank.

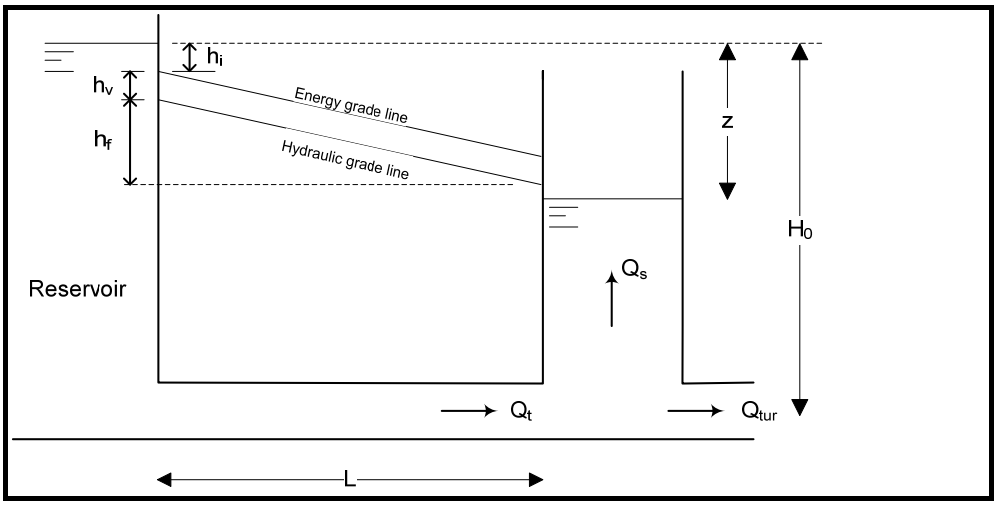

Figure 2-3: Simple surge tank, [6]

The dynamic equation is given applying the Newton's second law of motion; the rate of change of momentum is equal to the resultant force. The dynamic equation for a simple surge tank is given as follows

$$\frac{dQ_t}{dt} = \frac{gA_t}{L}\left(H - z + fQ|Q|\right) \tag{2.62}$$

The equation of continuity for the junction of the tunnel and the surge tank, shown in Figure 2-3, may be written as

$$Q_t = Q_s + Q_{tur} \tag{2.63}$$

where Q_s is the flow into the surge tank, Q_{tur} is the turbine flow. Since $Q_s = A_s\left(dz/dt\right)$, Equation (2.63) becomes

$$\frac{dz}{dt} = \frac{1}{A_s}\left(Q_t - Q_{tur}\right) \tag{2.64}$$

Equations (2.62) and (2.64) are for a simple surge tank located at the upstream side of a turbine. These equations are valid for a tailrace surge tank.

The period and the amplitude of the oscillations of the water surface in the surge tank for a frictionless system are given by:

$$T = 2\pi\sqrt{\frac{L}{g}\frac{A_S}{A_t}} \tag{2.65}$$

$$Z = Q_0\sqrt{\frac{L}{gA_SA_t}} \tag{2.66}$$

2.3.2 Surge Tank Mathematical Model

In a simple reservoir-surge tank system the unsteady flow can be modelled by a simple ordinary differential equation. The inclusion of surge tank effects is warranted in cases where dynamic performance is being simulated over many seconds to minutes. The surge tank equation is derived from the continuity of flow at the two junctions, Equation (2.64), and where the hydraulic losses at orifices of the surge tank are neglected. Normalizing Equation (2.64) yields

$$q = \frac{A_s H_0}{Q_0} \frac{dh}{dt} \tag{2.67}$$

The surge tank filling time, T_s, is defined as

$$T_s = \frac{A_s H_0}{Q_0} \tag{2.68}$$

The transfer function of flow rate and water pressure of upstream the surge tank is

$$\frac{h(s)}{q(s)} = \frac{1}{sT_s} \tag{2.69}$$

3 Hydraulic Turbines

This chapter contains the physical description of the hydraulic turbines and the deduction of the equations describing the appropriate mathematical models of the hydraulic turbine for their representation in power system dynamic studies. The turbine dynamics are characterized by the variations in flow and output mechanical torque with respect to turbine speed, gate opening, runner blade movement and the difference in pressure between the turbine inlet and outlet. Standard models are normally found in considerable number of relevant literature related hydropower plants modelling. Approaches based on approximate linear models assuming an ideal lossless turbine and ignoring the elasticity of the conduit system, are not suitable for the accurate study of the interaction between the hydraulic system and power system.

3.1 Hydraulic Turbines Overview

Hydraulic turbines derive the potential energy of the fluid into kinetic energy and a conversion of kinetic energy, or both kinetic and potential energy, into useful work. Hydraulic turbines derive power from the force exerted by water as it falls from an upper to a lower reservoir. Hydraulic turbines are divided according to their hydraulic action into two main classes: impulse turbines and reaction turbines. [1, 6, 8, 10, 21-22]

3.1.1 Impulse turbines

An impulse turbine has a runner with numerous spoon-shaped “buckets” attached to its periphery, which are driven by one or more jets of water issuing from fixed or adjustable nozzles. The kinetic energy is in the form of a high-speed jet that strikes the buckets, mounted on the periphery of the runner. As the water after striking the buckets falls into the tail water with little remaining energy, the casing can be light and serves the purpose of preventing splashing. Many impulse turbines use deflectors to allow rapid reduction of the power delivered to the turbine runner in cases where the flow cannot be changed quickly.

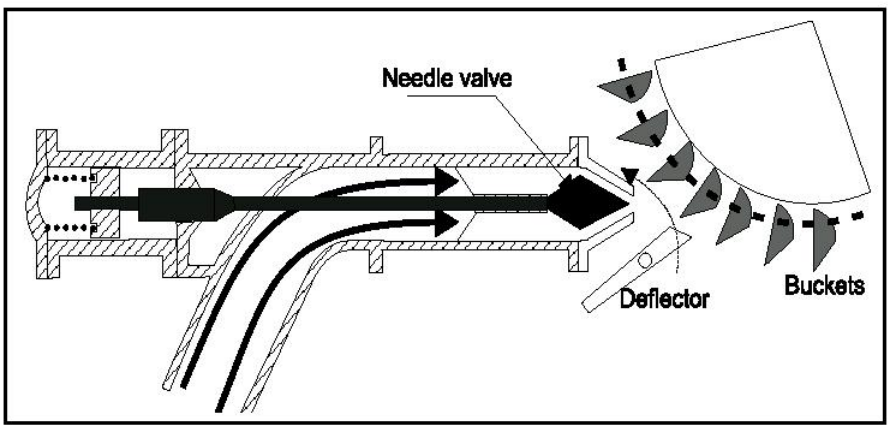

Figure 3-1: Impulse Turbine

Impulse or action type turbines are represented by the *Pelton* water-wheel, *Turgo* turbines and *Cross-flow* turbines. Impulse turbines are used in high-head, 300 meters or more, hydroelectric power plants.

Pressure transients in impulse turbine will only be induced at upstream side; at downstream there will be a canal with a transient free surface flow. Each nozzle will then actuate like a flow control valve.

3.1.2 Reaction Turbines

In reaction turbines, the entire flow from the headwater to tailwater takes place in a closed conduit system. Reaction turbines extract power from the kinetic energy of water because of the difference in pressure between the front and the back of each runner blade as the water flows through the runner. The water pressure can apply a force on the face of the runner blades. The turbine casing, with the runner fully immersed in water, must be strong enough to withstand the operating pressure.

Reaction turbines are represented by radial-flow Francis turbines; axial-flow Kaplan turbines with adjustable runner blades; axial-flow propeller turbines with fixed runner blades; diagonal-flow Deriaz turbines with adjustable runner blades.

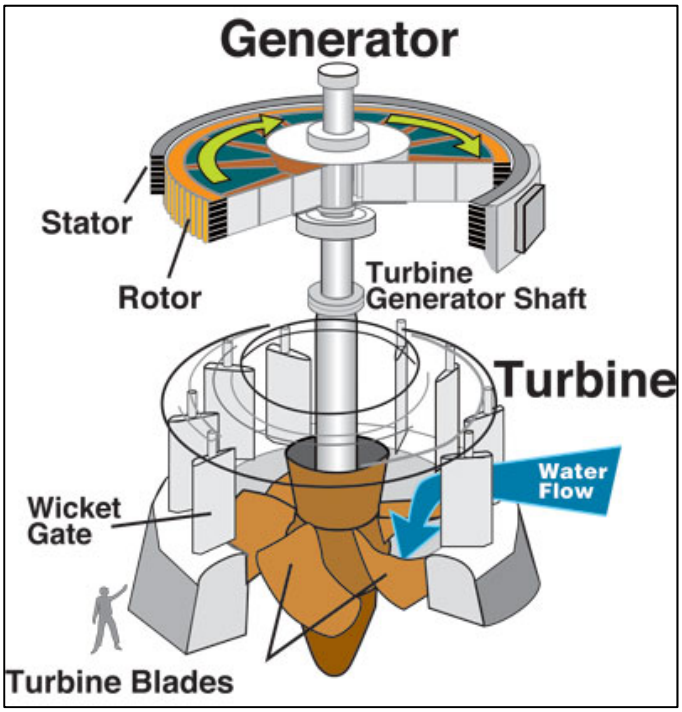

Figure 3-2: Francis Turbine

Upstream and downstream water columns are sensitive to flow disturbances at reaction type turbine. Pressure regulators or relief valves are used to temporarily allow part of the water to bypass the runner by flowing from the turbine spiral case directly to the tailrace during the quick closure of the wicket gates. The pressure regulators or relief valves prevent excessive water hammer, which is a severe pressure rise that results from rapid deceleration of the penstock water column.

3.2 General Technical Aspects

The hydroelectric generation is extremely site dependent because it depends on falling water. The basic elements of the Hydraulic Power Plant are depicted in Figure 3-3. The turbine proper is, according to standard practice, taken to begin at the entrance to the turbine casing and to end at a section of the tailrace just beyond the physical end of the draft tube. [9]

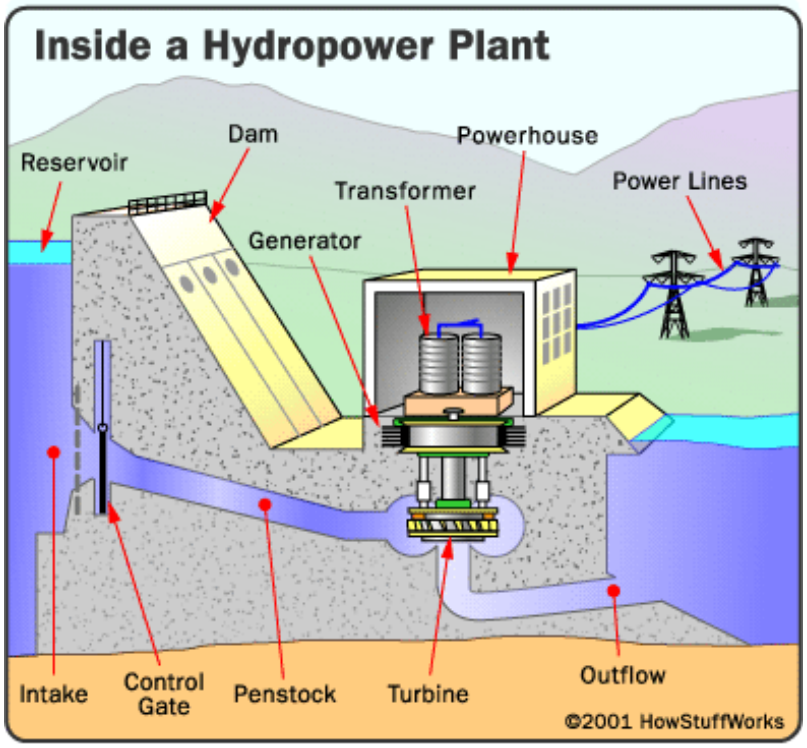

Figure 3-3: Schematic of Hydraulic Power Plant with a reaction turbine

3.2.1 Neat Head, Power and Efficiency

The **Neat Head** is the vertical height between the entrance level into the penstock and the discharge level from the turbine draft tube.

The **mechanical power** developed by the turbine is proportional to the product of the flow rate, the head and the efficiency. The power is controlled by regulating the flow into the turbine by wicket gates on the reaction turbines and by a needle on the impulse turbine. The nominal power is given by the following equation

$$P = \rho g Q H \eta \tag{3.1}$$

The **turbine efficiency** η represents the actual utilization of the available potential energy of the system. The turbine efficiency depends on the working fluid flow rate and the turbine characteristics. The turbine efficiency is defined as the ratio of power supplied by the turbine (mechanical power transmitted by the turbine shaft) to the absorbed power (hydraulic power equivalent to the measured discharge under the net head). [23]

The generator efficiency is usually considered constant over a wide operating range. However, the hydraulic efficiency depends significantly on both the water discharge and the net head. These relationships are generally represented in the so-called ***Turbine Hill Chart***.

3.2.2 Turbine Hill Charts

The mathematical modelling of the data for the flow and power output of a Francis turbine, and its transient behaviour is based on the characteristic curve of the hydraulic machine called ***Hill Charts.*** The Turbine Characteristics are curves representing the relationship between the net head and discharge. Although such curves are seldom used in specifications due to of difficulties of measurement, the speed-torque characteristics of a wide variety of hydraulic turbines have the general form with the torque falling off roughly in proportion to speed over wide ranges of speed and gate opening position. [6, 18, 24-27]

Static characteristic relationships of hydraulic turbines can be studied through the so-called *hill charts.* The plots of the prototype turbine characteristics are based in steady-state model test results. These turbine characteristics are assumed valid during the transient state. The turbine efficiency for any operating point given by runner speed, net head and gate position can be extracted from the *hill charts.*

An operating point of a hydraulic turbine is characterized by the specific energy, the discharge, the rotational speed, the torque and the gate opening position. Therefore, the graphical representation of a turbine characteristic requires the elimination of one of these quantities by the use of the hydraulic machines similitude laws. For transient analysis, it is more convenient to use dimensional factors where the specific energy is eliminated, [20]. The mathematical model of the characteristic of hydraulic turbine may be written as:

$$Q_{11} = f\left(n_{11}, y\right) \tag{3.2}$$

$$M_{11} = f\left(n_{11}, y\right) \tag{3.3}$$

However, there are still no detailed and precise mathematical models that can describe the unit flow rate Q_{11} and unit torque M_{11}. Q_{11} and M_{11} are usually obtained by interpolation method. The expression for the unit rotation speed n_{11}, and unit flow Q_{11} may be written as follows

$$n_{11} = \frac{nD_{ref}}{\sqrt{H}} \tag{3.4}$$

$$Q_{11} = \frac{Q}{D_{ref}^2\sqrt{H_n}} \tag{3.5}$$

$$M_{11} = \frac{M}{D_{ref}^3 H_n} \tag{3.6}$$

The characteristic curves are extrapolated for small wicket-gate openings. Therefore, the flow should be known when the turbine rotational speed is zero. The windage and friction losses should be known at wicket-gate openings below the speed no-load gate. The no-load gate is the lowest gate opening at which turbine rotates at synchronous speed with zero output. [6]

A typical Hill Chart for a Francis turbine is shown on Figure 5.2 of Chapter 5, page 131, of the textbook "*Applied Hydraulic Transients*". [6]

3.3 Hydraulic Turbine Modelling

The hydraulic turbine dynamics have a considerable influence on the dynamic stability of the power system. The block diagram of Figure 3-4 shows the basic elements of a hydro turbine within the power system environment.

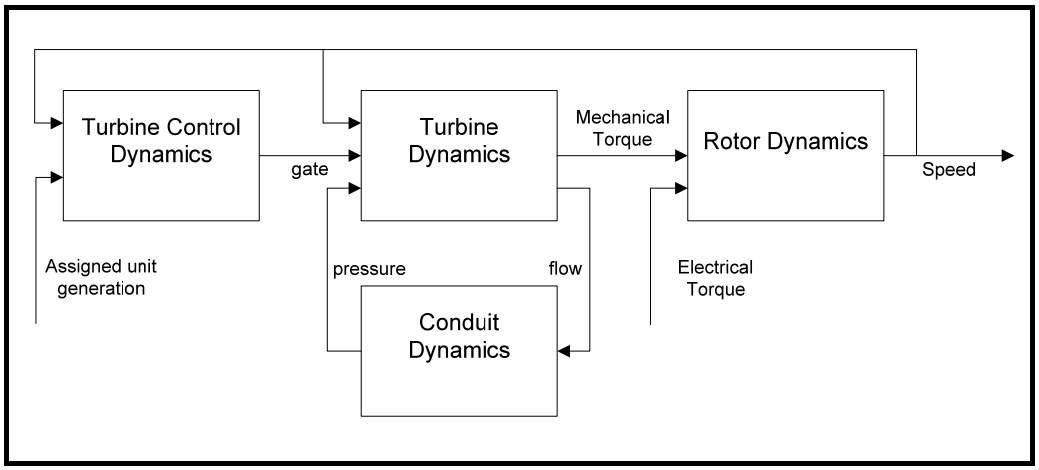

Figure 3-4: Functional Block Diagram of the hydro turbine, [1, 28]

The power developed by the turbine is a function of the water flow, the runner blade angle and the net head. The flow through the turbine is a function of the net head, rotational speed, gate opening position and runner blade angle. The nonlinear characteristic of a Francis turbine can be written as, [1, 6, 8, 16, 23, 25, 28-31]

$$p = f_p\left(h, n, y, \phi\right) \tag{3.7}$$

$$q = f_q\left(h, n, y, \phi\right) \tag{3.8}$$

The effect of the runner blade movement is not considered in the modelling of turbines with fixed blades, such as Francis turbines. The flow in an impulse turbine depends upon the head and the nozzle opening only.

The turbine dynamics is related to the generator dynamics through mechanical power P_m produced by the turbine. The relation between mechanical power P_m and mechanical torque M_m, expressed in per unit, is given by

$$p_m = \frac{n}{\omega_s} m_m \tag{3.9}$$

Normally, a simplifying assumption made is that $n = \omega_s$ at synchronous speed. This is not the same as saying that the speed is constant, it assumes that speed changes are small and do not have a significant effect. Thus, equation (3.9) yields

$$p_m = m_m \tag{3.10}$$

3.3.1 Simplified Nonlinear Turbine model

The nominal power obtained by a hydraulic turbine is proportional to the potential energy lost by the falling fluid. Due to the turbine is not 100% efficient, the no-load flow q_{NL} is subtracted from the actual flow. A damping effect that is dependent on gate opening is also present, so that at any load condition the turbine power can be expressed by

$$p_m = A_t h\left(q - q_{NL}\right)\eta - K_D\left(\omega_N - 1\right)y \tag{3.11}$$

Detailed information is available from turbine manufacturers on the variation of the turbine efficiency η with variation in the steady operating point of a turbine. The use of this data involves the use of a stored table and an interpolation procedure. Neglecting the variation of turbine efficiency, Equation (3.11) yields

$$p_m = A_t h\left(q - q_{NL}\right) - K_D\left(\omega_N - 1\right)y \tag{3.12}$$

The constant proportionality factor A_t is calculated using the turbine MW rating and generator MVA base. A_t is calculated by

$$A_t = \frac{1}{h\left(q - q_{NL}\right)}\frac{turbine\ power\left(MW\right)}{generator\ MVA\ rating} \tag{3.13}$$

The **pressure head across the turbine** is related to the per unit flow rate by assuming that the turbine can be represented by the valve characteristic

$$q = y\sqrt{h} \tag{3.14}$$

3.3.2 The linearized hydro turbine model

The most common hydraulic turbine representation for system stability studies consists of a transfer function obtained by linearizing the turbine characteristic curves around an operating point. The dynamics of the analyzed system with respect to the operating point can be observed by changing operating point. For the controller synthesis using linear synthesis method, Equations (3.7) and (3.8) can be represented by the Taylor series approximation for small variations in the vicinity of an operating point as, [25-26, 32-37]

$$\Delta m = \frac{\partial m}{\partial h}\Delta h + \frac{\partial m}{\partial n}\Delta n + \frac{\partial m}{\partial y}\Delta y \tag{3.15}$$

$$\Delta q = \frac{\partial q}{\partial h}\Delta h + \frac{\partial q}{\partial n}\Delta n + \frac{\partial q}{\partial y}\Delta y \tag{3.16}$$

The partial derivatives of flow and torque with respect to head, rotational speed and gate position are called ***Turbine Coefficients***. The turbine coefficients represent the nonlinear characteristics of a hydraulic turbine. The partial derivatives vary with the operating conditions of the turbine relative to gate opening position *y* and unit rotational speed n_{11}.

The influence of the turbine coefficients on the model accuracy is critical. These values have to be measured accurately on the field or taken from model tests.

The turbine coefficients of any operating point can be obtained by interpolation before simulation. For deviations around rated speed and pressure head, the turbine coefficients are deduced by differentiation of Equations (3.1) and (3.14), [11]. Differentiating Equations (3.12) and (3.14), the turbine coefficients are deduced for models neglecting the variation of the turbine efficiency, [37]. These parameters are detailed in Table 3-1.

Table 3-1: Turbine coefficients, [11, 37]

Partial Derivatives	IEEE Model, [11]	IEEE Model, [37]
$\frac{\partial q}{\partial h}$	$0.5\, y_0$	$\frac{y}{2\sqrt{h}}$
$\frac{\partial q}{\partial n}$	0.0	0.0
$\frac{\partial q}{\partial y}$	1.0	$\sqrt{h}$
$\frac{\partial m}{\partial h}$	$1.5\,\eta\, y_0$	$A_t\left(\frac{3}{2} y\sqrt{h} - q_{NL}\right)$
$\frac{\partial m}{\partial n}$	0.0	$-D_a y$
$\frac{\partial m}{\partial y}$	η	$A_t h^{3/2} - D_a\left(\omega_N - 1\right)$

The partial derivative of torque with respect to gate position, $\partial m/\partial y$, is called ***Turbine Gain.*** Turbine Gain is a critical parameter for an accurate approximation of hydro power plants dynamics, and has to be measured precisely in the field. The partial derivative of flow with respect to rotational speed, $\partial q/\partial n$, is usually considered to be negligible. The deviation of mechanical torque with rotational speed, $\partial m/\partial n$, is known as ***Turbine Self Regulation***. The value of the turbine self regulation is negative with an absolute value usually near unity.

Standard values for an ideal lossless turbine at full load and three linearized values of the turbine coefficients are shown in of Table 3-2. More accurate values of turbine parameters can be deduced from the Characteristic Curves of the turbine so-called Hill Charts, detailed in Chapter 3.2.2.

Table 3-2: Turbine Coefficients, [32]

Partial Derivatives	Generator Operating Conditions			IEEE model
	22.5 (MW)	84.3 (MW)	112.0 (MW)	
$\frac{\partial q}{\partial h}$	0.06	0.20	0.24	0.50
$\frac{\partial q}{\partial n}$	0.13	0.38	0.62	0.00
$\frac{\partial q}{\partial y}$	0.80	0.40	0.38	1.00
$\frac{\partial q}{\partial \phi}$	0.00	0.30	0.69	0.00
$\frac{\partial m}{\partial h}$	0.40	1.20	1.50	1.50
$\frac{\partial m}{\partial n}$	-0.39	-0.86	-0.75	0.00
$\frac{\partial m}{\partial y}$	0.88	0.90	0.34	1.00
$\frac{\partial m}{\partial \phi}$	0.00	0.50	0.52	0.00
$\frac{\partial \phi}{\partial y}$	0.00	2.30	1.00	0.00

It is worthy to notice that the linear models implemented in the Master's Thesis work uses the standard values according to IEEE model detailed in Table 3-2.

4 Synchronous Machine

This chapter deals with the mathematical modelling of the synchronous generator. Synchronous machines play an important role in power system stability. The physical characteristics of the synchronous generators and their performance affect the system stability. The complete mathematical modelling of the synchronous machine is fairly complex system for stability analysis of power systems. The classical model is used for simplified analysis of power system dynamics.

4.1 Synchronous Generator

Synchronous generators are the main source of electric energy in power systems. Hence, understanding of the theory and performance of the synchronous machines is fundamental to the study of power system stability. Synchronous generators can be classified as either high-speed generators, called turbo generators, driven by steam or gas, or low-speed generators driven by hydraulic turbines.

The synchronous machine is assumed to have a three-phase stator armature winding, a rotor field winding and two rotor damper winding –one in the d-axis and one in the q-axis. The armature winding carries the load current and supplies the power to the system. The armature winding usually operates at a voltage considerable higher than the field voltage. The rotor excitation winding is supplied with a direct current to produce a rotating magnetic flux. The rotor damper winding helps damp mechanical oscillations of the rotor. The notation follows the normal IEEE convention.

The following assumptions are made in order to develop the mathematical model of a synchronous machine. [2, 22, 38-40]

a) The three-phase stator winding is symmetrical distributed.
b) The capacitance of all the windings can be neglected.
c) Each of the distributed windings may be represented by a concentrated winding.
d) The change in the inductance of the stator windings due to rotor position is sinusoidal and does not contain higher harmonics.
e) Hysteresis loss is negligible but the influence of eddy currents can be included in the model of the damper windings.
f) In the transient and subtransient states the rotor speed is near synchronous speed.
g) The magnetic circuits are linear (not saturated) and the inductance values do not depend on the current.

4.2 Synchronous Generator Equations

The generator windings are magnetically coupled, hence, the flux in each winding depends on the currents in all the windings. The electrical dynamic performance of the machine is described by the flux-current relations and the voltage equations. The transformation of all the generator windings into the rotor reference frame is referred as the *0dq transformation* or *Park's transformation*. [41-43]

The electrical dynamic performance of the machine in terms of the *dq0* coordinate system may be described by the following set of equations.

Flux linkage equations

$$\begin{bmatrix}\psi_d\\ \psi_q\\ \psi_0\\ \psi_f\\ \psi_D\\ \psi_Q\end{bmatrix}=\begin{bmatrix}L_{ad}+L_l & 0 & 0 & L_{ad} & L_{ad} & 0\\ 0 & L_{aq}+L_l & 0 & 0 & 0 & L_{aq}\\ 0 & 0 & L_0 & 0 & 0 & 0\\ L_{ad} & 0 & 0 & L_{ad}+L_f & L_{ad} & 0\\ L_{ad} & 0 & 0 & L_{ad} & L_{ad}+L_D & 0\\ 0 & L_{aq} & 0 & 0 & 0 & L_{aq}+L_Q\end{bmatrix}\begin{bmatrix}-i_d\\ -i_q\\ -i_0\\ i_f\\ i_D\\ i_Q\end{bmatrix} \tag{4.1}$$

Stator voltage equations:

$$\begin{bmatrix}v_d\\ v_q\\ v_0\end{bmatrix}=\frac{1}{\omega_s}\frac{d}{dt}\begin{bmatrix}\psi_d\\ \psi_q\\ \psi_0\end{bmatrix}+\frac{\omega}{\omega_s}\begin{bmatrix}-\psi_q\\ \psi_d\\ 0\end{bmatrix}-\begin{bmatrix}R_a & 0 & 0\\ 0 & R_a & 0\\ 0 & 0 & R_a\end{bmatrix}\begin{bmatrix}i_d\\ i_q\\ i_0\end{bmatrix} \tag{4.2}$$

Rotor voltage equations:

$$\begin{bmatrix}v_f\\ 0\\ 0\end{bmatrix}=\frac{1}{\omega_s}\frac{d}{dt}\begin{bmatrix}\psi_f\\ \psi_D\\ \psi_Q\end{bmatrix}+\begin{bmatrix}R_f & 0 & 0\\ 0 & R_D & 0\\ 0 & 0 & R_Q\end{bmatrix}\begin{bmatrix}i_f\\ i_D\\ i_Q\end{bmatrix} \tag{4.3}$$

The transformer emfs, the $d\psi/dt$ terms, are referred to the armature emfs proportional to the rate change of the flux. The transformer emfs are due to changing currents in coils on the same axis as the one considered.

In addition to the equations describing the electrical dynamic performance, an expression for the electromechanical torque is required.

$$m_e=\frac{\omega_s}{\omega}\left[\psi_d i_q-\psi_q i_d\right] \tag{4.4}$$

Rotor mechanical Equations:

The rotor mechanical dynamic are given by the swing equation, which can be expressed via, [2]:

$$\frac{d\Delta\omega}{dt} = \frac{\omega_s}{2H}\left(m_m - m_e - K_D\Delta\omega\right) \tag{4.5}$$

$$\frac{\partial\delta}{\partial t} = \Delta\omega = \omega - \omega_s \tag{4.6}$$

In the above equations, all quantities are in per unit except time that is in seconds and ω and ω_s which are in rad/sec. In some literature, per unit speed $\omega_N = \omega/\omega_s$ is used. Therefore, Equations (4.5) and (4.6) yield

$$\frac{d\Delta\omega_N}{dt} = \frac{1}{2H}\left(m_m - m_e - K_D\left(\omega_N - 1\right)\right) \tag{4.7}$$

$$\frac{\partial\delta}{\partial t} = \omega_s\left(\omega_N - 1\right) \tag{4.8}$$

4.3 Synchronous Generator Models

The mathematical model of a synchronous machine is made up of Park's equations for the electrical dynamics, Equations (4.1), (4.2) and (4.3), and, two equations for mechanical dynamics, Equations (4.5) and (4.6). [44-45]

The larger number of differential equations required in the model, the greater the model complexity and the greater the time required to solve the differential equations. The complete ninth order nonlinear model is a complex system for stability analysis of power systems. It is highly desirable, to rephrase and simplify the full set of generator model in order to get a more acceptable form and easier to interface to the power system network equations, [22]. Some of the essential simplifications are:

- There are no zero-sequence currents in balanced operations.
- Changes in the generator speed are small, $\omega \approx \omega_s$.
- The transformer emfs ($d\psi_d/dt$ and $d\psi_q/dt$) are neglected because are small compared with the rotation emfs ($-\omega\psi_q$ and $+\omega\psi_d$).

The differential equations for the electrical dynamics, expressed in orthogonal phase quantities, used to model a number of different models are

$$T_{do}^{''}\frac{dE_q^{''}}{dt} = E_q^{'} - E_q^{''} + \left(X_d^{'} - X_d^{''}\right)I_d \tag{4.9}$$

$$T_{qo}^{''}\frac{dE_d^{''}}{dt} = E_d^{'} - E_d^{''} - \left(X_q^{'} - X_q^{''}\right)I_q \tag{4.10}$$

$$T_{do}^{'}\frac{dE_q^{'}}{dt}=E_f-E_q^{'}+\left(X_d-X_d^{'}\right)I_d \tag{4.11}$$

$$T_{qo}^{'}\frac{dE_d^{'}}{dt}=-E_d^{'}-\left(X_q-X_q^{'}\right)I_q \tag{4.12}$$

4.3.1 Synchronous Machine Represented by the Classical Model

The second-order synchronous generator model, referred to as the "classical" model, is widely used for simplified analysis of power system dynamics. In the classical model all the voltages, emfs and the currents are phasors in the network reference frame rather than their components resolved along the d- and q- axis.

Assume that the generator is connected to the infinite bus as shown in Figure 4-1 and that all the resistances and shunt impedances associated with the transformer and network are neglected. The time constant $T_{do}^{'}$ is relatively long and the changes in E_f and I_d are small. Additionally the rotor transient saliency is neglected.

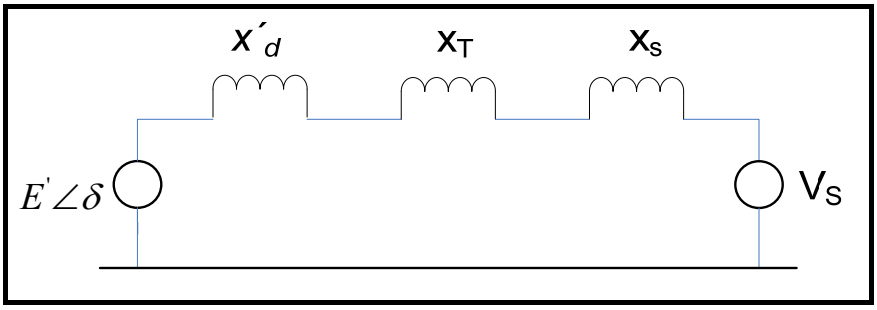

Figure 4-1: Equivalent circuit of the classical model of the generator

The classical synchronous generator model assumes that neither the d-axis armature current I_d nor the internal emf E_f representing the excitation voltage change very much during the transient state. In this model, the generator is represented by a constant emf E' throughout the study period behind the transient reactance X_d' and the rotor inertia equations, Equations (4.5) and (4.6). [22]

The equation describing the armature voltage yields

$$V=\left(E_q'+jE_d'\right)-jX_d'\left(I_q+jI_d\right)=E'-jX_d'I \tag{4.13}$$

The simplest second-order model is very approximate and only suitable for representing remote machines in the analysis of very large interconnected power systems or generators located a long way from the point of disturbance. It can also be useful for evaluating generator behaviour during the first rotor swing.

5 Turbine Governing Systems

The governing system is a system that regulates the turbine-governor speed and hence the frequency and the active power in response to load variation. The turbine governor regulates the inlet of water into a turbine, which in turn rotates the generator to produce electricity. This chapter details the modelling of the mechanical-hydraulic and electro-hydraulic turbine governing system.

5.1 Governing System

The main function of the turbine governing system is to regulate the turbine-generator speed and hence the frequency and the active power in response to load variation. The speed control mechanism includes equipment such as relays, servomotors, pressure or power amplifying devices, levers and linkages between the speed governor and governor-controlled gates. The speed governor normally actuates the governor-controlled gates that regulate the water input to the turbine through the speed control mechanism. [1-2, 6, 21-22, 46-49]

Hydro turbine governing systems are strongly influenced by the effects of water inertia and, as a result, two servomotors are used to provide the required force to move the control gate. The first *pilot servomotor*, low power, operates the *distributor or relay valve* of the second *main gate servomotor,* high-power. The pilot servomotor has a pilot valve that is controlled either by a mechanical governor or by an electronic regulator. The output of the speed-sensing devices is the deviation from the reference speed. [22]

The **permanent speed droop** R_P determines the amount of change in output a unit produces in response to a change in unit speed. The permanent speed droop can be developed either by using the wicket gate position or by using the unit output power. For isolated or islanded operation, the permanent speed droop can help to stabilize the unit speed control by providing an intermediate feedback that limits the over travel of the turbine control servomotors while controlling the unit speed. The permanent speed droop determines the amount of participation the unit produces when responding to disturbances in system frequency in operation while synchronized to an interconnected power system.

The **temporary droop** R_T is used to limit overshoot of the turbine control servomotor during a transient condition. The temporary droop may be developed either connecting a dashpot from the wicket gate position to the governor error summing point, or adding a filtered derivative of wicket gate position to the governor error summing point.

Hydro turbine governors are designed to have relatively large transient droop compensation with long resetting times. This ensures stable frequency regulation under isolated operating conditions. The response of a hydro turbine to speed changes or to changes in speed-changer setting is relatively slow.

5.2 Mechanical-hydraulic Governor

The Mechanical-Hydraulic Governing System uses the *Watt centrifugal mechanism* as the speed governor. Speed sensing, permanent droop feedback and computing functions are achieved through mechanical components and functions involving higher power are achieved through hydraulic components. The dashpot feedback is required in order to achieve stable performance. The schematic diagram of the mechanical-hydraulic governing system is shown in Figure 5-1.

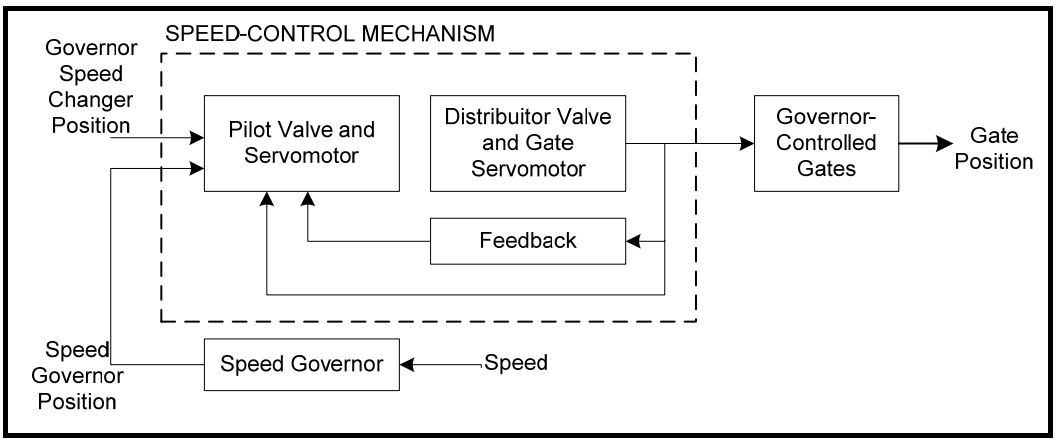

Figure 5-1: Schematic diagram of the Governing System, [48]

The main disadvantages of the Watt centrifugal governor are the present of deadbands and a relatively low accuracy. The size of the deadbands also tends to increase with time due to wear in the moving mechanical elements. The conventional *mechanical-hydraulic* governing system has been replaced by an *electro-hydraulic* governor.

5.2.1 Mathematical Modelling

Figure 5-2 shows a simplified mechanical-hydraulic governor. The variables used in the derivation of the transfer functions are per-unit derivatives from the initial steady-state values. [2, 22, 47]

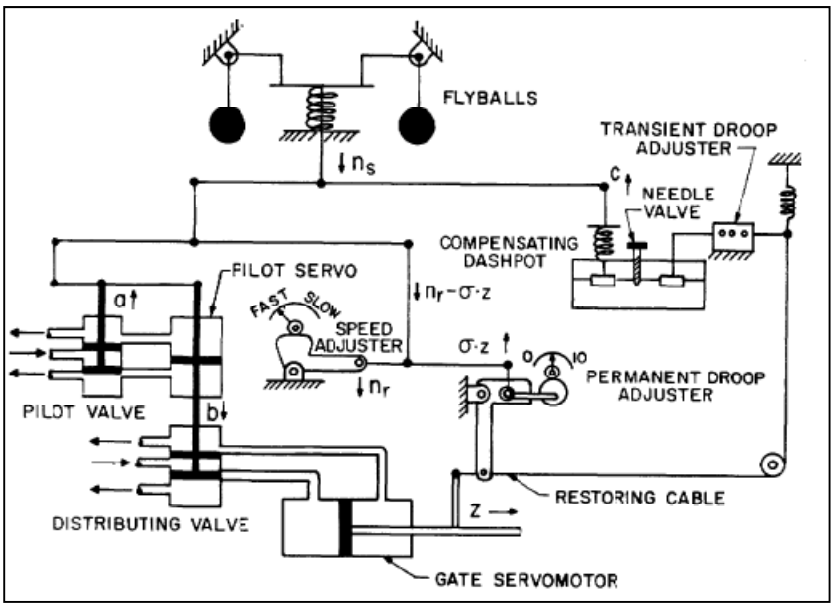

Figure 5-2: Mechanical-Hydraulic Governing System. [47]

The transfer function of the distributing valve and gate servomotor is

$$\frac{y}{b} = \frac{K_1}{s} \tag{5.1}$$

The transfer function of the pilot valve and pilot servomotor is

$$\frac{b}{a} = \frac{K_2}{1 + T_p s} \tag{5.2}$$

where K_2 is determined by the feedback lever ratio and T_p by the port areas of the pilot valve and K_2. Combining Equations (5.1) and (5.2) yields

$$\frac{y}{a} = \frac{K_1 K_2}{s\left(1 + T_P s\right)} = \frac{K_s}{s\left(1 + T_P s\right)} \tag{5.3}$$

The servomotor gain K_s is determined by the pilot valve feedback lever ratio and the port areas of the distributing valve and gate servomotor. The governor response time, $T_g = 1/K_s$, is related to the gate closing time T_c, where T_c is the time required for full-gate travel with the gates moving at maximum velocity, typically 5 to 10 seconds.

Assuming that the flow of dashpot fluid through the needle valve is proportional to the dashpot pressure, the dashpot transfer function is

$$\frac{c}{y} = R_T \frac{T_R s}{1 + T_R s} \tag{5.4}$$

The temporary droop R_T is determined by the selection of pivot-point for the lever connected to the input piston. The reset time T_R is determined by the needle valve setting.

The pilot valve input signal is produced adding the action of a system of floating levers, the reference speed, shaft speed, permanent droop, and temporary droop signals.

$$a = \omega_{ref} - \omega_s - R_P y - R_T \frac{T_R s}{1 + T_R s} \tag{5.5}$$

A combination of Equations (5.3), (5.4) and (5.5) gives

$$\frac{y}{\omega_{ref} - \omega_s} = \frac{\frac{1}{R_P}\left(1 + T_R s\right)}{\frac{T_P T_R T_g s^3}{R_P} + \frac{\left(T_P + T_R\right) T_g s^2}{R_P} + \frac{\left(T_g + T_R\left(R_P + R_T\right)\right) s}{R_P} + 1} \tag{5.6}$$

The block diagram of a typical hydro turbine governing system suitable for stability analysis is shown in Figure 5-3.

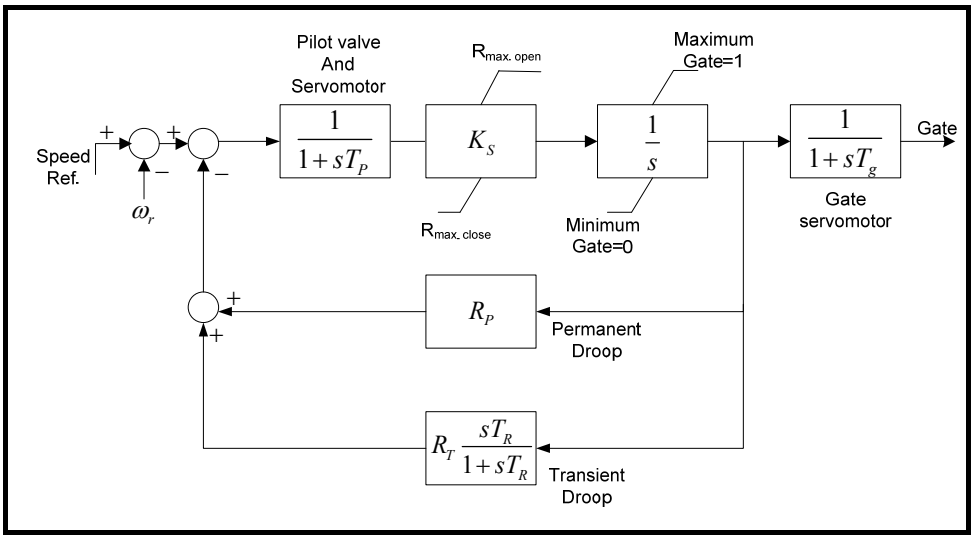

Figure 5-3: Model of governor for hydraulic turbines, [2]

As the pilot valve and servomotor time constant T_P is several times smaller than the time constants T_g and T_R, it may be neglected to give the second-order transfer function

$$\frac{y}{\omega_{ref}-\omega_s}=\frac{\frac{1}{R_P}\left(1+T_R s\right)}{\left(1+\frac{T_g+T_R\left(R_P+R_T\right)}{R_P}s\right)\left(1+\frac{T_R T_g}{T_g+T_R\left(R_P+R_T\right)}s\right)} \tag{5.7}$$

For stable operation under islanding conditions, the optimum choice of the temporary droop R_T and reset time T_R is given by; [2, 50]

$$R_T=\left[2.3-\left(T_W-1.0\right)0.15\right]\frac{T_W}{T_M} \tag{5.8}$$

$$T_R=\left[5.00-\left(T_W-1.00\right)0.50\right]T_W \tag{5.9}$$

Table 5-1 gives typical values and range of parameters for hydraulic governors.

Table 5-1: Typical values and range of Parameters, [47]

	Typical values	Range
T_R	5.00	2.50 – 25.0
T_g	0.20	0.20 – 0.40
T_W	1.00	0.50 – 5.00
T_M (2H)	8.00	6.00 – 12.0
T_c	5.00	5.00 – 10.0
R_P	0.04	0.03 – 0.06
R_T	0.31	0.20 – 1.00

5.3 Electro-Hydraulic Governing System

The Electro-Hydraulic Governing System operation is very similar to that of mechanical-hydraulic governors. Speed sensing, droop compensation, and computing functions are performed electrically. The output signal drives an electrical-mechanical transducer, which operates a pilot valve and pilot-valve servomotor. The turbine rotor speed is measured electronically with high accuracy. [2, 18, 47-49]

5.3.1 Mathematical Model

The Electro-Hydraulic governor uses the three-term controllers with proportional-integral-derivative action, PID-controller, to perform the low-power functions. The proportional term produces a control action proportional to the size of the error input, and an immediate response to an error level input. The proportional term response has a significant influence on the stability of the governed system. The integral term produces a control action that accumulates at a rate proportional to the size of the error input. The integral term also trims out the error input to the governor controller to determine the steady-state accuracy of the governed system. The derivative term produces a control action that is proportional to the rate of change of the error input. The derivative term helps to extend the stability limits of the governed system by allowing higher proportional and integral gains while maintaining a stable control system. [1, 21, 35, 40, 47, 51-52]

The block diagram of a PID controller is shown in Figure 5-4. The permanent-droop feedback may be obtained from generator terminal power rather than from gate position to eliminate the nonlinearity of the gate-position versus power curve. [47]

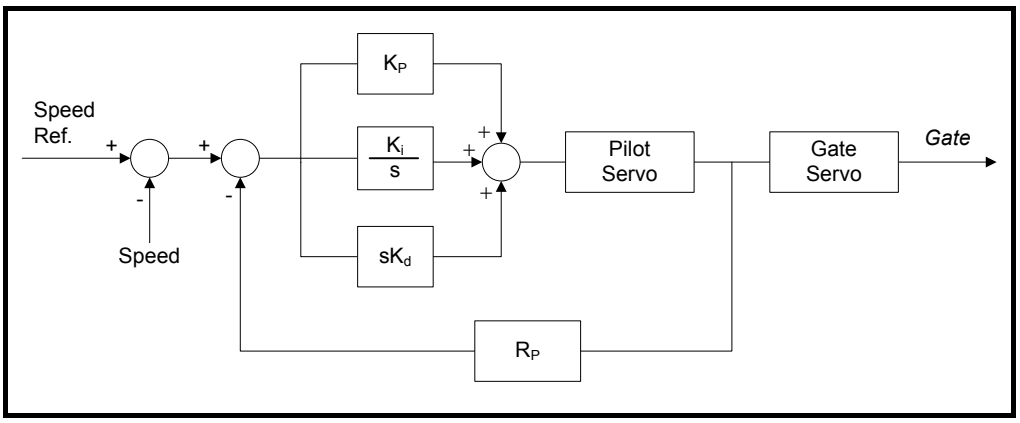

Figure 5-4: Typical PID Governor Controller, [2]

The transfer function of the PID governor expressed in terms of proportional, integral and derivative gains, is

$$\frac{y}{\omega_{ref}-\omega_s}=\frac{1}{R_P}\left[\frac{K_d s^2+K_p s+K_i}{K_d s^2+\left(K_p+1/R_P\right)s+K_i}\right] \tag{5.10}$$

The optimum parameters suggested in [53] are expressed as follows

$$K_p = 0.80\frac{T_M}{T_W} \tag{5.11}$$

$$K_i = 0.24\frac{T_M}{T_W^2} \tag{5.12}$$

$$K_d = 0.27T_M \tag{5.13}$$

The use of a high derivative gain will result in excessive oscillations and possibly instability when the generating unit is connected to an interconnected system. When the derivative gain is set to zero, the transfer function of PID-controller is equivalent to that of the mechanical-hydraulic governor. The design is based on linear control theory at one load condition and then de-tuned for worst operating conditions. This controller design does not guarantee the close loop system to remain stable at all operating conditions. The transfer function of the PI governor yields

$$\frac{y}{\omega_{ref} - \omega_s} = \frac{1}{R_P}\frac{K_p s + K_i}{\left(K_p + \frac{1}{R_P}\right)s + K_i} \tag{5.14}$$

Adding a small time constant, Equation (5.14) may be improved as

$$\frac{y}{\omega_{ref} - \omega_s} = \frac{1}{R_P}\frac{1 + \frac{K_p}{K_i}s}{\left(1 + \frac{K_p R_P + 1}{K_i R_P}s\right)(1 + 0.1s)^2} \tag{5.15}$$

6 Hydraulic Power Plant Models

Hydroelectric power generating system is a high-order, uncertain and nonlinear system. The power output of a hydro power plant varies constantly according to the network needs that involve a reaction of the control system. The representation of each component of the power system by means of appropriate mathematical models is essential for the understanding of system stability.

This chapter deals with the development of advanced mathematical models of each component of a typical Hydraulic Power Generating System equipped with Francis turbines for their representation in power system dynamic studies.

The stability analysis of different models for synchronous machines and turbine governing system are beyond of the scope of the Master's Thesis work. The enhancement of the hydraulic power generating system is studied by means of analysis of the dynamic behaviour of different models of the hydraulic machine and water conduit system.

Appropriate models of the hydraulic turbine and water conduit system are implemented in various degrees of detail. Firstly, nonlinear models for a simple turbine without surge tank considering the inelastic and elastic travelling wave effects have been developed. After that, nonlinear models considering the inelastic and elastic travelling wave effects for a turbine with surge tank for Hydropower Systems with long length penstocks are implemented. Finally, the nonlinear models for a turbine with long length penstocks are linearized at an operating point are developed considering the nonlinear turbine characteristics and the travelling wave effects.

6.1 Hydropower Plant Models

A hydroelectric development includes in some form a water-diverting structure, conduit to carry the water to the turbines and governors, generators, control and switching apparatus, housing for the equipment, transformers, and electrical network. Depending upon the requirement of the hydroelectric plants, a surge tank can be placed at upstream and/or downstream side of the powerhouse.

A hydroelectric power plant may be considered as a system consisting of several subsystems: the penstock including any surge chamber, the hydraulic machine, the speed governor, the tailrace and, finally, the generator and electrical network. The diagram of Figure 6-1 depicts the functional blocks for the elements of a Hydraulic Turbine Generating System.

The turbine governing system is modelled by a mechanical-hydraulic turbine governing model and it is detailed in Chapter 5. The subsystem of the governor control considers the turbine speed dead zone, valve saturation, and limitation. The block diagram of a typical hydro turbine governing system used for the stability analysis is depicted in Figure 5-3. The transfer function of a mechanical-hydraulic governor is given by Equation (5.6).

For stability and control studies, the synchronous generator is modelled by a detailed model with damping, which consists of one field winding, one damper winding in d-axis and one damper winding in q-axis with saturation included. The modelling of the synchronous machine is detailed in Chapter 4.

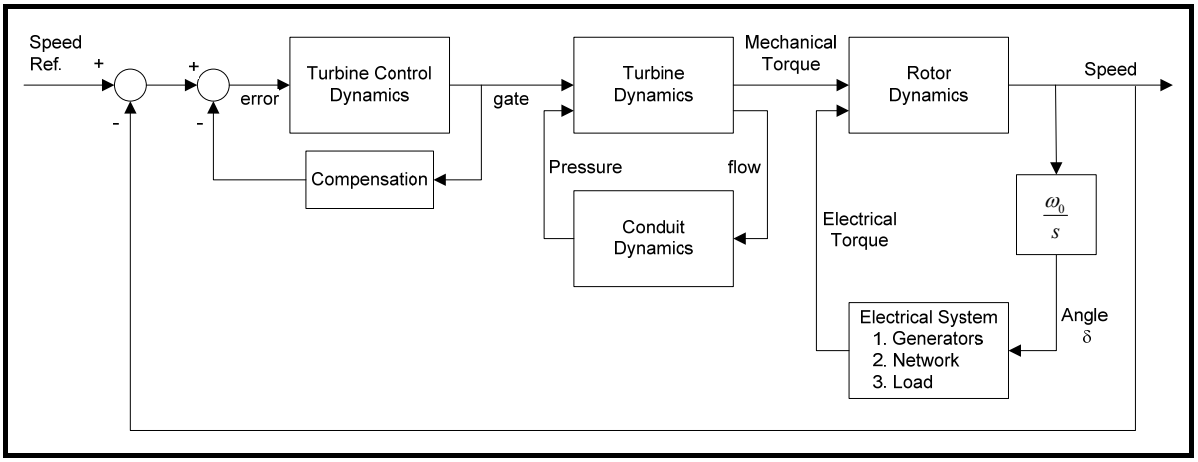

Figure 6-1: Functional Block Diagram of the Hydraulic Turbine Generating System

The most common classification of the hydraulic power plant models consists in linear and nonlinear models. This classification is based on the complexity of the equations involved in the models. The accurate mathematical models of the hydraulic components of a hydro power plant include the dynamic representation of penstock, surge tank, upstream and/or downstream tunnel and the hydraulic losses of all these elements. [1, 6, 11, 18, 24, 28-29, 31-32, 36-37, 42, 46, 48, 50, 54-64]

The hydraulic power generating system for the stability analysis has been designed with a third-order synchronous generator model, a mechanical-hydraulic governing system model, and a hydraulic turbine.

The hydraulic turbine is modelled with varying degrees of detail. The mathematical models of the hydraulic turbine developed for the stability analysis of a Hydraulic Power Generating System are

- Simplified Nonlinear Turbine Model
- Nonlinear Turbine Model without Surge Tank assuming Inelastic Water Column
- Nonlinear Turbine Model without Surge Tank including Elastic Water Column Effect
- Nonlinear Turbine Model with Surge Tank assuming Inelastic Water Columns in Penstock and Tunnel
- Nonlinear Turbine Model with Surge Tank assuming Elastic Water Column in Penstock and Inelastic Water Column in Tunnel
- Linear Turbine Model with Surge Tank considering Inelastic Water Columns in Penstock and Tunnel and, turbine characteristics
- Linear Turbine Model with Surge Tank including Elastic Water Column in Penstock and turbine characteristics

6.2 Nonlinear Turbine Models

Nonlinear turbine models are required when speed and power changes are large during an islanding, load rejection and system restoration conditions. Hydrodynamics and mechanic-electric dynamics are involved in nonlinear systems. It is important in a system with long penstock.

The nonlinear models of the hydraulic turbine developed and studied are

- Simplified Nonlinear Turbine Model
- Nonlinear Turbine Model without Surge Tank assuming Inelastic Water Column
- Nonlinear Turbine Model without Surge Tank including Elastic Water Column Effect
- Nonlinear Turbine Model with Surge Tank assuming Inelastic Water Columns in Penstock and Tunnel
- Nonlinear Turbine Model with Surge Tank assuming Elastic Water Column in Penstock and Inelastic Water Column in Tunnel

6.2.1 Simplified Nonlinear Turbine Model

The *Simplified Nonlinear Turbine Model* is based upon a simple hydraulic turbine with a short length penstock, unrestricted head and tailrace, and without surge tank. The penstock is modelled assuming an inelastic conduit and incompressible fluid. Neglecting friction losses in the penstock, the transfer function of flow rate and water pressure of a simple Penstock system is described by Equation (2.61).

In the modelling of the turbine itself, both its hydraulic characteristics and mechanical output power must be modelled. The nonlinear characteristics of hydraulic turbine are neglected in this model. The hydraulic turbine model is described by Equations (3.12) and (3.14).

The block diagram representing the dynamic characteristics of a simplified nonlinear turbine model is shown in Figure 6-2. Equating (2.61), (3.12) and (3.14) gives the transfer function for a simplified nonlinear turbine model. The input and output signal of the transfer function are the per unit deviations in gate opening position and turbine output torque, respectively.

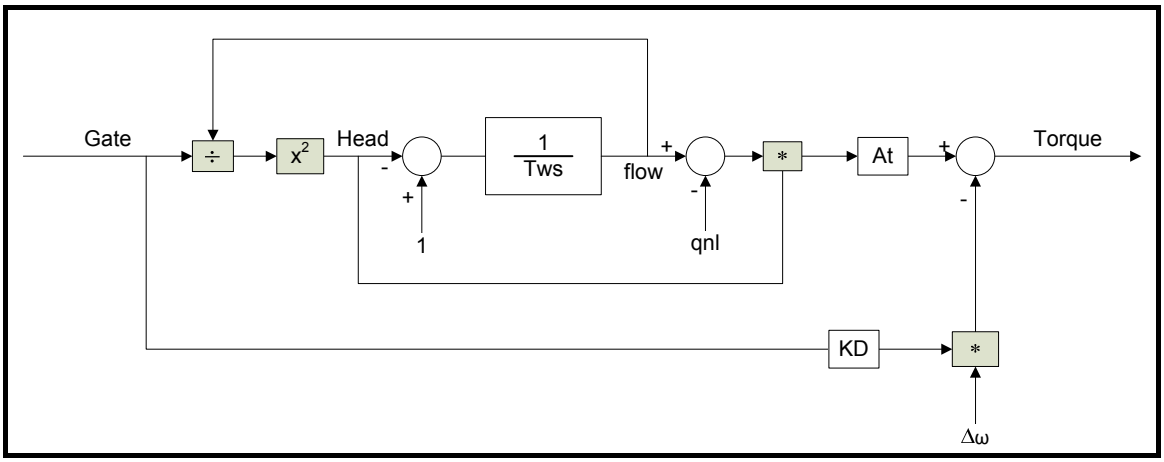

Figure 6-2: Simplified Nonlinear Turbine Model

6.2.2 Nonlinear Model without Surge Tank assuming Inelastic Water Column

The *Nonlinear Model without Surge Tank assuming Inelastic Water Column* is based upon the Simplified Nonlinear Turbine Model, described in Chapter 6.2.1. The penstock is modelled assuming an inelastic conduit and incompressible fluid where the travelling pressure wave effects are relatively insignificant.

The head losses h_f are proportional to flow squared and depends on the conduit dimensions and friction coefficient f_p. It suffices in this model assume that the head losses are proportional to flow squared and the head loss coefficient. The transfer function relating the flow rate and water pressure of a simple Penstock system is described by Equation (2.60).

In the modelling of the turbine itself, both its hydraulic characteristics and mechanical output power must be modelled. The hydraulic turbine model is described by Equations (3.12) and (3.14). Figure 6-3 shows the block diagram of a Nonlinear Model without Surge Tank assuming Inelastic Water Column.

Equating (2.60), (3.12) and (3.14) gives the transfer function for a nonlinear model without surge tank assuming inelastic water column. The input and output signal of the transfer function are the per unit deviations in gate opening position and turbine output torque, respectively. This model is depicted in Figure 2 in the report *"Hydraulic Turbine and Turbine Control Models for System Dynamic Studies"*. [1]

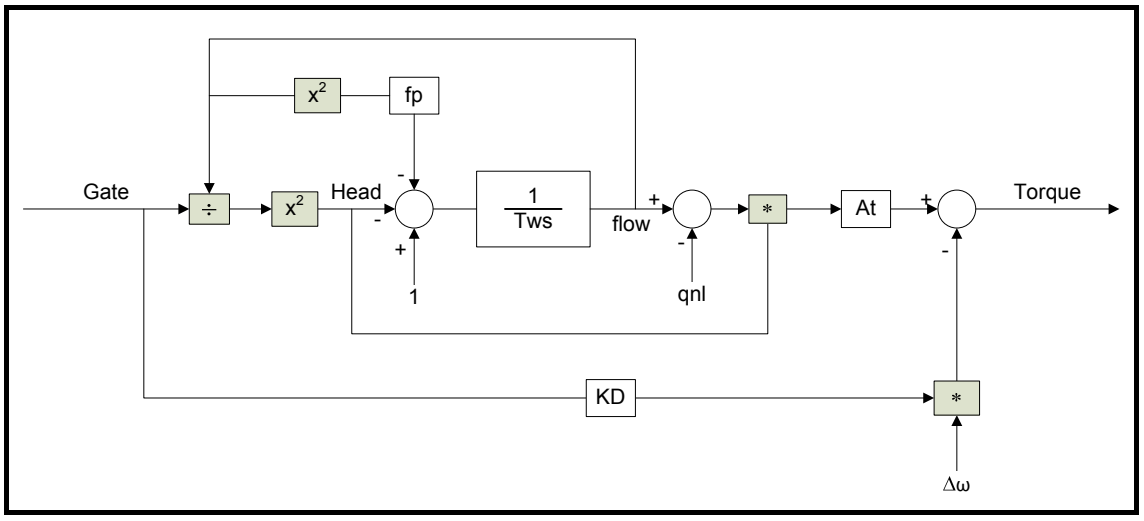

Figure 6-3: Nonlinear Model without Surge Tank assuming Inelastic Water Column

6.2.3 Nonlinear Model without surge tank including Elastic Water Column Effect

The modelling of inelastic water column effect is adequate only in short or medium length penstocks. The travelling wave effects and the travel time of the pressure are considered in hydropower plant models with long penstocks. Penstock is modelled taking into account the elastic water hammer theory and neglecting the hydraulic friction losses.

The classical wave solution taking into account the elastic water hammer theory is described in Equation (2.59). The water hammer occurrence in penstock in mathematical terminology is represented by a delay e^{-s2T_e} in the hydraulic structure.

The mechanical power output and hydraulic characteristics of a turbine are described by Equations (3.12) and (3.14), respectively. The block diagram of the Nonlinear Model without Surge Tank including Elastic Water Column Effect is shown in Figure 6-4.

Equating (2.59), (3.12) and (3.14), the transfer function for a Nonlinear Model without Surge Tank including Elastic Water Column Effect relating the turbine output torque to the deviations in gate position is gotten. This model is depicted in Figure 4 in the report *"Hydraulic Turbine and Turbine Control Models for System Dynamic Studies"*. [1]

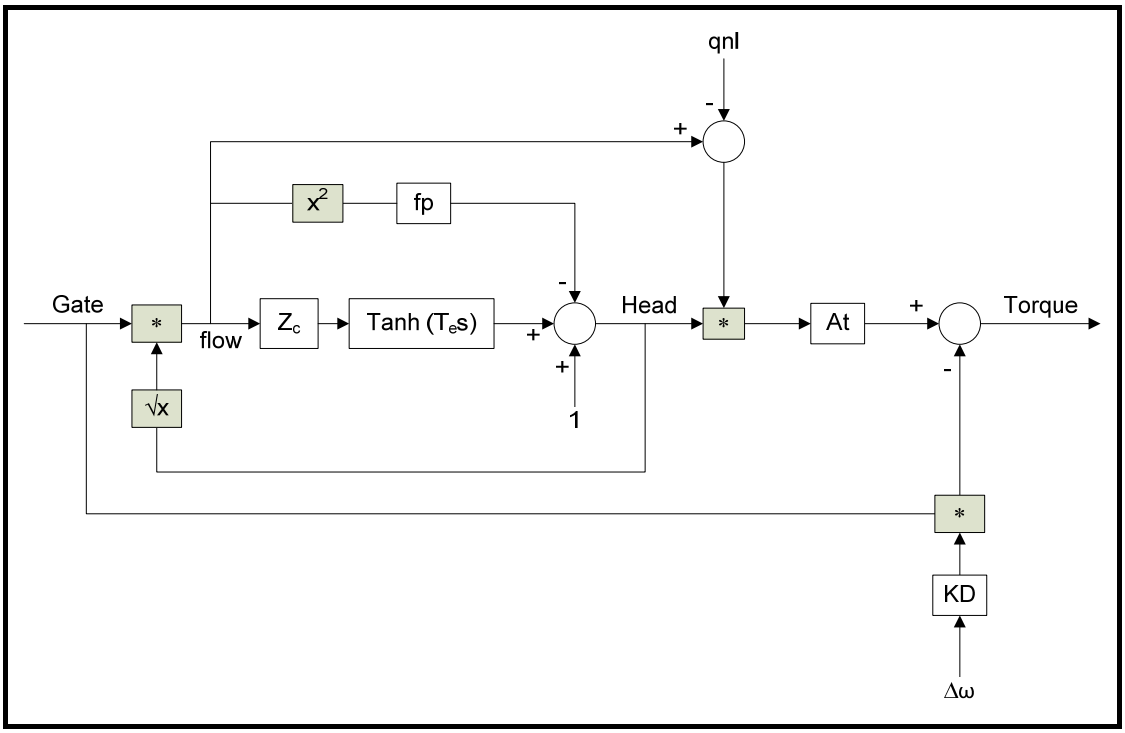

Figure 6-4: Nonlinear Model without surge tank including Elastic Water Column Effect

6.2.4 Nonlinear Model with Surge Tank assuming Inelastic Water Columns

Hydro power plants with long conduits use surge tank to provide some hydraulic isolation of the turbine from the head deviations generated by transients in the conduit. The Nonlinear Model with Surge Tank assuming Inelastic Water Columns is based upon a simple turbine with an upstream water tunnel, a surge tank and a long length penstock.

The block diagram of the Nonlinear Model with Surge Tank assuming Inelastic Water Columns is shown in Figure 6-5. The upstream water tunnel and penstock are modelled assuming an incompressible fluid and a rigid conduit where the travelling pressure wave effects are relatively insignificantly. It suffices in this model assume that the upstream water tunnel and penstock head losses are proportional to flow squared through loss coefficients f_{p1} and f_{p2}, respectively. The transfer function relating the flow rate and water pressure of a simple Penstock system is described by Equation (2.60).

The mechanical power output and hydraulic characteristics of a turbine are described by Equations (3.12) and (3.14), respectively. The nonlinear characteristics of hydraulic turbine are considered in this model.

The hydraulic model of the surge tank includes an orifice that dissipates the energy of hydraulic oscillations and produces damping. Head losses in the orifice of the surge tank are proportional to loss coefficients f_0 times flow rate times absolute value of flow rate to maintain the direction of head loss. The transfer function of flow rate and water pressure of the surge tank is described by Equation (2.69).

Equating (2.60), (2.69), (3.12) and (3.14) gives the transfer function for a Nonlinear Model with Surge Tank assuming Inelastic Water Columns. The input and output signal of the transfer function are the per unit deviations in gate opening position and turbine torque, respectively. This model is depicted in Figure 5 in the report *"Hydraulic Turbine and Turbine Control Models for System Dynamic Studies"*. [1]

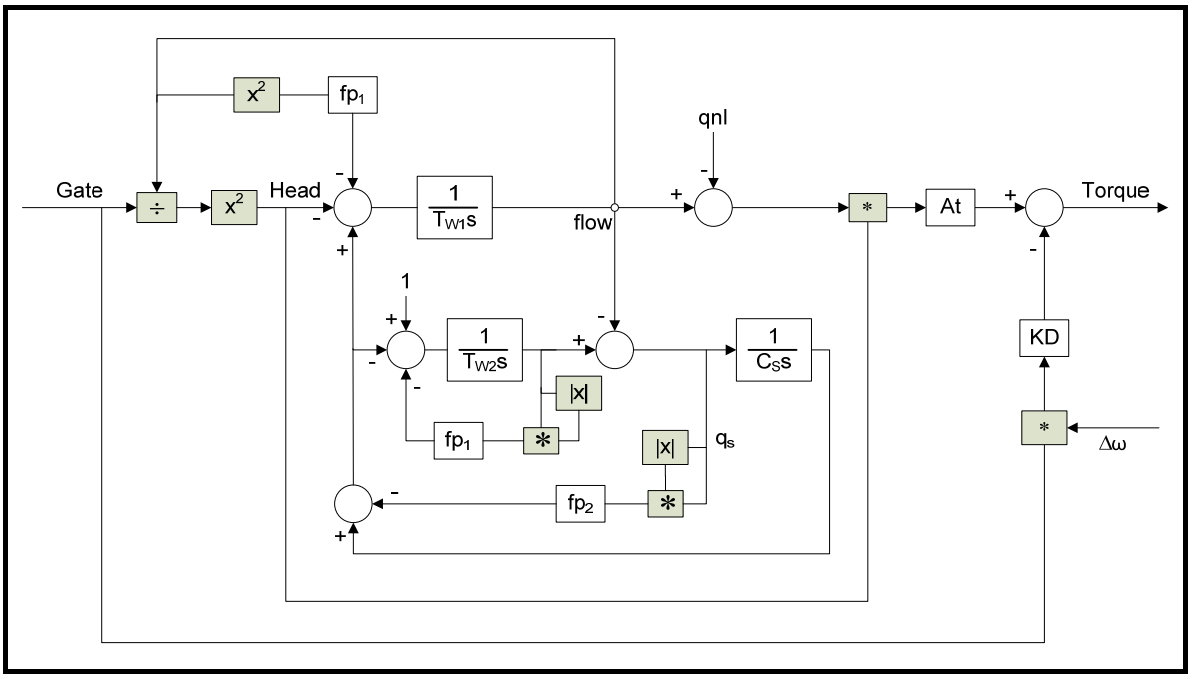

Figure 6-5: Nonlinear Model with Surge Tank assuming Inelastic Water Columns

6.2.5 Nonlinear Model with Surge Tank assuming Elastic Water Column in Penstock and Inelastic Water Column in Upstream Tunnel

The *Nonlinear Model with Surge Tank assuming Elastic Water Column in Penstock and Inelastic Water Column in Upstream Tunnel* is based upon a Nonlinear Model with Surge Tank assuming Inelastic Water Columns in cases where the travelling wave effects in the penstock are essential. The block diagram of Figure 6-5 is modified to a block diagram that represents the dynamic characteristic of a simple turbine with an upstream inelastic tunnel, a surge tank and a long length elastic penstock. Figure 6-6 shows the block diagram of a nonlinear model with surge tank including elastic water column in penstock and inelastic water column in upstream tunnel.

The dynamic effects of the upper tunnel contribute with low frequency oscillations, in the order of 0.10 Hz. The dynamic behaviour of the penstock contributes with high frequency oscillation due to the penstock is subject to abrupt gate or flow changes.

The hydraulic model of the surge tank includes an orifice, which dissipates the energy of hydraulic oscillations and produces damping. Head losses in the orifice of the surge tank are proportional to loss coefficients f_0 times flow rate times absolute value of flow rate to maintain the direction of head loss.

The transfer function of flow deviation and water pressure deviation of the upstream water tunnel is described by Equation (2.60). The transfer function of the penstock taking into account the elastic water hammer theory is described in Equation (2.59). The transfer function of flow rate and water pressure of the surge tank is described by Equation (2.69). The mechanical power output and hydraulic characteristics of a turbine are described by Equations (3.12) and (3.14), respectively. The nonlinear characteristics of hydraulic turbine are not considered in this model.

Equating (2.59), (2.60), (2.69), (3.12) and (3.14) gives the transfer function for a Nonlinear Model with Surge Tank assuming Elastic Water Column in Penstock and Inelastic Water Column in Upstream Tunnel. The input and output signal of the transfer function are the per unit deviations in gate opening position and turbine torque, respectively. This model is depicted in Figure 6 in the report *"Hydraulic Turbine and Turbine Control Models for System Dynamic Studies"*. [1]

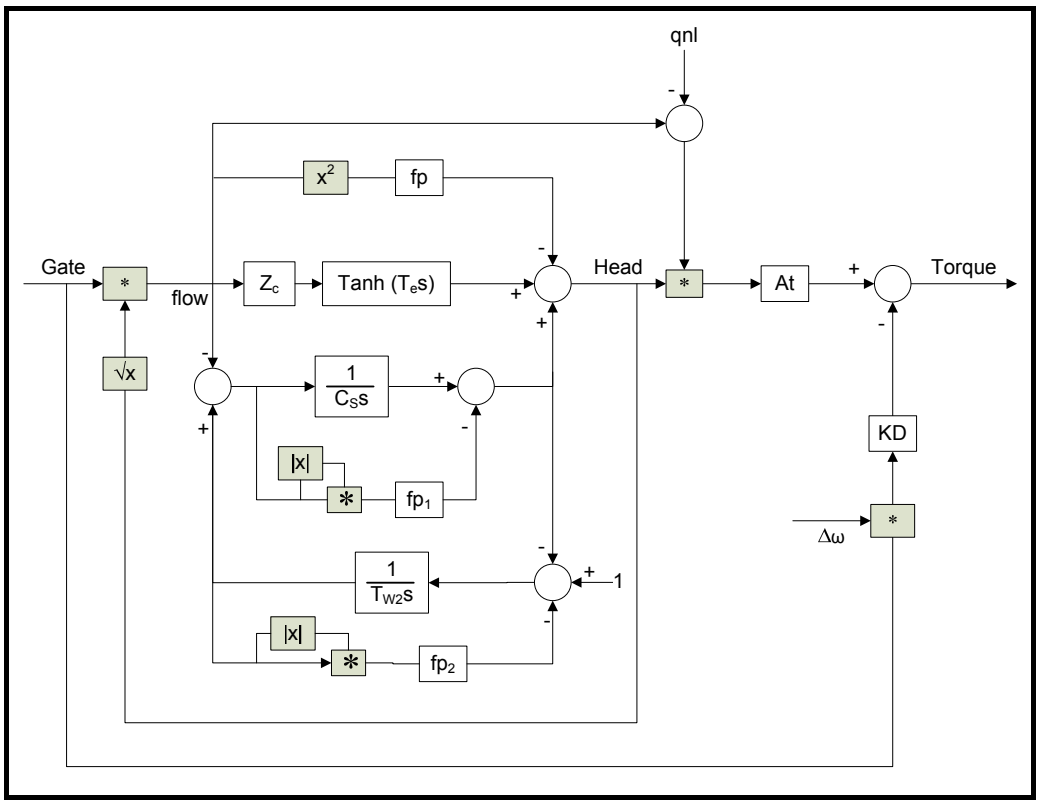

Figure 6-6: Nonlinear Model with surge tank assuming elastic water column in penstock and inelastic water column in upstream tunnel

6.3 Hydro Turbine Linear Models

The nonlinear characteristics of the hydro power plant models can be approximated by linear models. Linear equations or lower step transfer function are used for studies of control system stability limited to small perturbations around a stable operating point. The dynamics of the analyzed system with respect to the operating point can be observed by changing operating point. The nonlinear turbine characteristics and the travelling wave effects are considered in these models. [15, 18, 33]

The linear models of the hydraulic turbine, including the nonlinear turbine characteristics extracted from the Hill Charts, developed and studied are

- Linear Turbine Model with Surge Tank considering Inelastic Water Columns in Penstock and Tunnel and, turbine characteristics
- Linear Turbine Model with Surge Tank including Elastic Water Column in Penstock and turbine characteristics

These linear models of the hydraulic turbine consider its characteristic curves and coefficients that must be extracted and calculated from the Hill Charts of the test model.

6.3.1 Linear Turbine Model with Surge Tank assuming Inelastic Water Columns

The *Linear Model with Surge Tank assuming Inelastic Water Columns* is based upon a simple turbine with an upstream tunnel, a surge tank and a penstock. The upstream tunnel and penstock are modelled assuming an inelastic conduit and incompressible fluid where the travelling pressure wave effects are relatively insignificant. The nonlinear characteristics of hydraulic turbine and the inelastic water hammer effect are considered in this model. This model is based on the paper *"Basic Modelling and Simulation Tool for Analysis of Hydraulic Transients in Hydroelectric Power Plants".* [18]

The transfer function of flow deviation and water pressure deviation of the outlet of the upstream water tunnel is described by Equation (2.60). The transfer function relating incremental water pressure and flow of penstock can be written as

$$\left(T_{W2}s + H_{f2}\right)q_2 = -\left(h_2 - h_1\right) \tag{6.1}$$

where the suffix 1 is related to the upstream tunnel and the suffix 2 corresponds to Penstock.

The transfer function of flow rate and water pressure of the surge tank is described by Equation (2.69) where the hydraulic losses in the orifice are neglected.

The mathematical model of the Francis turbine is represented by Equations (3.15) and (3.16) for small variations in the vicinity of an operating point. The six partial derivatives, which represent the nonlinear characteristic of the turbine, are taken from model tests. Prototype turbine characteristics are plotted in the ***Hill Charts***. The turbine efficiency for any operating point given by runner speed, pressure head and gate position can be extracted from the Hill Charts.

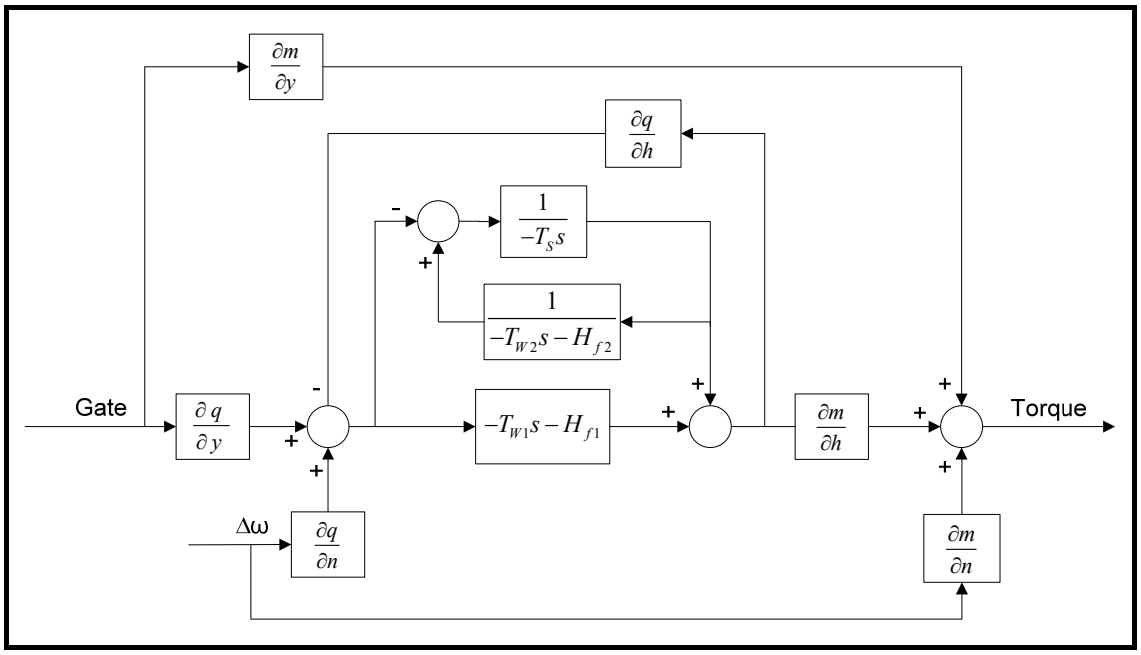

Figure 6-7: Linear Model with Surge Tank assuming Inelastic Water Columns

Equating (2.60), (2.69), (3.15), (3.16) and (6.1) gives the transfer function relating the per unit deviations turbine torque to gate position for a Linear Model with Surge Tank assuming Inelastic Water Columns. Figure 6-7 shows the block diagram of a Linear Model with Surge Tank assuming Inelastic Water Columns.

6.3.2 Linear Turbine Model with Surge Tank assuming Elastic Water Column in Penstock

The *Linear Model with Surge Tank assuming Elastic Water Column in Penstock* is based upon a simple turbine with an upstream tunnel, a surge tank and a penstock. The upstream tunnel is modelled assuming an inelastic conduit and incompressible fluid where the travelling pressure wave effects are relatively insignificant. Penstock is modelled taking into account the elastic water hammer theory and neglecting the hydraulic friction losses. The nonlinear characteristics of hydraulic turbine are considered in this model. This model is based on the paper *"Basic Modelling and Simulation Tool for Analysis of Hydraulic Transients in Hydroelectric Power Plants".* [18]

The block diagram of Figure 6-7 is modified to a block diagram that represents the dynamic characteristic of a simple turbine with an inelastic upstream tunnel, a surge tank and an elastic penstock. Figure 6-8 shows the block diagram of a Linear Model with Surge Tank assuming Elastic Water Column in Penstock.

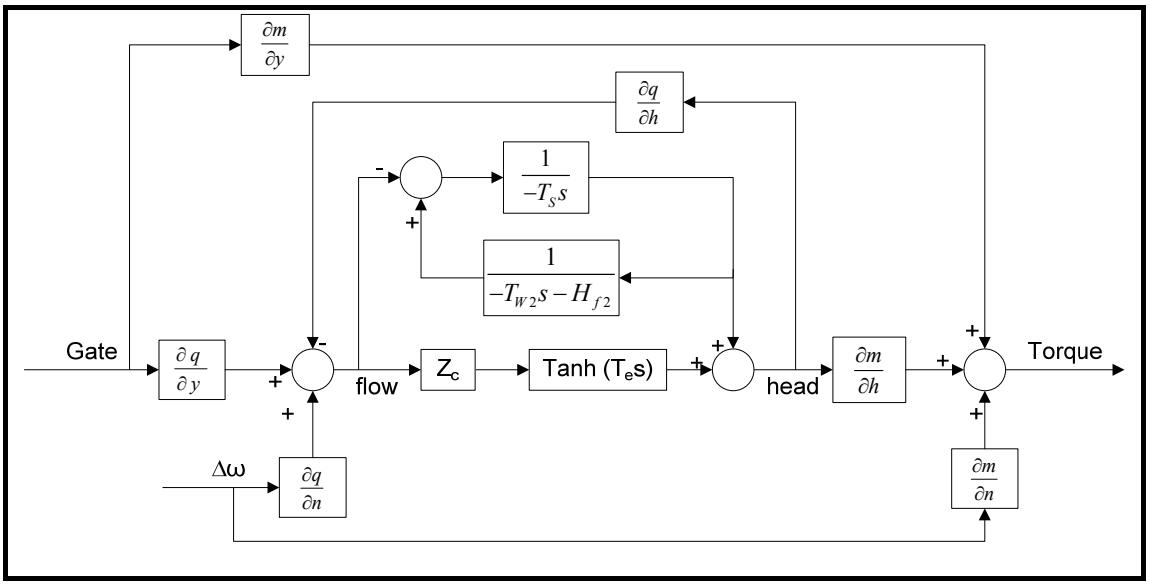

Figure 6-8: Linear Model with Surge Tank assuming Elastic Water Column in Penstock

The transfer function of flow deviation and water pressure deviation of the outlet of the upstream water tunnel is described by Equation (2.60). The transfer function relating incremental water pressure and flow of penstock can be written as

$$\left(\frac{T_{W2}}{T_e}\tanh\left(sT_e\right)\right)q_2 = -\left(h_2 - h_1\right) \tag{6.2}$$

Where the suffix 1 is related to the upstream tunnel and the suffix 2 corresponds to Penstock.

The transfer function of flow rate and water pressure of the surge tank is described by Equation (2.69) where the hydraulic losses in the orifice are neglected.

The mathematical model of the Francis turbine is represented by Equations (3.15) and (3.16) for small variations in the vicinity of an operating point. The six partial derivatives which represent the nonlinear characteristic of the turbine are taken from model tests. Prototype turbine characteristics are plotted in the ***Hill Charts***. The turbine efficiency for any operating point given by runner speed, pressure head and gate position can be extracted from the Hill Charts.

Equating (2.60), (2.69), (3.15), (3.16) and (6.2) gives the transfer function relating the per unit deviations turbine torque to gate position for a Linear Model with Surge Tank assuming Elastic Water Column in Penstock.

7 Hydroelectric Power Plant Modelling by Structure Matrix Method

This chapter shows an alternative method of Hydroelectric Power Plant modelling for stability studies. The Hydroelectric power plant is modelled by the Structure Matrix Method. Hermod Brekke introduced this mathematical method. This improved model covers a wide range of parameters such as influence of the turbine characteristics, frictional damping of oscillatory flow in elastic conduits, influence of the generator load and the analysis of the turbine governing system.

The Hydroelectric Power Plant mathematical model may consist of many different elements. The representation of each component of the Hydro Power System is presented by means of appropriate block diagrams. The Structure Matrix Method uses the Laplace transformed equations for the system stability study. The turbine characteristics are linearized at an operating point. The stability study of a dynamic system is based in the frequency response analysis and free vibration analysis. This method is only presented for illustration purposes.

7.1 Definition of the Method

The Structure Matrix Method was introduced by Hermod Brekke for the governing stability analysis and the study of frictional damping of oscillatory flow in complex conduits. The combination of isolated operation, long transmission lines, and long and complex tunnel systems require a thorough stability analysis of the speed control of the units in the systems. The origin of the Structure Matrix Method may be traced to the Structure Analysis theory and terminologies such as “Element”, "Node" as well as "Local" and "Global" matrices have been used. *Element Matrix* representations of each of the elements for the modelling of the overall system are used as ***“bricks”*** to construct the *Global Structure Matrix*. [6, 16, 30]

An Element Matrix representation has the following general form

$$\mathbf{A}(\mathbf{s})\mathbf{b} = \mathbf{c} \tag{7.1}$$

The dimension of the *Element Matrix* ***A(s)*** is mxn. The vector ***b***, dimension nx1, is often referred to as the “pressure vector”. The vector ***c*** of dimension mx1 is referred to as “flow vector”. The *Element Matrix* is the lowest level of the Structure Matrix.

A matrix representation of the group of elements interconnected may be established by incorporating all the Element Matrices together. The *Global Structure Matrix*, which is normally regular, can be solved if the number of known components in the vector ***b*** is equal to the number of unknown components in the vector ***c***.

7.2 Matrix representations of the Basic Elements in Hydro Power Systems

The Structure Matrix method is based on the same functional equations that Transfer Method and Impedance Method. The essential part of the Structure Matrix Method is to establish the Element Structure Matrices of each component. The Hydro Power Plant mathematical model may consist of many different elements such as tunnels, surge tanks, throttles, junctions, pumps, turbine sets and so on. The representation of each component of the Hydro Power System is presented by means of appropriate block diagrams.

7.2.1 Pipes and Tunnels

The pipe or tunnel is one of the most important elements of the hydropower plant modelling. The dynamic behaviour of the elastic fluid in a closed-conduit is described in Chapter 2.2. The Element Matrix representation for a pipe based on the transfer function detailed in Equation (2.56) is

$$\begin{bmatrix} -\dfrac{1}{Z_c \tanh(zT_e)} & \dfrac{1}{Z_c \sinh(zT_e)} \\ \dfrac{1}{Z_c \sinh(zT_e)} & -\dfrac{1}{Z_c \tanh(zT_e)} \end{bmatrix} \begin{bmatrix} h_i(s) \\ h_{i+1}(s) \end{bmatrix} = \begin{bmatrix} q_i(s) \\ q_{i+1}(s) \end{bmatrix} \tag{7.2}$$

Using the following expressions:

$$T = \frac{1}{Z_c \tanh(zT_e)} \tag{7.3}$$

$$S = \frac{1}{Z_c \sinh(zT_e)} \tag{7.4}$$

The general pipe matrix, Equation (7.2) yields

$$\begin{bmatrix} -T & S \\ S & -T \end{bmatrix} \begin{bmatrix} h_i(s) \\ h_{i+1}(s) \end{bmatrix} = \begin{bmatrix} q_i(s) \\ q_{i+1}(s) \end{bmatrix} \tag{7.5}$$

7.2.2 Surge tanks or air accumulators

The Element Matrix expression for surge tank or air accumulator may be written as either a one-terminal element or a virtual two-terminal element. The Element matrix for a surge tank written as one-terminal element is

$$\left[-\frac{H_0 A_s}{Q_0} s \right] \left[h_i(s) \right] = \left[q_i(s) \right] \tag{7.6}$$

The Element matrix expression for a surge tank written as a virtual two-terminal element, considering $h_{i+1} = q_{i+1} = 0$, is

$$\begin{bmatrix} 1 & 0 \\ 0 & -\dfrac{H_0 A_s}{Q_0} s \end{bmatrix} \begin{bmatrix} h_{i+1}(s) \\ h_i(s) \end{bmatrix} = \begin{bmatrix} q_{i+1}(s) \\ q_i(s) \end{bmatrix} \tag{7.7}$$

For a free water surface of an open surge tank, the most convenient representation for a surge tank is a two-terminal Element by incorporating Equations (7.6) and (7.7) together.

$$\begin{bmatrix} -T - T_F & S \\ S & -T \end{bmatrix} \begin{bmatrix} h_i(s) \\ h_{i+1}(s) \end{bmatrix} = \begin{bmatrix} 0 \\ q_{i+1}(s) \end{bmatrix} \tag{7.8}$$

where

$$T_F = \frac{H_0 A_s}{Q_0} s \tag{7.9}$$

7.2.3 Local Losses

The Element Matrix describing the damping caused by local variations in cross sections of the conduit or for fixed partial open valves may be established as follows

$$\begin{bmatrix} -\dfrac{1}{K_{re}} & \dfrac{1}{K_{re}} \\ \dfrac{1}{K_{re}} & -\dfrac{1}{K_{re}} \end{bmatrix} \begin{bmatrix} h_i(s) \\ h_{i+1}(s) \end{bmatrix} = \begin{bmatrix} q_i(s) \\ q_{i+1}(s) \end{bmatrix} \tag{7.10}$$

For throttles, K_{re} is given by

$$K_{re} = \frac{Q_t Q_0}{g H_0} \xi \left(\frac{1}{A_s^2} - \frac{1}{A_b^2} \right) \tag{7.11}$$

In Equation (7.11), A_s is the smallest cross section and A_b is the largest cross section. A loss constant ξ is included.

For T joints, K_{re} is given by

$$K_{re} = \frac{k Q_0^2}{3 g A_s^2 H_0} q + \frac{Q_t Q_0}{g A_b^2 H_0} \tag{7.12}$$

In Equation (7.12), k is the geometry constant.

7.2.4 Hydro Turbine

The analysis of the stability is valid for frequencies domains normally up to about 6 rad/sec, and resonance frequencies in the turbine runner and guide vane system can be neglected. In this frequency range, the influence from the turbine may be evaluated from the turbine characteristic diagram, which is assumed valid for small oscillations with low frequencies around a steady state value. A linearization around the steady state may also be carried out within acceptable accuracy.

7.2.4.1 Hydro Turbine Characteristics

The **mechanical power** developed by the turbine is given by differentiating Equation (3.1)

$$dP = \frac{\partial P}{\partial Q} dQ + \frac{\partial P}{\partial H} dH + \frac{\partial P}{\partial \eta} d\eta \tag{7.13}$$

Dividing through by $P_0 = \rho g H_0 \eta_0 Q_0$, Equation (7.13) yields

$$\Delta p = \Delta q + \Delta h + \Delta \eta \tag{7.14}$$

The values of Δq, Δh and $\Delta \eta$ may be found by studying the characteristic diagram of the turbine.

The **flow** through a Francis turbine depends upon the net head, rotational speed of the turbine and wicket-gate opening position. The equation of the flow yields

$$\Delta q = Q_y \Delta y + Q_n \Delta n - \frac{1}{2}\left(1 - Q_n\right) \Delta h + Q_\phi \Delta \phi \tag{7.15}$$

The values Q_n, Q_y and Q_ϕ may be determined by means of the turbine characteristic diagram. The expressions for Q_n, Q_y and Q_ϕ are

$$Q_n = \left.\frac{\partial Q_{11}}{\partial n_{11}}\right|_0 \frac{\left(n_{11}\right)_0}{\left(Q_{11}\right)_0} \tag{7.16}$$

$$Q_y = \left.\frac{\partial Q_{11}}{\partial Y}\right|_0 \frac{Y_0}{\left(Q_{11}\right)_0} \tag{7.17}$$

$$Q_\phi = \left.\frac{\partial Q_{11}}{\partial \phi}\right|_0 \frac{\phi_0}{\left(Q_{11}\right)_0} \tag{7.18}$$

The **efficiency** is defined as the ratio of power supplied by the turbine to the absorbed power. The relative efficiency can be expressed as follows

$$\Delta \eta = E_q \Delta q - \frac{1}{2}\left(E_q - E_n\right) \Delta h + E_n \Delta n + E_\phi \Delta \phi \tag{7.19}$$

The values E_n, E_y and E_ϕ may be determined by means of the turbine characteristic diagram. The expressions for E_n, E_y and E_ϕ are

$$E_q = \left.\frac{\partial \eta}{\partial Q_{11}}\right|_0 \frac{Q_0}{\eta_0} \tag{7.20}$$

$$E_n = \left.\frac{\partial \eta}{\partial n_{11}}\right|_0 \frac{(n_{11})_0}{\eta_0} \tag{7.21}$$

$$E_\phi = \left.\frac{\partial \eta}{\partial \phi}\right|_0 \frac{\phi_0}{\eta_0} \tag{7.22}$$

The **runner blade** servomotor has a time constant T_L that describes the runner blades movement as a function of the guide vane movement. The transfer function describing the **runner blades movement** is

$$F_\phi = \frac{K_L}{1+T_L s} \tag{7.23}$$

The runner blades normally are stopped mechanically before the guide vanes are fully closed. The cam transmission constant K_L must take into account only about 75% of the guide vane stroke regarded versus the runner blade stroke.

For turbines with fixed runner blades, such as Francis turbines, the runner blade movement is zero, ϕ=0.

7.2.4.2 Hydro Turbine Matrix Representation

Consider the flow positive out of the turbine on both sides and rising pressure to be positive in the same way as for pipe elements. The pressure Δh in Equations (7.15) and (7.19) is regarded to pressure difference between the right hand side and the left hand side. The equations of continuity for flow through the turbine, head upstream and downstream of the turbine is given by

$$\Delta q = \Delta q_i \tag{7.24}$$

$$\Delta q_{i+1} + \Delta q_i = 0 \tag{7.25}$$

$$\Delta h = \Delta h_{i+1} - \Delta h_i \tag{7.26}$$

Substituting η and h from Equations (7.19) and (7.26) into Equation (7.14), yields

$$\left(1+E_q\right)\Delta q + \left(1-\frac{1}{2}\left(E_q+E_n\right)\right)\left(\Delta h_{i+1} - \Delta h_i\right) + E_n \Delta n + E_\phi \Delta\phi - \Delta p = 0 \tag{7.27}$$

Further by substituting ϕ, q and h by Equations (7.23) and (7.26) into Equation (7.15), yields

$$\left(1-\frac{1}{2}\left(E_q+E_n\right)\right)\left(\Delta h_{i+1}-\Delta h_i\right)+E_n\Delta n+E_\phi F_\phi\Delta y-\Delta p-\left(1+E_q\right)\Delta q_{i+1}=0 \tag{7.28}$$

Substituting ϕ and q h by Equations (7.23), (7.24), (7.25) and (7.26) into Equation (7.27), yields

$$\frac{1}{2}\left(1-Q_n\right)\Delta h_{i+1}+Q_n\Delta n+\left(Q_y-Q_\phi F_\phi\right)\Delta y-\frac{1}{2}\left(1-Q_n\right)\Delta h_i=\Delta q_{i+1} \tag{7.29}$$

$$\frac{1}{2}\left(1-Q_n\right)\Delta h_{i+1}+Q_n\Delta n+\left(Q_y-Q_\phi F_\phi\right)\Delta y-\frac{1}{2}\left(1-Q_n\right)\Delta h_i=-\Delta q_i \tag{7.30}$$

The complete turbine matrix may be established by means of Equations (7.28), (7.29) and (7.30)

$$\begin{bmatrix} -B & -C & B & -Q & 0 \\ J & L & -J & K & M \\ B & C & -B & Q & 0 \end{bmatrix}\begin{bmatrix} h_{i+1} \\ y \\ h_i \\ n \\ p \end{bmatrix}=\begin{bmatrix} q_{i+1} \\ 0 \\ q_i \end{bmatrix} \tag{7.31}$$

The turbine matrix will be established with vectors describing all inputs and variables which have to be solved; where

$$B=\frac{1}{2}\left(1-Q_n\right) \tag{7.32}$$

$$C=Q_y+Q_\phi F_\phi \tag{7.33}$$

$$Q=Q_n \tag{7.34}$$

$$J=\frac{3-E_n-\left(1+E_q\right)Q_n}{2\left(1+E_q\right)} \tag{7.35}$$

$$K=Q_n+\frac{E_n}{1+E_q} \tag{7.36}$$

$$L=Q_y+Q_\phi F_\phi+\frac{E_\phi F_\phi}{1+E_q} \tag{7.37}$$

$$M=-\frac{1}{1+E_q} \tag{7.38}$$

7.2.5 The synchronous generator and the electric grid

As a first approach, the synchronous generator model for a generator-infinite bus system may be simplified. The simplified generator model only includes the analysis of the hydraulic system with the influence of the frictional damping and the turbine characteristics. The synchronous generator model for a generator-infinite bus system may be simplified by assuming:

- The electric load is pure resistive and there is no rotating mass (except the generator itself) in the system,
- The transients of the electric system are much faster than those of hydraulic-mechanic system, and therefore may be ignored.

The simplified equation of the generator taking account of load characteristic may be simplified by the following simple function

$$p - p_g = \left(T_a s + F_g\right) n \tag{7.39}$$

The transfer function F_g is the adjusting load coefficient which describes an isolated load condition or a grid system. Ta is inertia mass time constant of the generator (mechanical inertia constant).

For a frequency response analysis for ω<2 rad/sec, the transfer function, described in Equation (7.39) may be simplified to be $F_g = e_b$, where e_b is the permanent load droop (voltage droop) or self-regulating in the load as a function of the speed droop of the generator. The worst scenario is a resistive load $F_g = 0$.

The simplified Element Matrix yields:

$$\begin{bmatrix} 0 & 0 \\ N & 1 \end{bmatrix} \begin{bmatrix} n \\ p(s) \end{bmatrix} = \begin{bmatrix} 0 \\ p_g(s) \end{bmatrix} \tag{7.40}$$

where

$$N = -\left(T_a s + F_g\right) \tag{7.41}$$

For studies of the interaction of hydraulic system and power systems, it is possible to establish a complete sub matrix for the electric grid including the torque-angle oscillations of the synchronous machine. This matrix may be included in the global matrix of the system.

7.2.6 Turbine Speed Governor

Despite of the large variety of turbine governors, there is no great difference on the general mathematical representation for them. The most common used governors may be divided into two types:

- Mechanical dashpot governor (PI type)
- Electric-Hydraulic PID governor

7.2.6.1 Traditional Governor

The traditional governor is described with the following equations

$$F_n n - R_P p_r + \frac{GR_P + 1}{GC} y = n_{ref} \tag{7.42}$$

$$p_{ref} + p_\omega = p_r \tag{7.43}$$

where

$$C = \frac{1}{1 + T_p s} \tag{7.44}$$

$$G = \frac{1 + T_D s}{R_T T_D s} \tag{7.45}$$

Assuming p_ω=0 in Equation (7.43) if there is no power adjustment signal from the water level controller. Equations (7.42) and (7.43) in matrix form yield

$$\begin{bmatrix} F_n & -R_P & \frac{GR_P + 1}{CG} \\ 0 & 1 & 0 \end{bmatrix} \begin{bmatrix} n \\ p_r \\ y \end{bmatrix} = \begin{bmatrix} n_{ref} \\ p_{ref} \end{bmatrix} \tag{7.46}$$

Equation (7.46) may be simplified assuming P_{ref} as a possible port of excitation of little importance in stability or vibration analysis. Hence, Equation (7.46) yields

$$\begin{bmatrix} F_n & \frac{GR_P + 1}{CG} \end{bmatrix} \begin{bmatrix} n \\ y \end{bmatrix} = \begin{bmatrix} n_{ref} \end{bmatrix} \tag{7.47}$$

7.2.6.2 PID Governor

The following equations describe the turbine governing system when the turbine governor is assumed a PID type.

$$\begin{bmatrix} K_n & E & F \\ 0 & 1 & 0 \end{bmatrix} \begin{bmatrix} n \\ p_r \\ y \end{bmatrix} = \begin{bmatrix} n_{ref} \\ p_{ref} \end{bmatrix} \tag{7.48}$$

Where

$$E = -\left(R_p + \frac{1}{G} \right) \tag{7.49}$$

$$F = \frac{GR_p + 1}{GC} \tag{7.50}$$

$$C = \frac{1}{\left(1 + T_y s\right)\left(1 + T_x s\right)} \tag{7.51}$$

$$G = K_p + \frac{K_i}{s} + K_d s \tag{7.52}$$

Assuming $p_r = p_{ref}$, Equation (7.48) yields

$$\begin{bmatrix} K_n & F \end{bmatrix} \begin{bmatrix} n \\ y \end{bmatrix} = \begin{bmatrix} n_{ref} \end{bmatrix} \tag{7.53}$$

It should be noted that the constant K_n is used for choosing between open and closed loop analysis. It is assumed $K_n = 0$ for the open loop analysis, and $K_n = 1$ for close loop analysis.

7.3 Composition of the Global Structure Matrix

The Structure Matrix of a complex system could be built from Element and Local Matrixes. Every element in the system is designed in order with an element number. The points where the elements terminals join are referred as nodes. The Element Matrixes are connected together in series or in parallel according to some general rules. The Element Matrixes are incorporated into the Global System Structure Matrix according to the system indexing.

The general rules for the composition of the System Structure Matrix are detailed below.

1. The dimension of a *Global Structure Matrix* **A** is equal to the number of nodes of the complete system.
2. An *m*-dimension element has connection to *m* nodes.
3. Two elements may share *m* common nodes if they share *m* common variables.
4. The *Global Structure Matrix* **A** has a dimension of nxn. Each of its entries $\mathbf{A}_{ij}$ is equal to the sum of Element Structure Matrixes.
5. A group of elements, incorporated together, may be treated as an element, and the *Local Structure Matrix* can be used as the *Element Matrix*.

In stability analysis for hydro power plants, the following boundary conditions have been established in order to built the Complete Structure Matrix

- For open water surfaces, the vector ***h*** is equal to zero (***h*** = 0),
- For closed ends, the vector ***q*** is equal to 0 (***q*** = 0)

7.4 Structure Matrix of the Hydro Turbine Unit

The *Group Structure Matrix* for a hydro turbine set includes the hydraulic turbine, generator and turbine speed governor. The Element Matrixes of the turbine, generator and PID governor have been described in Equations (7.31), (7.40) and (7.48), respectively. The *Structure Matrix* for the hydro turbine set is built by incorporating Equations (7.31), (7.40) and (7.48) together. There are six nodes connected to six independent variables for the complete turbine set.

Numbering the variables as h_R=1, n=2, y=3, p_r=4, p=5 and h_L=6. The Structure Matrix may be determined as

$$\begin{bmatrix} -B & -Q & -C & 0 & 0 & B \\ 0 & K_n & F & E & 0 & 0 \\ J & K & L & 0 & M & -J \\ 0 & 0 & 0 & 1 & 0 & 0 \\ 0 & N & 0 & 0 & 1 & 0 \\ B & Q & C & 0 & 0 & -B \end{bmatrix} \begin{bmatrix} h_R(s) \\ n \\ y \\ p_r \\ p(s) \\ h_L(s) \end{bmatrix} = \begin{bmatrix} q_R(s) \\ n_{ref} \\ 0 \\ p_{ref} \\ p_g(s) \\ q_L(s) \end{bmatrix} \tag{7.54}$$

7.5 Hydro Power Plant Structure Matrix

The hydro power plant chosen for this study is shown in Figure 7-1. This hydro power plant consists of 5 elements. The elements can be written in matrixes according to the indexing.

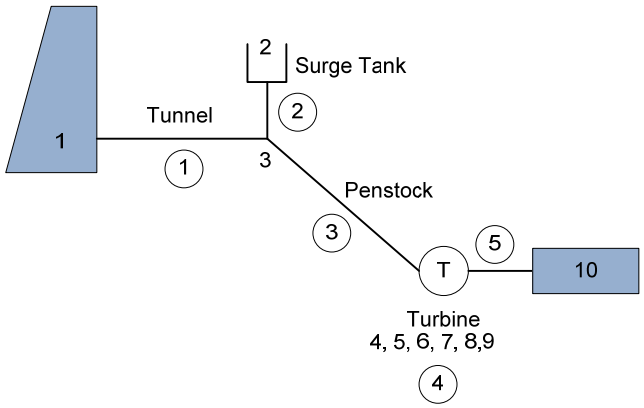

Figure 7-1: Layout of Hydro Power Plant for Structure Matrix Method Modelling

The Element 1 is the tunnel connecting to the reservoir and the surge tank (node 1 and 3)

$$\begin{bmatrix} -T_1 & S_1 \\ S_1 & -T_1 \end{bmatrix}\begin{bmatrix} h_1(s) \\ h_3(s) \end{bmatrix}=\begin{bmatrix} q_1(s) \\ q_3(s) \end{bmatrix} \tag{7.55}$$

The Element 2 is the surge tank, node number 2, connected to node 3

$$\begin{bmatrix} -T_{F2}-T_2 & S_2 \\ S_2 & -T_2 \end{bmatrix}\begin{bmatrix} h_2(s) \\ h_3(s) \end{bmatrix}=\begin{bmatrix} 0 \\ q_3(s) \end{bmatrix} \tag{7.56}$$

The Element 3 is the tunnel connecting to the surge tank and the turbine, (node 3 and 4)

$$\begin{bmatrix} -T_3 & S_3 \\ S_3 & -T_3 \end{bmatrix}\begin{bmatrix} h_3(s) \\ h_4(s) \end{bmatrix}=\begin{bmatrix} q_3(s) \\ q_4(s) \end{bmatrix} \tag{7.57}$$

The Element 4 is the Structure Matrix for the Hydro Turbine Unit. The *Group Structure Matrix* for a hydro turbine set is described in Chapter 7.4. Numbering the nodes as follows h_R=4, n=5, y=6, p_r=7, p=8 and h_L=9.

$$\begin{bmatrix} -B & -Q & -C & 0 & 0 & B \\ 0 & K_n & F & E & 0 & 0 \\ J & K & L & 0 & M & -J \\ 0 & 0 & 0 & 1 & 0 & 0 \\ 0 & N & 0 & 0 & 1 & 0 \\ B & Q & C & 0 & 0 & -B \end{bmatrix}\begin{bmatrix} h_4(s) \\ n \\ y \\ p_r \\ p(s) \\ h_9(s) \end{bmatrix}=\begin{bmatrix} q_4(s) \\ n_{ref} \\ 0 \\ p_{ref} \\ p_g(s) \\ q_9(s) \end{bmatrix} \tag{7.58}$$

The Element 5 is the tailrace, connecting to node 9 to 10

$$\begin{bmatrix} -T_5 & S_5 \\ S_5 & -T_5 \end{bmatrix} \begin{bmatrix} h_9(s) \\ h_{10}(s) \end{bmatrix} = \begin{bmatrix} q_9(s) \\ q_{10}(s) \end{bmatrix} \tag{7.59}$$

The Global Structure Matrix expression for the Hydro Power Plant, shown in Figure 7-1, according to the indexing is

$$\begin{bmatrix} -T_1 & 0 & S_1 & 0 & 0 & 0 & 0 & 0 & 0 & 0 \\ 0 & -T_{F2}-T_2 & S_2 & 0 & 0 & 0 & 0 & 0 & 0 & 0 \\ S_1 & S_2 & -T_1-T_2-T_3 & S_3 & 0 & 0 & 0 & 0 & 0 & 0 \\ 0 & 0 & S_3 & -T_3-B & -Q & -C & 0 & 0 & B & 0 \\ 0 & 0 & 0 & 0 & K_n & F & E & 0 & 0 & 0 \\ 0 & 0 & 0 & J & K & L & 0 & M & -J & 0 \\ 0 & 0 & 0 & 0 & 0 & 0 & 1 & 0 & 0 & 0 \\ 0 & 0 & 0 & 0 & N & 0 & 0 & 1 & 0 & 0 \\ 0 & 0 & 0 & B & Q & C & 0 & 0 & -B-T_5 & S_5 \\ 0 & 0 & 0 & 0 & 0 & 0 & 0 & 0 & S_5 & -T_5 \end{bmatrix} \begin{bmatrix} 0 \\ h_2 \\ h_3 \\ h_4 \\ n \\ y \\ p_r \\ p \\ h_9 \\ 0 \end{bmatrix} = \begin{bmatrix} q_1 \\ 0 \\ 0 \\ 0 \\ n_{ref} \\ 0 \\ p_{ref} \\ p_g \\ 0 \\ q_{10} \end{bmatrix} \tag{7.60}$$

In stability studies for hydro power plants, the system responses to power reference setting are often ignored. Hence, Equation (7.60) can be reduced as

$$\begin{bmatrix} -T_1 & 0 & S_1 & 0 & 0 & 0 & 0 & 0 & 0 \\ 0 & -T_{F2}-T_2 & S_2 & 0 & 0 & 0 & 0 & 0 & 0 \\ S_1 & S_2 & -T_1-T_2-T_3 & S_3 & 0 & 0 & 0 & 0 & 0 \\ 0 & 0 & S_3 & -T_3-B & -Q & -C & 0 & B & 0 \\ 0 & 0 & 0 & 0 & K_n & F & 0 & 0 & 0 \\ 0 & 0 & 0 & J & K & L & M & -J & 0 \\ 0 & 0 & 0 & 0 & N & 0 & 1 & 0 & 0 \\ 0 & 0 & 0 & B & Q & C & 0 & -B-T_5 & S_5 \\ 0 & 0 & 0 & 0 & 0 & 0 & 0 & S_5 & -T_5 \end{bmatrix} \begin{bmatrix} 0 \\ h_2 \\ h_3 \\ h_4 \\ n \\ y \\ p \\ h_9 \\ 0 \end{bmatrix} = \begin{bmatrix} q_1 \\ 0 \\ 0 \\ 0 \\ n_{ref} \\ 0 \\ p_g \\ 0 \\ q_{10} \end{bmatrix} \tag{7.61}$$

For an ideal lossless, Q_y = 1, Q_n=0 and η=constant. Equation (7.61) is simplified to

$$\begin{bmatrix} -T_1 & 0 & S_1 & 0 & 0 & 0 & 0 & 0 & 0 \\ 0 & -T_{F2}-T_2 & S_2 & 0 & 0 & 0 & 0 & 0 & 0 \\ S_1 & S_2 & -T_1-T_2-T_3 & S_3 & 0 & 0 & 0 & 0 & 0 \\ 0 & 0 & S_3 & -T_3-0.5 & 0 & -C & 0 & 0.5 & 0 \\ 0 & 0 & 0 & 0 & K_n & F & 0 & 0 & 0 \\ 0 & 0 & 0 & 1.5 & 0 & 1 & -1 & 1.5 & 0 \\ 0 & 0 & 0 & 0 & N & 0 & 1 & 0 & 0 \\ 0 & 0 & 0 & 0.5 & 0 & 1 & 0 & -0.5-T_5 & S_5 \\ 0 & 0 & 0 & 0 & 0 & 0 & 0 & S_5 & -T_5 \end{bmatrix} \begin{bmatrix} 0 \\ h_2 \\ h_3 \\ h_4 \\ n \\ y \\ p \\ h_9 \\ 0 \end{bmatrix} = \begin{bmatrix} q_1 \\ 0 \\ 0 \\ 0 \\ n_{ref} \\ 0 \\ p_g \\ 0 \\ q_{10} \end{bmatrix} \quad (7.62)$$

7.6 Dynamic Analysis

The stability analysis of a dynamic system is based in the frequency response analysis and free vibration analysis.

7.6.1 Frequency Response Analysis

The frequency response analysis is based on the study of the steady-oscillatory flow responses to a large harmonic excitation over a range of frequencies. The frequency response of the system is determined directly with *s* replaced by *jω*. The frequency response of the system to the excitation can be obtained by solving Equation (7.1) repeatedly with a selected *ω* within the frequency range $\omega_1 < \omega > \omega_2$.

The input signal may be applied to any device and the outputs are studied. A constant, usually 1, must be assigned to one of the components in vector **q** in Equation (7.1) according to where the excitation is imposed.

The frequency responses to load disturbances can be calculated assuming p_g = 1 and n_{ref} = 0. The response n/p_g is the most important measure to study the stability of the system.

The open-loop speed response to speed setting can be evaluated by the criteria of Nyquist-Bode on open-loop $n - n_{ref}$ responses. The $n - n_{ref}$ responses can be measured setting n_{ref} = 1 and p_g = 0 1.

7.6.2 Free Vibration Analysis

The free vibration analysis is a study of the dynamic characteristics of the system assuming no external excitation imposed on the system. The dynamic characteristic of a linear system depend on its eigenvalues and the mode shapes. The eigenvalues determine the natural frequencies and damping of the system, and the modes determine the shape of the vibrations.

8 Power System Stability Analysis

Stability problems in a power system may be manifested in different ways depending on the system configuration and operating mode. Analysis of elementary power system configurations by means of idealized models illustrates some of the fundamental stability properties of power systems. *Small-signal stability* is the ability of a power system to reach a steady-state operating point, which is identical, or close to, the initial condition after being subjected to small disturbances. Small-signal analysis uses linear techniques to provide valuable information about the dynamic characteristics of the power system.

This chapter describes fundamental aspects and analytical techniques in the study of stability of dynamic systems, and identifies factors influencing them. The stability of the generator-infinite busbar system following a small disturbance is discussed.

8.1 Power System Stability

Power System Stability is defined as the ability of a power system to remain in a state of operating equilibrium under normal conditions and to regain an acceptable state of equilibrium after being subjected to a physical disturbance. An electrical power system is composed of many individual elements connected together to form a large, complex and dynamic system that is able to generate, transmits and distribute energy over a geographical area. The two main causes of power system dynamic are the behaviour of the system to both a changing power demand and to various types of disturbances. [2, 22, 45, 65-66]

The power system stability can be divided into rotor angle stability, frequency stability and voltage stability. Rotor angle and voltage stability can be study into small- and large disturbance stability.

8.1.1 Small-Signal Stability Analysis

A system is steady state stable for a particular operating point if, following any small disturbance, it reaches a steady-state operating point which is identical, or close to, the predisturbance condition. This is known as *small-signal stability.* Small-signal analysis uses linear techniques to provide valuable information about the dynamic characteristics of the power system. Instability may be a result of steady increase in rotor angle due to lack of sufficient synchronous torque, or rotor oscillations of increasing amplitude due to lack of sufficient damping torque. [22, 67]

The dynamics of the generator, and its stability, are affected by automatic control of the generator and the turbine. The stability of a linear system is independent of the input, and the state of a stable system with zero input will always return to the origin of the state space. The stability of a nonlinear system depends on the type and magnitude of input and the initial state.

8.2 Fundamentals of Power System Stability

The behaviour of a dynamic power system is described by a set of *n* first order nonlinear differential equations. This set of equations can be written in the form

$$\dot{\mathbf{x}} = \mathbf{f}\left(\mathbf{x}, \mathbf{u}, t\right) \tag{8.1}$$

The vector **x** is referred as the *state vector,* and its entries x_i as state variables. The inputs of the system are represented by the vector **u.** The derivate of a state variable *x* with respect to time *t* is denoted by $\dot{\mathbf{x}}$. The state of a system is the minimum amount of information of the system at any instant in time. The system is **autonomous** when the derivatives of the state variables are not explicit functions of time. Equation (8.1) is simplified to

$$\dot{\mathbf{x}} = \mathbf{f}\left(\mathbf{x}, \mathbf{u}\right) \tag{8.2}$$

To observe the output variables of the system, the state variables and the input variables can be expressed in the following form

$$\mathbf{y} = \mathbf{g}\left(\mathbf{x}, \mathbf{u}\right) \tag{8.3}$$

The outputs of the system are represented by vector **y.** The vector **g** is a vector of the nonlinear functions relating state and input variables to output variables.

The singular or equilibrium points are the characteristic of the dynamic system behaviour. The singular point must satisfy the following equation

$$\mathbf{f}\left(\mathbf{x}_0\right) = 0 \tag{8.4}$$

A linear system has only one equilibrium state. There may be more than one equilibrium point for a nonlinear system.

The linearized forms of Equations (8.2) and (8.3), evaluated at the equilibrium point about which the small disturbance is analyzed, are

$$\Delta\dot{\mathbf{x}} = \mathbf{A}\Delta\mathbf{x} + \mathbf{B}\Delta\mathbf{u} \tag{8.5}$$

$$\Delta\mathbf{y} = \mathbf{C}\Delta\mathbf{x} + \mathbf{D}\Delta\mathbf{u} \tag{8.6}$$

The Laplace transforms of $\Delta\mathbf{x}$ and $\Delta\mathbf{y}$ are the Laplace transforms of the free and zero-state components of the state and output vectors. These Laplace transforms have a component dependent on the initial conditions and other component dependent on the inputs. The poles of $\Delta\mathbf{x}$ and $\Delta\mathbf{y}$ are the roots of the equation

$$\det\left[s\mathbf{I} - \mathbf{A}\right] = 0 \tag{8.7}$$

Equation (8.7) is referred to as the *characteristic equation* of matrix **A.** The values of s that satisfy the characteristic equation are known as *eigenvalues* of the matrix **A.**

8.3 Eigenvalue Analysis

8.3.1 Eigenvalues and Eigenvectors

A scalar parameter λ is called eigenvalue of a matrix ***A*** if there is a nonzero column vector $\mathbf{\Phi}$ satisfying

$$\mathbf{A}\Phi = \lambda\Phi \tag{8.8}$$

A non-trivial solution of Equation (8.8) is given by

$$\det\left[\mathbf{A} - \lambda\mathbf{I}\right] = 0 \tag{8.9}$$

For every eigenvalues λ_i, the vector $\mathbf{\Phi}_i$ which satisfies Equation (8.8) is called the right eigenvector associated with ***A*** the eigenvalue λ_i. Therefore,

$$\mathbf{A}\Phi_i = \lambda_i\Phi_i \tag{8.10}$$

Similarly, the left eigenvector associated with the eigenvalue λ_i is the vector $\boldsymbol{\Psi_i}$ which satisfies Equation (8.11)

$$\Psi_i\mathbf{A} = \lambda_i\Psi_i \tag{8.11}$$

The left and right eigenvectors corresponding to different eigenvalues are orthogonal. The eigenvectors can be normalized. The product of the normalized left and right eigenvectors corresponding to the same eigenvalue is

$$\Psi_i\Phi_i = 1 \tag{8.12}$$

8.3.2 Eigenvalue Analysis

The time dependent characteristic of a mode corresponding to an eigenvalue λ_i is given by $e^{\lambda i t}$. The eigenvalues of Equation (8.7) leads to the following conclusions, which are important for the analysis of the power system dynamics:

A. The original system is asymptotically stable when the eigenvalues have negative real parts.
B. The original system is unstable when at least one of the eigenvalues has a positive real part.
C. The stability of the original system is not possible to determinate when the eigenvalues have real parts equal to zero.
D. A real eigenvalue corresponds to a non-oscillatory mode. A negative real eigenvalue represents a decaying mode. The larger its magnitude, the faster the decay. A positive real eigenvalue represents aperiodic stability.
E. Each conjugate pair of complex eigenvalues introduces to the response oscillatory modes. The oscillatory mode is stable is the real part of the eigenvalue is negative.

A complex eigenvalue λ is represented by

$$\lambda = \sigma \pm j\omega \tag{8.13}$$

The real component of the eigenvalues gives the damping and the imaginary component gives the frequency of oscillation.

The damping ratio determines the rate of decay of the amplitude of the oscillation. The damping ratio is given by

$$\zeta = -\frac{\sigma}{\sqrt{\sigma^2 + \omega^2}} \tag{8.14}$$

Eigenvalue Analysis is performed using special linear power systems analysis programs. These determinate the eigenvalues and eigenvectors associated with the system model. Local modes of oscillation have natural frequencies of about 1 to 2 Hz.

In practice, damping of rotor swings is considered to be satisfactory if the damping ratio $\zeta \geq 0.05$.

8.3.3 Modal and Sensitivity Analysis

The left eigenvectors carry information about the controllability of the individual modal variable by individual state variables. The left eigenvector weights the contribution of the activity of the state variables to mode *i*.

The right eigenvectors carry information about the observability of the individual modal variable by individual state variables. The right eigenvector gives the mode shape. The mode shape represents the relative activity of the state variables when a particular mode is excited. The mode shape represents an inherent feature of a linear dynamic system and does not depend of the disturbance applied.

The **sensitivity** of an eigenvalue λ_i to the elements of the state matrix is equal to the product of the left eigenvector element and the right eigenvector element. Multiplying the right and left eigenvectors as follows

The **participation factor matrix** combines the right and left eigenvalues as a measure of the relationship between the state variables and the modes.

$$p_{ki} = \Phi_{ki}\Psi_{ik} \tag{8.15}$$

Coefficients p_{ki} are referred to as the participation factors. Each participation factor is a product of the *k*th element of the *i*th left and right eigenvectors. It quantifies the sensibility of the ith eigenvalue to the kth diagonal element of the state matrix. Participation factor contains information about the observability and controllability.

Participation factors can be used to determine enhancing system stability.

8.4 Small-Signal Stability Analysis of a generator-infinite bus system

Assume that the generator is connected to the infinite busbar, with the generator represented by the synchronous machine classical model detailed in Chapter 4.3.1. The initial disturbed conditions are $\Delta\delta\left(t=0^{+}\right)=\Delta\delta_0\neq 0$ and $\Delta\omega=0$. The incremental swing equation, Equations (4.7) and (4.8), written in the matrix form becomes

$$\begin{bmatrix}\dfrac{\partial\Delta\omega_N}{\partial t}\\ \dfrac{\partial\Delta\delta}{\partial t}\end{bmatrix}=\begin{bmatrix}-\dfrac{K_D}{2H} & -\dfrac{K_{E'}}{2H}\\ \omega_s & 0\end{bmatrix}\begin{bmatrix}\Delta\omega_N\\ \Delta\delta\end{bmatrix}+\begin{bmatrix}\dfrac{1}{2H}\\ 0\end{bmatrix}\Delta m_m \tag{8.16}$$

The transient synchronizing power coefficient $K_{E'}$ by definition is:

$$K_{E'}=\frac{\partial P_e}{\partial\delta}=\frac{E'V_S}{x_d}\cos\delta \tag{8.17}$$

where $x_d=X_d+X$ and $X=X_T+X_S$ is the combined reactance of the step up transformer and the equivalent network.

The eigenvalues of this state matrix can be determined from solving

$$\det\begin{bmatrix}-\lambda-\dfrac{K_D}{2H} & -\dfrac{K_{E'}}{2H}\\ \omega_s & -\lambda\end{bmatrix}=\lambda^2+\frac{K_D}{2H}\lambda+\omega_s\frac{K_{E'}}{2H}=0 \tag{8.18}$$

Equation (8.18) may be rewritten as the standard second-order differential equation

$$\lambda^2+2\zeta\omega_{nat}\lambda+\omega_{nat}^2=0 \tag{8.19}$$

Thus, the **undamped natural frequency** ω_{nat} of rotor swings for small oscillations is given by

$$\omega_{nat}=\sqrt{K_{E'}\frac{\omega_s}{2H}} \tag{8.20}$$

The **damping ratio** ζ determines the amount of damping present in the system response expressing how quickly the amplitude of rotor swings decreases during subsequent periods. The damping ratio is

$$\zeta=\frac{1}{2}\frac{K_D}{2H\omega_{nat}}=\frac{1}{2}\frac{K_D}{\sqrt{K_{E'}2H\omega_s}} \tag{8.21}$$

The **damped natural frequency** ω_d of rotor swings is

$$\omega_d = \omega_{nat}\sqrt{1-\zeta^2} \tag{8.22}$$

The characteristic equation has two roots λ_1 and λ_2 given by

$$\lambda_{1,2} = -\zeta\omega_{nat} \pm j\omega_{nat}\sqrt{1-\zeta^2} \tag{8.23}$$

The results of the roots $\lambda_{1,2}$ depends on the actual values of $K_{E'}$, K_D and *H.* The inertia constant *H* is constant while both K_D and $K_{E'}$ depends on the generator loading.

8.5 Dynamic Analysis

The dynamic behaviour of a hydraulic power plant may be analyzed either in the time domain by using Method of the Characteristics or in the frequency domain. The best-known methods for frequency domain analysis are Impedance Method and Transfer Matrix Method.

The partial differential equations describing the unsteady flow are converted into ordinary differential equations in the ***Time Domain Analysis***. The nonlinear friction losses and the nonlinear boundary conditions may be included in the Method of the Characteristics.

The equations describing the unsteady flow in the time domain are converted into the ***Frequency Time Domain*** by assuming a sinusoidal variation of the pressure head and the flow. The nonlinear friction losses and the nonlinear boundary conditions are linearized for solution in these methods. The system response is determined by superposition of individual responses. As the frequency response for the analysis is small, these methods are suitable for general studies.

The analysis of transients in the Hydraulic Power System Model is subdivided in water-hammer response and mass-oscillation response.

- The elastic pressure frequency describes the oscillation along the penstock. The characteristic frequency does not vary with the load and depends only upon the dimensions of the penstock. The natural frequency is typically in the order of 1.00 Hz.
- The natural frequency resulting from the pendulum action between the reservoir and the surge shaft called mass-oscillations. The mass-oscillations can take several minutes to get the steady-state.

8.5.1 Natural frequency analysis

The analysis of transients in hydroelectric systems is subdivided in mass-oscillation response and waterhammer response. Ordinary differential equations describe the mathematical model for mass-oscillation (or rigid water column) between the reservoir and the surge tank. Partial differential equations show the mathematical model for waterhammer along the penstock and draft tube. [15-20, 56, 58]

The first natural frequency of the penstock corresponds to the frequency corresponding to the fundamental period of the system, described in Equation (2.4). The first natural frequency of the penstock can be written as

$$f_0 = \frac{a}{4L} \tag{8.24}$$

The period of oscillation of the water surface in a simple surge tank is described in Equation (2.65). The natural frequency of the mass-oscillation between the upstream reservoir and the surge tank is given by

$$f_0 = \frac{1}{2\pi}\frac{1}{\sqrt{\frac{L}{g}\frac{A_S}{A_t}}} \tag{8.25}$$

8.5.2 Frequency Response Analysis

The frequency response of a system is the steady-state response of the system to a sinusoidal input signal. The transfer function of a system can by determined experimentally by frequency response tests. The design of a system in the frequency response method provides the designer with control over the system bandwidth and over the effect of noise and disturbance on the system response. [43]

The response of a linear time-invariant system to sinusoidal input $r(t) = A\sin(\omega t)$ is given by

$$c(t) = A\left|G(j\omega)\right|\sin\left[\omega t + \theta(\omega)\right] \tag{8.26}$$

Where the transfer function *G(jω)* is obtained by substituting *jω* for *s* in the expression for *G(s).* The most common graphical representation of a frequency response function is the Bode Plot.

The frequency response characteristics of the operational parameters and related them to standard parameters can be examined in SIMPOW. Such characteristics provide useful insight into the dynamic behaviour of the machine. To demonstrate the dynamic nonlinear effects, a perturbation signal is applied to any input device in open loop conditions. The input and outputs may be associated with the network equations as well as the dynamic devices. [2]

9 Test System Model

A hydroelectric development includes in some form a water-diverting structure, conduit to carry water to the turbines and governors, generators, control and switching apparatus, housing for the equipment, transformers, and transmission lines to electrical network. In some cases, a surge tank is provided to minimize the hydraulic transient effects.

The general configuration of the test Electric Power System consists of a single synchronous machine connected to a large system through a transmission line. The synchronous machine is driven by a hydraulic turbine type Francis. For the purpose of stability analysis, the system was reduced to a single machine infinite bus bar configuration.

This chapter presents the physical characteristics and capability of the components of the test system such as water upstream tunnel, surge tank, penstock, a hydraulic turbine, speed governor, generator, and electrical network. The dynamic behaviour of these components is described by a set of nonlinear equations and is modelled in the power simulation software SIMPOW.

9.1 Overview of the test System

The test system model used for stability studies is composed of a synchronous machine infinite bus power system shown in Figure 9-1. The hydraulic turbine is connected to a synchronous generator and the generator is connected to an infinite bus through a transmission line. The generated power is fed into the transmission system via a step-up transformer. The transmission system nominal voltage is 132kV.

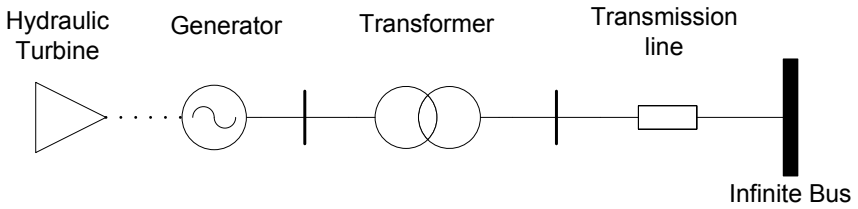

Figure 9-1: Single machine infinite bus power system

The network reactances of the test system, depicted in Figure 9-1 are in per unit on 50MVA, 24kV base. The network reactance values are based on the exercise 12.2 of the Chapter 12, page 732, of the textbook *"Power System Stability and Control"*, [2]. Resistances are assumed negligible. The system parameters and initial operating condition of the electrical network are as follows.

Table 9-1: System parameters and operating conditions

Generator	Rated apparent power	45.00 + j15.00 [MVA]
	Rated phase to phase voltage	24.00∠36.01° [kV]
	Frequency	50.00 [Hz]
	Number of pairs of poles	6.00 [-]
	Inertia Time Constant	2.70 [MWs/MVA]
Transformer	Reactance	0.15 [pu]
	Rated Voltage	24.00/132.00 [kV]
Transmission line	Reactance	0.50 [pu]
Infinite Bus	Rated voltage	0.995 ∠0.00° [pu]

9.2 Models of the different components

9.2.1 Power Plant Model

The hydroelectric power plant includes a canal to carry the water flow from the reservoir, a surge tank, a penstock to convey the water to the powerhouse, a powerhouse for the turbine and generator, and a tailrace. The synchronous generator is mechanically coupled to the turbine, and the electrical output power of the generator is carried by the transmission lines to the electric grid. A governing system is provided to correct any changes in the system frequency by opening or closing the wicket gates of the turbine. [6, 10]

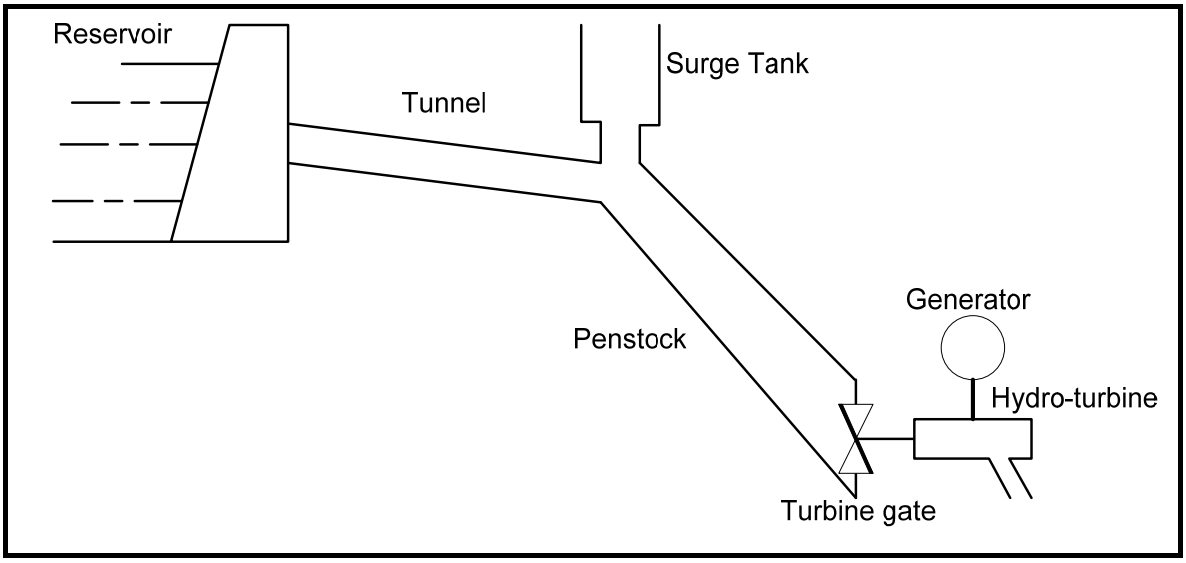

Figure 9-2: A general Layout of Hydro Power Plant, [19]

The layout of hydroelectric power plant used for the stability studies is shown in Figure 9-2. The water conduit system has a static head between 220.0 m and 200.0 m. The power plant is composed of an upstream reservoir, a 1307 meters long gallery, a surge tank, a 435 meters long penstock, a turbine and 100 meters long discharge tailrace. The power plant has a Francis unit. The main parameters of the hydraulic circuit are summarized in Table 9-2.

Table 9-2: Hydraulic Power Plant Model

Tunnel	Length	1307.00	[m]
	Diameter	3.90	[m]
	Friction constant, f	0.06	[-]
Surge Tank	Diameter	5.00	[m]
	Water level measured	300.00	[m]
	Friction constant, f	0.05	[-]
Penstock	Length	435.00	[m]
	Diameter	2.00	[m]
	Friction constant, f	0.01	[-]
Francis Turbine	Rated mechanical power	46.15	[MW]
	Rated speed	500.00	[rpm]
	Rated discharge	25.00	[m^3/s]
	Rated head	200.00	[m]
	Reference diameter	3.90	[m]
	Hydraulic efficiency	0.96	[-]
	Rated efficiency	0.94	[-]
Tailrace/outlet	Length	100.00	[m]
	Diameter	3.90	[m]
	Friction constant, f	0.06	[-]

The value considered for the pressure wave velocity a is 1200 m/s. The dimensionless pipe friction factor is a function of the Reynolds number and the relative roughness height, described in Chapter 2.1.3. The friction factor is selected from the Moody diagram.

9.2.2 Hydraulic Turbine

The hydraulic turbine is a type Francis. In a reaction turbine having long pressure tunnels, the dynamic response of both upstream and downstream water columns must be studied in order to avoid excessive pressure or over speed problems.

The hydraulic turbine is designed by models of varying degrees of detail for the stability analysis of The Hydraulic Power Generating System. The hydraulic turbine parameters used in the modelling and simulation of the hydro turbine models are given in Table 9-3.

Table 9-3: Hydraulic Turbine Parameters

Parameter		**Value**	
Turbine Damping	K_D	0.500	[-]
Gate Position at Rated Condition		0.900	[pu]
Gate Opening at Full Load	y_{FL}	0.960	[pu]
Gate Opening at No-Load	y_{NL}	0.172	[pu]
No-load Load	Q_{NL}	4.300	[m^3/s]
Constant Proportionality	A_t	1.250	[-]
Water Time Constant in Penstock	T_{W1}	1.764	[s]
Water Time Constant in Upstream Tunnel	T_{W2}	1.394	[s]
Surge Tank Filling Time	T_s	157.079	[s]

The mathematical models of the hydraulic turbine developed, simulated and analyzed for the stability analysis of a hydraulic power generating system are listed in Table 9-4. It is worthy to notice that the linear models uses the typical values recommend by IEEE, detailed in Table 3-2.

Table 9-4: Hydraulic Turbine Models

Model	Description
1	Simplified Nonlinear Turbine Model assuming Inelastic Water Column
2	Nonlinear Turbine Model without Surge Tank assuming Inelastic Water Column
3	Nonlinear Turbine Model without Surge Tank including Elastic Water Column Effect
4	Nonlinear Turbine Model with Surge Tank assuming Inelastic Water Columns in Penstock and Tunnel
5	Nonlinear Turbine Model with Surge Tank assuming Elastic Water Column in Penstock and Inelastic Water Column in Tunnel
6	Linear Turbine Model with Surge Tank considering Inelastic Water Columns in Penstock and Tunnel, and turbine coefficients recommend by IEEE
7	Linear Turbine Model with Surge Tank including Elastic Water Column in Penstock, and turbine coefficients recommend by IEEE

9.2.3 Synchronous Generator

The synchronous generator is modelled by a detailed model with damping, TYPE 2, which consists of one field winding, one damper winding in d-axis and one damper winding in q-axis with saturation included. The synchronous machine is modelled without automatic voltage regulator. This synchronous machine model TYPE 2 is a standard component in the simulation software SIMPOW that is described in detail in the SIMPOW User Manual.

The synchronous machine parameters used in the modelling of the synchronous generator are shown in Table 9-5. These parameters are based on typical values of standard parameters detailed in the Table 4.2 of the Chapter 4 of the textbook “Power System Stability and Control”, [2]. The reactance values are in per unit using the machine rated values as the base values and the time constants are in seconds.

Table 9-5: Synchronous machine Parameters

Parameter		Value
Stator Resistance	R_a	0.003 [pu]
Direct-axis synchronous reactance	x_d	1.174 [pu]
Direct-axis transient reactance	x_d'	0.300 [pu]
Direct-axis subtransient reactance	x_d''	0.215 [pu]
Quadrature-axis synchronous reactance	x_q	0.770 [pu]
Quadrature-axis subtransient reactance	x_q''	0.150 [pu]
Stator leakage reactance	x_l	0.101 [pu]
Open-circuit d-axis transient time constant	T_{d0}'	8.500 [sec]
Open-circuit d-axis subtransient time constant	T_{d0}''	0.050 [sec]
Open-circuit q-axis subtransient time constant	T_{q0}''	0.250 [sec]

9.2.4 Governing Systems for Hydraulic Turbines

The turbine governing system is modelled by a general speed-governing model TYPE SG1. The physical characteristics and capability of the turbine governing system are detailed in Chapter 5. The governor model type SG1 is available in the DSL-libraries in the software SIMPOW that is documented in the SIMPOW User Manual. The rotor speed ω_r is set as the input speed signal. The input signal for the permanent droop compensation is the pilot or main servomotor position *y*.

The turbine governing system parameters used on the test system are based on the governor model detailed in the Figure 9.10 of the Chapter 9 of the textbook in Reference [2]. These values are shown in given as typical values in Table 9-6.

Table 9-6: Typical Values of parameters of turbine governing system

Parameter		Value
Pilot valve time constant	T_P	0.05 [s]
Servo gain	K_s	5.00 [-]
Main servomotor time constant	T_g	0.20 [s]
Permanent droop	R_P	0.04 [-]
Temporary droop	R_T	0.40 [-]
Reset time	T_R	5.00 [sec]
Maximum gate opening rate	*YPMAX*	0.10 [pu/s]
Maximum gate closing rate	*YPMIN*	-0.10 [pu/s]
Maximum gate position limit	*YMAX*	1.00 [-]
Minimum gate position limit	*YMIN*	0.00 [-]

9.3 Power Flow Analysis

The power flow analysis involves the study of the flow of active and reactive power, losses, and the voltage profile for normal symmetrical steady operating condition in the given system. The Power Flow module OPTPOW, part of SIMPOW, calculates initial power flows in the network.

The test system, shown in Figure 9-1, contains three buses. The synchronous generator is connected in the bus 1. The generation at bus 1 is modelled as UP-node. The transformer is connected between bus 1 and bus 2. Bus 3 is the swing bus and represents an infinite bus. Table 9-7 shows the power-flow results from the OPTPOW calculation.

Table 9-7: Power Flow results

Name	U p.u.	U kV	FI(u) Deg.	P1 MW	Q1 Mvar	P2 MW	Q2 Mvar
BUS1	1.0000	24.0000	36.0109				
TR2 BUS1 BUS2 0				-45.0000	-15.0107	45.0000	8.2597
PROD SYNKRONGEN				45.0000	15.0107	0.0000	0.0000
BUS2	0.9645	127.3090	27.9646				
LINE BUS2 BUS3 0				-45.0000	-8.2597	45.0000	-14.2433
TR2 BUS1 BUS2 0				-45.0000	-15.0107	45.0000	8.2597
BUS3	0.9950	131.3400	0.0000				
LINE BUS2 BUS3 0				-45.0000	-8.2597	45.0000	-14.2433
PROD SWING				-45.0000	14.2433	0.0000	0.0000

9.4 Power System Stability Analysis – Theoretical Results

9.4.1 Eigenvalue Analysis

The circuit model representing the initial operating condition with all the parameters expressed in per unit is shown in Figure 9-3. The synchronous generator is modelled by the classical model and all the resistances neglected.

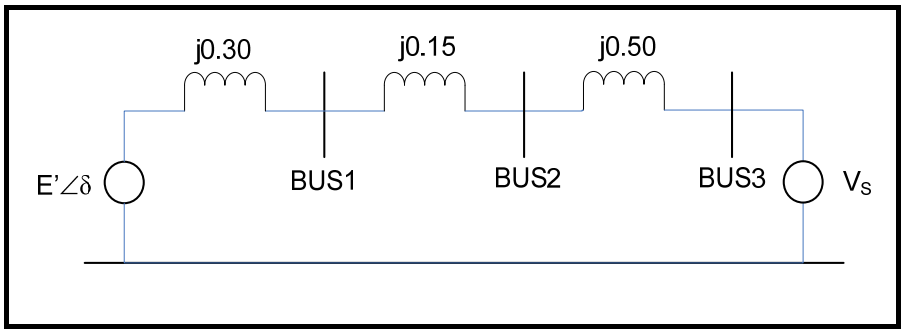

Figure 9-3: Circuit model of the test system

Assuming the generator voltage to be reference, the generator stator current is

$$I_0 = \left(\frac{P + jQ}{V_g}\right)^* = \frac{P - jQ}{V_g} = \frac{0.90 - j0.30}{1.00\angle -36.01^\circ} = 0.9487\angle 17.5760^\circ \tag{9.1}$$

The internal voltage for the transient state is:

$$E' = V_g + jX_d' I_0 = \left(1.00\angle 36.01^\circ\right) + j0.3 \cdot \left(0.95\angle 17.58^\circ\right) = 1.1229\angle 49.9234^\circ \tag{9.2}$$

The transient synchronizing power coefficient $K_{E'}$ is:

$$K_{E'} = \frac{E'V_S}{x_d}\cos\delta = \frac{1.123 \cdot 0.995}{0.95}\cos 49.92^\circ = 0.7572 \tag{9.3}$$

Linearized system equations, from Equation (8.16), give

$$\begin{bmatrix} \dfrac{\partial \Delta\omega_N}{\partial t} \\ \dfrac{\partial \Delta\delta}{\partial t} \end{bmatrix} = \begin{bmatrix} -0.1852K_D & -0.1402 \\ 100\pi & 0 \end{bmatrix} \begin{bmatrix} \Delta\omega_N \\ \Delta\delta \end{bmatrix} + \begin{bmatrix} 0.1852 \\ 0 \end{bmatrix} \Delta m_m \tag{9.4}$$

The eigenvalues of the state matrix, Equation (9.4), are given by

$$\det \begin{bmatrix} -\lambda - 0.1852K_D & -0.1402 \\ 100\pi & -\lambda \end{bmatrix} = \lambda^2 + 0.1852K_D\lambda + 14.0212\pi = 0 \tag{9.5}$$

The undamped natural frequency, from Equation (8.20), gives

$$\omega_{nat} = \sqrt{0.1402 \frac{100\pi}{2*2.7}} = 6.6372 \text{ rad/s} = 1.0563 \text{ Hz} \tag{9.6}$$

The damping ratio, from Equation (8.21), is

$$\zeta = \frac{1}{2} \frac{K_D}{2*2.7*6.6372} = 0.0140 K_D \tag{9.7}$$

The theoretical results for this test system for different values of K_D are detailed in Table 9-8.

Table 9-8: Results of the Synchronous machine represented by Classical Model

Description	*Results*		
Eigenvalues, λ	0.00 ± j6.6372	-0.0463 ± j6.6371	-0.0926 ± 6.6366
Damping coefficient, K_D	0.00	0.50	1.00
Damping Ratio, ζ	0.00	0.0070	0.0140
Damped frequency, ω_d	1.0563 [Hz]	1.0563 [Hz]	1.0562 [Hz]
Undamped natural frequency, ω_{nat}	1.0563 [Hz]	1.0563 [Hz]	1.0563 [Hz]

9.4.2 Natural frequency analysis

The first natural frequency of the penstock corresponds to the frequency corresponding to the fundamental period of the system, described in Equation (2.4). The first natural frequency of the penstock is

$$f_0 = \frac{a}{4L} = \frac{1200}{4*435} = 0.8305 \tag{9.8}$$

The natural frequency of the mass-oscillation between the upstream reservoir and the surge tank is given by

$$f_0 = \frac{1}{2\pi} \frac{1}{\sqrt{\frac{L}{g}\frac{A_S}{A_t}}} = \frac{1}{2\pi} \frac{1}{\sqrt{\frac{1307.00}{9.81}\left(\frac{2.50}{3.90}\right)^2}} = 0.010755 \tag{9.9}$$

10 Dynamic Simulations in SIMPOW

Once the Hydro Power Plant models are established, the different models are implemented, simulated and studied in the software SIMPOW. SIMPOW is a software system for digital Simulation and analysis of electrical Power systems. Digital models, static and dynamic, of most elements in a power system are available for the conventional calculation of power flow, fault currents and time simulation of short-term dynamics. SIMPOW has been designed with a numerical technique and events handling, which are robust and give accurate results.

This chapter deals with the study of the system stability characteristics of the different hydro turbine models within a typical hydraulic power generating system implemented in the software SIMPOW. The objective of the dynamic modelling of the test system is to analyze the stability characteristics of the Hydro Power System about the steady-state operating condition following a three-phase fault to ground at t=1 s. This disturbance is simulated for a period of 5.0 ms. The sampling period is 50 seconds.

The hydraulic power generating system for the stability analysis has been designed with a detailed synchronous generator model with damping, a general speed-governing model, and a turbine. The hydraulic turbine is modelled with varying degrees of detail. The mathematical models of the hydraulic turbine are detailed in Table 9-4, and listed below

Model 1 Simplified Nonlinear Turbine Model
Model 2 Nonlinear Turbine Model without Surge Tank assuming Inelastic Water Column
Model 3 Nonlinear Turbine Model without Surge Tank including Elastic Water Column Effect
Model 4 Nonlinear Turbine Model with Surge Tank assuming Inelastic Water Columns
Model 5 Nonlinear Turbine Model with Surge Tank assuming Elastic Water Column in Penstock and Inelastic Water Column in Upstream Tunnel
Model 6 Linear Turbine Model with Surge Tank considering Inelastic Water Columns in Penstock and Tunnel, and turbine characteristics based in the turbine coefficients recommend by IEEE
Model 7 Linear Turbine Model with Surge Tank including Elastic Water Column in Penstock, and turbine characteristics based in the turbine coefficients recommend by IEEE

Frequency response analysis as well as transient analysis is performed to evaluate the effects of the detailed modelling of the turbine and conduit system to the stability analysis and the dynamic performance of the hydraulic power generating system.

The dynamic performance of the different Hydro Power System models has been investigated utilizing the eigenvalue analysis to analyze the behaviour of a single unit connected to a power system. The computed eigenvalues are analyzed in Dynpow of the software SIMPOW. The values of the real part of the eigenvalues are measured in [1/s] and the imaginary part is measured in [Hz].

10.1 MODEL 1: Simplified Nonlinear Turbine Model

The hydraulic turbine in the model 1 is design by a *Simplified Nonlinear Turbine Model*, described in Chapter 6.2.1. The penstock is modelled assuming an inelastic conduit, incompressible fluid and neglecting friction losses. The nonlinear characteristics of hydraulic turbine are neglected in this model. The block diagram of this hydro power plant model is shown in Figure 6-2.

The parameters of the hydro power plant and operating conditions are detailed in Chapter 9. The simplified nonlinear turbine model, type ***HYTUR***, is available in the SIMPOW DSL-library that is documented in the SIMPOW User's Manual.

10.1.1 Eigenvalue Analysis

Table 10-1 shows the real-valued eigenvalues, non-real-valued eigenvalues and the state variables that have the highest participation of the test system with a simplified nonlinear turbine model.

Table 10-1: Eigenvalues and the state variable for a model 1

	Eigenvalue			Damping Ratio	Frequency [Hz]	Dominant States
	Real, [1/s]		Imag, [Hz]			
1	-23.0168		0.0000	-	-	$\Delta\psi_D$
2	-17.5102		0.0000	-	-	
3,4	-0.4073	±	1.0538	0.06140	1.05383	$\Delta\omega$ and $\Delta\delta$
5	-6.7770		0.0000	-	-	$\Delta\psi_Q$
6,7	-3.7911	±	0.1221	0.98015	0.12205	
8	-1.2927		0.0000	-	-	
9	-0.0167		0.0000	-	-	
10	-0.1773		0.0000	-	-	$\Delta\psi_f$
11	-1.0000		0.0000	-	-	

It is seen in Table 10-1 that

- All eigenvalues have negative real part.
- The system is stable.
- λ_1, λ_2, λ_5, λ_8, λ_9, λ_{10} and λ_{11} influence the dynamic system with pure damping,
- $\lambda_{3,4}$ and $\lambda_{6,7}$ influence the dynamic simulation with both damping and oscillation.
- The oscillatory mode $\lambda_{3,4}$ have a damped frequency of 1.0538 Hz. The oscillations decay with a time constant of 1/0.4073 seconds. This corresponds to a damping ratio ζ of 0.0614.

The magnitudes of the participation factors, computed in SIMPOW, are shown in Table 10-2. The angles of the participation factors do not provide any useful information. From the participation matrix, $\Delta\delta$ and $\Delta\omega$ have a high participation in the oscillatory mode associated to the eigenvalues $\lambda_{3,4}$. The field flux linkage has a high participation in the non-oscillatory mode represented by the eigenvalue λ_{10}. The d-axis flux linkage has a high participation on the non-oscillatory mode represented by the eigenvalue λ_1. The q-axis flux linkage has a high participation on the non-oscillatory mode represented by the eigenvalue λ_5.

Table 10-2: Participation matrix for a model 1

	λ_1	λ_2	λ_3	λ_4	λ_5	λ_6	λ_7	λ_8	λ_9	λ_{10}
$\Delta\delta$	0.00627	0.00037	0.54104	0.54104	0.02714	0.22094	0.22094	0.06553	0.00391	0.00088
$\Delta\omega$	0.00582	0.00290	0.53081	0.53081	0.01898	0.08866	0.08866	0.00244		0.00043
$\Delta\psi_f$	0.00575	0.00001	0.00751	0.00751	0.00036	0.00849	0.00849	0.00812	0.00016	0.98838
$\Delta\psi_D$	1.00647	0.00044	0.01323	0.01323	0.00085	0.00455	0.00455	0.00015	0.00000	0.00888
$\Delta\psi_Q$	0.00004	0.00006	0.03267	0.03267	0.99570	0.07283	0.07283	0.00203	0.00000	0.00185

10.1.2 Dynamic Simulation Analysis

Figure 10-1 shows the result of simulating a three-phase fault to ground on bus BUS2 at t=1 s. This disturbance is simulated for a period of 5.0 ms. The simulation results of a simple turbine without surge tank represented by model 1 shows the dynamic behaviour of the angle, speed, mechanical torque, gate position, flow rate and head pressure.

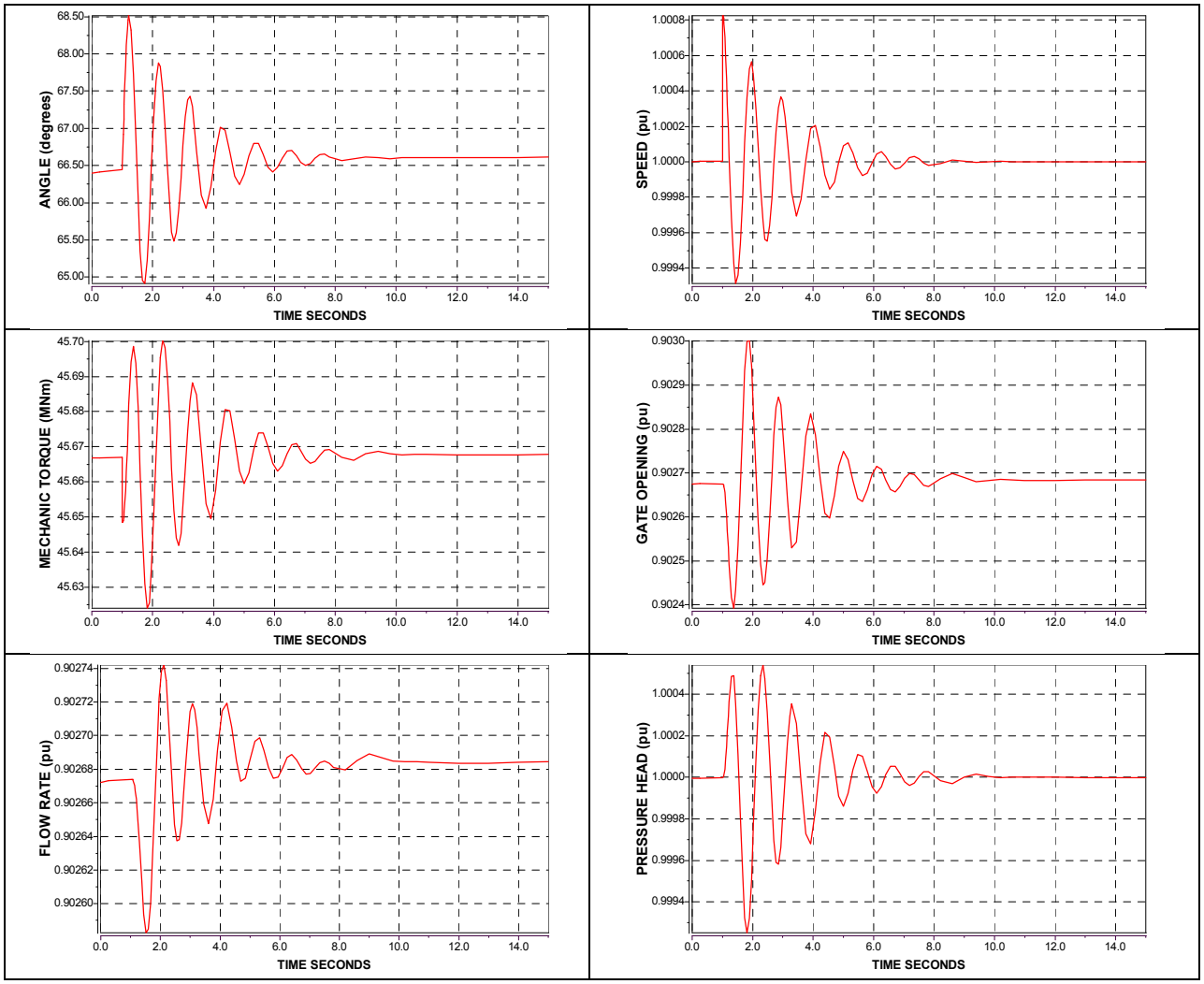

Figure 10-1: Fault simulation results: (a) angle, (b) speed, (c) mechanical torque, (d) gate position, (e) flow rate and (f) head pressure of Model 1

The initial value of the Mechanical Power is 45.5214 MW. After the fault is simulated, the mechanical power drops to 0.00 MW. The mechanical power oscillates for a period of 6 seconds, approximately.

The electrical angle oscillates for a period of 7.80 seconds. The minimum value is 64.9139° at 1.74 seconds and the maximum value is 68.51° at 1.22 seconds. The value of the electrical angle at steady-state is 66.61°.

The rotational speed oscillates between the values of 0.9993 pu and 1.0008 pu. The rotational speed recovers stability after 8 seconds, demonstrating that the dynamic response of the hydro power plant is efficient.

The initial value of Mechanical Torque and Electric Torque are 45.67 MNm and -45.66 MNm, respectively. The Mechanic Torque oscillates for a period of 8 seconds, between the values of 45.62 MNm and 45.70 MNm. The Mechanical Torque at steady state is 45.6678 MNm. The period of oscillation of Electrical Torque is 5.50 seconds, approximately. Electrical Torque oscillates between the values of -47.08 MNm and -1.38 MNm. The Electrical Torque at steady state is -45.67 MNm.

The variables such as gate opening, flow rate and water pressure head are measured in per unit. The gate position oscillates between 0.9024 and 0.9030. The flow rate varies between 0.9025 and 0.9027. The pressure head oscillates between 0.9993 and 1.0005. The values of gate position, flow rate and water pressure at steady-state are 0.9027, 0.9027 and 1.0000, respectively.

10.1.3 Frequency Response Analysis

The magnitude and phase of the transfer function from gate position to Mechanical Power of a Simplified Nonlinear Model are plotted in Figure 10-2. The perturbation signal is applied to the gate position in open loop conditions and the signal mechanical power is monitored.

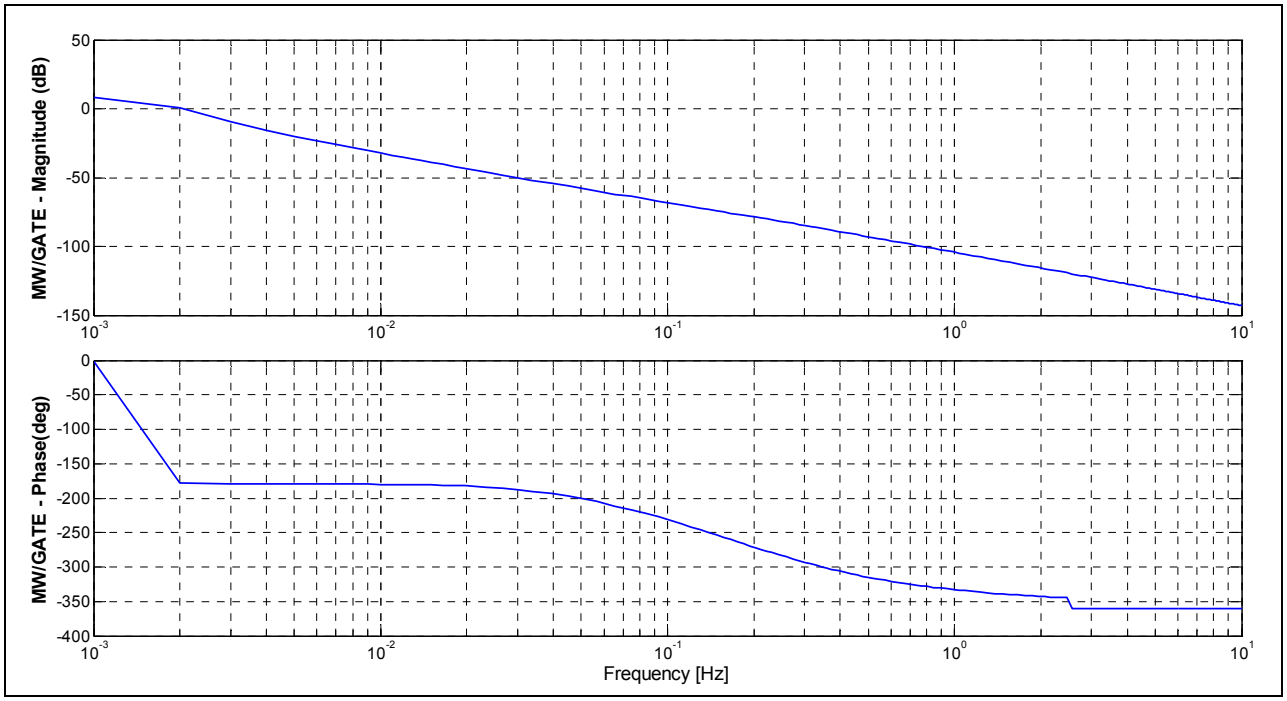

Figure 10-2: Frequency response of the transfer function from Gate position to Mechanical Power of model 1

The relationship between the mechanical torque and the variation of gate position is studied in order to analyze the dynamic behaviour of the system. The perturbation signal is applied to the gate position in open loop conditions and the signal mechanical torque is monitored. The magnitude and phase of the frequency response of the transfer function of the hydraulic turbine are plotted in Figure 10-3.

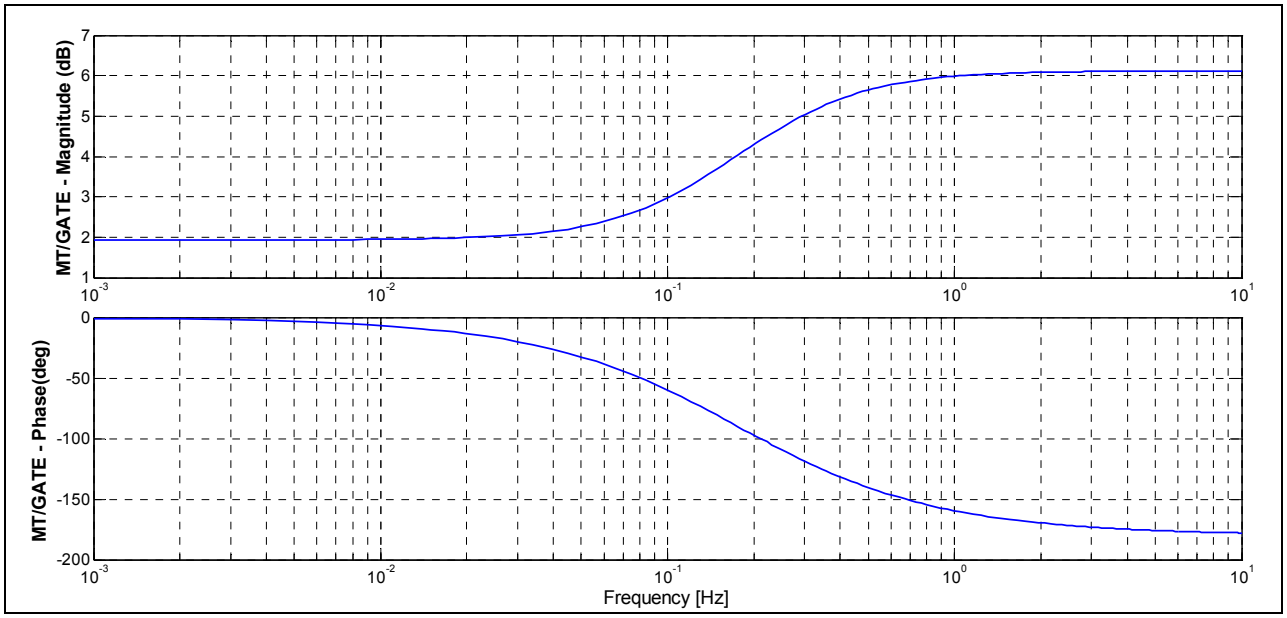

Figure 10-3: Frequency response of the transfer function from Gate position to Mechanical Torque of Model 1

Figure 10-4 plots the computed frequency response of the transfer function of the conduit system of a Simplified Nonlinear Turbine Model. The transfer function of the conduit system relates the water pressure to gate position.

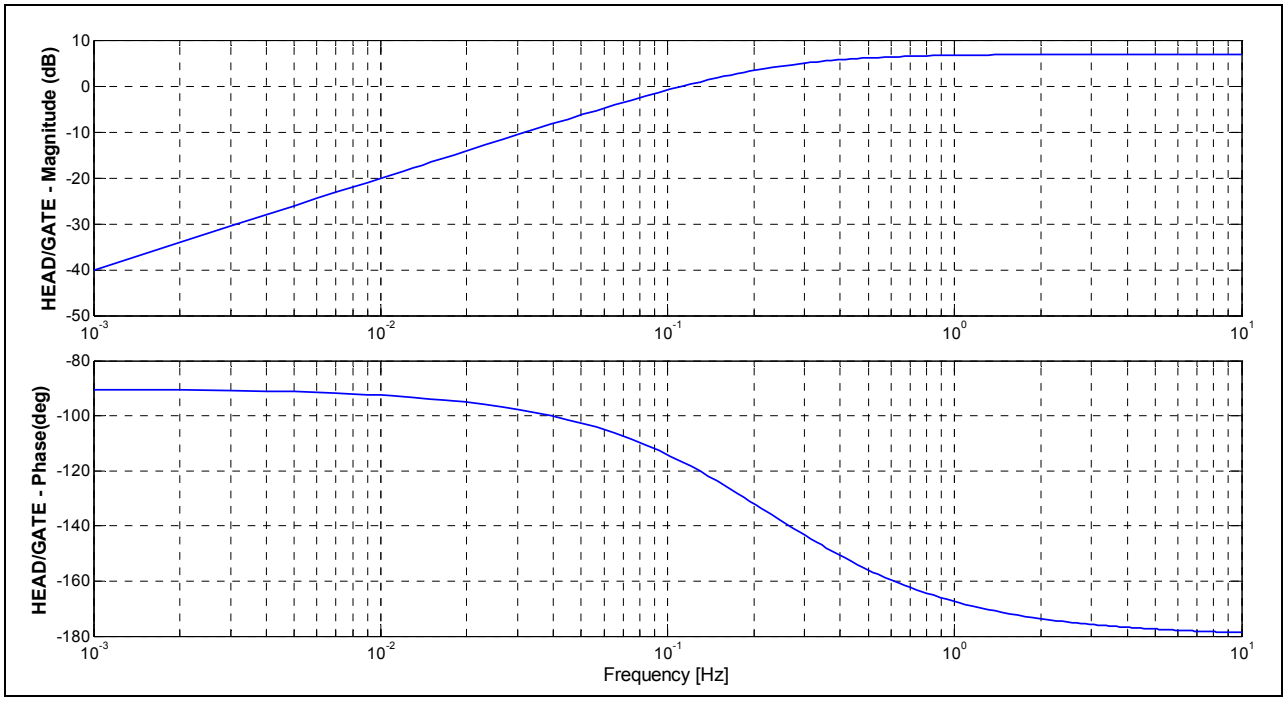

Figure 10-4: Frequency response of the transfer function of the conduit system of Model 1

Figure 10-5 plots the magnitude and phase of the transfer function from gate position to Electrical Power Angle.

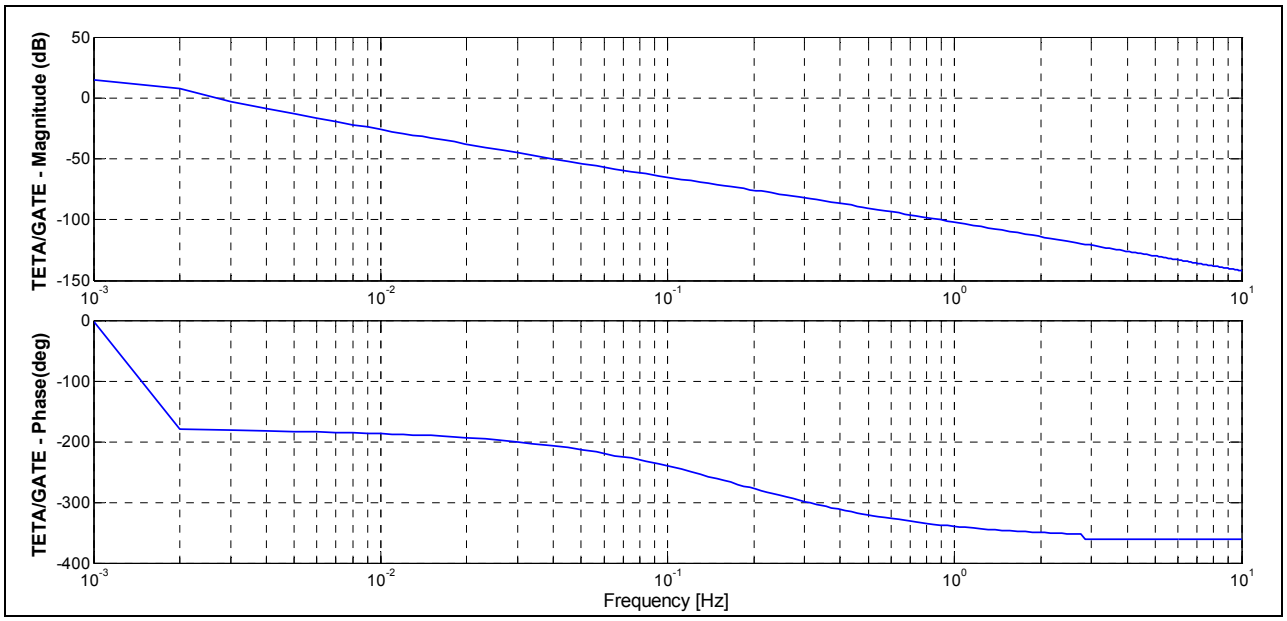

Figure 10-5: Frequency response of the transfer function from gate position to electrical angle of Model 1

The magnitude and phase of the transfer function of the mechanical-hydraulic governor of a Simplified Nonlinear Model are plotted in Figure 10-6. The transfer function of the governor relates the gate position to speed changes.

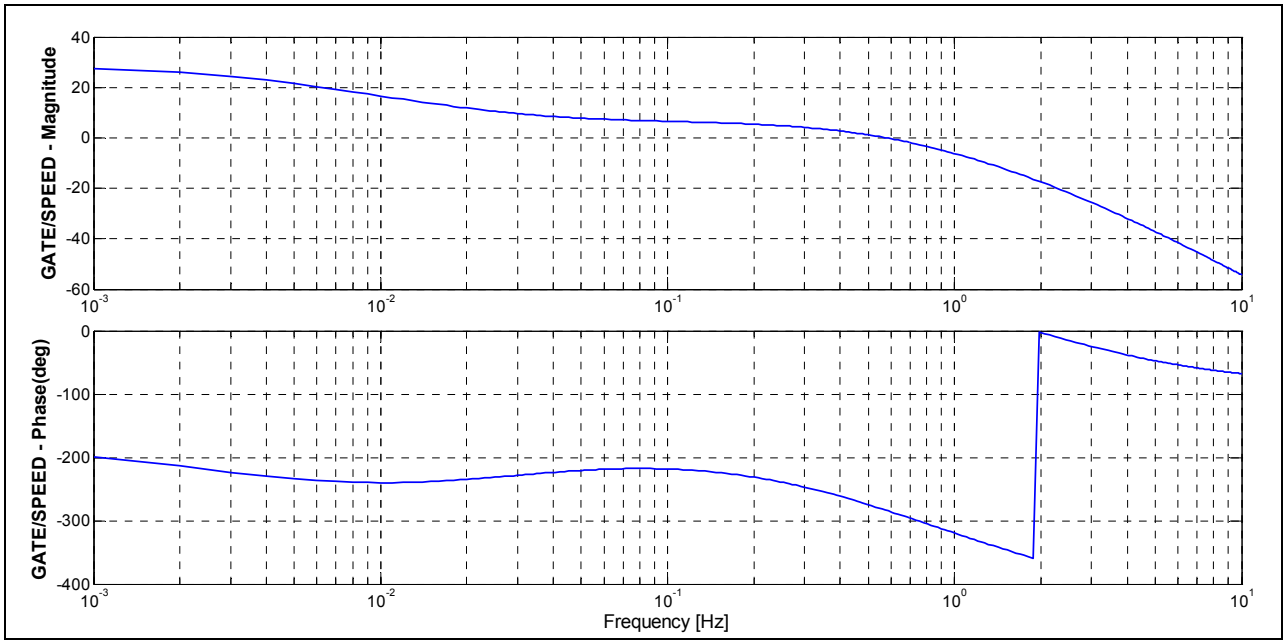

Figure 10-6: Frequency response of the transfer function of the mechanical-hydraulic governor of Model 1

10.2 MODEL 2: Nonlinear Turbine Model without Surge Tank assuming Inelastic Water Column

The hydraulic turbine in the model 2 is represented by a *Nonlinear Turbine Model without Surge Tank assuming Inelastic Water Column*, described in Chapter 6.2.2. The Penstock is modelled assuming an inelastic conduit and incompressible fluid where the travelling pressure wave effects are relatively insignificant. The nonlinear characteristics of the hydraulic turbine are neglected in this model. The block diagram of this configuration is shown in Figure 6-3.

The parameters of the Hydro Power Plant and operating conditions are detailed in Chapter 9. This model was implemented in DSL Code Generator which is a tool used for making self-defined dynamic models for dynamic simulation in SIMPOW.

10.2.1 Eigenvalue Analysis

Table 10-3 shows the real-valued eigenvalues, non-real-valued eigenvalues and the state variables that have the highest participation of the test system with a Nonlinear Turbine Model without Surge Tank assuming Inelastic Water Column.

Table 10-3: Eigenvalues and the state variable for Model 2

	Eigenvalue			Damping Ratio	Frequency [Hz]	Dominant States
	Real, [1/s]		Imag, [Hz]			
1	-23.0319		0.0000	-	-	$\Delta\psi_D$
2	-17.5091		0.0000	-	-	
3,4	-0.4203	±	1.0649	0.06270	1.06485	$\Delta\omega$ and $\Delta\delta$
5	-6.7511		0.0000	-	-	$\Delta\psi_Q$
6,7	-3.7861	±	0.1176	0.98148	0.11762	
8	-1.2895		0.0000	-	-	Δq
9	-0.0167		0.0000	-	-	
10	-0.1814		0.0000	-	-	$\Delta\psi_f$
11	-1.0000		0.0000	-	-	

It is seen in Table 10-3 that

- All eigenvalues have negative real part.
- The system is stable.
- λ_1, λ_2, λ_5, λ_8, λ_9, λ_{10}, and λ_{11} influence the dynamic system with pure damping.
- $\lambda_{3,4}$, and $\lambda_{6,7}$ influence the dynamic simulation with both damping and oscillation.
- The oscillatory mode $\lambda_{3,4}$ have a damped frequency of 1.0649 Hz. The oscillations decay with a time constant of 1/0.4203 s. This corresponds to a damping ratio ζ of 0.0627.

The magnitudes of the participation factors, computed in SIMPOW, are shown in Table 10-4. The angles of the participation factors do not provide any useful information. From the participation matrix, $\Delta\delta$ and $\Delta\omega$ have a high participation in the oscillatory mode associated to the eigenvalues $\lambda_{3,4}$. The field flux linkage has a high participation in the non-oscillatory mode represented by the eigenvalue λ_{10}. The d-axis flux linkage has a high participation on the non-oscillatory mode represented by the eigenvalue λ_1. The q-axis flux linkage has a high participation on the non-oscillatory mode represented by the eigenvalue λ_5.

Table 10-4: Participation factors matrix of a turbine Model 2

	λ_1	λ_2	λ_3	λ_4	λ_5	λ_6	λ_7	λ_8	λ_9	λ_{10}
$\Delta\delta$	0.0061	0.0004	0.5412	0.5412	0.0291	0.2246	0.2246	0.0636	0.0036	0.0008
$\Delta\omega$	0.0057	0.0028	0.5316	0.5316	0.0203	0.0893	0.0893	0.0023		0.0004
$\Delta\psi_f$	0.0057	0.0000	0.0071	0.0071	0.0004	0.0084	0.0084	0.0077	0.0001	0.9886
$\Delta\psi_D$	1.0062	0.0004	0.0128	0.0128	0.0009	0.0045	0.0045	0.0001	0.0000	0.0087
$\Delta\psi_Q$	0.0000	0.0001	0.0350	0.0350	0.9947	0.0801	0.0801	0.0021	0.0000	0.0019

10.2.2 Dynamic Response Analysis

Figure 10-7 shows the result of simulating a three-phase fault to ground on bus BUS2 at t=1 s. This disturbance is simulated for a period of 5.0 ms. The simulation results of a simple turbine without surge tank represented by model 2 shows the dynamic behaviour of the power angle, rotational speed, mechanical torque, gate position, flow rate and head pressure.

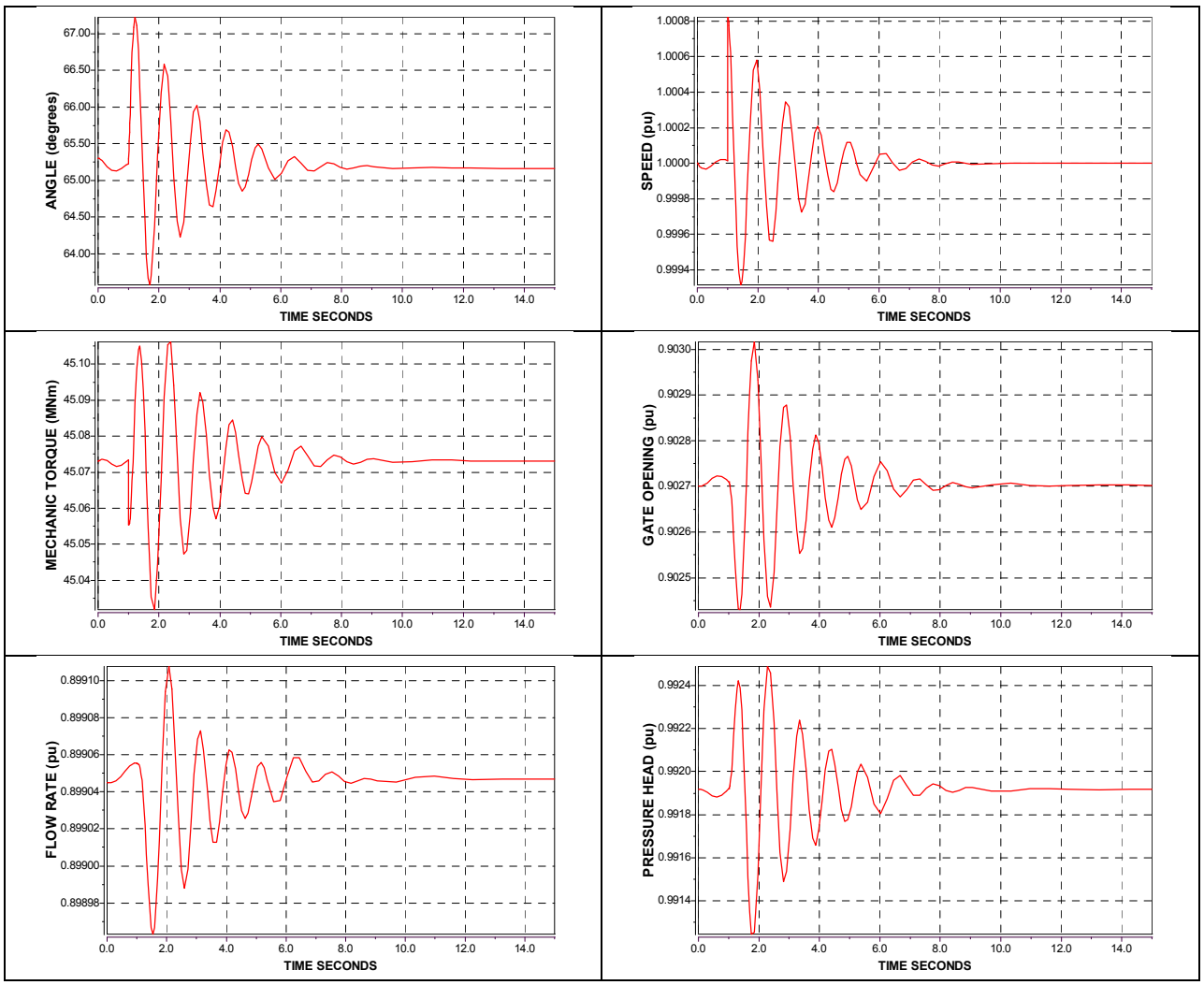

Figure 10-7: Fault simulation Results: (a) Power angle, (b) Speed, (c) Mechanical Torque, (d) Gate Position, (e) Flow Rate and (f) Head Pressure of Model 2

The initial value of the Mechanical Power is 45.00 MW. After the fault is simulated, the Mechanical Power drops to 0.00 MW. The Mechanical Power oscillates for a period of 5.2 seconds, approximately.

The electrical angle oscillates for a period of 7.60 seconds. The minimum value is 63.5775° at 1.69 seconds and the maximum value is 67.2254° at 1.22 seconds. The value of the electrical angle at steady-state is 65.16°.

The rotational speed oscillates between the values of 0.9993 pu and 1.0008 pu. The rotational speed recovers stability after 8 seconds, demonstrating that the dynamic response of the hydro power plant is efficient.

The initial value of Mechanical Torque and Electric Torque are 45.07 MNm and -45.14 MNm, respectively. The Mechanic Torque oscillates for a period of 8 seconds, between the values of 45.03 MNm and 45.10 MNm. The Mechanical Torque at steady state is 45.0732 MNm. The period of oscillation of Electrical Torque is 5.50 seconds, approximately. Electrical Torque oscillates between the values of -46.49 MNm and -1.38 MNm. The Electrical Torque at steady state is -45.07 MNm.

The variables Gate Opening, Flow rate and Pressure Head are measured in per unit. Gate opening oscillates between 0.9024 and 0.9030. The flow varies between 0.8989 and 0.8991. The pressure head oscillates between 0.9919 and 0.9925. The values of Gate position, Flow rate and Pressure Head at steady-state are 0.9027, 0.8990 and 0.9919, respectively.

10.2.3 Frequency Response Analysis

The magnitude and phase of the transfer function from gate position to Mechanical Power of a Nonlinear Turbine Model without Surge Tank assuming Inelastic Water Column are plotted in Figure 10-8. The perturbation signal is applied to the gate position in open loop conditions and the signal mechanical power is monitored.

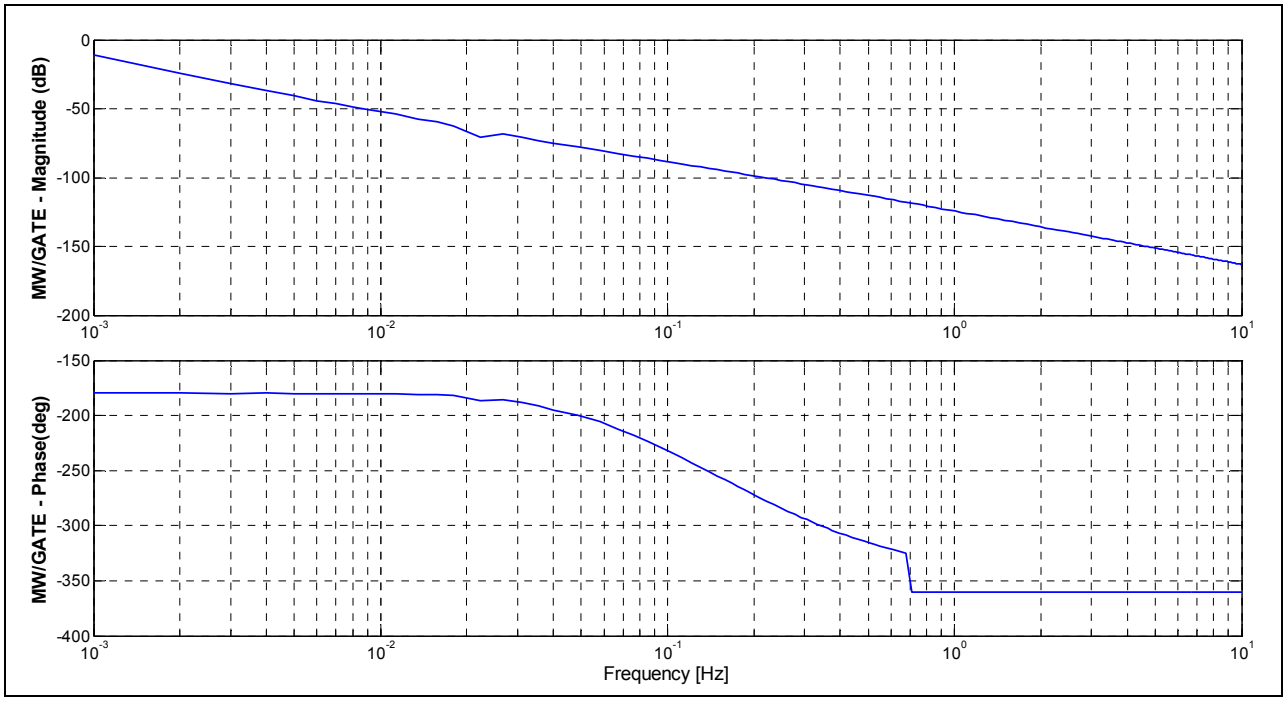

Figure 10-8: Frequency response of the transfer function from Gate position to Mechanical Power of Model 2

The relationship between the mechanical torque and the variation of gate position is studied in order to analyze the dynamic behaviour of the system. The perturbation signal is applied to the gate position in open loop conditions and the signal mechanical torque is monitored. The magnitude and phase of the frequency response of the transfer function of the hydraulic turbine are plotted in Figure 10-9.

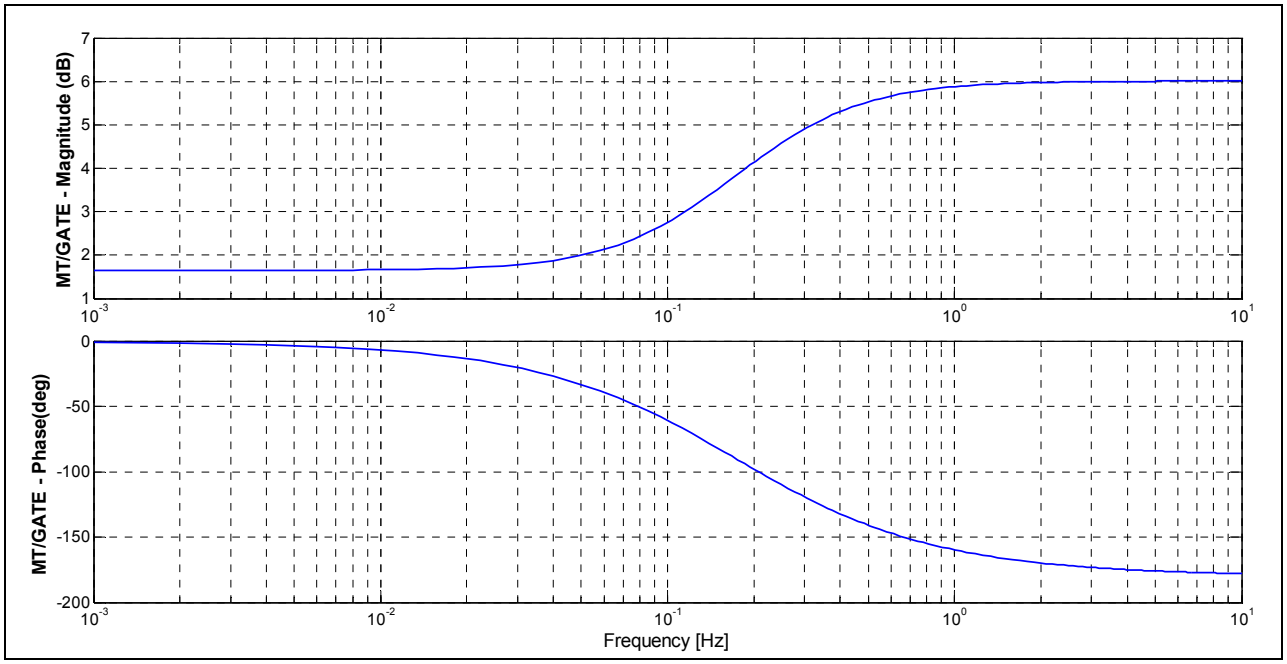

Figure 10-9: Frequency response of the transfer function from Gate position to Mechanical Torque of Model 2

Figure 10-10 plots the computed frequency response of the transfer function of the conduit system of the Model 2. The transfer function of the conduit system relates the Pressure Head to gate position.

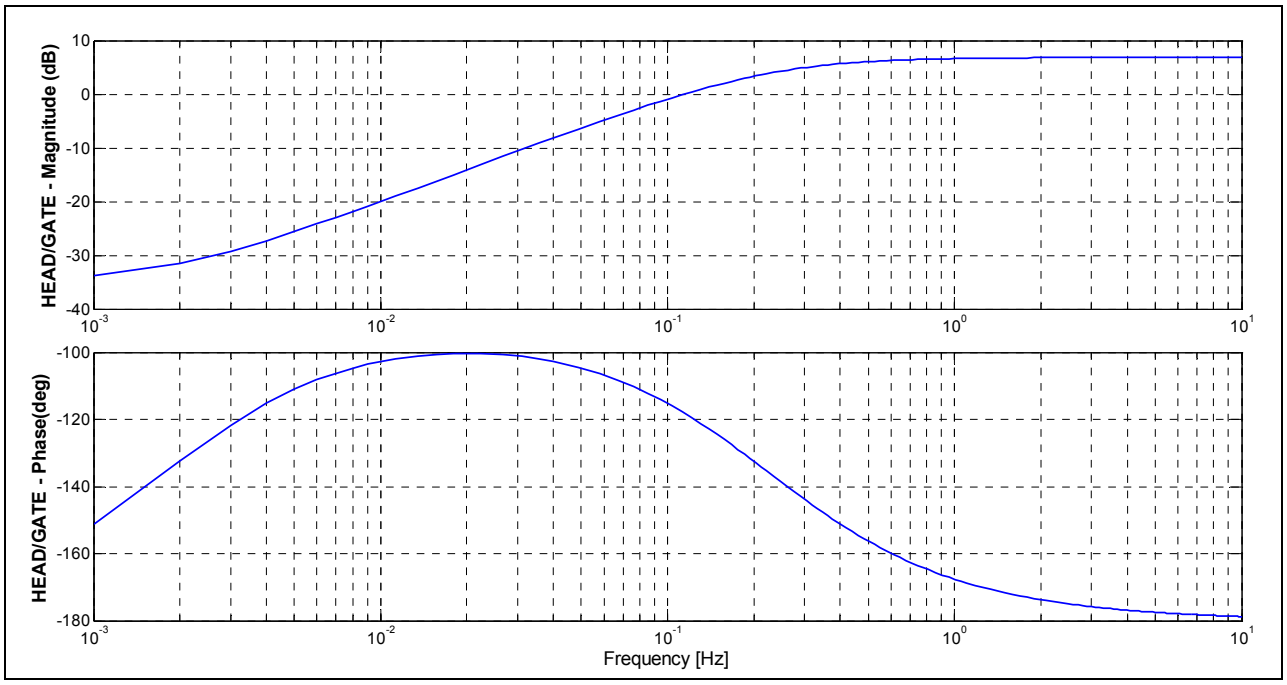

Figure 10-10: Frequency response of the transfer function of the conduit system of Model 2

Figure 10-11 plots the magnitude and phase of the transfer function from gate position to Electrical Power Angle.

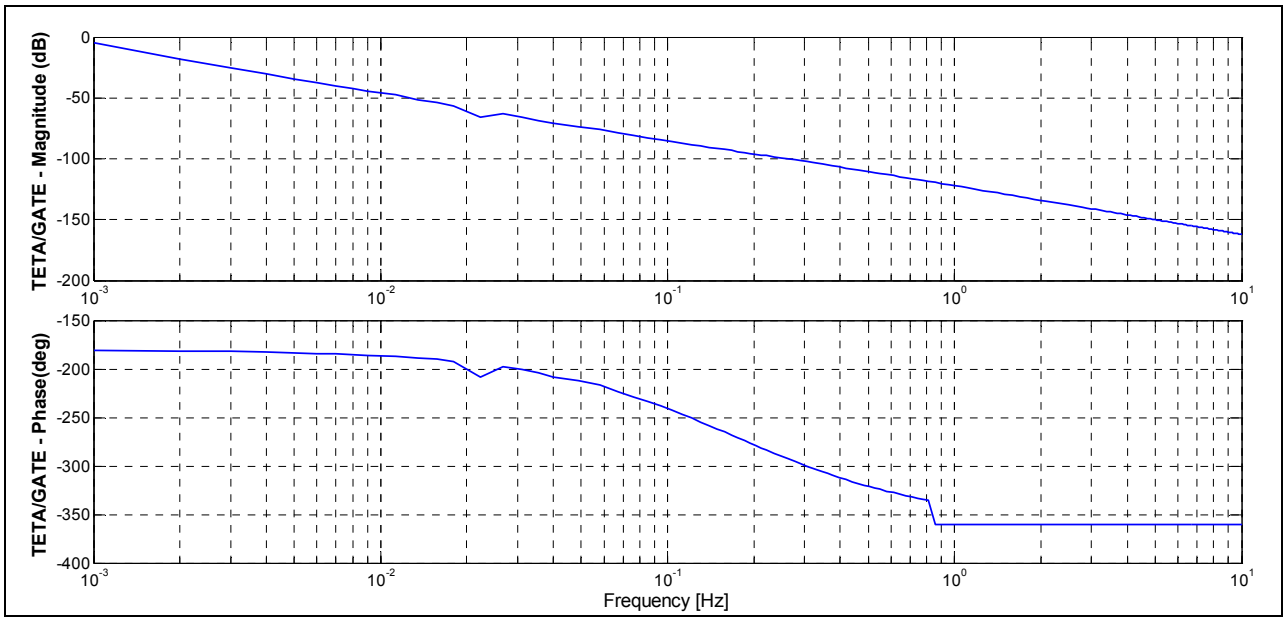

Figure 10-11: Frequency response of the transfer function from Gate position to Electrical Angle of Model 2

The magnitude and phase of the transfer function of the mechanical-hydraulic governor are plotted in Figure 10-12. The transfer function of the governor relates the gate position to speed changes.

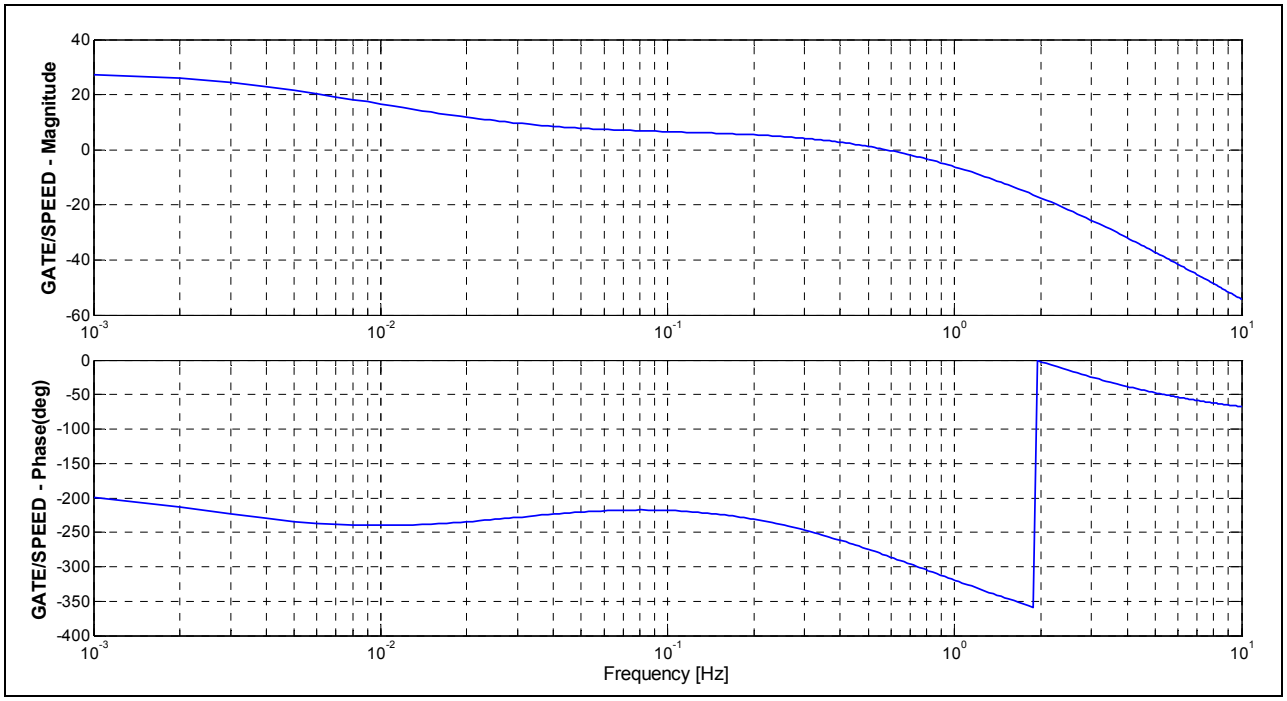

Figure 10-12: Frequency Response of the transfer function of the mechanical-hydraulic governor of Model 2

10.3 MODEL 3: Nonlinear Turbine Model without Surge Tank including Elastic Water Column Effects

The hydraulic turbine in the model 3 is represented by a *Nonlinear Turbine Model without Surge Tank including Elastic Water Column Effects,* described in Chapter 6.2.3. The Penstock is modelled taking into account the elastic water hammer theory and the hydraulic friction losses. The nonlinear characteristics of the hydraulic turbine are neglected in this model. The block diagram of this configuration is shown in Figure 6-4.

The parameters of the Hydro Power Plant and operating conditions are detailed in Chapter 9. This model was implemented in DSL Code Generator which is a tool used for making self-defined dynamic models for dynamic simulation in SIMPOW.

10.3.1 Eigenvalue Analysis

Table 10-5 shows the real-valued eigenvalues, non-real-valued eigenvalues and the state variables that have the highest participation of the test system with a Nonlinear Turbine Model without Surge Tank including Elastic Water Column Effects.

Table 10-5: Eigenvalues and the state variable for the Turbine Model 3

	Eigenvalue			Damping Ratio	Frequency [Hz]	Dominant States
	Real, [1/s]		Imag, [Hz]			
1	-23.0313		0.0000	-	-	$\Delta\psi_D$
2	-17.5710		0.0000	-	-	Δy
3,4	-0.5188	±	1.0587	0.07775	1.05872	$\Delta\omega$ and $\Delta\delta$
5	-6.8018		0.0000	-	-	$\Delta\psi_Q$
6,7	-3.6763	±	0.2128	0.93977	0.21280	Δy
8	-1.3377		0.0000	-	-	
9	-0.0167		0.0000	-	-	Δy
10	-0.1814		0.0000	-	-	$\Delta\psi_f$
11	-1.0000		0.0000	-	-	

It is seen in Table 10-5 that

- All eigenvalues have negative real part.
- The system is stable.
- λ_1, λ_2, λ_5, λ_8, λ_9, λ_{10}, and λ_{11} influence the dynamic system with pure damping.
- $\lambda_{3,4}$ and $\lambda_{6,7}$ influence the dynamic simulation with both damping and oscillation.
- The oscillatory mode $\lambda_{3,4}$ have a damped frequency of 1.0587 Hz. The oscillations decay with a time constant of 1/0.5188 s. This corresponds to a damping ratio ζ of 0.0778.

The magnitudes of the participation factors, computed in SIMPOW, are shown in Table 10-6. The angles of the participation factors do not provide any useful information. From the participation matrix, $\Delta\delta$ and $\Delta\omega$ have a high participation in the oscillatory mode associated to the eigenvalues $\lambda_{3,4}$. The field flux linkage has a high participation in the non-oscillatory mode represented by the eigenvalue λ_{10}. The d-axis flux linkage has a high participation on the non-oscillatory mode represented by the eigenvalue λ_1. The q-axis flux linkage has a high participation on the non-oscillatory mode represented by the eigenvalue λ_5.

Table 10-6: Participation factors matrix of a Turbine Model 3

	λ_1	λ_2	λ_3, λ_4	λ_5	λ_6, λ_7	λ_8	λ_9	λ_{10}
$\Delta\delta$	0.00614	0.00076	0.55712	0.02676	0.22299	0.10336	0.00337	0.00081
$\Delta\omega$	0.00572	0.00584	0.54235	0.01463	0.08774	0.00410		0.00042
$\Delta\psi_f$	0.00572	0.00002	0.00742	0.00027	0.00784	0.01188	0.00013	0.98850
$\Delta\psi_D$	1.00644	0.00087	0.01325	0.00064	0.00436	0.00025	0.00000	0.00873
$\Delta\psi_Q$	0.00004	0.00013	0.03659	0.97540	0.06619	0.00365	0.00000	0.00192

10.3.2 Dynamic Simulation Analysis

Figure 10-13 shows the result of simulating a three-phase fault to ground on bus BUS2 at t=1 s. This disturbance is simulated for a period of 5.0 ms. The simulation results of a simple turbine without surge tank represented by model 3 shows the dynamic behaviour of the power angle, rotational speed, mechanical torque, gate position, flow rate and head pressure.

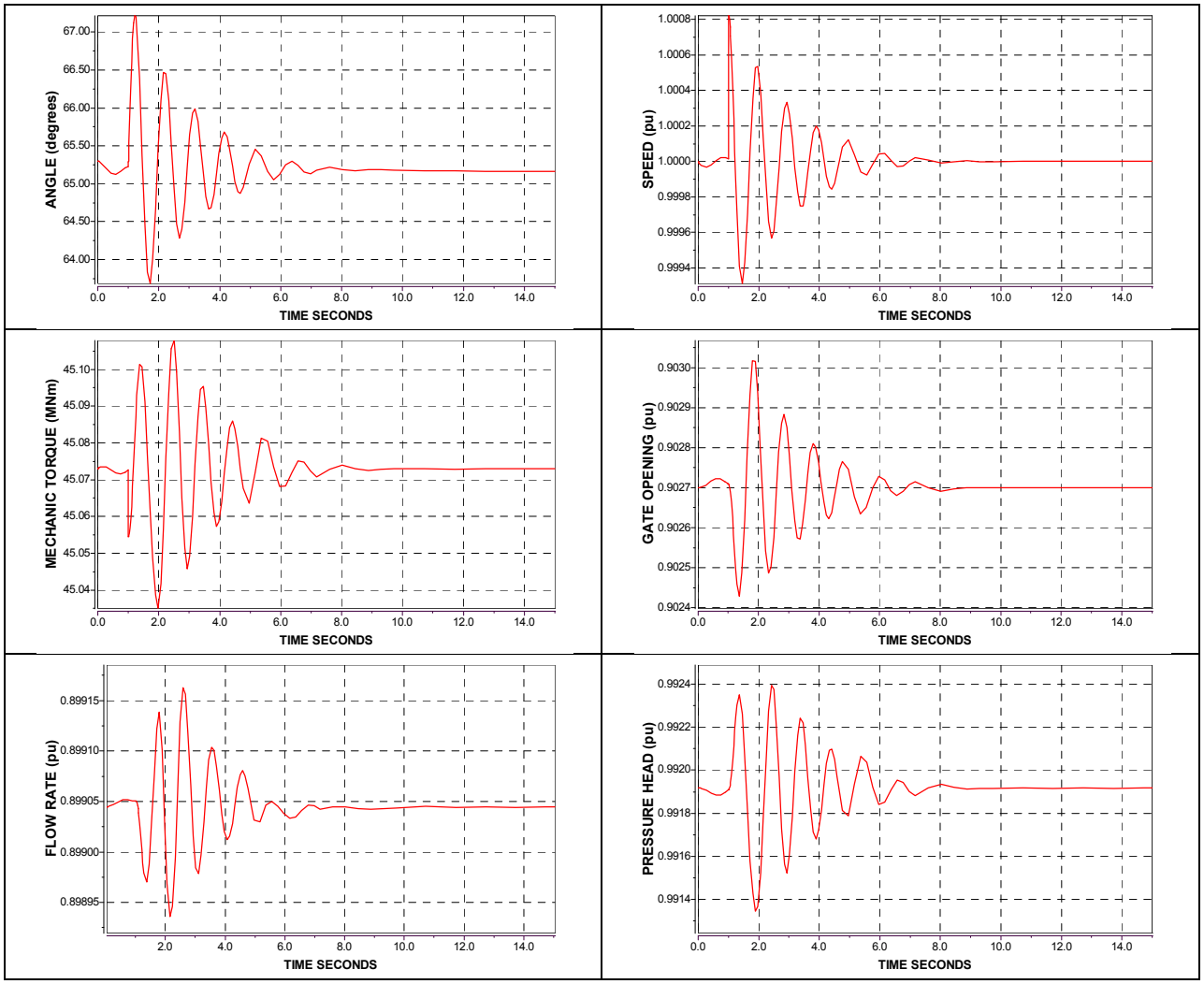

Figure 10-13: Fault simulation results: (a) angle, (b) speed, (c) mechanical torque, (d) gate position, (e) flow rate and (f) water pressure of Model 3

The initial value of the Mechanical Power is 44.94 MW. After the fault is simulated, the Mechanical Power drops to 0.00 MW. The Mechanical Power oscillates for a period of 5.5 seconds, approximately.

The electrical angle oscillates for a period of 7.60 seconds. The minimum value is 63.6860° at 1.72 seconds and the maximum value is 67.2146° at 1.21 seconds. The value of the electrical angle at steady-state is 65.16°.

The rotational speed oscillates between the values of 0.9993 pu and 1.0008 pu. The rotational speed recovers stability after 8 seconds, demonstrating that the dynamic response of the hydro power plant is efficient.

The initial value of Mechanical Torque and Electric Torque are 45.07 MNm and -45.14 MNm, respectively. The Mechanic Torque oscillates for a period of 8 seconds, between the values of 45.04 MNm and 45.11 MNm. The Mechanical Torque at steady state is 45.0730 MNm. The period of oscillation of Electrical Torque is 5.50 seconds, approximately. Electrical Torque oscillates between the values of -46.49 MNm and -1.38 MNm. The Electrical Torque at steady state is -45.07 MNm.

The variables Gate Opening, Flow rate and Pressure Head are measured in per unit. Gate opening oscillates between 0.9024 and 0.9030. The flow varies between 0.8989 and 0.8991. The pressure head oscillates between 0.9913 and 0.9923. The values of Gate position, Flow rate and Pressure Head at steady-state are 0.9027, 0.8990 and 0.9919, respectively.

10.3.3 Frequency Response Analysis

The magnitude and phase of the transfer function from gate position to Mechanical Power of a Nonlinear Turbine Model without Surge Tank including Elastic Water Column Effects are plotted in Figure 10-8. The perturbation signal is applied to the gate position in open loop conditions and the signal mechanical power is monitored.

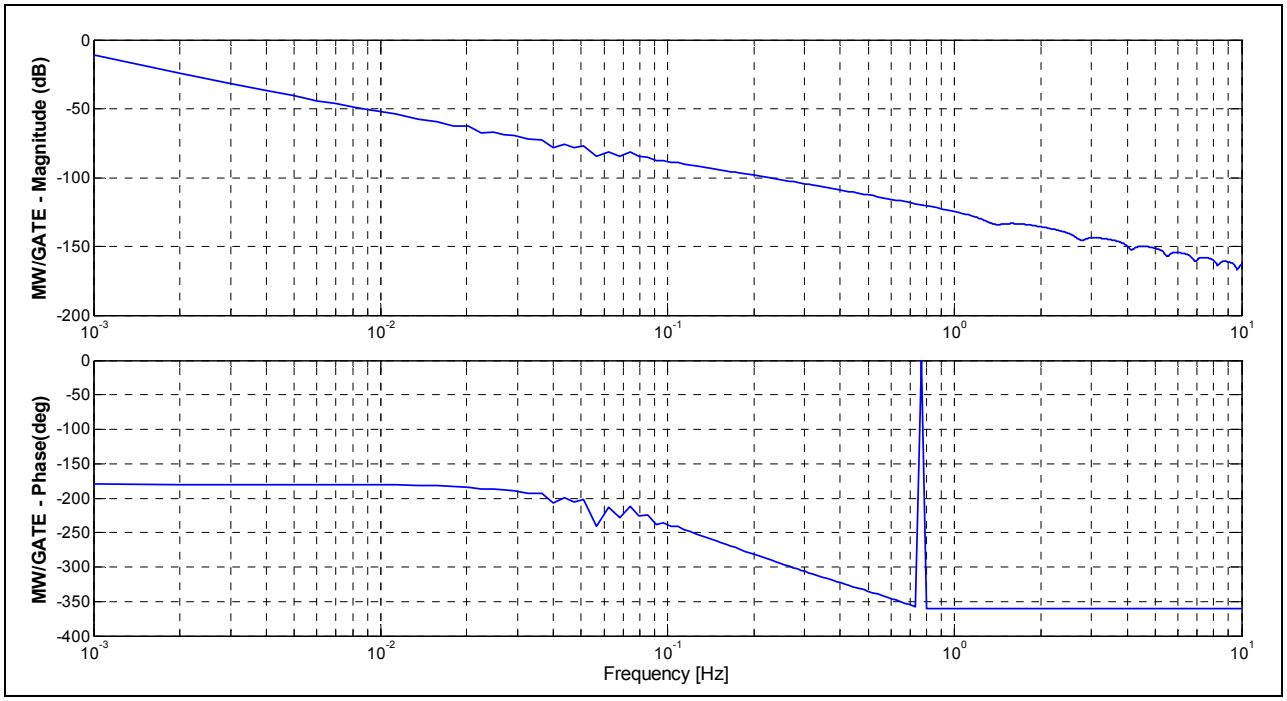

Figure 10-14: Frequency response of the transfer function from Gate position to Mechanical Power of Model 3

The relationship between the mechanical torque and the variation of gate position is studied in order to analyze the dynamic behaviour of the system. The perturbation signal is applied to the gate position in open loop conditions and the signal mechanical torque is monitored. The magnitude and phase of the frequency response of the transfer function of the hydraulic turbine are plotted in Figure 10-15.

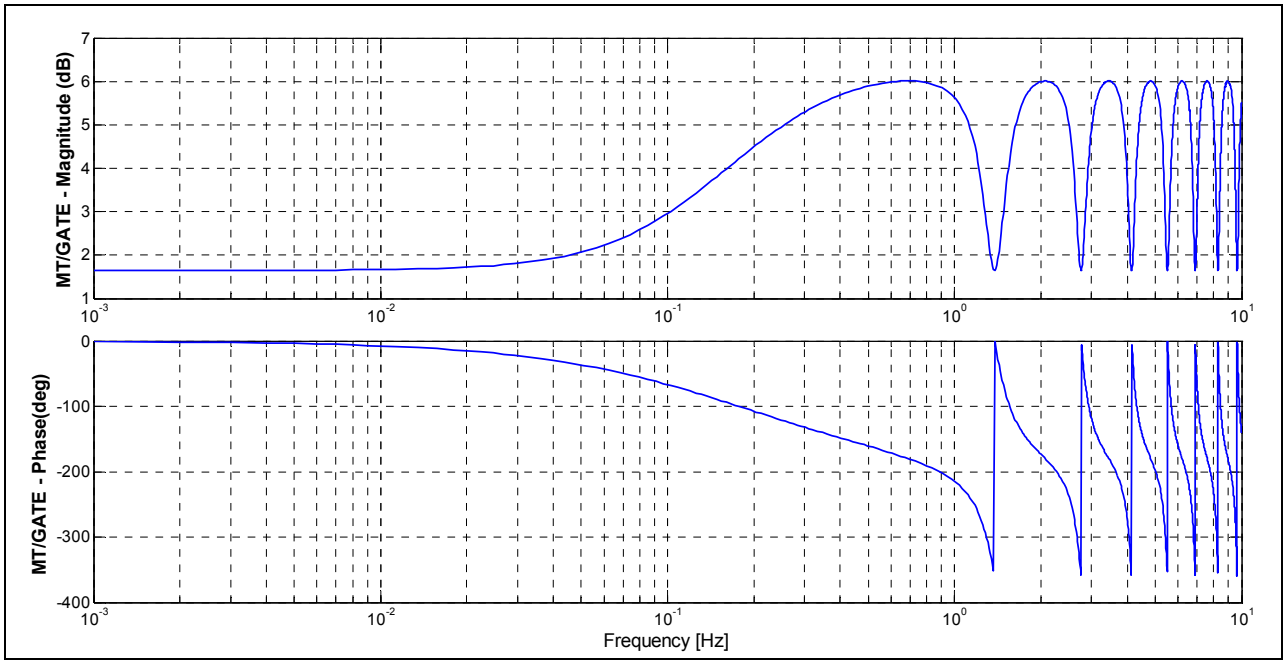

Figure 10-15: Frequency response of the transfer function from Gate position to Mechanical Torque of Model 3

Figure 10-16 plots the computed frequency response of the transfer function of the conduit system of the Model 3. The transfer function of the conduit system relates the water pressure to gate position.

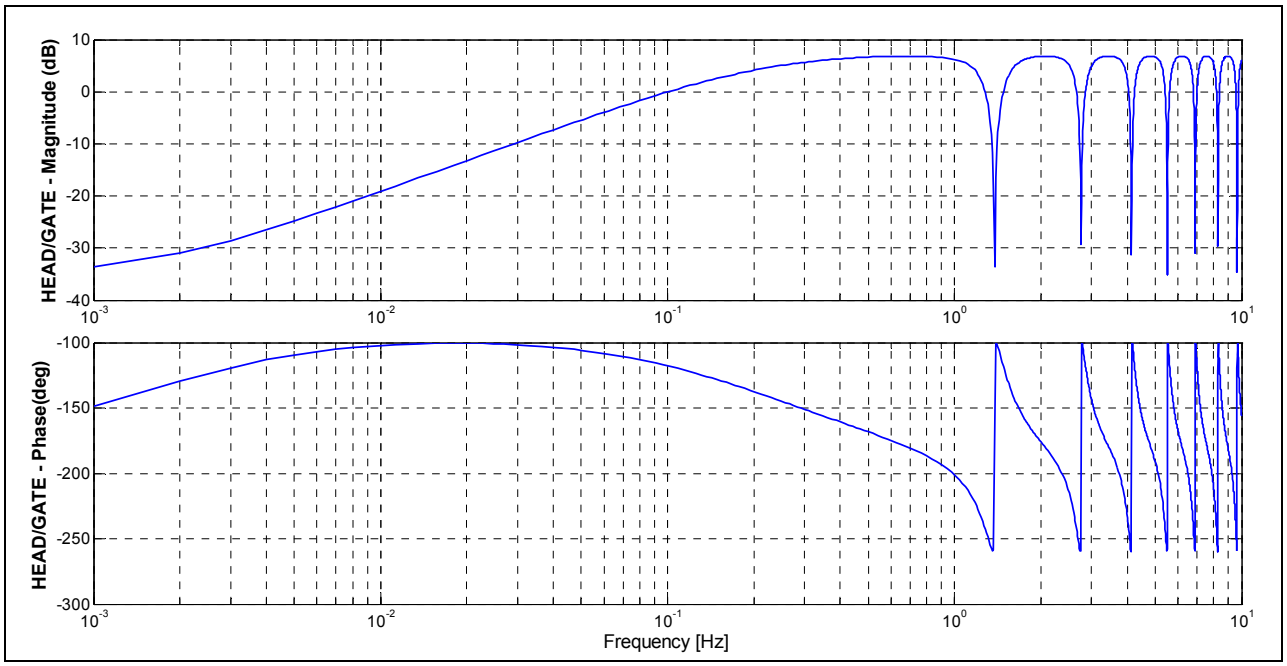

Figure 10-16: Frequency Response of the transfer function of the conduit system of Model 3

Figure 10-17 plots the magnitude and phase of the transfer function from gate position to Electrical Power Angle.

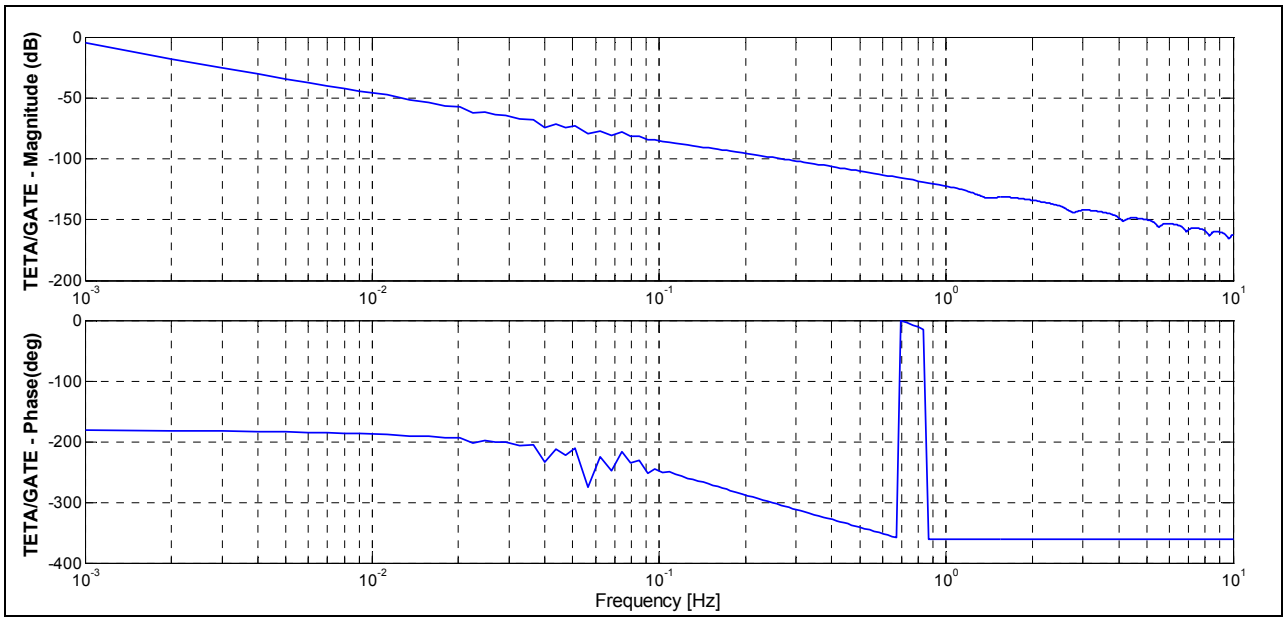

Figure 10-17: Frequency response of the transfer function from Gate position to Electrical Angle of Model 3

The magnitude and phase of the transfer function of the mechanical-hydraulic governor are plotted in Figure 10-18. The transfer function of the governor relates the gate position to speed changes.

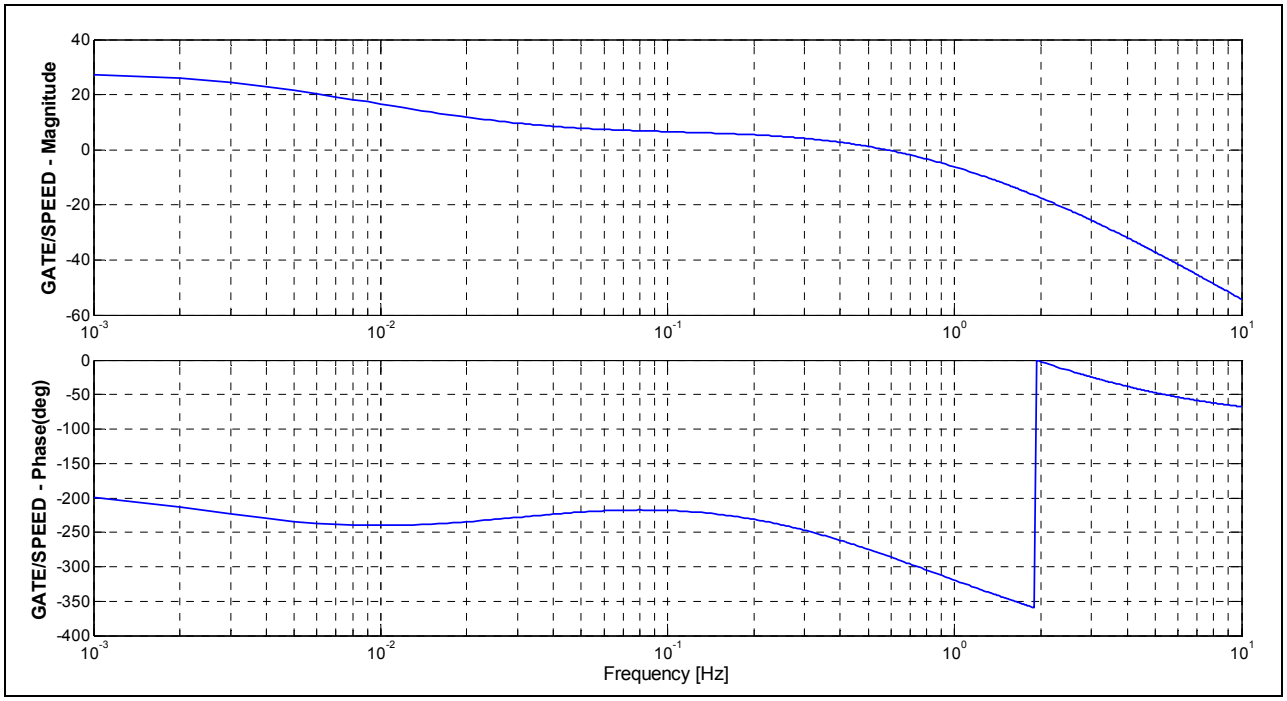

Figure 10-18: Frequency Response of the transfer function of the mechanical-hydraulic governor of Model 3

10.4 MODEL 4: Nonlinear Turbine Model with Surge Tank assuming Inelastic Water Columns

The hydraulic turbine in the model 4 is represented by a *Nonlinear Turbine Model with Surge Tank assuming Inelastic Water Columns in Penstock and Tunnel,* described in Chapter 6.2.4. The upstream tunnel and penstock are modelled assuming an incompressible fluid and a rigid conduit where the travelling pressure wave effects are relatively insignificantly. The nonlinear characteristics of hydraulic turbine are neglected in this model. The block diagram of this configuration is shown in Figure 6-5. The parameters of the Hydro Power Plant and operating conditions are detailed in Chapter 9. This model was implemented in DSL Code Generator which is a tool used for making self-defined dynamic models for dynamic simulation in SIMPOW.

10.4.1 Eigenvalue Analysis

Table 10-7 shows the real-valued eigenvalues, non-real-valued eigenvalues and the state variables that have the highest participation of the test system with a Nonlinear Turbine Model with Surge Tank Assuming Inelastic Water Columns in Penstock and Tunnel.

Table 10-7: Eigenvalues and the state variable for the turbine Model 4

	Eigenvalue			Damping Ratio	Frequency [Hz]	Dominant States
	Real, [1/s]		Imag, [Hz]			
1	-23.1362		0.0000	-	-	$\Delta\psi_D$
2	-17.5026		0.0000	-	-	
3,4	-0.5102	±	1.1313	0.07160	1.13126	$\Delta\omega$ and $\Delta\delta$
5	-6.5735		0.0000	-	-	$\Delta\psi_Q$
6,7	-3.7469	±	0.0840	0.99021	0.08405	Δy
8	-1.1626		0.0000	-	-	
9	-0.0167		0.0000	-	-	
10,11	-0.0392	±	0.0091	0.56646	0.00909	
12	-0.2060		0.0000	-	-	$\Delta\psi_f$
13	-1.0000		0.0000	-	-	

It is seen Table 10-7 that

- All eigenvalues have negative real part.
- The system is stable.
- λ_1, λ_2, λ_5, λ_8, λ_9, λ_{12}, and λ_{13} influence the dynamic system with pure damping.
- $\lambda_{3,4}$, $\lambda_{6,7}$ and $\lambda_{10,11}$ influence the dynamic simulation with both damping and oscillation.
- The oscillatory mode $\lambda_{3,4}$ have a damped frequency of 1.1313 Hz. The oscillations decay with a time constant of 1/0.5102 s. This corresponds to a damping ratio ζ of 0.0716.

The magnitudes of the participation factors, computed in SIMPOW, are shown in Table 10-8. The angles of the participation factors do not provide any useful information. From the participation matrix, $\Delta\delta$ and $\Delta\omega$ have a high participation in the oscillatory mode associated to the eigenvalues $\lambda_{3,4}$. The field flux linkage has a high participation in the non-oscillatory mode represented by the eigenvalue λ_{12}. The d-axis flux linkage has a high participation on the non-oscillatory mode represented by the eigenvalue λ_1. The q-axis flux linkage has a high participation on the non-oscillatory mode represented by the eigenvalue λ_5.

Table 10-8: Participation factors matrix of a hydraulic turbine Model 4

	λ_1	λ_2	λ_3, λ_4	λ_5	λ_6, λ_7	λ_8	λ_9	$\lambda_{10}, \lambda_{11}$	λ_{12}
$\Delta\delta$	0.00508	0.00041	0.54296	0.04179	0.27162	0.04706	0.00244	0.00032	0.00048
$\Delta\omega$	0.00465	0.00244	0.53682	0.02836	0.10359	0.00131			0.00035
$\Delta\psi_f$	0.00556	0.00001	0.00514	0.00049	0.00893	0.00540	0.00006	0.00004	0.98932
$\Delta\psi_D$	1.00424	0.00030	0.01042	0.00106	0.00451	0.00006			0.00785
$\Delta\psi_Q$	0.00005	0.00008	0.04992	0.98495	0.14922	0.00199	0.00000		0.00223

10.4.2 Dynamic Simulation Analysis

Figure 10-19 shows the result of simulating a three-phase fault to ground on bus BUS2 at t=1 s. This disturbance is simulated for a period of 5.0 ms. The simulation results of a simple turbine with surge tank represented by model 4 show the dynamic behaviour of the power angle, rotational speed, mechanical torque, gate position, flow rate and head pressure.

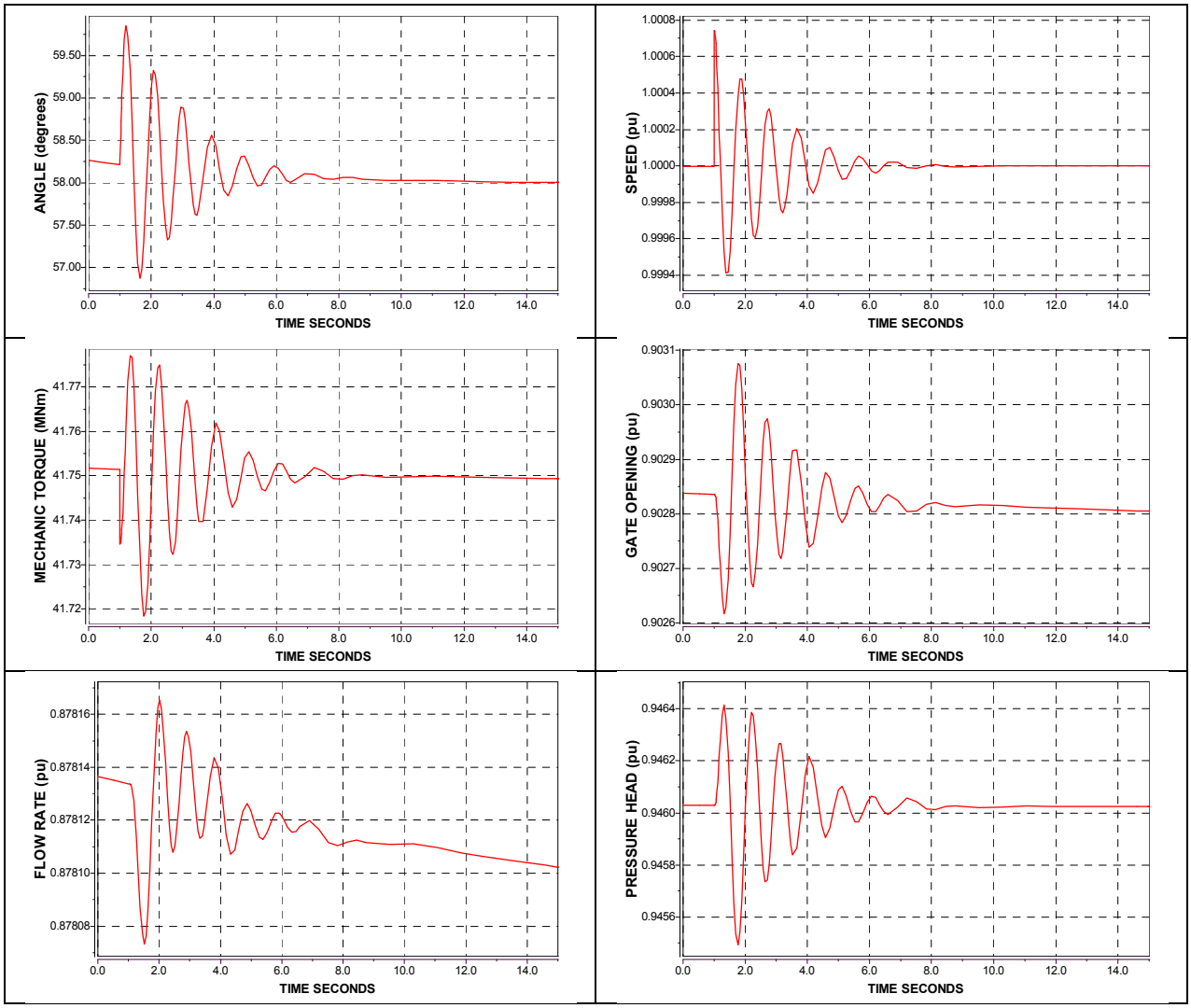

Figure 10-19: Fault simulation results: (a) angle, (b) Speed, (c) Mechanical Torque, (d) Gate Position, (e) Flow Rate and (f) Head Pressure of Model 4

The initial value of the Mechanical Power is 41.64 MW. After the fault is simulated, the Mechanical Power drops to 0.00 MW. The Mechanical Power oscillates for a period of 5.3 seconds, approximately.

The electrical angle oscillates for a period of 8.90 seconds. The minimum value is 56.8832° at 1.63 seconds and the maximum value is 59.8531° at 1.20 seconds. The value of the electrical angle at steady-state is 58.00°.

The rotational speed oscillates between the values of 0.9994 pu and 1.0007 pu. The rotational speed recovers stability after 8 seconds, demonstrating that the dynamic response of the hydro power plant is efficient.

The initial value of Mechanical Torque and Electric Torque are 41.75 MNm and -41.75 MNm, respectively. The Mechanic Torque oscillates for a period of 8 seconds, between the values of 41.7182 MNm and 41.7776 MNm. The Mechanical Torque at steady state is 41.7492 MNm. The period of oscillation of Electrical Torque is 5.50 seconds, approximately. Electrical Torque oscillates between the values of -43.1007 MNm and -1.43839 MNm. The Electrical Torque at steady state is -41.7492 MNm.

The variables Gate Opening, Flow rate and Pressure Head are measured in per unit. Gate opening oscillates between 0.9026 and 0.9030. The flow varies between 0.878059 and 0.878164. The pressure head oscillates between 0.945495 and 0.946452. The values of Gate position, Flow rate and Pressure Head at steady-state are 0.9028, 0.8781 and 0.946032, respectively.

10.4.3 Frequency Response Analysis

The magnitude and phase of the transfer function from gate position to Mechanical Power of a Nonlinear Turbine Model with Surge Tank assuming Inelastic Water Columns in Penstock and Tunnel are plotted in Figure 10-20. The perturbation signal is applied to the gate position in open loop conditions and the signal mechanical power is monitored.

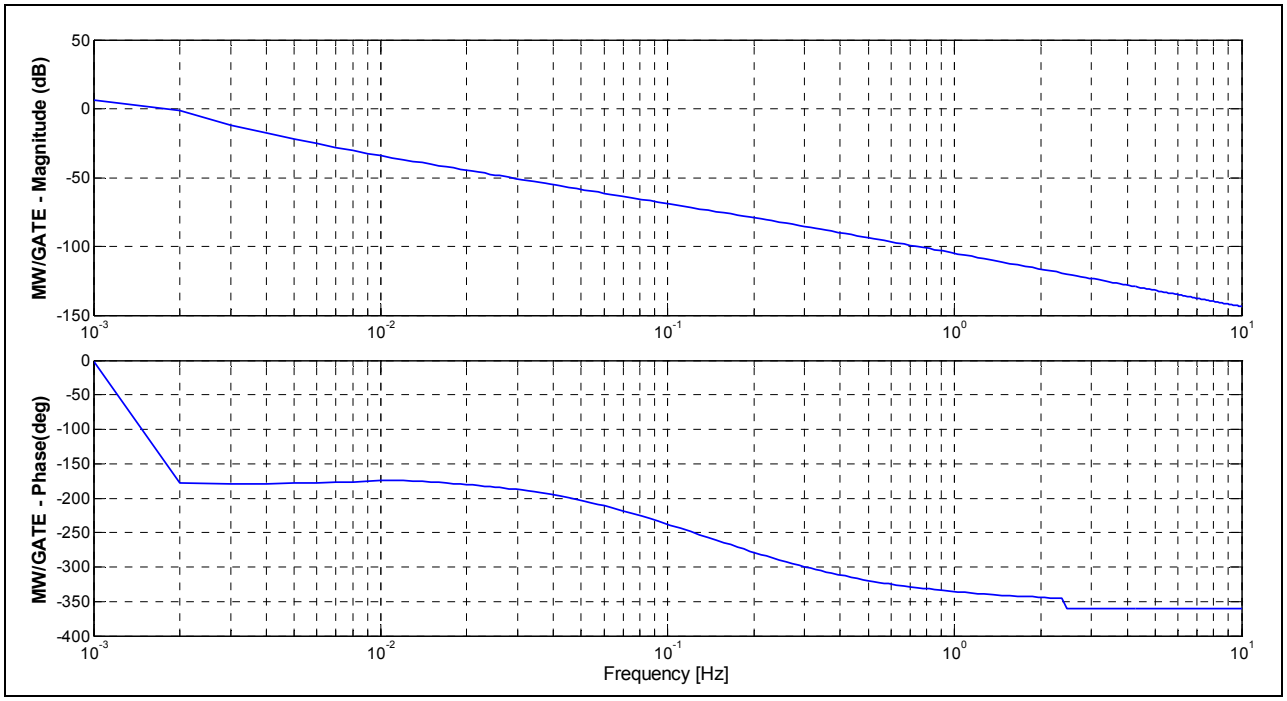

Figure 10-20: Frequency response of the transfer function from Gate position to Mechanical Power of Model 4

The relationship between the mechanical torque and the variation of gate position is studied in order to analyze the dynamic behaviour of the system. The perturbation signal is applied to the gate position in open loop conditions and the signal mechanical torque is monitored. The magnitude and phase of the frequency response of the transfer function of the hydraulic turbine are plotted in Figure 10-21.

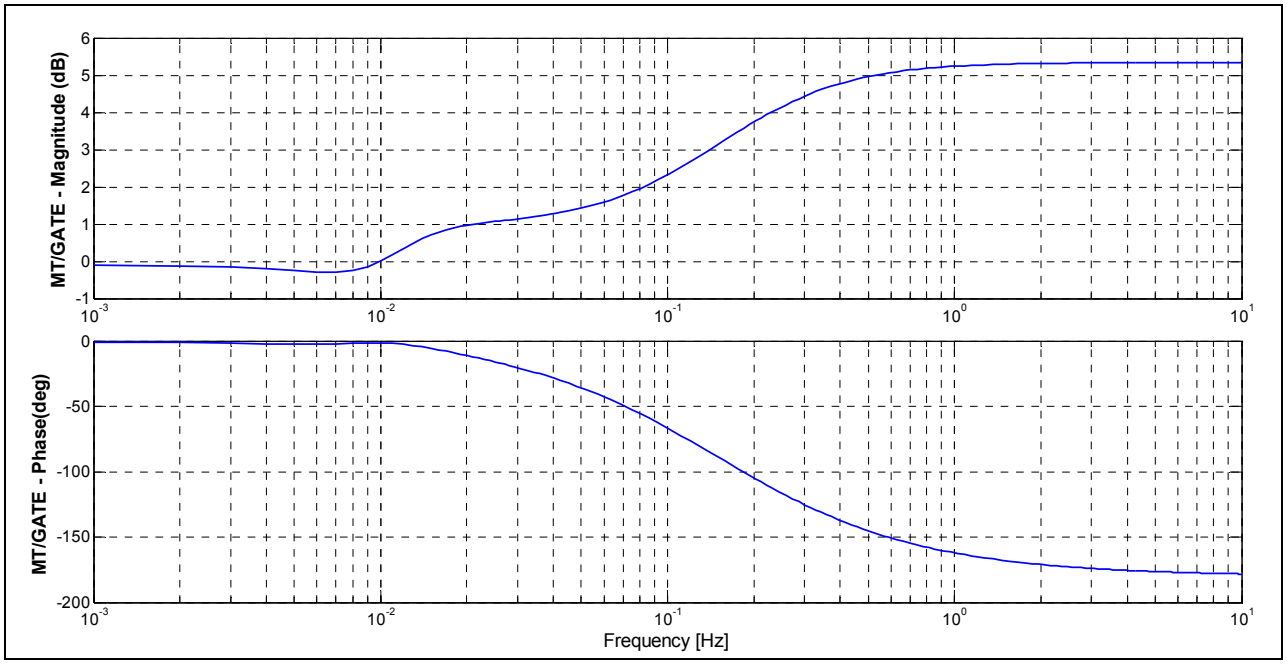

Figure 10-21: Frequency response of the transfer function from Gate position to Mechanical Torque of Model 4

Figure 10-22 plots the computed frequency response of the transfer function of the conduit system of model 4. The transfer function of the conduit system relates the Pressure Head to gate position.

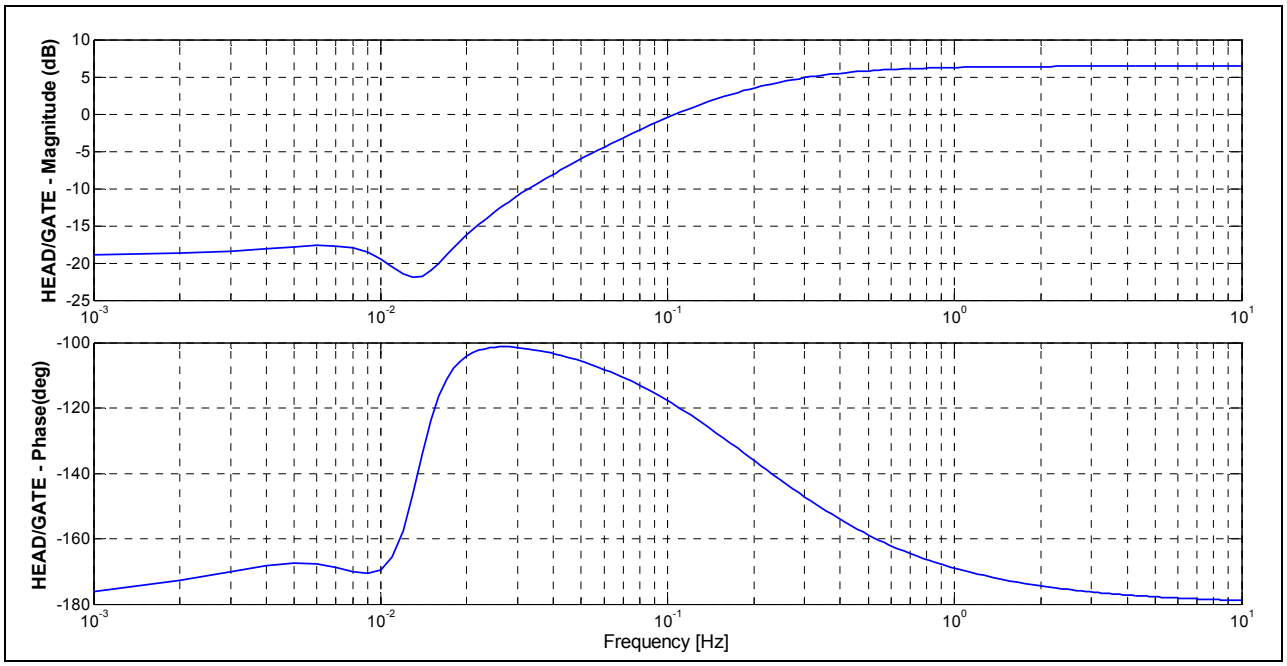

Figure 10-22: Frequency Response of the transfer function of the conduit system of Model 4

Figure 10-23 plots the magnitude and phase of the transfer function from gate position to Electrical Power Angle.

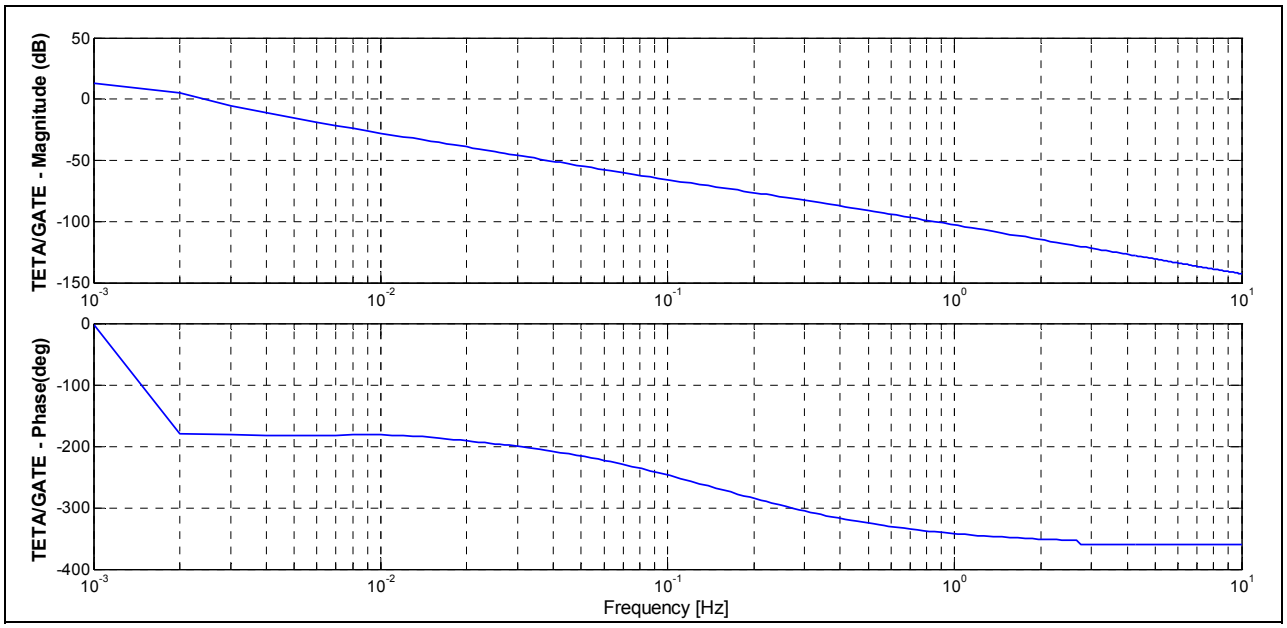

Figure 10-23: Frequency response of the transfer function from Gate position to Electrical Angle of Model 4

The magnitude and phase of the transfer function of the mechanical-hydraulic governor are plotted in Figure 10-24. The transfer function of the governor relates the gate position to speed changes.

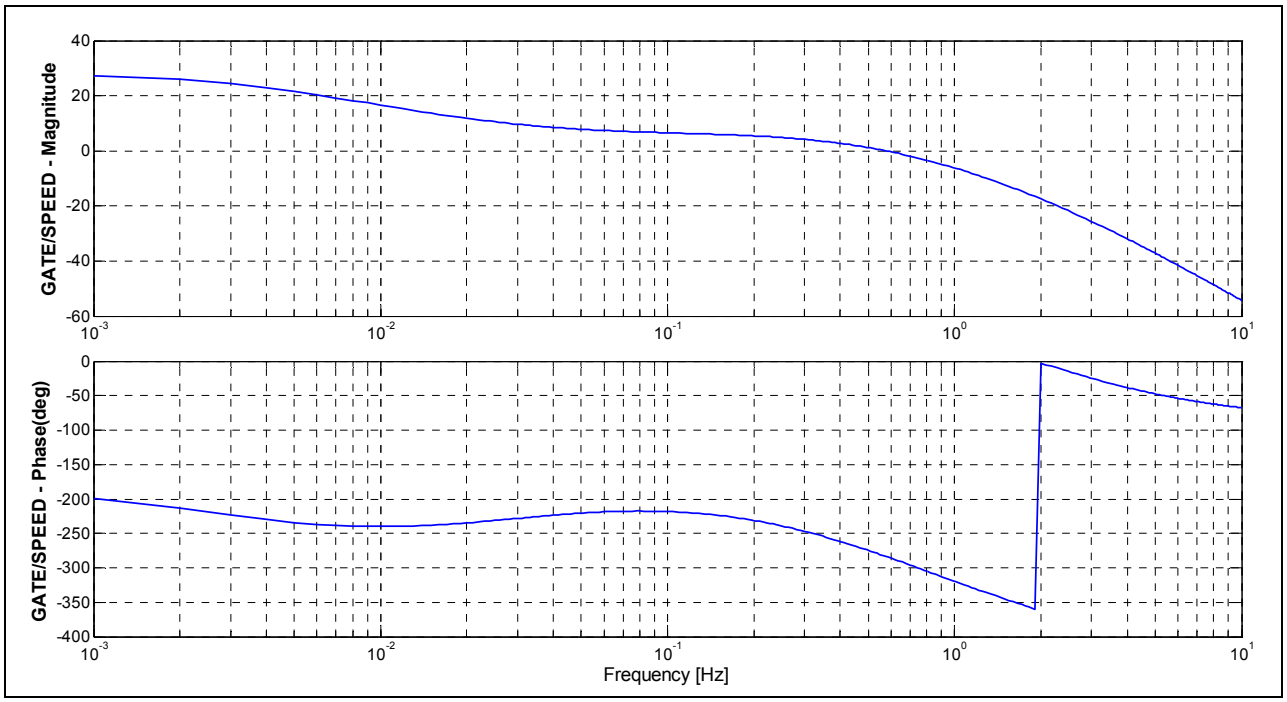

Figure 10-24: Frequency Response of the transfer function of the mechanical-hydraulic governor of Model 4

10.5 MODEL 5: Nonlinear Model with Surge Tank assuming Elastic Water Column in Penstock and Inelastic Water Column in Tunnel

The hydraulic turbine in the model 5 is represented by a *Nonlinear Turbine Model with Surge Tank assuming Elastic Water Column in Penstock and Inelastic Water Column in Tunnel,* described in Chapter 6.2.5. Penstock is modelled taking into account the elastic water hammer theory. The nonlinear characteristics of hydraulic turbine are not considered in this model. The block diagram of this configuration is shown in Figure 6-6. This model was implemented in DSL Code Generator which is a tool used for making self-defined dynamic models for dynamic simulation in SIMPOW. The parameters of the Hydro Power Plant and operating conditions are detailed in Chapter 9.

10.5.1 Eigenvalue Analysis

Table 10-9 shows the real-valued eigenvalues, non-real-valued eigenvalues and the state variables that have the highest participation of the test system with a Nonlinear Model with Surge Tank assuming Elastic Water Column in Penstock and Inelastic Water Column in Tunnel.

Table 10-9: Eigenvalues and state variables for Model 5

	Eigenvalue			Damping Ratio	Frequency [Hz]	Dominant States
	Real, [1/s]		Imag, [Hz]			
1	-23.1350		0.0000	-	-	$\Delta\psi_D$
2	-17.5566		0.0000	-	-	Δy
3,4	-0.5933	±	1.1269	0.08350	1.12692	$\Delta\omega$ and $\Delta\delta$
5	-6.6476		0.0000	-	-	$\Delta\psi_Q$
6,7	-3.6479	±	0.1899	0.95044	0.18991	Δy
8	-1.3158		0.0000	-	-	
9,10	-0.0392	±	0.0091	0.56646	0.00909	
11	-0.0167		0.0000	-	-	Δy
12	-0.2059		0.0000	-	-	$\Delta\psi_f$
13	-1.0000		0.0000	-	-	

It is seen in Table 10-9 that

- All eigenvalues have negative real part.
- The system is stable.
- λ_1, λ_2, λ_5, λ_8, λ_{11}, λ_{12}, and λ_{13} influence the dynamic system with pure damping.
- $\lambda_{3,4}$, $\lambda_{6,7}$ and $\lambda_{9,10}$ influence the dynamic simulation with both damping and oscillation.
- The oscillatory mode $\lambda_{3,4}$ have a damped frequency of 1.1269 Hz. The oscillations decay with a time constant of 1/0.5933 s. This corresponds to a damping ratio ζ of 0.0835.

The magnitudes of the participation factors, computed in SIMPOW, are shown in Table 10-10. The angles of the participation factors do not provide any useful information. From the participation matrix, $\Delta\delta$ and $\Delta\omega$ have a high participation in the oscillatory mode associated to the eigenvalues $\lambda_{3,4}$. The field flux linkage has a high participation in the non-oscillatory mode represented by the eigenvalue λ_{12}. The d-axis flux linkage has a high participation on the non-oscillatory mode represented by the eigenvalue λ_1. The q-axis flux linkage has a high participation on the non-oscillatory mode represented by the eigenvalue λ_5.

Table 10-10: Participation factors matrix for Model 5

	λ_1	λ_2	λ_3, λ_4	λ_5	λ_6, λ_7	λ_8	λ_9, λ_{10}	λ_{11}	λ_{12}
$\Delta\delta$	0.00510	0.00083	0.55426	0.03864	0.21962	0.09201	0.00019	0.00225	0.00049
$\Delta\omega$	0.00469	0.00500	0.54516	0.02059	0.08119	0.00334			0.00035
$\Delta\psi_f$	0.00556	0.00001	0.00528	0.00034	0.00662	0.00887	0.00002	0.00006	0.98932
$\Delta\psi_D$	1.00443	0.00062	0.01068	0.00077	0.00349	0.00017			0.00785
$\Delta\psi_Q$	0.00005	0.00017	0.05161	0.95721	0.09945	0.00473		0.00000	0.00223

10.5.2 Dynamic Simulation Analysis

Figure 10-25 shows the result of simulating a three-phase fault to ground on bus BUS2 at t=1 s. This disturbance is simulated for a period of 5.0 ms. The simulation results of a simple turbine with surge tank represented by model 5 shows the dynamic behaviour of the power angle, rotational speed, mechanical torque, gate position, flow rate and head pressure.

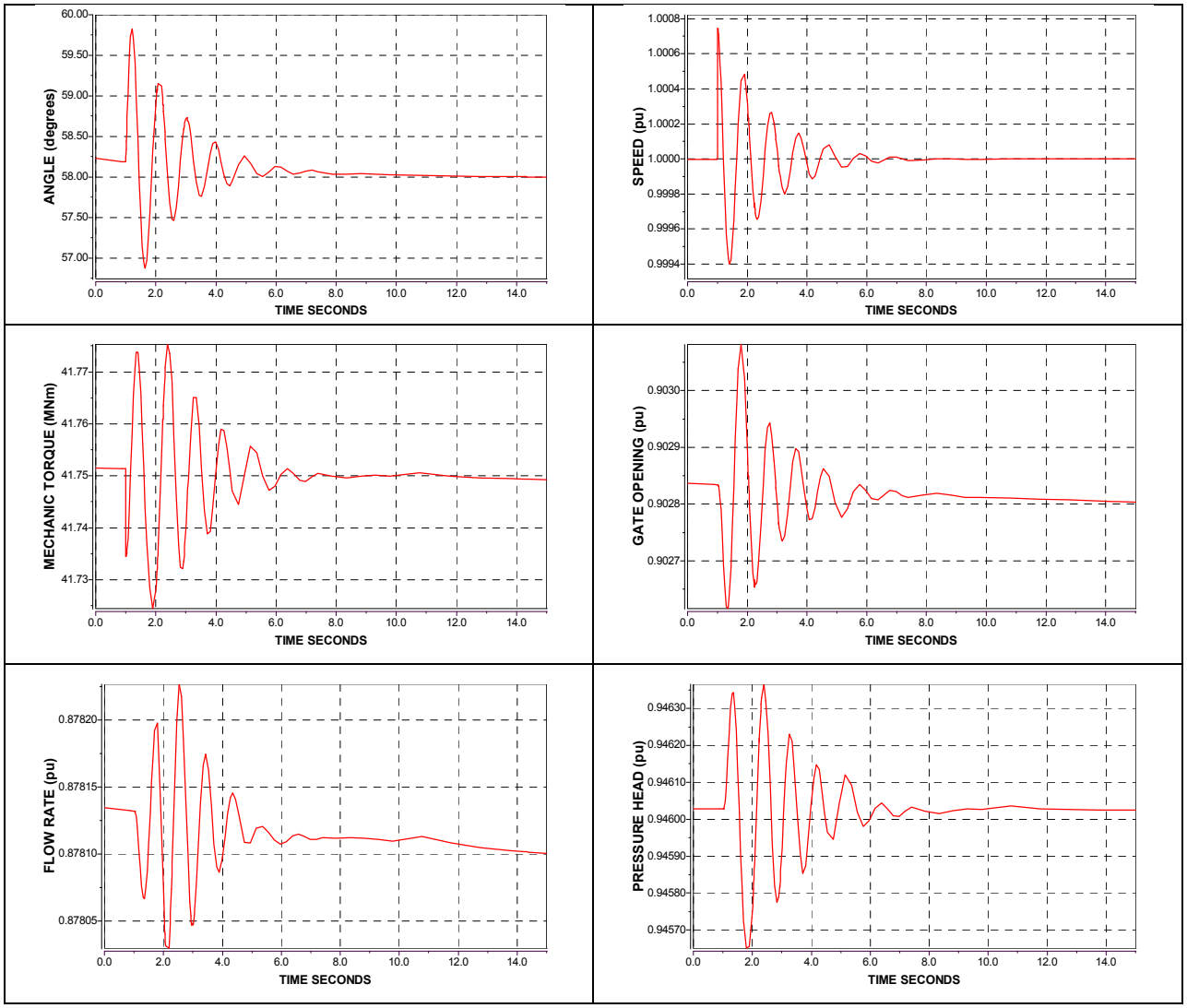

Figure 10-25: Fault simulation Results: (a) angle, (b) Speed, (c) mechanical torque, (d) gate position, (e) flow rate and (f) water pressure of Model 5

The initial value of the Mechanical Power is 41.64 MW. After the fault is simulated, the Mechanical Power drops to 0.00 MW. The Mechanical Power oscillates for a period of 4.4 seconds, approximately.

The electrical angle oscillates for a period of 7.60 seconds. The minimum value is 56.8765° at 1.65 seconds and the maximum value is 59.8244° at 1.21 seconds. The value of the electrical angle at steady-state is 57.99°.

The rotational speed oscillates between the values of 0.9994 pu and 1.0008 pu. The rotational speed recovers stability after 8 seconds, demonstrating that the dynamic response of the hydro power plant is efficient.

The initial value of Mechanical Torque and Electric Torque are 41.7515 MNm and -41.75 MNm, respectively. The Mechanic Torque oscillates for a period of 8 seconds, between the values of 41.7245 MNm and 41.7753 MNm. The Mechanical Torque at steady state is 41.7493 MNm. The period of oscillation of Electrical Torque is 5.50 seconds, approximately. Electrical Torque oscillates between the values of -43.1092 MNm and -1.43937 MNm. The Electrical Torque at steady state is -41.7493 MNm.

The variables Gate Opening, Flow rate and Pressure Head are measured in per unit. Gate opening oscillates between 0.9026 and 0.9031. The flow varies between 0.8780 and 0.8782. The pressure head oscillates between 0.9457 and 0.9464. The values of Gate position, Flow rate and Pressure Head at steady-state are 0.9028, 0.8780 and 0.9460, respectively.

10.5.3 Frequency Response Analysis

The magnitude and phase of the transfer function from gate position to Mechanical Power of a Nonlinear Model with Surge Tank assuming Elastic Water Column in Penstock and Inelastic Water Column in Upstream Tunnel are plotted in Figure 10-26. The perturbation signal is applied to the gate position in open loop conditions and the signal mechanical power is monitored.

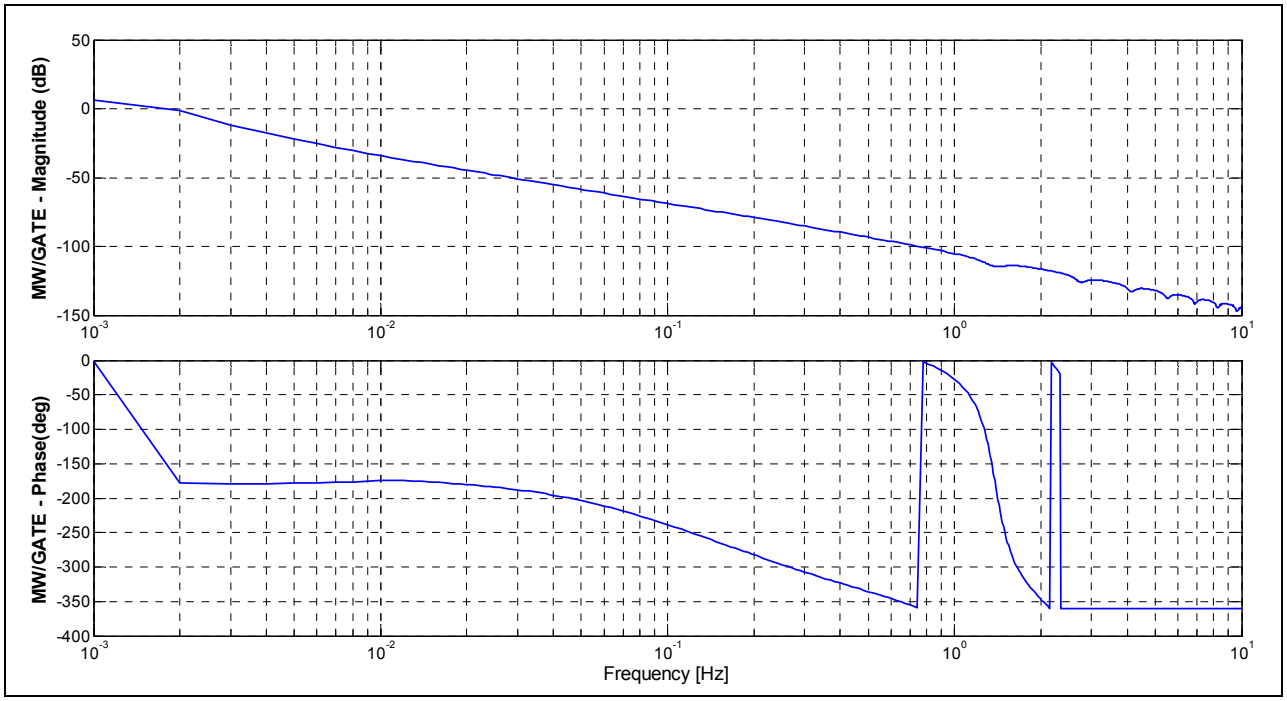

Figure 10-26: Frequency response of the transfer function from Gate position to Mechanical Power of Model 5

The relationship between the mechanical torque and the variation of gate position is studied in order to analyze the dynamic behaviour of the system. The perturbation signal is applied to the gate position in open loop conditions and the signal mechanical torque is monitored. The magnitude and phase of the frequency response of the transfer function of the hydraulic turbine are plotted in Figure 10-27.

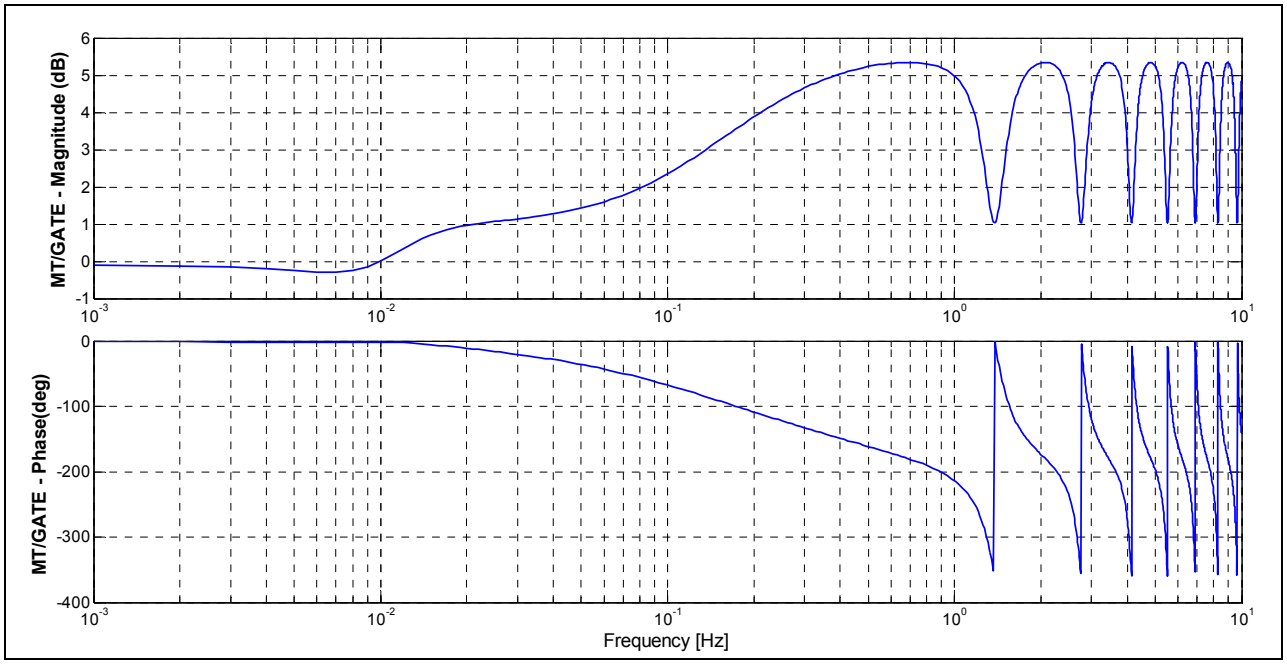

Figure 10-27: Frequency response of the transfer function from Gate position to Mechanical Torque of Model 5

Figure 10-28 plots the computed frequency response of the transfer function of the conduit system of model 5. The transfer function of the conduit system relates the Pressure Head to gate position.

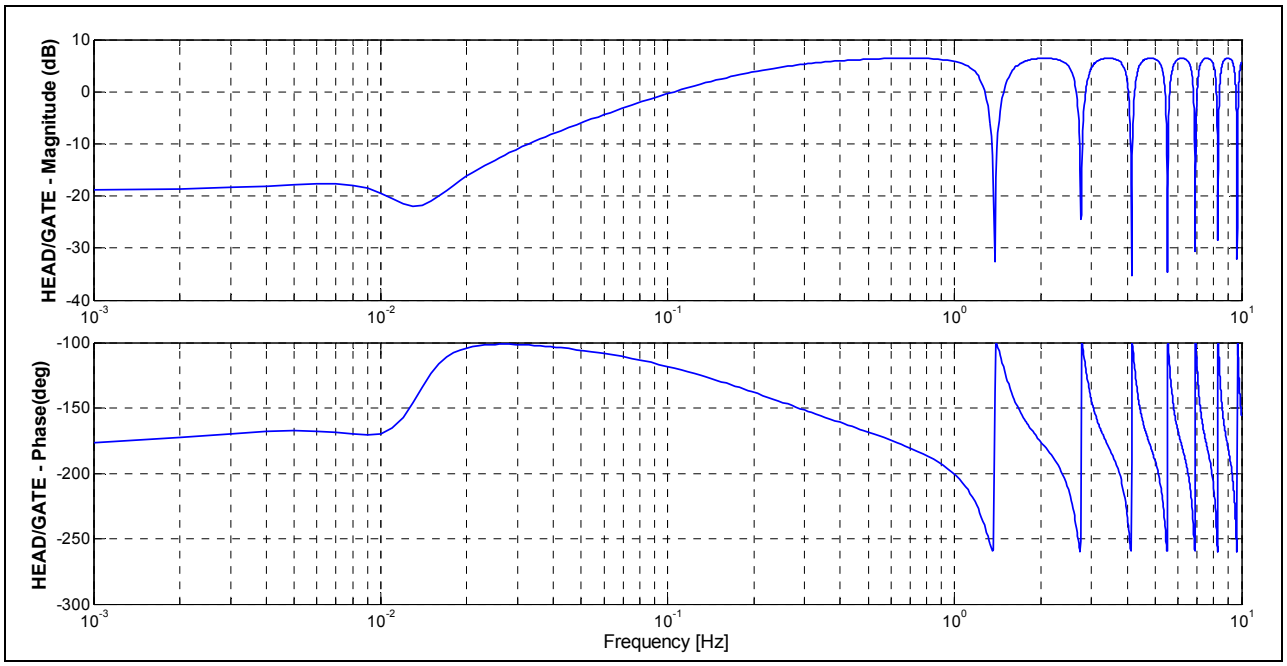

Figure 10-28: Frequency Response of the transfer function of the conduit system of Model 5

Figure 10-29 plots the magnitude and phase of the transfer function from gate position to Electrical Power Angle.

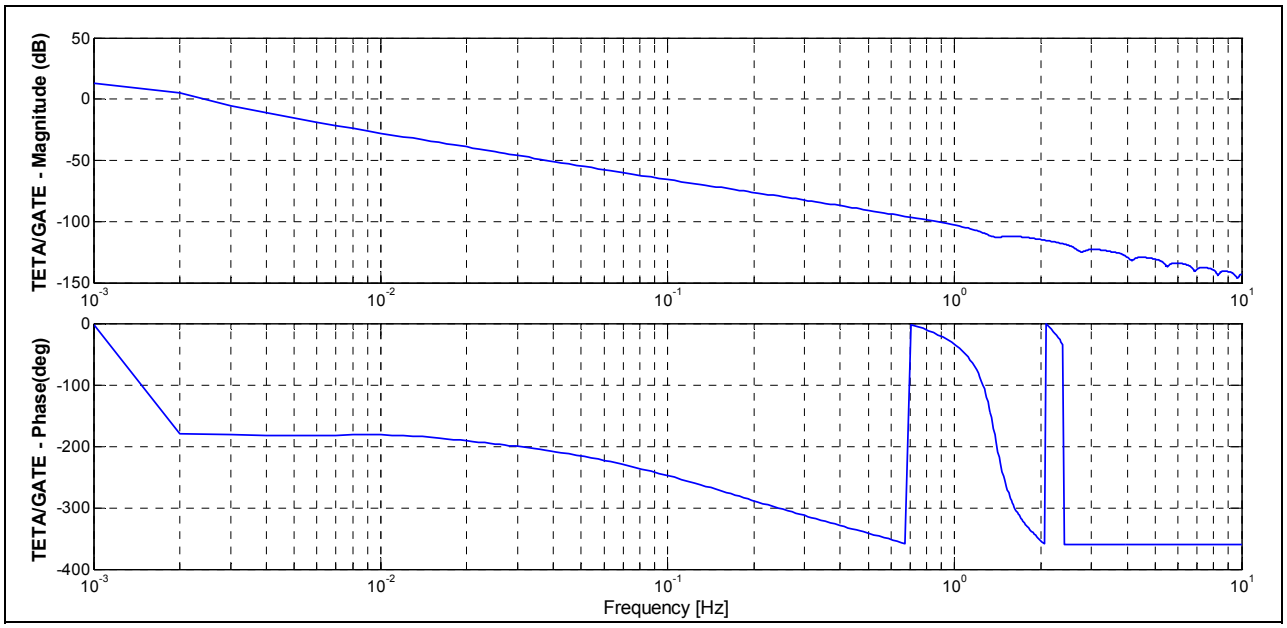

Figure 10-29: Frequency response of the transfer function from Gate position to Electrical Angle of Model 5

The magnitude ratio and phase of the transfer function of the mechanical-hydraulic governor are plotted in Figure 10-30. The transfer function of the governor relates the gate position to speed changes.

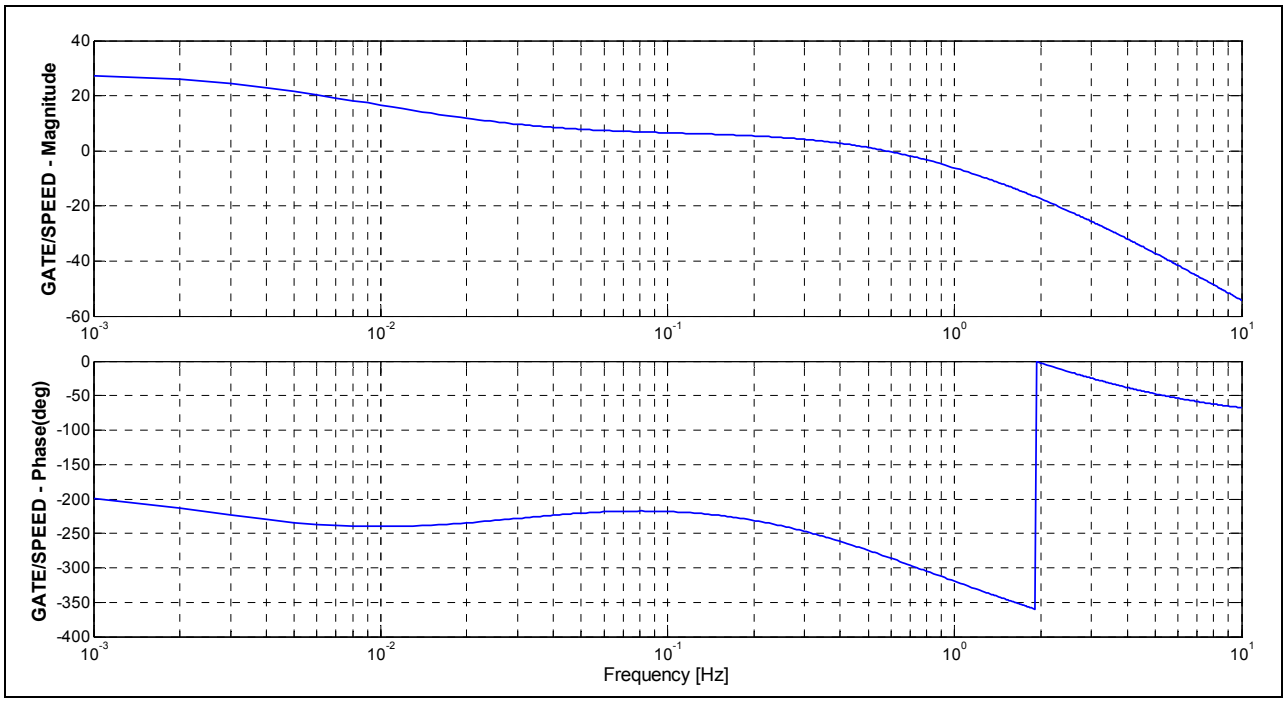

Figure 10-30: Frequency Response of the transfer function of the mechanical-hydraulic governor of Model 5

10.6 MODEL 6: Linear Turbine Model with Surge Tank assuming Inelastic Water Columns

The hydraulic turbine in the model 6 is represented by a *Linear Turbine Model with Surge Tank assuming Inelastic Water Columns in Penstock and Tunnel,* described in Chapter 6.3.1. The nonlinear characteristics of hydraulic turbine and the inelastic water hammer effect are considered in this model. The block diagram of this configuration is shown in Figure 6-7. The parameters of the Hydro Power Plant and operating conditions are detailed in Chapter 9. This model was implemented in DSL Code Generator which is a tool used for making self-defined dynamic models for dynamic simulation in SIMPOW.

10.6.1 Eigenvalue Analysis

Table 10-11 shows the real-valued eigenvalues, non-real-valued eigenvalues and the state variables that have the highest participation of the test system with a Linear Turbine Model with Surge Tank assuming Inelastic Water Columns in Penstock and Tunnel.

Table 10-11: Eigenvalues and the state variable for Model 6

	Eigenvalue			Damping Ratio	Frequency [Hz]	Dominant States
	Real, [1/s]		Imag, [Hz]			
1	-23.0473		0.0000	-	-	$\Delta\psi_D$
2	-17.4271		0.0000	-	-	Δy
3,4	-0.2925	±	1.0890	0.04270	1.08896	$\Delta\omega$ and $\Delta\delta$
5	-6.5781		0.0000	-	-	$\Delta\psi_Q$
6	-5.2853		0.0000	-	-	Δy
7	-2.5995		0.0000	-	-	Δy
8	-0.0167		0.0000	-	-	
9, 10	-0.0037	±	0.0108	0.05513	0.01076	
11	-0.1851		0.0000	-	-	$\Delta\psi_f$
12	-1.0000		0.0000	-	-	

It is seen in Table 10-11 that

- All eigenvalues have negative real part.
- The system is stable.
- λ_1, λ_2, λ_5, λ_6, λ_7, λ_8, λ_{11}, and λ_{12} influence the dynamic system with pure damping.
- $\lambda_{3,4}$ and $\lambda_{9,10}$ influence the dynamic simulation with both damping and oscillation.
- The oscillatory mode $\lambda_{3,4}$ have a damped frequency of 1.0890 Hz. The oscillations decay with a time constant of 1/0.2925 s. This corresponds to a damping ratio ζ of 0.0470.

The magnitudes of the participation factors, computed in SIMPOW, are shown in Table 10-12. The angles of the participation factors do not provide any useful information. From the participation matrix, $\Delta\delta$ and $\Delta\omega$ have a high participation in the oscillatory mode associated to the eigenvalues $\lambda_{3,4}$. The field flux linkage has a high participation in the non-oscillatory mode represented by the eigenvalue λ_{11}. The d-axis flux linkage has a high participation on the non-oscillatory mode represented by the eigenvalue λ_1. The q-axis flux linkage has a high participation on the non-oscillatory mode represented by the eigenvalue λ_5.

Table 10-12: Participation factors matrix of a Model 6

	λ_1	λ_2	λ_3, λ_4	λ_5	λ_6	λ_7	λ_8	λ_9, λ_{10}	λ_{11}
$\Delta\delta$	0.00592	0.00018	0.51300	0.03538	0.02546	0.03901	0.00290	0.00038	0.00088
$\Delta\omega$	0.00543	0.00127	0.51623	0.04673	0.02780	0.00641			0.00041
$\Delta\psi_f$	0.00570	0.00000	0.00634	0.00092	0.00102	0.00203	0.00010	0.00004	0.98949
$\Delta\psi_D$	1.00554	0.00018	0.01184	0.00200	0.00124	0.00037	0.00000		0.00860
$\Delta\psi_Q$	0.00004	0.00003	0.03431	1.13006	0.06890	0.00521	0.00000		0.00198

10.6.2 Dynamic Simulation Analysis

Figure 10-31 shows the result of simulating a three-phase fault to ground on bus BUS2 at t=1 s. This disturbance is simulated for a period of 5.0 ms. The simulation results of a simple turbine with surge tank represented by model 5 shows the dynamic behaviour of the power angle, rotational speed, mechanical torque, gate position, flow rate and head pressure.

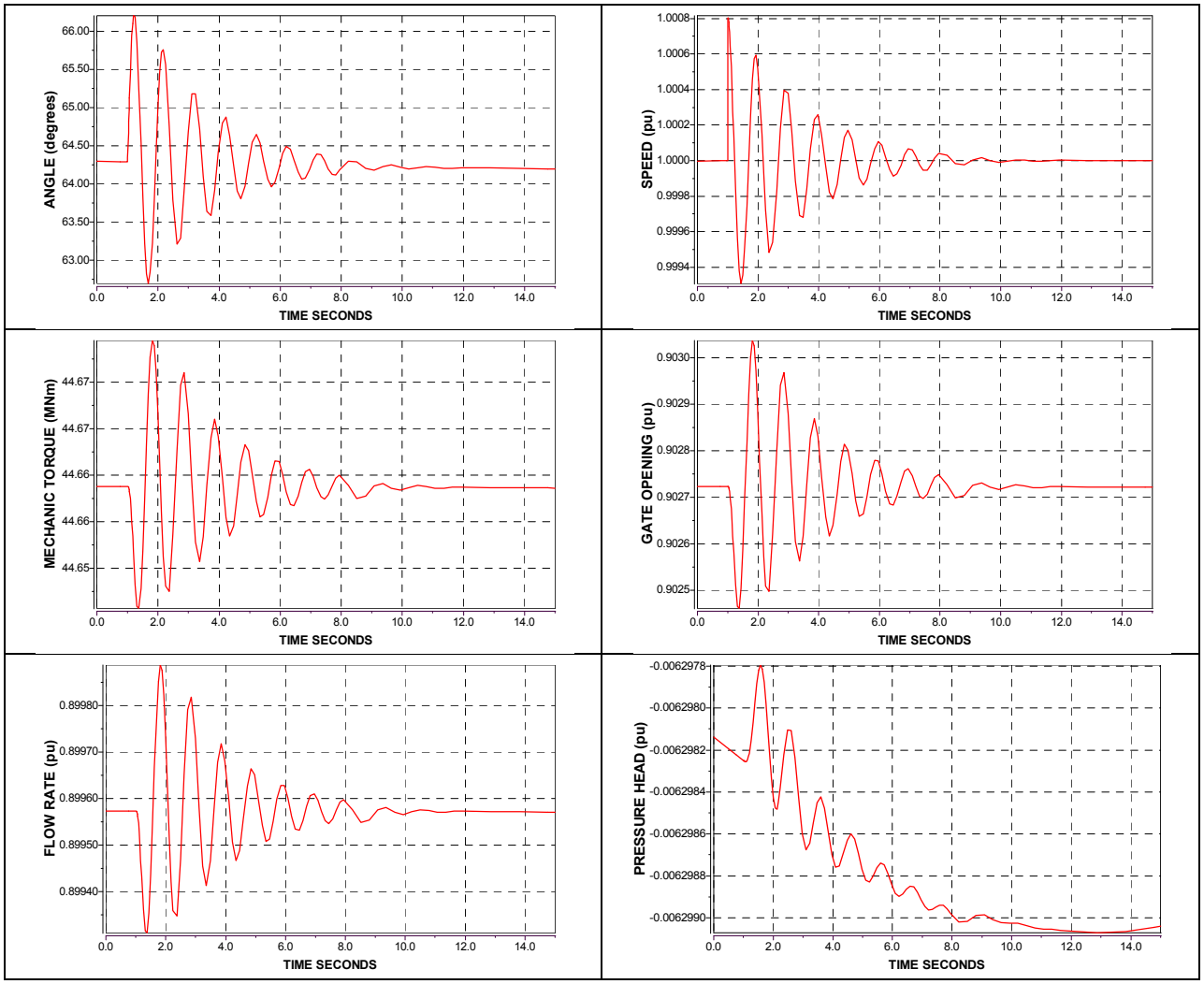

Figure 10-31: Fault simulation Results: (a) angle, (b) speed, (c) mechanical torque, (d) gate position, (e) flow rate and (f) water pressure of Model 6

The initial value of the Mechanical Power is 44.53 MW. After the fault is simulated, the Mechanical Power drops to 0.00 MW. The Mechanical Power oscillates for a period of 5.5 seconds, approximately.

The electrical angle oscillates for a period of 6.80 seconds. The minimum value is 62.696° at 1.69 seconds and the maximum value is 66.20° at 1.19 seconds. The value of the electrical angle at steady-state is 64.19°.

The rotational speed oscillates between the values of 0.9993 pu and 1.0008 pu. The rotational speed recovers stability after 7.8 seconds, demonstrating that the dynamic response of the hydro power plant is efficient.

The initial value of Mechanical Torque and Electric Torque are 44.66 MNm and -44.66 MNm, respectively. The Mechanic Torque oscillates for a period of 8 seconds, between the values of 44.6507 MNm and 44.6795 MNm. The Mechanical Torque at steady state is 44.6636 MNm. The Electrical Torque oscillates between the values of -46.0743 MNm and -1.3905 MNm. The Electrical Torque at steady state is -44.6633 MNm.

The variables Gate Opening and Flow rate are measured in per unit. Gate opening oscillates between 0.9024 and 0.9030. The flow varies between 0.8993 and 0.8999. The values of Gate position and Flow rate at steady-state are 0.8996, and 1.0794, respectively.

10.6.3 Frequency Response Analysis

The magnitude and phase of the transfer function from gate position to Mechanical Power of a Linear Turbine Model with Surge Tank assuming Inelastic Water Columns in Penstock and Upstream tunnel are plotted in Figure 10-32. The perturbation signal is applied to the gate position in open loop conditions and the signal mechanical power is monitored.

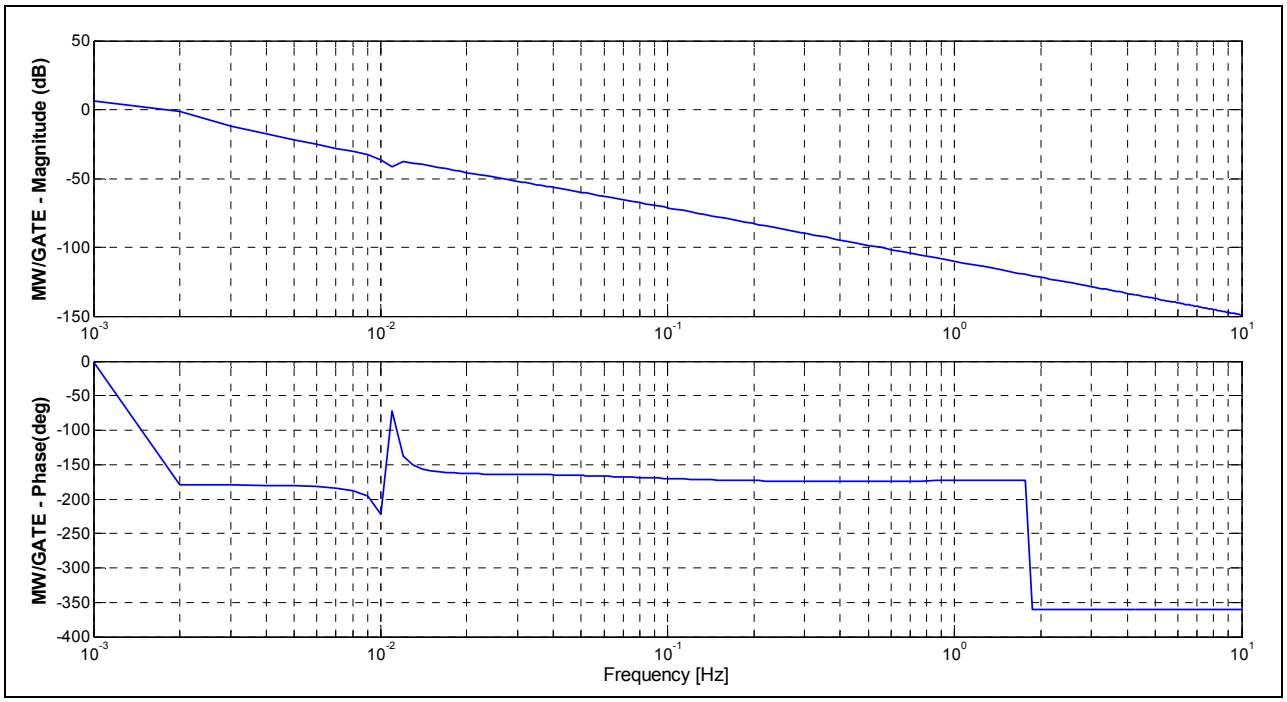

Figure 10-32: Frequency response of the transfer function from Gate position to Mechanical Power of Model 6

The relationship between the mechanical torque and the variation of gate position is studied in order to analyze the dynamic behaviour of the system. The perturbation signal is applied to the gate position in open loop conditions and the signal mechanical torque is monitored. The magnitude and phase of the frequency response of the transfer function of the hydraulic turbine are plotted in Figure 10-33.

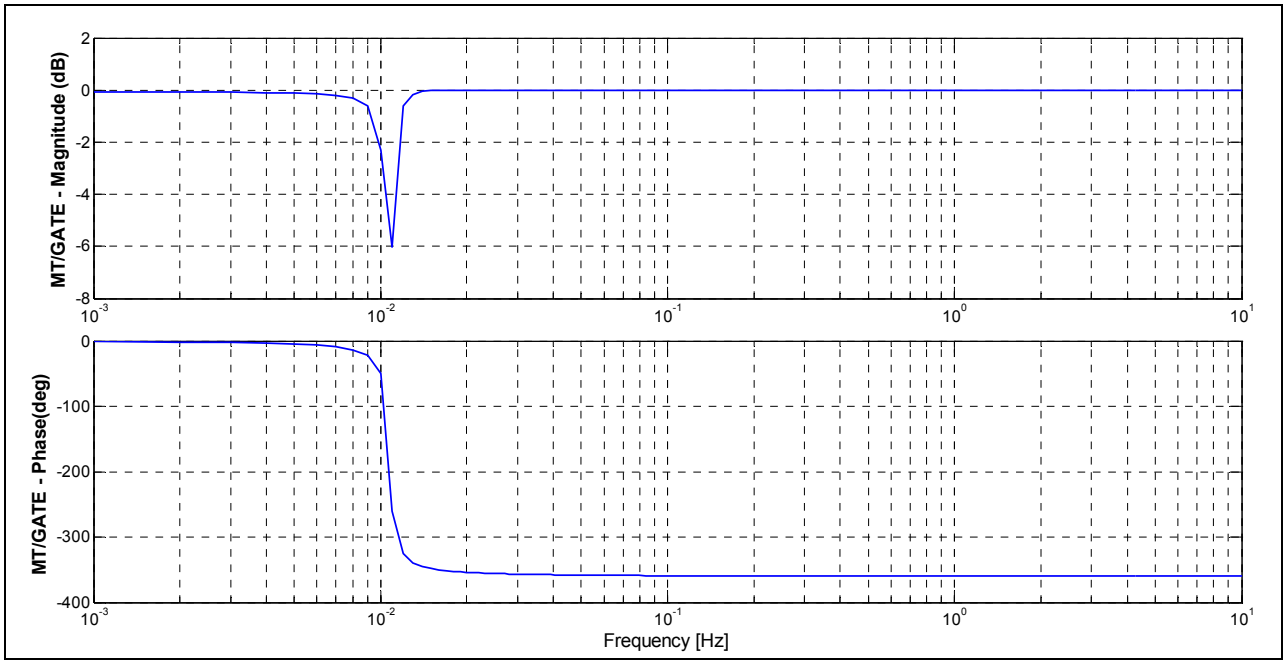

Figure 10-33: Frequency response of the transfer function from Gate position to Mechanical Torque of Model 6

Figure 10-34 plots the computed frequency response of the transfer function of the conduit system of a Linear Turbine Model with Surge Tank assuming Inelastic Water Columns. The transfer function of the water supply system relates the Pressure Head to gate position.

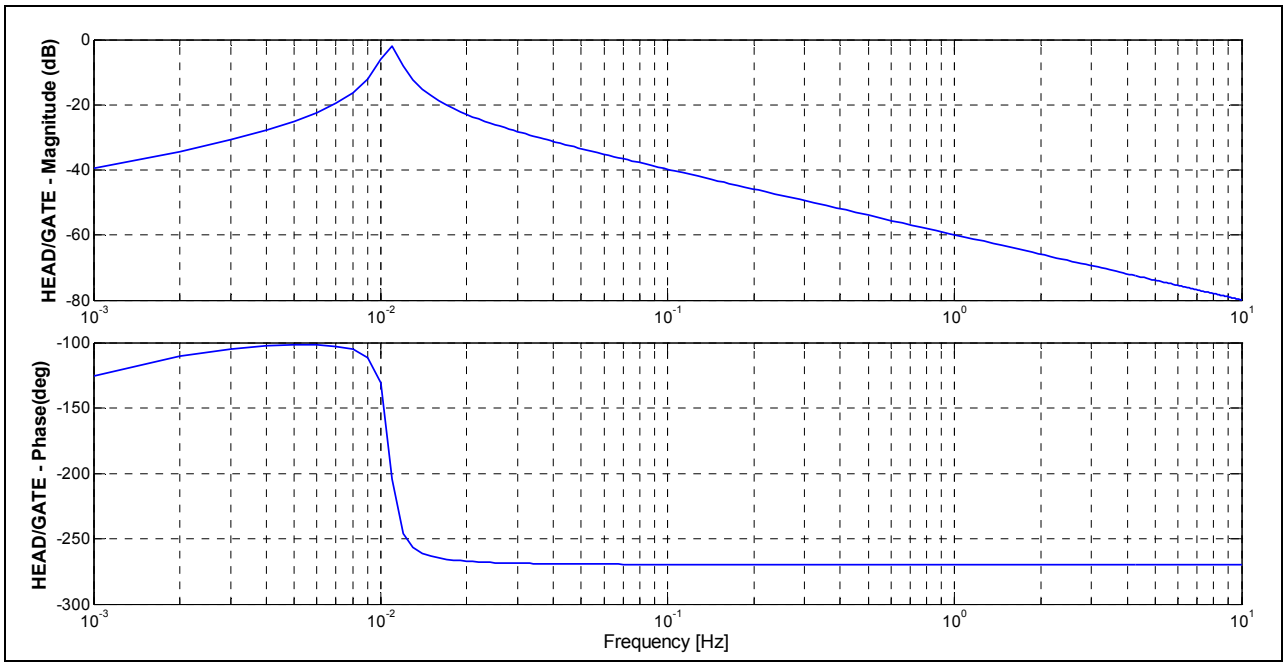

Figure 10-34: Frequency Response of the transfer function of the conduit system of Model 6

Figure 10-35 plots the magnitude and phase of the transfer function from gate position to Electrical Power Angle.

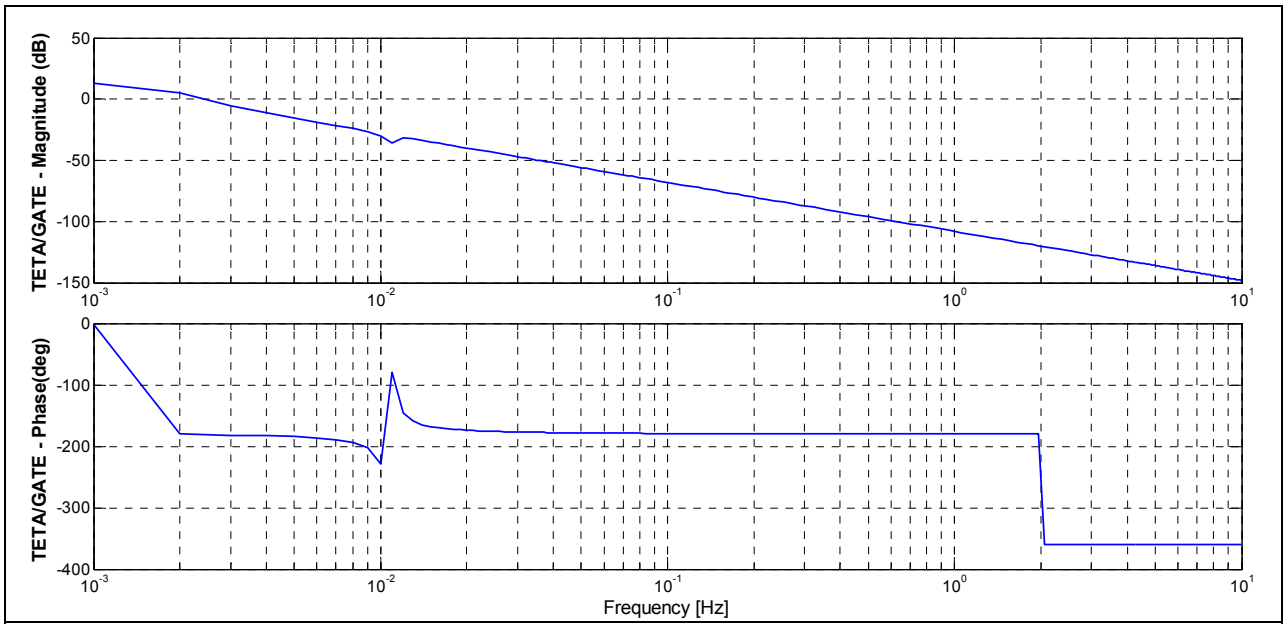

Figure 10-35: Frequency response of the transfer function from Gate position to Electrical Angle of Model 6

The magnitude ratio and phase of the transfer function of the mechanical-hydraulic governor are plotted in Figure 10-36. The transfer function of the governor relates the gate position to speed changes.

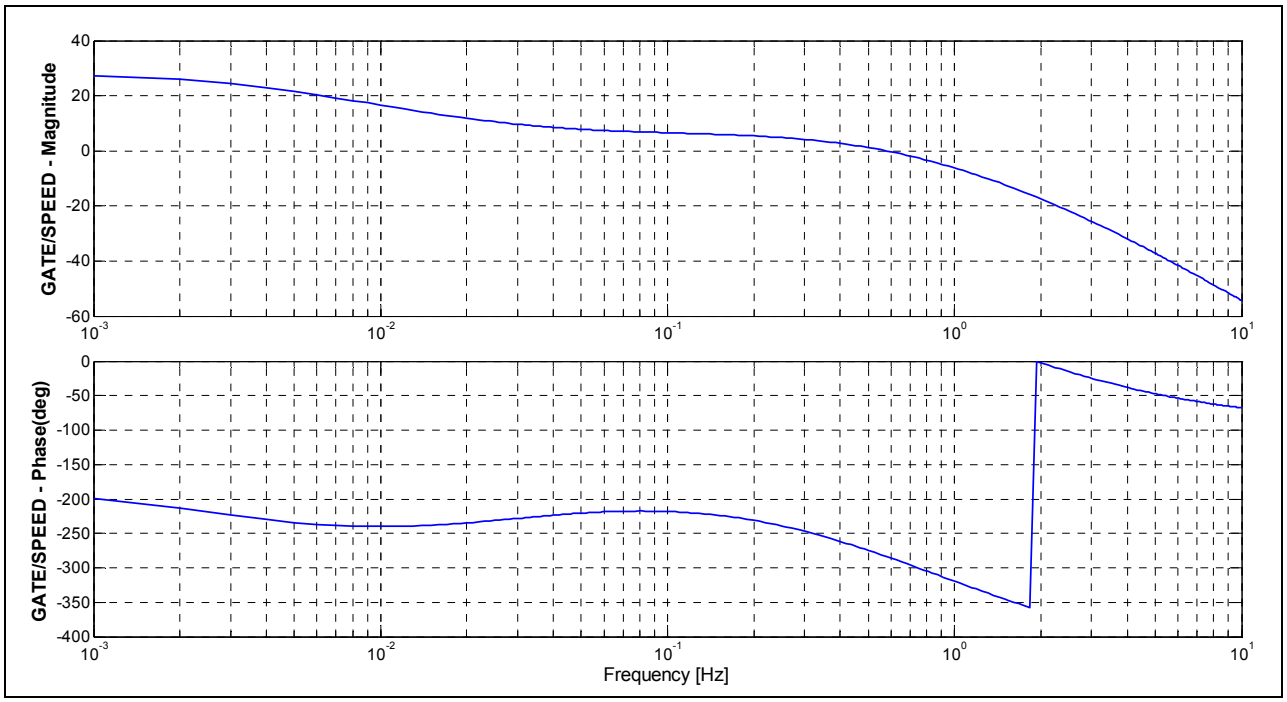

Figure 10-36: Frequency Response of the transfer function of the mechanical-hydraulic governor of Model 6

10.7 MODEL 7: Linear Turbine Model with Surge Tank assuming Elastic Water Column in Penstock

The hydraulic turbine in the model 7 is modelled by a *Linear Model with Surge Tank assuming Elastic Water Column in Penstock*, described in Chapter 6.3.2. The Penstock is modelled taking into account the elastic water hammer theory and neglecting the hydraulic friction losses. The nonlinear characteristics of hydraulic turbine are considered in this model. The block diagram of this configuration is shown in Figure 6-8. The parameters of the Hydro Power Plant and operating conditions are detailed in Chapter 9. This model was implemented in DSL Code Generator which is a tool used for making self-defined dynamic models for dynamic simulation in SIMPOW.

10.7.1 Eigenvalue Analysis

Table 10-13 shows the real-valued eigenvalues, non-real-valued eigenvalues and the state variables that have the highest participation of the test system with a Linear Model with Surge Tank assuming Elastic Water Column in Penstock.

Table 10-13: Eigenvalues and the state variable for the Model 7

Eigenvalue				Damping Ratio	Frequency [Hz]	Dominant States
	Real, [1/s]		Imag, [Hz]			
1	-23.0440		0.0000	-	-	$\Delta\psi_D$
2	-17.5548		0.0000	-	-	Δy
3,4	-0.4674	±	1.0695	0.06939	1.06950	$\Delta\omega$ and $\Delta\delta$
5	-6.7715		0.0000	-	-	$\Delta\psi_Q$
6,7	-3.6698	±	0.1773	0.95688	0.17731	Δy
8	-1.2029		0.0000	-	-	
9	-0.0167		0.0000	-	-	Δy
10,11	-0.0037	±	0.0108	0.05504	0.01077	
12	-0.1846		0.0000	-	-	$\Delta\psi_f$
13	-1.0000		0.0000	-	-	

It is seen in Table 10-13 that

- All eigenvalues have negative real part.
- The system is stable.
- λ_1, λ_2, λ_5, λ_8, λ_9, λ_{12}, and λ_{13} influence the dynamic system with pure damping.
- $\lambda_{3,4}$, $\lambda_{6,7}$ and $\lambda_{10,11}$ influence the dynamic simulation with both damping and oscillation.
- The oscillatory mode $\lambda_{3,4}$ have a damped frequency of 1.0695 Hz. The oscillations decay with a time constant of 1/0.4674 s. This corresponds to a damping ratio ζ of 0.06939.

The magnitudes of the participation factors, computed in SIMPOW, are shown in Table 10-14. The angles of the participation factors do not provide any useful information. From the participation matrix, $\Delta\delta$ and $\Delta\omega$ have a high participation in the oscillatory mode associated to the eigenvalues $\lambda_{3,4}$. The field flux linkage has a high participation in the non-oscillatory mode represented by the eigenvalue λ_{12}. The d-axis flux linkage has a high participation on the non-oscillatory mode represented by the eigenvalue λ_1. The q-axis flux linkage has a high participation on the non-oscillatory mode represented by the eigenvalue λ_5.

Table 10-14: Participation factors matrix of a Model 7

	λ_1	λ_2	λ_3, λ_4	λ_5	λ_6, λ_7	λ_8	λ_9	$\lambda_{10}, \lambda_{11}$	λ_{12}
$\Delta\delta$	0.00599	0.00068	0.55228	0.02888	0.22085	0.07832	0.00280	0.00019	0.00094
$\Delta\omega$	0.00555	0.00502	0.53969	0.01667	0.08406	0.00245			0.00041
$\Delta\psi_f$	0.00570	0.00002	0.00704	0.00030	0.00789	0.01018	0.00010	0.00002	0.98890
$\Delta\psi_D$	1.00608	0.00073	0.01279	0.00072	0.00415	0.00014	0.00000		0.00862
$\Delta\psi_Q$	0.00004	0.00012	0.03773	0.97929	0.07153	0.00246	0.00000		0.00197

10.7.2 Dynamic Simulation Analysis

Figure 10-37 shows the result of simulating a three-phase fault to ground on bus BUS2 at t=1 s. This disturbance is simulated for a period of 5.0 ms. The simulation results of a simple turbine with surge tank represented by model 7 show the dynamic behaviour of the power angle, rotational speed, mechanical torque, gate position, flow rate and head pressure.

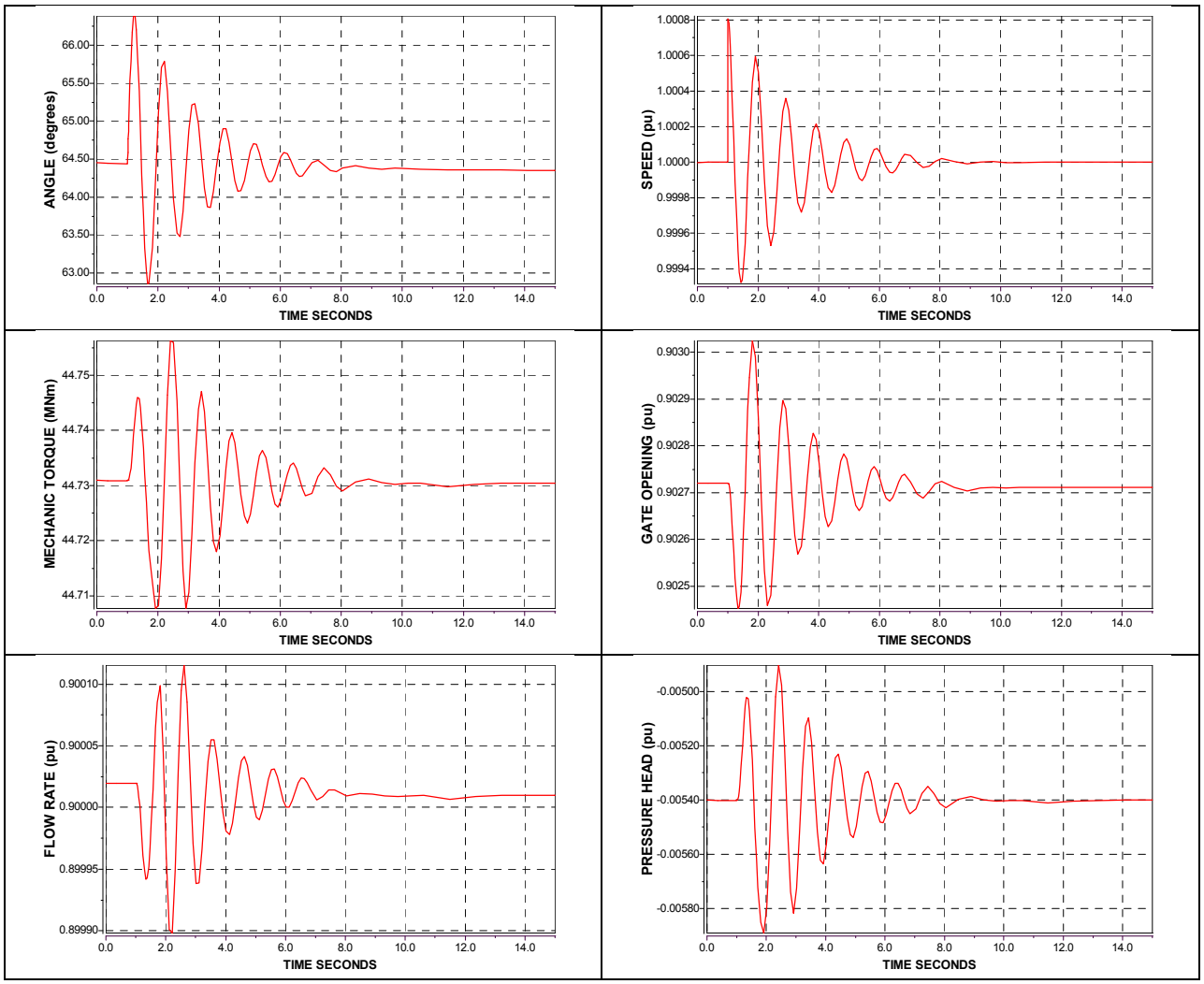

Figure 10-37: Fault simulation Results: (a) Power angle, (b) Speed, (c) Mechanical Torque, (d) Gate Position, (e) Flow Rate and (f) Head Pressure of Model 7

The initial value of the Mechanical Power is 44.59 MW. After the fault is simulated, the Mechanical Power drops to 0.00 MW. The Mechanical Power oscillates for a period of 5.5 seconds, approximately.

The electrical angle oscillates for a period of 6.80 seconds. The minimum value is 64.8585° at 1.66 seconds and the maximum value is 66.39° at 1.24 seconds. The value of the electrical angle at steady-state is 64.35°.

The rotational speed oscillates between the values of 0.9993 pu and 1.0008 pu. The rotational speed recovers stability after 7.0 seconds, demonstrating that the dynamic response of the hydro power plant is efficient.

The initial value of Mechanical Torque and Electric Torque are 44.71 MNm and -44.72 MNm, respectively. The Mechanic Torque oscillates for a period of 8 seconds, between the values of 44.708 MNm and 44.756 MNm. The Mechanical Torque at steady state is 44.731 MNm. The Electrical Torque oscillates between the values of -46.146 MNm and -1.389 MNm. The Electrical Torque at steady state is -44.7304 MNm.

The variables Gate Opening and Flow rate are measured in per unit. Gate opening oscillates between 0.9025 and 0.9030. The flow varies between 0.8999 and 0.9001. The values of Gate position and Flow rate at steady-state are 0.9027, and 0.9000, respectively.

10.7.3 Frequency Response Analysis

The magnitude and phase of the transfer function from gate position to Mechanical Power of a Linear Model with Surge Tank assuming Elastic Water Column in Penstock are plotted in Figure 10-38. The perturbation signal is applied to the gate position in open loop conditions and the signal mechanical power is monitored.

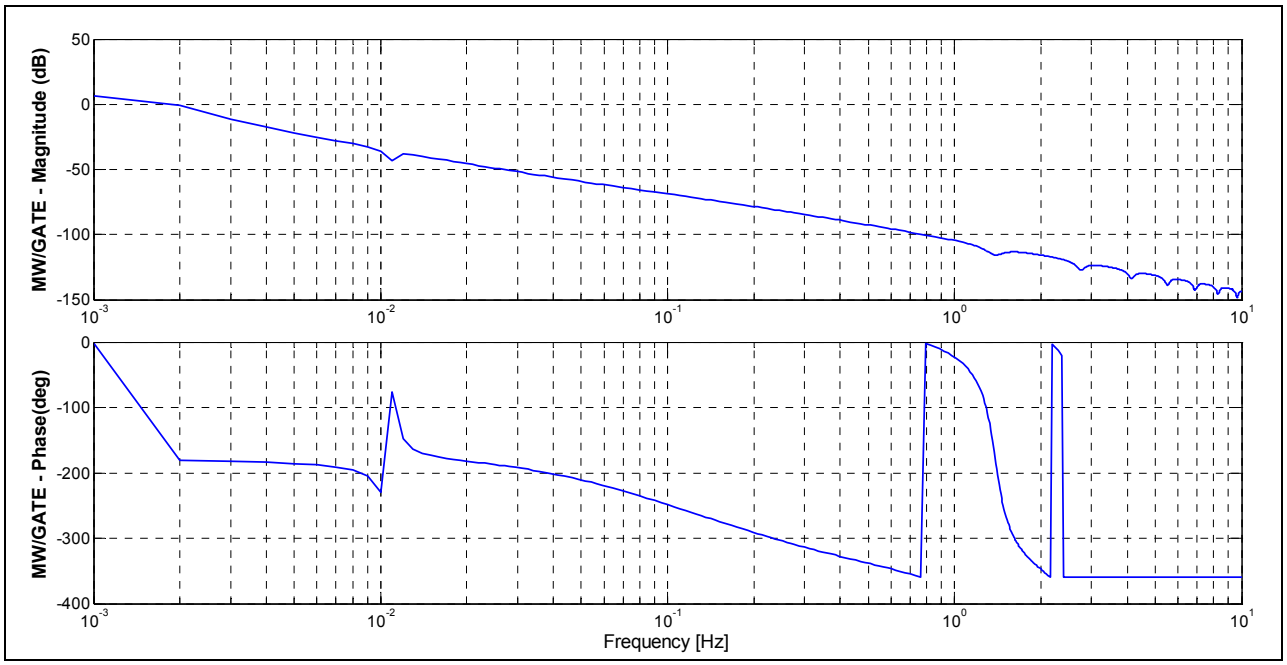

Figure 10-38: Frequency response of the transfer function from Gate position to Mechanical Power of Model 7

The relationship between the mechanical torque and the variation of gate position is studied in order to analyze the dynamic behaviour of the system. The perturbation signal is applied to the gate position in open loop conditions and the signal mechanical torque is monitored. The magnitude and phase of the frequency response of the transfer function of the hydraulic turbine are plotted in Figure 10-39.

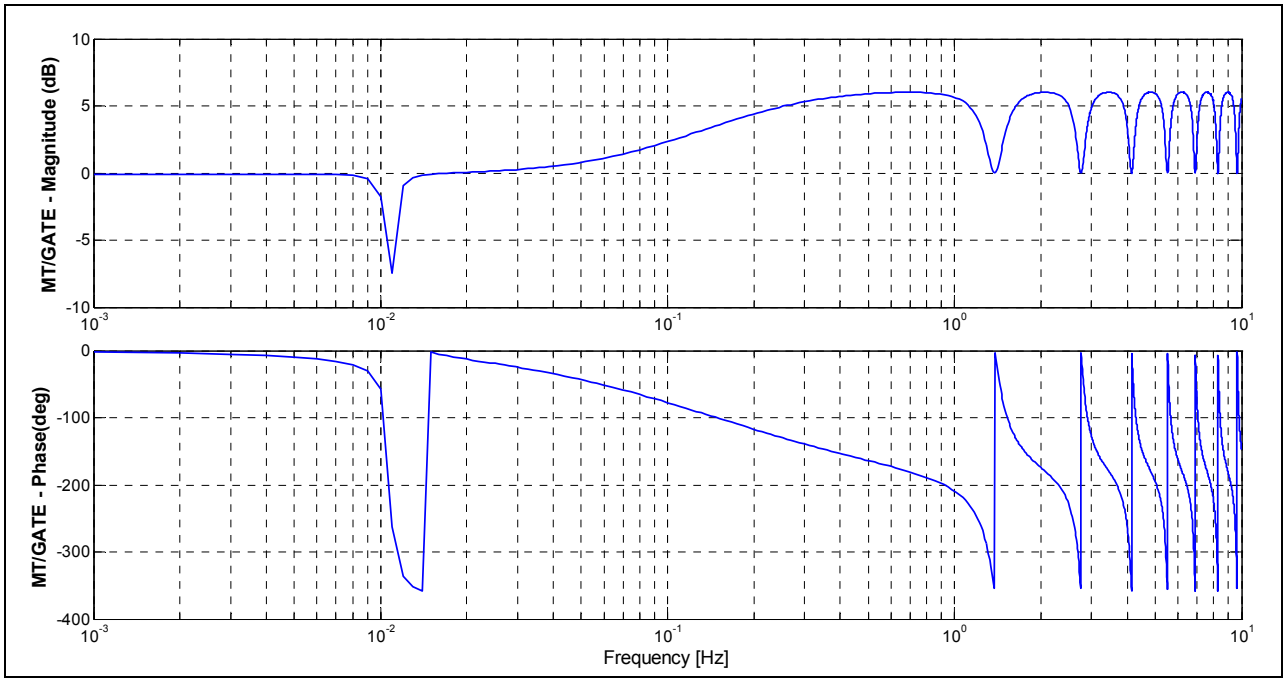

Figure 10-39: Frequency response of the transfer function from Gate position to Mechanical Torque of Model 7

Figure 10-40 plots the computed frequency response of the transfer function of the conduit system of a Linear Model with Surge Tank assuming Elastic Water Column in Penstock. The transfer function of the conduit system relates the Pressure Head to gate position.

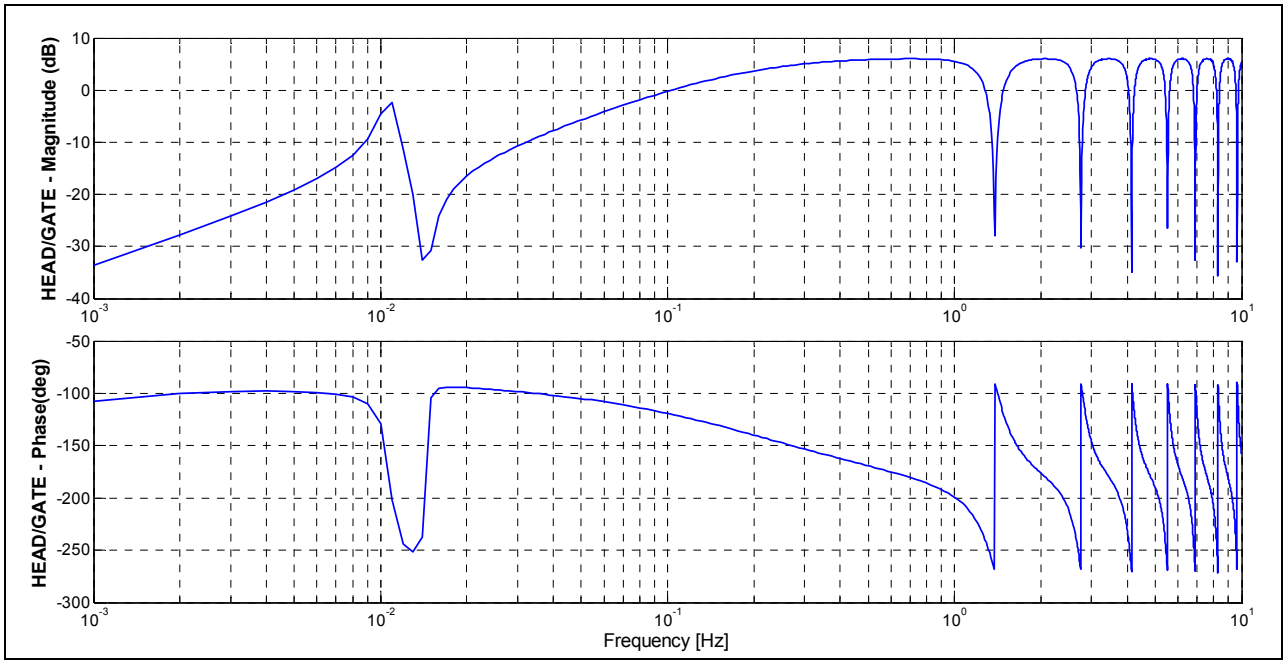

Figure 10-40: Frequency Response of the transfer function of the conduit system of Model 7

Figure 10-41 plots the magnitude and phase of the transfer function from gate position to Electrical Power Angle.

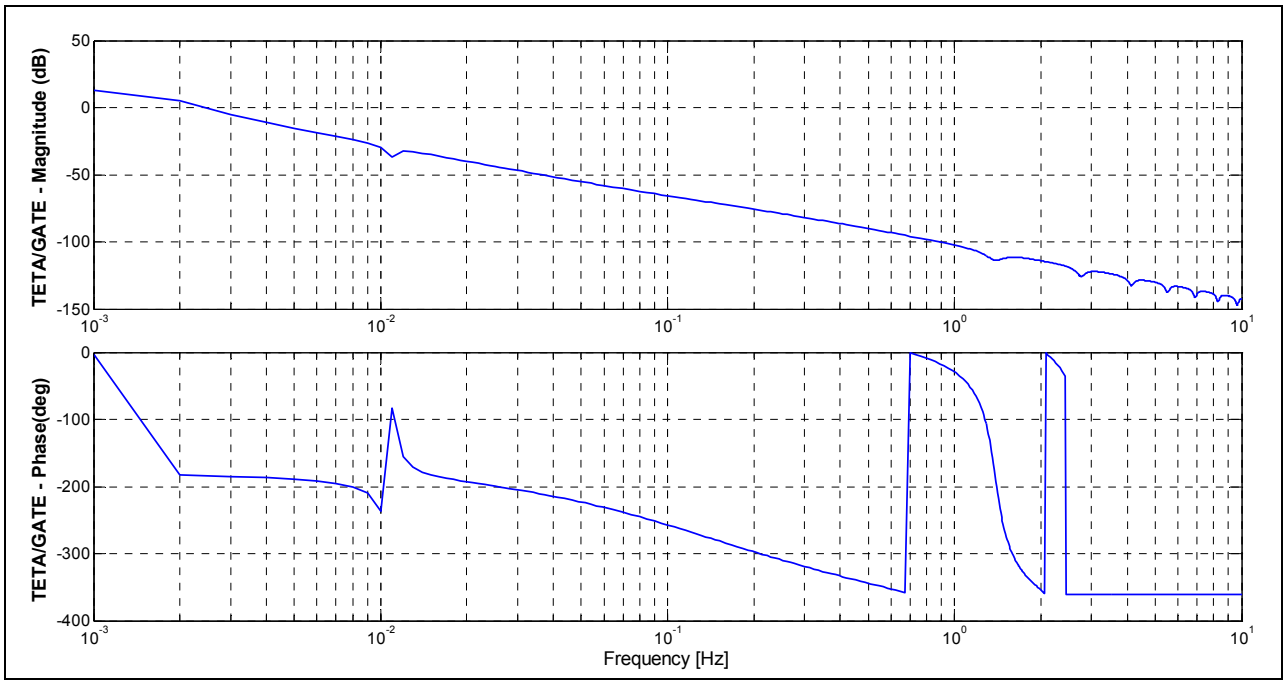

Figure 10-41: Frequency response of the transfer function from Gate position to Electrical Angle of Model 7

The magnitude and phase of the transfer function of the mechanical-hydraulic governor are plotted in Figure 10-42. The transfer function of the governor relates the gate position to speed changes.

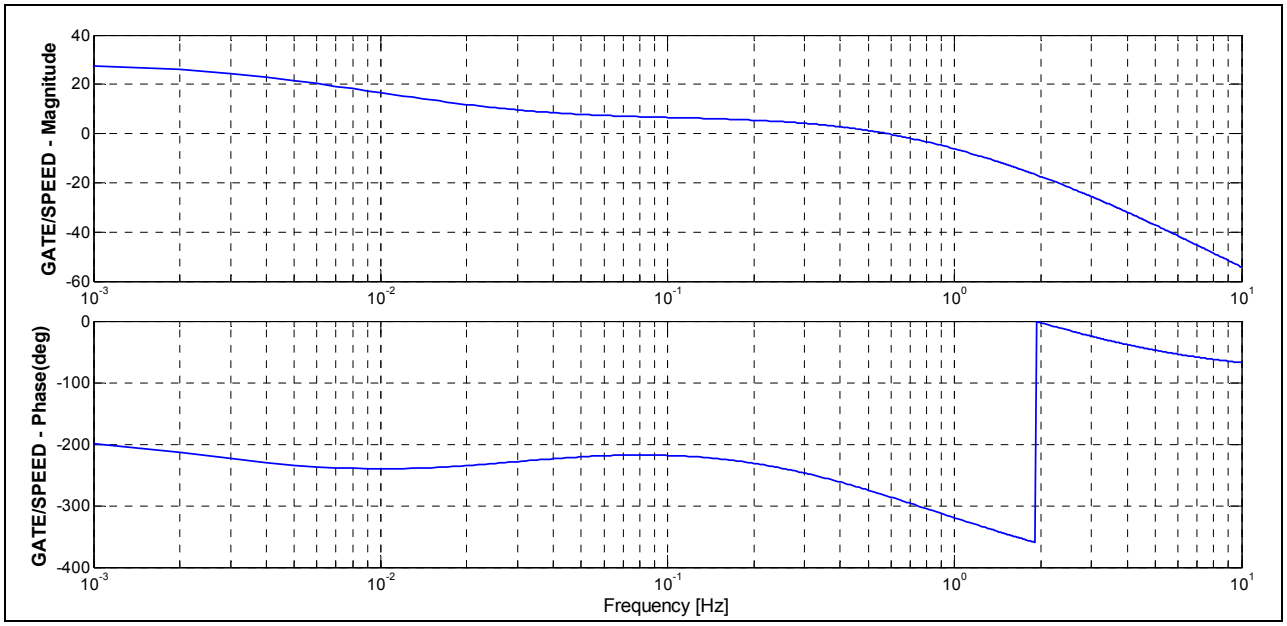

Figure 10-42: Frequency Response of the transfer function of the mechanical-hydraulic governor of Model 7

11 Power System Modelled in LVTrans

LVTrans is a general hydraulic dynamic simulation tool used to calculate all kinds of systems consisting mainly of fluid-filled pipes and open channels. The general configuration of the Hydro Power Plant modelled in LVTrans contains the essential components of a hydraulic power system such as reservoir, an upstream tunnel to carry the water from the reservoir, a surge tank, a penstock, a hydraulic turbine, speed governor and a tailrace through the water is released back to the river.

This chapter studies the system dynamic characteristics of the test hydraulic system, detailed in Chapter 9, modelled in the dynamic simulation tool LVTrans. The dynamic behaviour of the hydraulic power system is analyzed in the program LVTrans version LVTrans8_1.1.2 and version LVTrans86_1.3.1_T. Afterwards, the frequency response of the transfer function relating the Pressure Head to Gate position simulated in the two different versions are compared and studied.

11.1 Description of LVTrans

LVTrans is a general hydraulic dynamic simulation tool built in Lab VIEW. LVTrans may be used to calculate all kinds of systems consisting mainly of fluid-filled pipes and open channels. It can also be used to calculate the acoustics of gas-filled tubes. LVTrans uses the *Method* of *Characteristic* to solve the differential equations describing the hydraulic conduits. A detailed one-dimension Euler equation system is used to calculate the full dynamic behaviour of the test system. LVTrans has been used in several projects in the North Sea, including the fire water system, acoustic calculations in gas pipes on Heidrun, cooling water system for Ormen Lange. Hydropower is a special field for LVTrans, as most items are custom made for this purpose. [68]

LVTrans has had many enhancements. The dynamic behaviour of the test Hydraulic Power System is simulated and analyzed in two versions of LVTrans.

LVTrans version LVTrans8_1.1.2 is a version created specifically for the study of the dynamic performance and interaction between the hydraulic system and power system of a power plant equipped with Francis units. This version was specially designed for detailed grid/waterway interaction in January 2005.

LVTrans version LVTrans86_1.3.1_T is the newest version of the program. LVTrans version 86_1.3.1_T includes many upgrades to the front panel, block diagram and related functionality to the study of the dynamic performance of the hydraulic system. The new version of LVTrans does not have some of the tools developed in the version LVTrans8_1.1.2.

11.2 Hydraulic System Modelling

The general configuration of the Hydro Power Plant modelled in LVTrans contains the essential components of a hydraulic power system such as a reservoir, an upstream tunnel, a surge tank, a penstock, a hydraulic turbine, speed governor and a tailrace through the water is released back to the river. The power plant has a Francis unit. The simplified sketch of a typical hydraulic power system is depicted in Figure 9-2. The accuracy of the dynamic analysis of the Hydro Power Plant modelled in LVTrans is at least 90% due to the damping of these elements can be adjusted.

Figure 11-1 shows the block diagram of the test system modelled in LVTrans. The elements needed in the block diagram to model the sketch, shown in Figure 9-2, such as pipes, surge shaft, turbine and PID control, are dragged and dropped from **Function Palette >> LVTrans** in the block diagram. These elements must be wired after all the elements are inserted and named. Each element must have a unique name. The main parameters of the hydraulic circuit are summarized in Table 9-2.

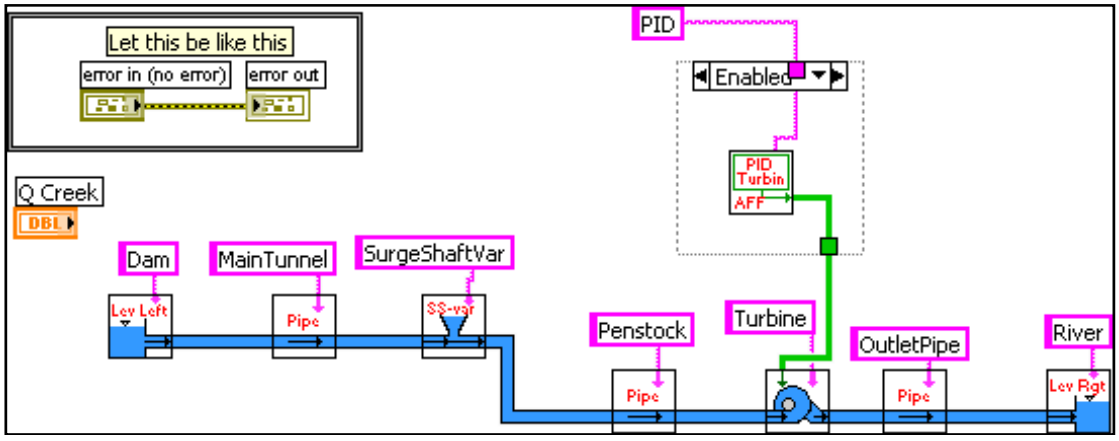

Figure 11-1: Block Diagram of the Hydraulic System Model

The data must be set up for each element before the simulation begins. The data are stored in separate data files. LVTrans sets initial values for each element after running the program for first time. These data files are edited directly in each element while the program is run by press the indicator *data* in the window of each element or in a plain text editor.

The input data used for each of the components of the test system model are described in detail in Chapter 9. The given parameters are set according to the Hydraulic Grade Line (HGL), which shows the height corresponding to elevation and pressure head. The HGL is the height to which the liquid would rise in a piezometer tube attached to the flow. [14]

The value considered for the pressure wave velocity a is 1200 m/s. The dimensionless pipe friction factor is a function of the Reynolds number and the relative roughness height, described in Chapter 2.1.3. The friction factor is selected from the Moody diagram.

11.3 Dynamic Simulation

The frequency response analysis as well as transient response analysis to evaluate the dynamic performance of the Hydraulic Power System Model, depicted in Figure 11-1, is implemented in the dynamic simulation tool LVTrans version LVTrans8_1.1.2 and version LVTrans86_1.3.1_T. The Hydraulic Power System Model is simulated with and without droop in LVTrans8_1.1.2. The frequency response of the transfer function relating the water pressure to gate opening position implemented in the different versions are compared and studied.

The feedback from the gate opening position to the controller is included when the simulation is performed with droop. The droop is usually 4% to 8%.

The analysis of transients in the Hydraulic Power System Model is subdivided in water-hammer response and mass-oscillation response.

- The elastic pressure frequency describes the oscillation along the penstock. The characteristic frequency does not vary with the load and depends only upon the dimensions of the penstock. The natural frequency is typically in the order of 1.00 Hz.
- The natural frequency resulting from the pendulum action between the reservoir and the surge shaft called mass-oscillations. The mass-oscillations can take several minutes to get the steady-state.

Both the water-hammer and mass-oscillation responses are calculated by shutting down the turbine in the interface and block diagram. The water-hammer and mass-oscillations responses depend of the length of the conduit. The oscillation mode could be analyzed at the graph of the Penstock and Turbine in the block diagram.

Figure 11-2 shows the oscillations of the hydraulic power plant modelled in LVTrans86_1.3.1_T. The parameters of the Hydro Power Plant and operating conditions are detailed in Chapter 9.

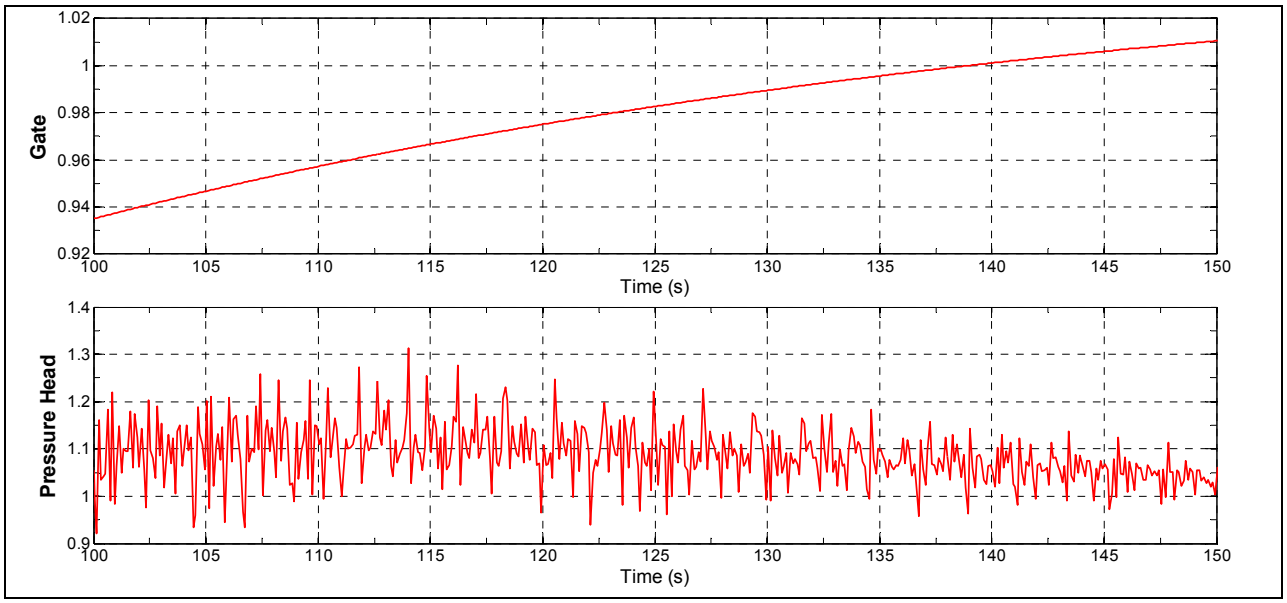

Figure 11-2: Simulation Results: (a) gate opening position, (b) Pressure Head of the Hydraulic Test Model in LVTrans86_1.3.1_T

11.3.1 Frequency Response Analysis computed in LVTrans8_1.1.2

The frequency response of the transfer function from gate position to pressure head of the hydraulic power plant modelled without droop in LVTrans8_1.1.2 is shown in Figure 11-3.

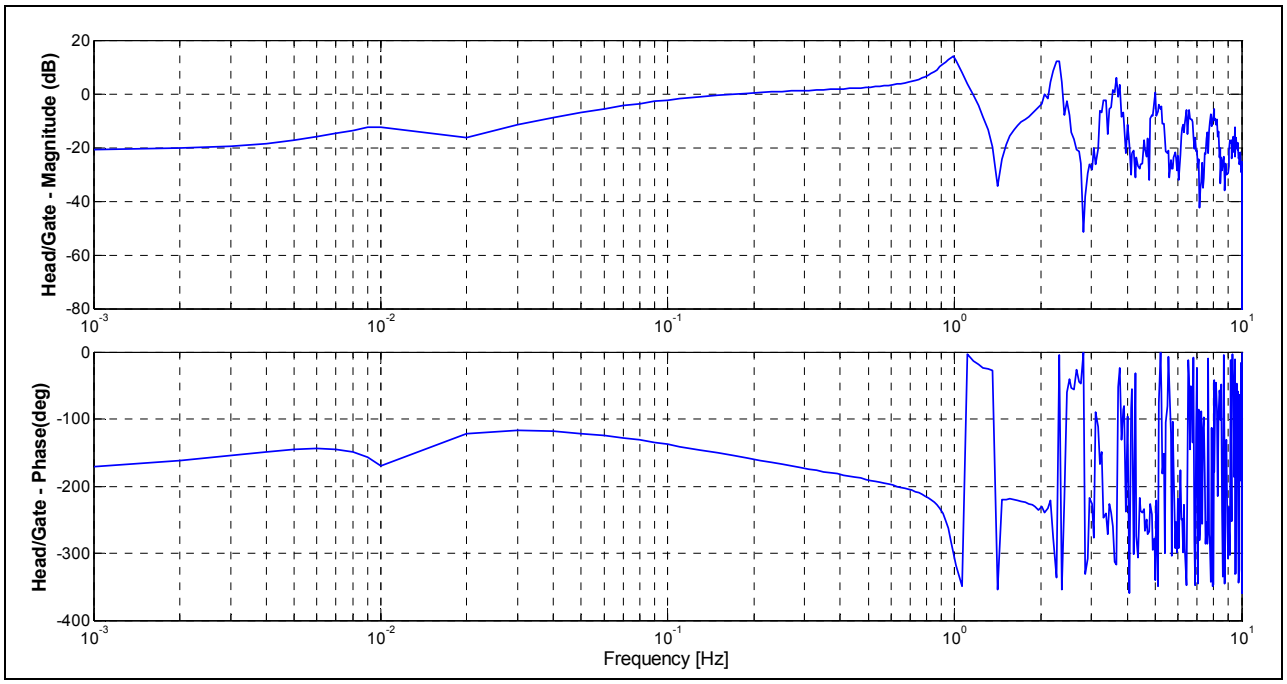

Figure 11-3: Frequency Response of the transfer function from gate position to pressure head of the hydraulic power plant simulated without droop in LVTrans8_1.1.2

Figure 11-4 shows the magnitude and phase of the frequency response of the hydraulic power plant modelled with droop in LVTrans8_1.1.2.

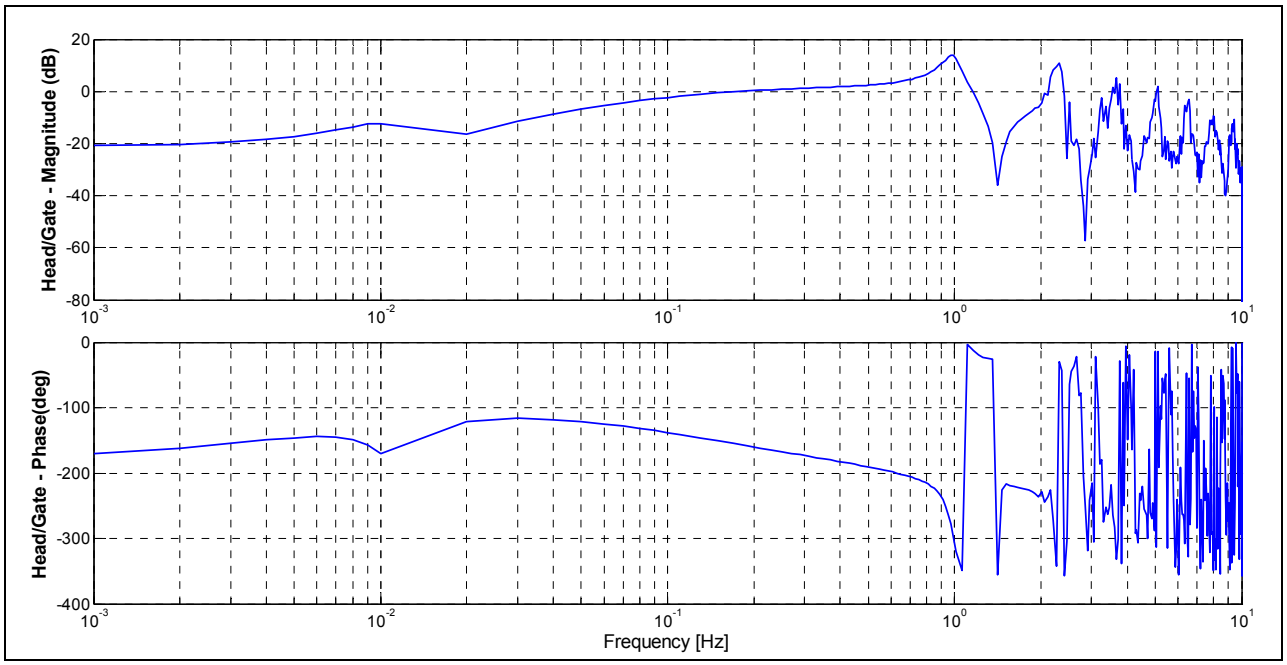

Figure 11-4: Frequency Response of the transfer function from gate position to pressure head of the hydraulic power plant simulated with droop in LVTrans8_1.1.2

Comparison between the magnitude and phase of the frequency response of the transfer functions from gate position to pressure head of the hydraulic system model simulated with and without droop can be examined in Figure 11-5.

In Figure 11-5, the dynamic performance of the blue solid line represents the hydraulic system model simulated without droop, and the green dashed line represents the hydraulic system model simulated with droop.

The hydraulic system model without droop agrees well with the hydraulic system model with droop representation model. The magnitudes of both models reach a peak at a resonance frequency around 0.01 Hz. This frequency corresponds to the natural frequency of the mass-oscillation between the reservoir and the surge tank. The magnitudes of both models reach a higher peak at a resonance frequency around 0.8 Hz. This frequency corresponds to the first natural frequency of the penstock. The effects of the droop has very little different on the phase.

The oscillations at higher frequencies are due to the elasticity of the conduit system.

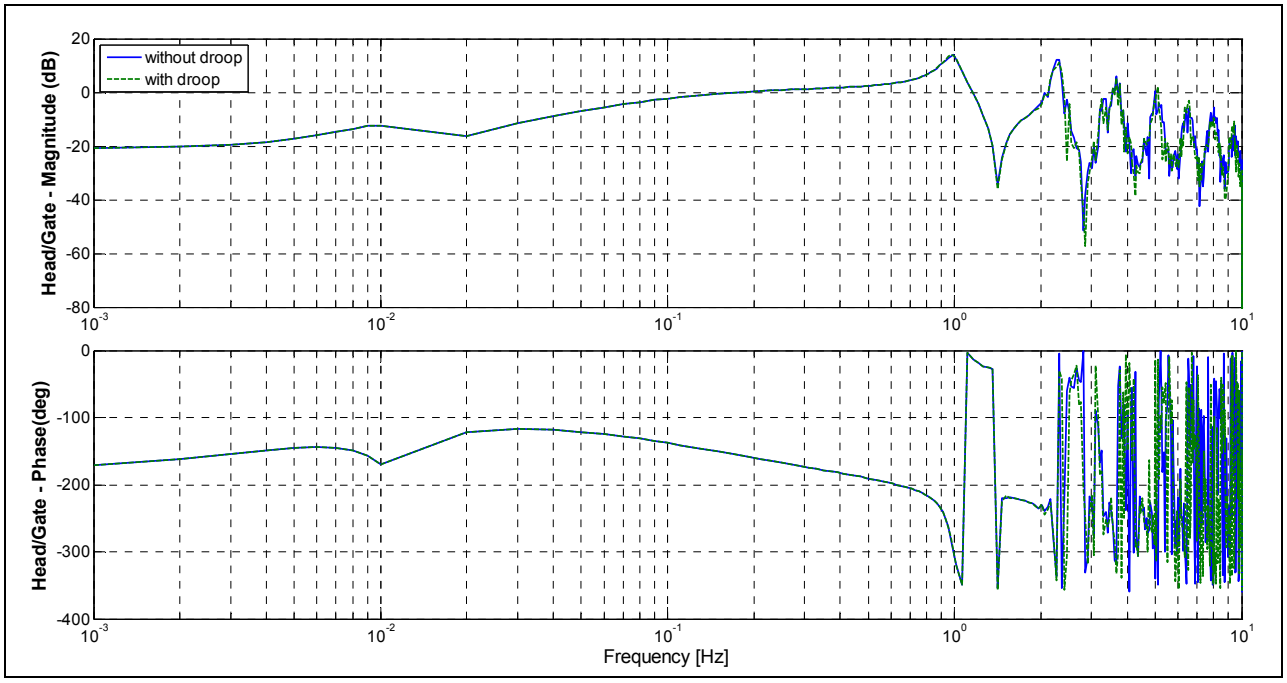

Figure 11-5: Frequency Response of the transfer function from gate position to pressure head of the hydraulic power plant simulated without and with droop in LVTrans8_1.1.2

The feedback from the gate opening position to the controller is included when the simulation is performed with droop. The droop is usually 4% to 8%.

11.3.2 Frequency Response Analysis computed in LVTrans86_1.3.1_T

The magnitude and phase of the frequency response of the transfer function from gate position to Pressure Head of the Hydraulic Power System is plotted in Figure 11-6.

The magnitude of the transfer function reaches a peak value at 0.01 Hz that corresponds to the natural frequency of the mass-oscillation between the reservoir and the surge tank. The theoretical value is given by Equation (9.9). The magnitude reaches a second peak value at approximate 1 Hz. This value corresponds to the resonance frequency of the penstock which theoretical value is given by Equation (9.8).

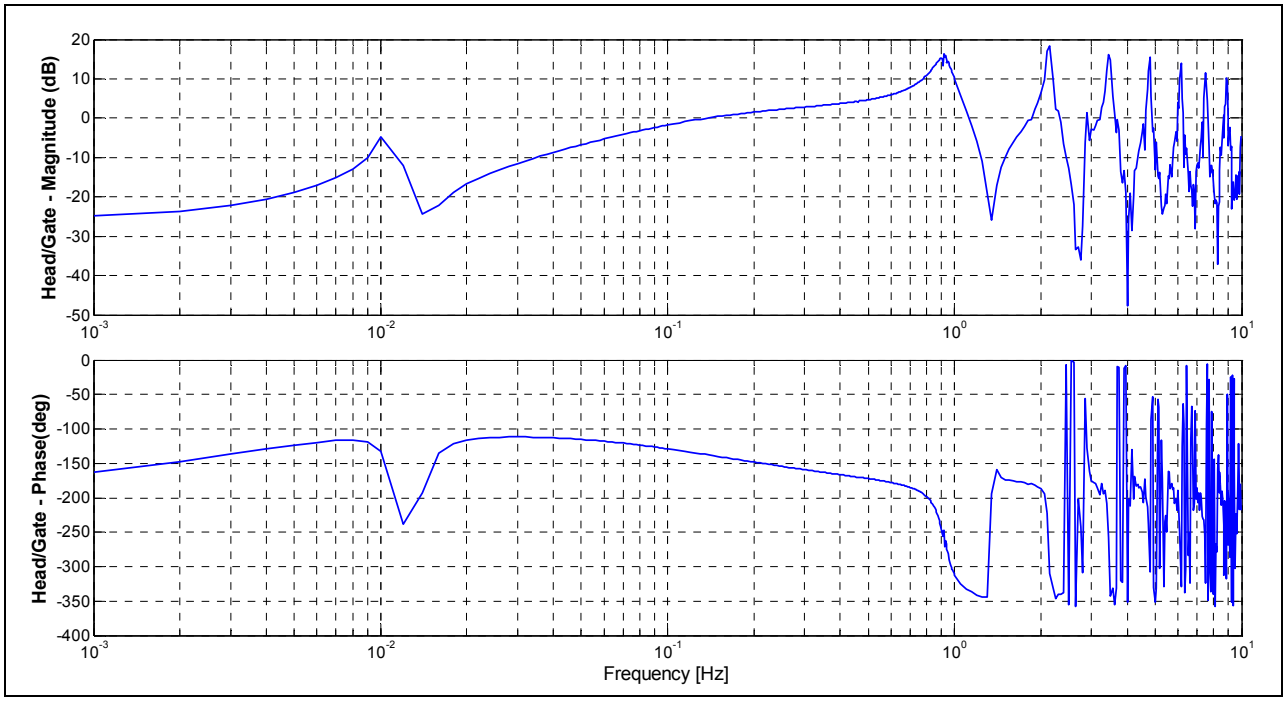

Figure 11-6: Frequency Response of the transfer function from gate position to pressure head of the hydraulic power plant simulated in LVTrans86_1.3.1_T

11.3.3 Comparison of the Frequency Response Analysis of the Hydraulic Power Plant computed in LVTrans8_1.1.2 and LVTrans86_1.3.1_T

The frequency response of the hydraulic power system model has been simulated and analyzed in the dynamic tool LVTrans version LVTrans8_1.1.2 and LVTrans86_1.3.1_T. The hydraulic power system model includes the essential components such as the reservoir, upstream tunnel, a surge tank, a penstock, a Francis turbine, a PID governor and tailrace.

In Figure 11-7 and Figure 11-8, the blue solid line represents the frequency response of the hydraulic power generating system simulated in LVTrans8_1.1.2 and the green dashed line is the hydraulic power plant simulated in LVTrans86_1.3.1_T.

The magnitude and phase of the relationship between the gate opening position and water pressure head of the hydraulic power generating system simulated without droop in LVTrans8_1.1.2 and computed in LVTrans86_1.3.1_T can be compared in Figure 11-7. The magnitude of the hydraulic power generating system simulated in LVTrans8_1.1.2 is slightly different to that computed in LVTrans86_1.3.1_T.

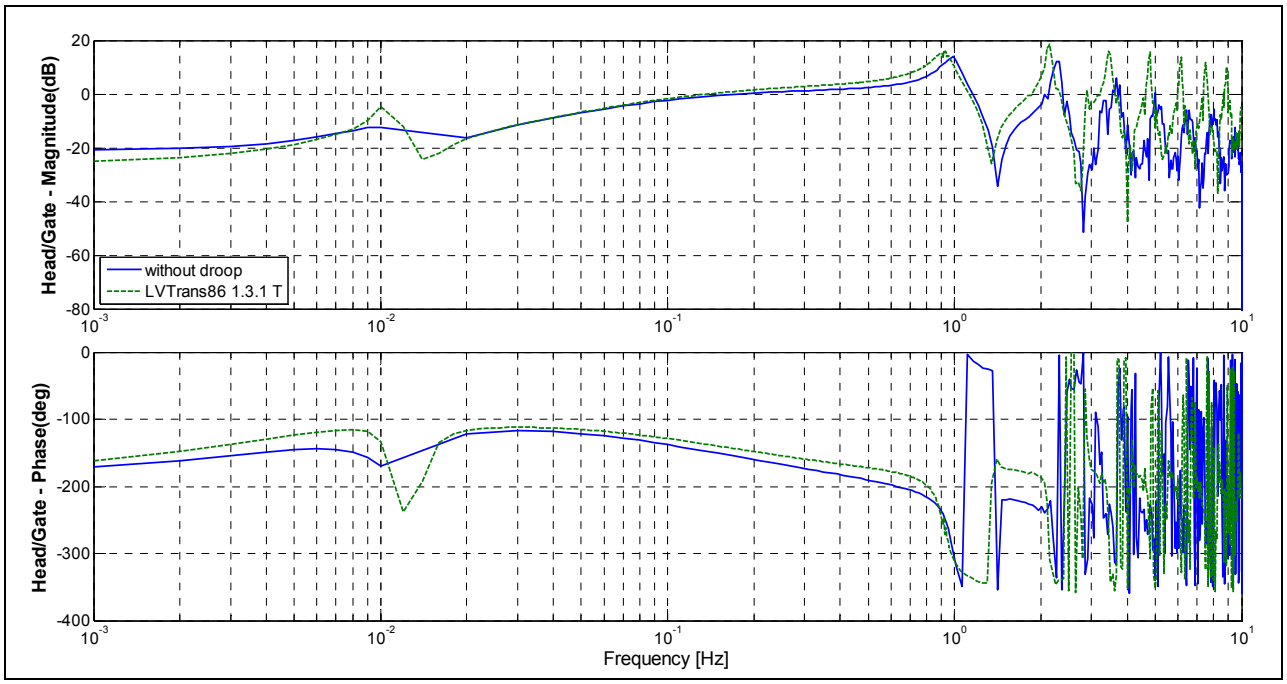

Figure 11-7: Comparison of the Frequency response of the hydraulic power generating system simulated without droop in LVTrans8_1.1.2 and computed in LVTrans86_1.3.1_T

Comparison of the magnitude and phase of the relationship between the water pressure head and gate opening position of the hydraulic power generating system simulated with droop in LVTrans8_1.1.2 and computed in LVTrans86_1.3.1_T can be analyzed in Figure 11-8. The magnitude of the hydraulic power generating system simulated in LVTrans8_1.1.2 is slightly different to that computed in LVTrans86_1.3.1_T.

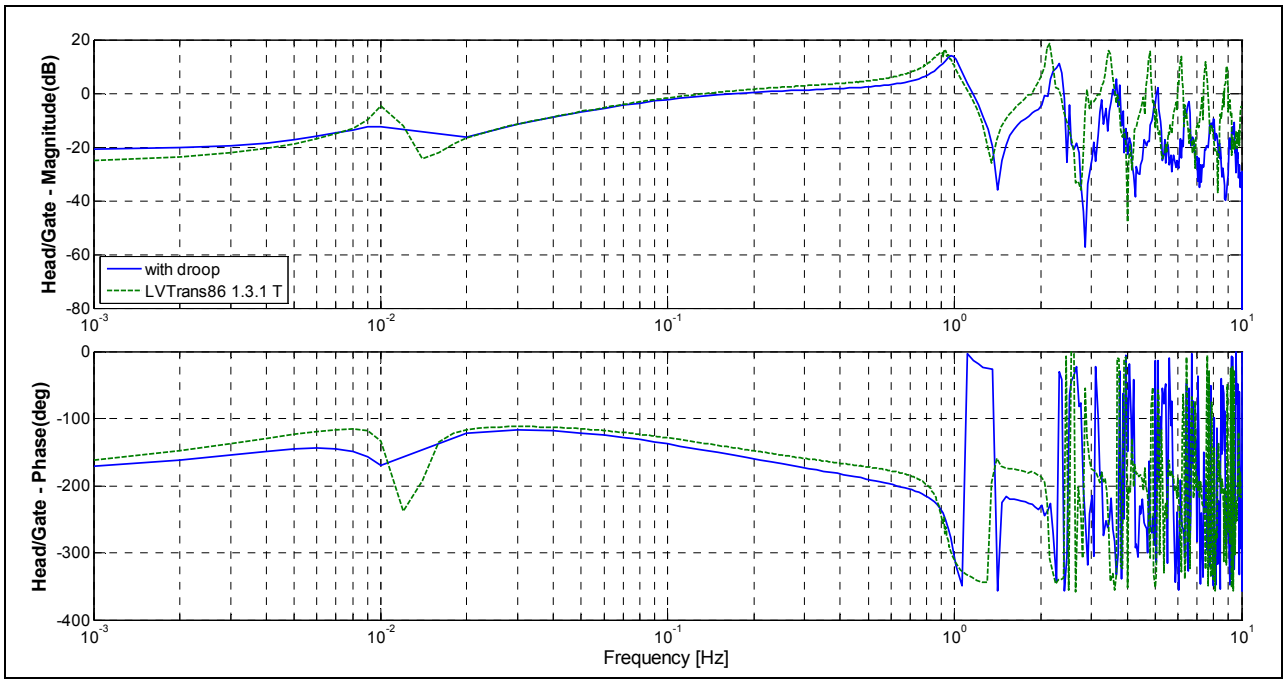

Figure 11-8: Comparison of the Frequency Response of the hydraulic power generating system simulated with droop in LVTrans8_1.1.2 and computed in LVTrans86_1.3.1_T

In Figure 11-7 and Figure 11-8, the magnitude of the transfer function of the hydraulic power generating system simulated in LVTrans8_1.1.2 is a little different to that computed in LVTrans86_1.3.1_T. The frequency response of the hydraulic power generating system simulated in LVTrans86_1.3.1_T has more damping.

LVTrans8_1.1.2 is a version created specifically for the detailed grid/waterway interaction. LVTrans8_1.1.2 has more details than the newest version LVTrans86_1.3.1_T. The modelling of the generator, grid and PID governor is more detailed in LVTrans version LVTrans8_1.1.2.

The magnitude of the hydraulic power generating system simulated LVTrans86_1.3.1_T has a lower value at the early frequency range but slowly increases. The magnitude of the model simulated in LVTrans86_1.3.1_T reaches higher values than the magnitude of the model simulated in LVTrans8_1.1.2.

The magnitudes of both models reach a peak at a resonance frequency around 0.01 Hz. This frequency corresponds to the natural frequency of the mass-oscillation between the reservoir and the surge tank. The magnitudes of both models reach a higher peak at a resonance frequency around 0.8 Hz. This frequency corresponds to the first natural frequency of the penstock. The oscillations at higher frequencies are due to the elasticity of the conduit system.

12 Discussion

The simulation system of a typical hydroelectric power plant has been implemented in the software SIMPOW and the simulaton tool LVTrans. The hydroelectric power system has a reservoir, an upstream tunnel, a long length penstock with an upstream surge tank and is equipped with a Francis turbine. In order to test the accuracy and effectiveness of the hydraulic power system, some simulations have been conducted.

This chapter presents the summary of the results of the frequency response analysis as well as transient response analysis of the models implemented in SIMPOW and LVTrans. The models implemented in SIMPOW are compared and analyzed. After that, these models are compared with the models developed in LVTrans8_1.1.2.

12.1 Summary of Simulation Results of the models computed in SIMPOW

The hydraulic power generating system, which is developed in this work for the stability analysis, has been implemented in SIMPOW with a detailed synchronous generator model with damping, a general speed-governing model, and a hydraulic turbine. The hydraulic turbine is modelled with varying degrees of detail. The mathematical models of the hydraulic turbine are detailed in Table 9-4, and listed below

Model 1 Simplified Nonlinear Turbine Model
Model 2 Nonlinear Turbine Model without Surge Tank assuming Inelastic Water Column
Model 3 Nonlinear Turbine Model without Surge Tank including Elastic Water Column Effect
Model 4 Nonlinear Turbine Model with Surge Tank assuming Inelastic Water Columns
Model 5 Nonlinear Turbine Model with Surge Tank assuming Elastic Water Column in Penstock and Inelastic Water Column in Upstream Tunnel
Model 6 Linear Turbine Model with Surge Tank considering Inelastic Water Columns in Penstock and Tunnel, and turbine characteristics based in the turbine coefficients recommend by IEEE
Model 7 Linear Turbine Model with Surge Tank including Elastic Water Column in Penstock, and turbine characteristics based in the turbine coefficients recommend by IEEE

In order to test the accuracy and effectiveness of the hydro power generating system, frequency response analysis as well as transient response analysis is performed to evaluate the effects of the detailed modelling of the turbine and conduit system to the stability analysis and the dynamic performance.

The frequency response analysis has been performed to the relationships of the mechanical power, mechanical torque, and pressure head to gate position. The angular frequency of the input sinusoidal was varied between 0.001 and 10 Hz.

12.2 Summary of the Eigenvalue analysis computed in SIMPOW

The dynamic performance of the models implemented in SIMPOW is investigated utilizing the Eigenvalue analysis. The Eigenvalue analysis of the models shows that the all the models have one oscillatory mode associated with the rotor angle and speed. This mode is called electromechanical oscillatory mode and corresponds to the synchronous machine natural frequency that depends on rotating inertias. Table 12-1 shows the electromechanical oscillatory mode of the models of the Hydro Power System implemented in Chapter 10.

Table 12-1: Summary of the electromechanical oscillatory mode of the models of the models

	Models	Eigenvalue	Damping Ratio	Frequency [Hz]
1	Simplified Nonlinear Turbine Model	-0.4073 ± j 6.6214	0.06140	1.05383
2	Nonlinear Turbine Model without Surge Tank assuming Inelastic Water Column	-0.4203 ± j 6.6906	0.06270	1.06485
3	Nonlinear Turbine Model without Surge Tank including Elastic Water Column Effect	-0.5188 ± j 6.6521	0.07775	1.05872
4	Nonlinear Turbine Model with Surge Tank assuming Inelastic Water Columns	-0.5102 ± j 7.1079	0.07160	1.13126
5	Nonlinear Turbine Model with Surge Tank assuming Elastic Water Column in Penstock	-0.5933 ± j 7.0806	0.08350	1.12692
6	Linear Turbine Model with Surge Tank considering Inelastic Water Columns, and turbine characteristics	-0.2925 ± j 6.8421	0.04270	1.08896
7	Linear Turbine Model with Surge Tank including Elastic Water Column in Penstock, and turbine characteristics	-0.4674 ± j 6.7198	0.06939	1.06950

The error in the frequency of oscillation between the calculated eigenvalues with K_D=0.50, Table 9-8, and the computed eigenvalues of the different models are shown in Table 12-2. The error calculated between the computed models and the calculated eigenvalues is less that the 10% in all the representations.

Table 12-2: Error between the calculated eigenvalues and the computed eigenvalues

Model	Error, [%]
Simplified Nonlinear Turbine Model	0.1450
Nonlinear Turbine Model without Surge Tank assuming Inelastic Water Column	0.9068
Nonlinear Turbine Model without Surge Tank including Elastic Water Column Effect	0.3193
Nonlinear Turbine Model with Surge Tank assuming Inelastic Water Columns	7.1986
Nonlinear Turbine Model with Surge Tank assuming Elastic Water Column in Penstock	6.7817
Linear Turbine Model with Surge Tank considering Inelastic Water Columns, and turbine characteristics	3.1904
Linear Turbine Model with Surge Tank including Elastic Water Column in Penstock, and turbine characteristics	1.3427

12.3 Comparison of the results of the models in SIMPOW

Frequency response analysis is developed by "Frequency Scanning" in Linear Analysis in DYNPOW in order to identify the transfer function and other parameters of the models of the hydraulic turbine and conduit system, detailed in Table 9-4. To demonstrate the dynamic nonlinear effects, a perturbation signal is applied to the gate opening position in open loop conditions. The open loop condition is obtained by assuming H=9999999 for the synchronous machine model. That means that the effects of the speed in the block diagram can be omitted.

12.3.1 Comparison of Nonlinear Turbine Models without surge tank

Herein, frequency response analysis as well as transient response analysis is performed to evaluate the effects to the stability analysis of a simple hydraulic turbine without surge tank modelled by

- the simplified nonlinear model (Model 1),
- the nonlinear model assuming inelastic water column (Model 2) and
- the nonlinear model including elastic water column effects (Model 3)

In Figure 12-1 to Figure 12-4, the dynamic performance of the blue solid line represents the simplified nonlinear turbine model (Model 1), the green dashed line represents the nonlinear model assuming inelastic water column (Model 2), and the red dash-dotted line represents the nonlinear model including elastic water column effects (Model 3).

Comparison between the dynamic behaviour of variables such as power angle, rotational speed, mechanical torque, gate position, flow rate and head pressure of a hydraulic power system model simulated by Model 1, 2 and 3 can be examined in Figure 12-1. The stability analysis of the hydraulic power system model is tested by simulating a three-phase fault to ground at t=1 s. This disturbance is simulated for a period of 5.0 ms.

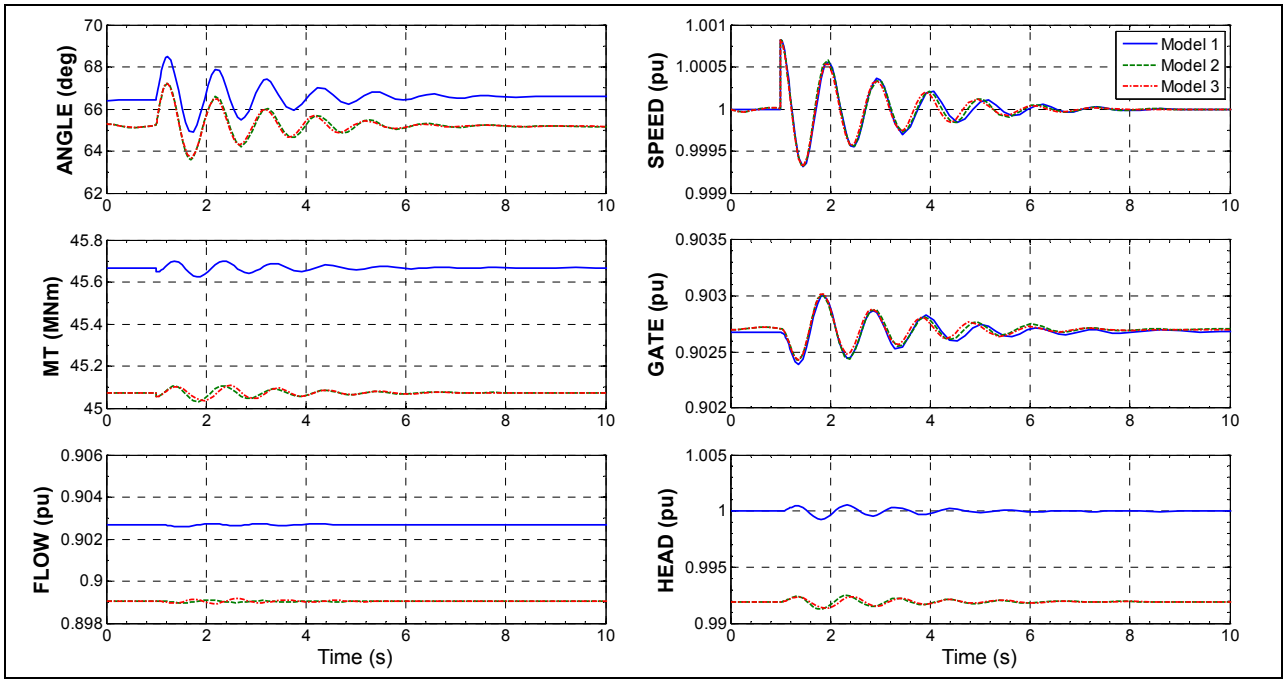

Figure 12-1: Fault Simulation Results of hydraulic turbine represented by model 1, 2 and 3

It is seen from Figure 12-1, the angle and speed of the generator are almost the same for models 2 and 3, and is slightly different for model 1. It means that the effect of different hydro turbine models on the power system transient stability simulation is comparatively small. The variables such as mechanical torque, flux rate, and pressure head that are closely related to the conduit system have a little difference between model 1, and models 2 and 3. The speed of the generator and gate position are almost the same for the three models. The gate opening position in the hydraulic power system model changes slightly.

The dynamic behaviour of Model 2 and Model 3 are very similar. It can be concluded that the simulation results of Model 1 is slightly different. The difference between model 1 and model 2 and 3 is small. The difference between models 1, and model 2 and 3 is little different because of the simplified nonlinear model neglects the hydraulic losses.

The static behaviour is established by the relationship between the steady-state values of gate position and turbine developed power. Figure 12-2 compares the gate position-turbine developed power relationship of the hydraulic turbine model 1, 2 and 3. There is a good agreement between the magnitude of the transfer functions of model 2 and 3. The magnitude of the transfer functions of model 1 and, model 2 and 3 have a little difference due to the head losses. It is observed a significant difference in the phase of model 1, 2 and 3 at very low frequencies up to 0.002 Hz. The phase is slightly different for the rest of the bandwidth.

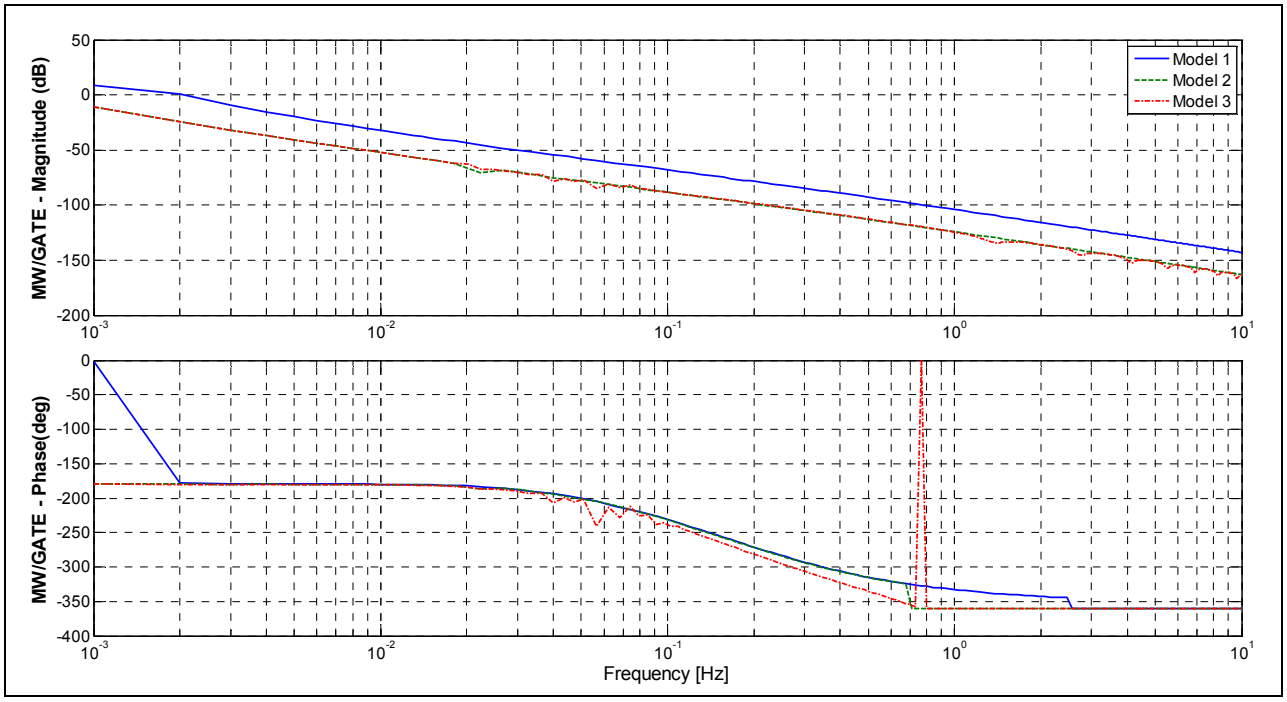

Figure 12-2: Frequency response of the transfer functions from Gate position to Mechanical Power of a simple hydraulic turbine represented by Model 1, 2 and 3

Figure 12-3 compares the magnitude and phase of the transfer function relating the mechanical torque to variations of the gate position of the hydraulic power system represented by model 1, 2 and 3. It is observed that model 1, 2 and 3 have a slight difference between each other at low frequencies up to 0.7 Hz. However, significant difference in model 3 is observed at high frequencies. Model 3 shows oscillations due to the elasticity of the conduit system. The natural frequencies corresponding to higher modes of the conduit system oscillations are visible.

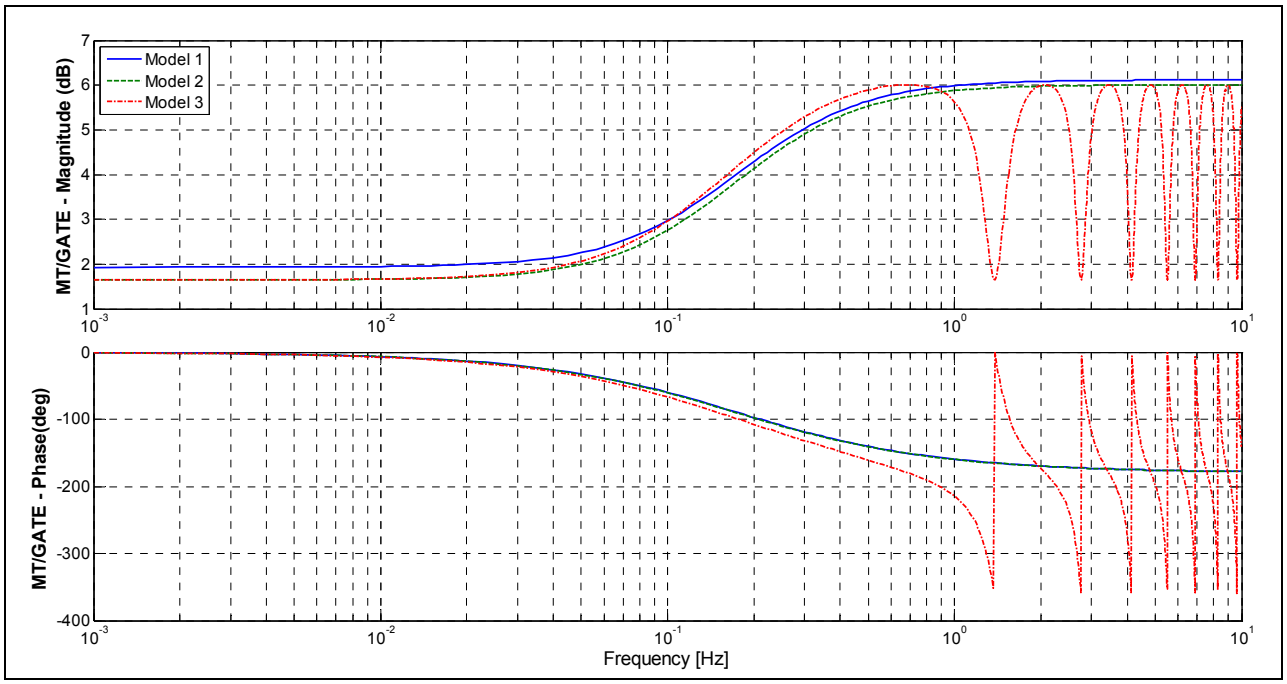

Figure 12-3: Frequency response of the transfer function from Gate position to Mechanical Torque of a hydraulic turbine represented by Model 1, 2 and 3

The frequency responses of transfer function of head pressure and gate position of a hydraulic turbine represented by model 1, 2 and 3 are compared in Figure 12-4. The magnitude and phase of the three transfer functions are similar for frequencies up to 1.0 Hz. The transfer function features the first natural frequency of the penstock with a high amplitude at 0.7 Hz. For higher frequencies, the transfer functions of model 1 and 2 cannot represent the conduit dynamics with any acceptable degree of accuracy. This is evident when observing the frequency response between 1 and 10 Hz.

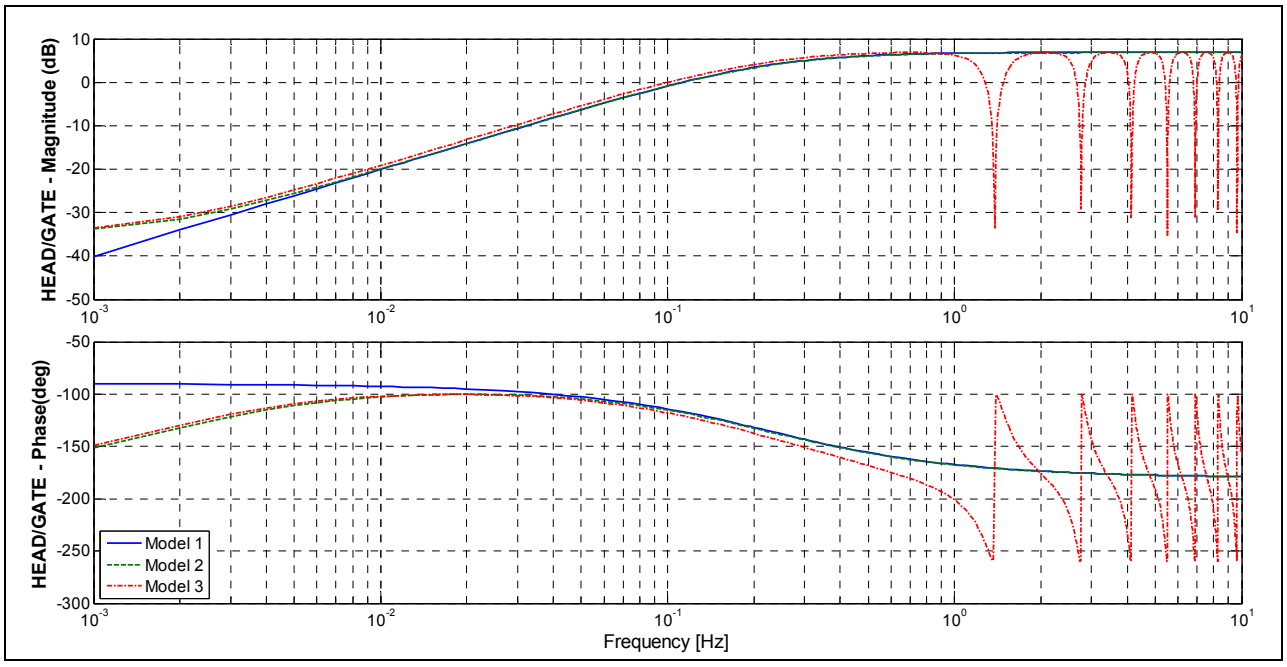

Figure 12-4: Frequency response of the transfer functions of the conduit system of Model 1, 2 and 3

12.3.2 Comparison of Turbine Models with Surge Tank

The following studies involve frequency response analysis as well as transient response analysis to evaluate the effects to the stability analysis of a simple hydraulic turbine with surge tank modelled by

- the nonlinear model assuming Inelastic water columns in penstock and tunnel (Model 4)
- the nonlinear model assuming elastic water column in penstock (Model 5)
- the linear model assuming inelastic water columns in penstock and tunnel (Model 6)
- the linear model including elastic water column effects in the penstock (Model 7)

In Figure 12-5 to Figure 12-8, the dynamic performance of the blue solid line represents the model 4, the green dashed line represents the model 5, the red dotted line represents the model 6, and the turquoise dash-dotted line represents the model 7.

Comparison between the dynamic behaviour of variables such as power angle, rotational speed, mechanical torque, gate position, flow rate and head pressure of the hydraulic system model simulated by Model 4, 5, 6 and 7 can be examined in Figure 12-5. The stability analysis of the hydraulic power generating system is tested by simulating a three-phase fault to ground at t=1 s. This disturbance is simulated for a period of 5.0 ms. The sampling period is 50 s.

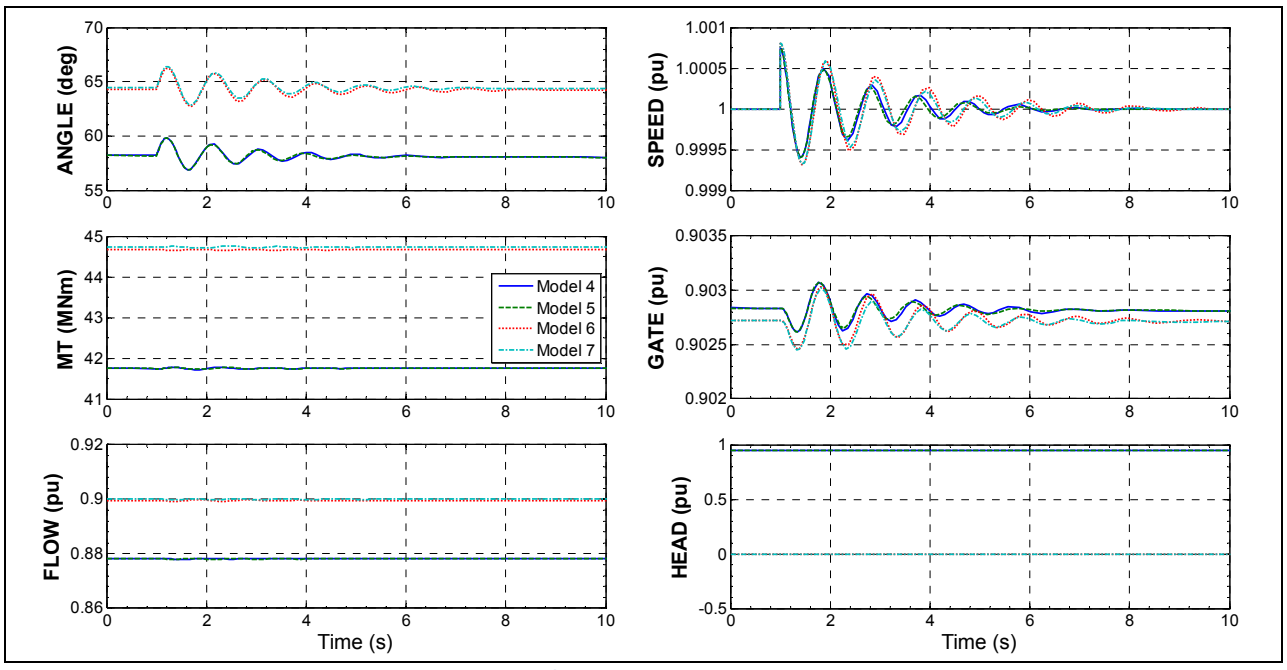

Figure 12-5: Fault Simulation Results of hydraulic turbine represented by Model 4, 5, 6 and 7

It is seen from Figure 12-5, the angle of the generator are almost the same for model 4 and 5, and is slightly different for the model 6 and 7. The speed of the generator is very similar for model 4, 5, 6 and 7; this means that the effect of different hydro turbine models on the power system transient stability simulation is comparatively small. The variables such as mechanical torque, flux rate, and pressure head that are closely related to the conduit system have a little difference between nonlinear models and linear models.

The changes of speed of the generator and the gate position are almost the same for the four models. The gate opening position in the hydraulic power system model changes slightly. The

dynamic behaviour of the linear models, model 6 and 7, are very similar. It can be concluded that the simulation results of the nonlinear models are slightly different of the linear models.

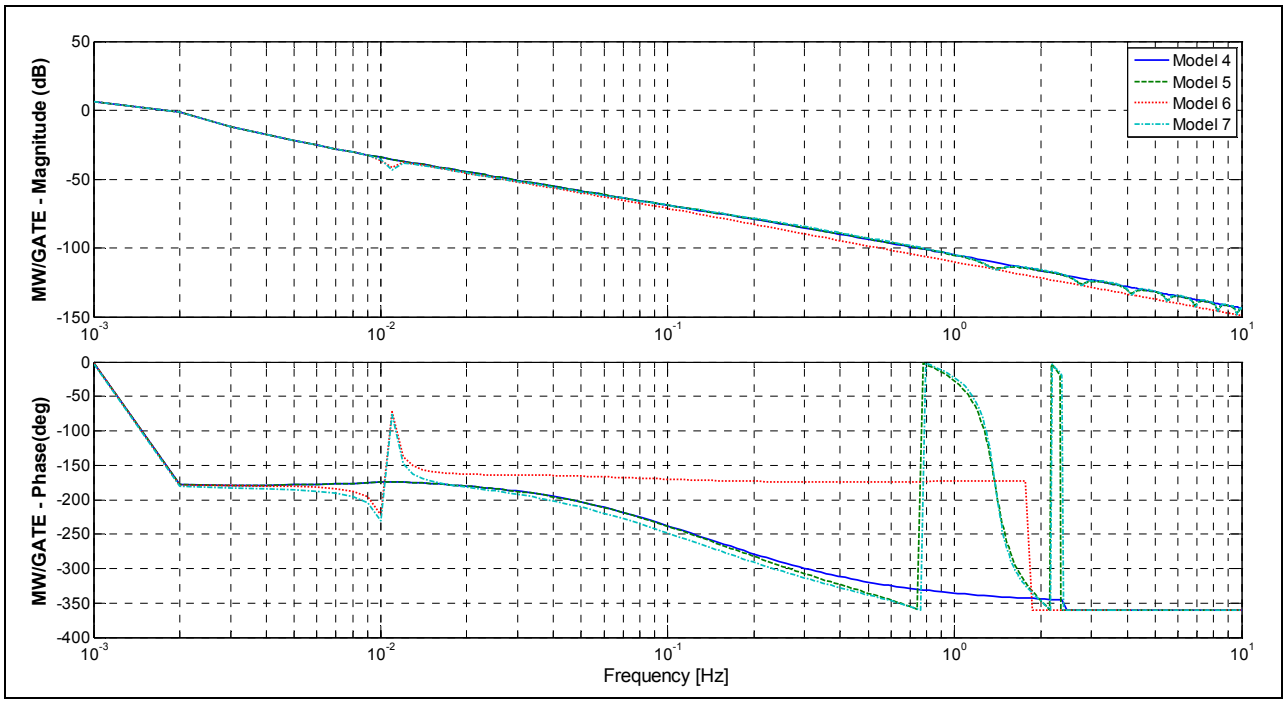

Figure 12-6: Frequency response of the transfer function from gate position to Mechanical Power of Model 4, 5, 6 and 7

Figure 12-6 compares the gate position-turbine developed power relationship of the hydraulic turbine model 4, 5, 6 and 7. The magnitude of the transfer functions of model 4, 5, 6 and 7 are very similar in the entire bandwidth. Model 4, 5, 6 and 7 shows significant difference in the phase.

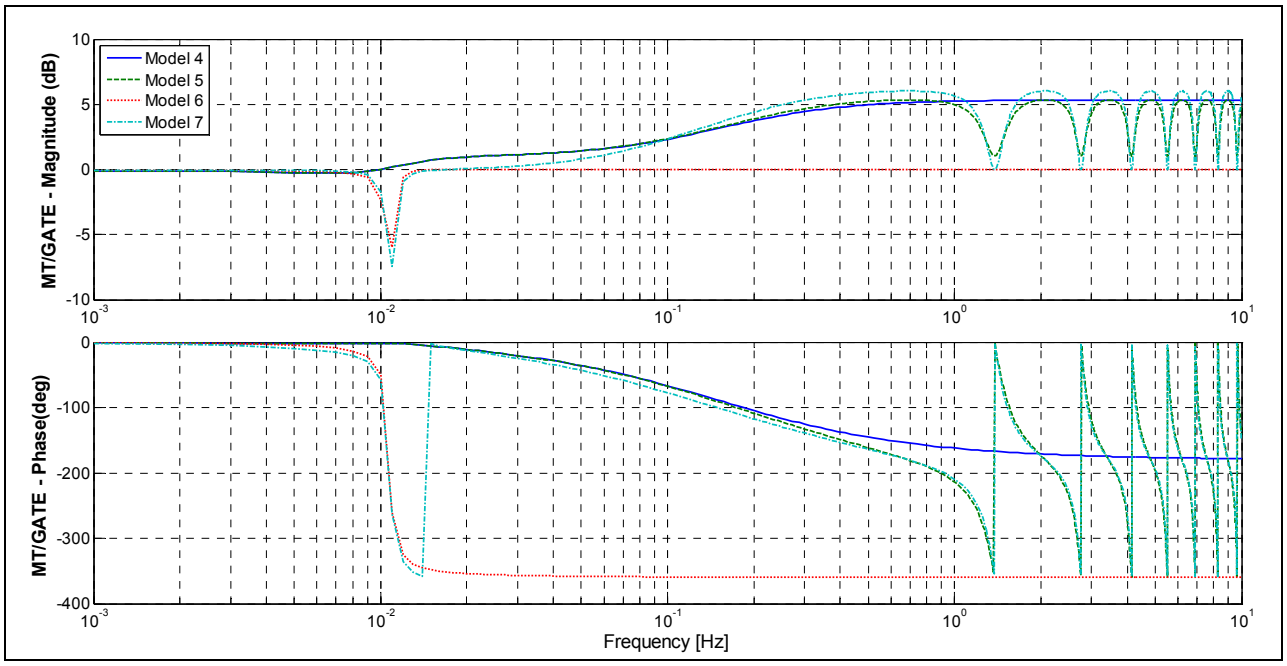

Figure 12-7: Frequency Response of the transfer function from Gate position to Mechanical Torque of a simple hydraulic turbine represented by Model 4, 5, 6 and 7

Figure 12-7 compares the magnitude and phase of the transfer function relating the mechanical torque to the gate position of the turbine represented by model 4, 5, 6 and 7. It is observed that model 4, 5 and 7 have a slight difference at low frequencies up to 0.8 Hz. However, significant difference is observed at high frequencies. The natural frequencies corresponding to higher modes of the conduit system of model 5 and 7 are shown.

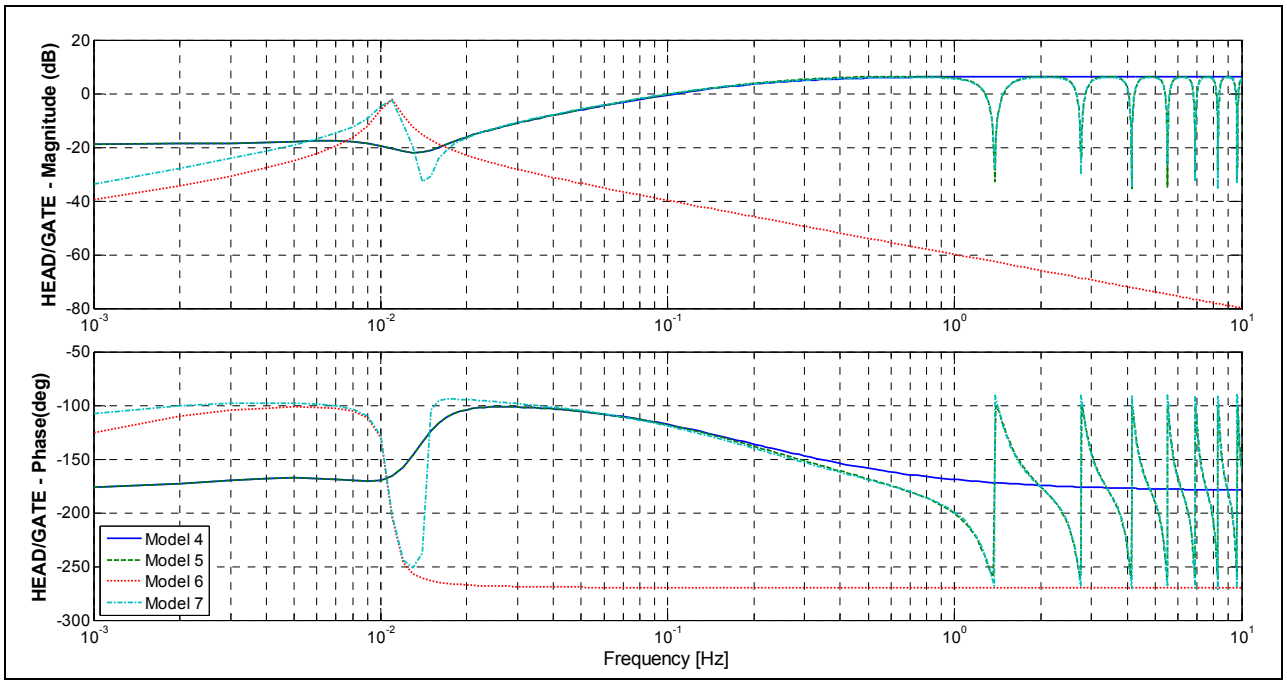

Figure 12-8: Frequency response of the transfer function of the conduit system of Model 4, 5, 6 and 7

The frequency response of the transfer function of head pressure and gate position of a simple hydraulic turbine with surge tank represented by model 4, 5, 6 and 7 are compared in Figure 12-8. It can easily be noticed that the frequency responses of the elastic models, model 5 and 7, are similar even though their parametric models are significantly different. A large difference in the phase of model 4 and 6 are shown.

The transfer functions of model 6 and 7 feature a natural frequency with a high amplitude at 0.01 Hz. This frequency corresponds to the natural frequency of the mass-oscillation between the reservoir and the surge tank. The calculated natural frequency of the mass-oscillation is given by Equation (9.9). The transfer functions of model 4, 5 and 7 feature the natural frequency of the penstock with a higher amplitude at 0.8 Hz. The natural frequency of the penstock is described in Equation (9.8). For higher frequencies, the transfer function of model 4 and 6 cannot represent the conduit dynamics with any acceptable degree of accuracy. This is evident when observing the frequency response between 1 and 10 Hz.

The simulation results of Model 4 and 5 do not show the natural frequency of the mass-oscillation between the reservoir and the surge tank. The implementation of Model 4 and 5 must be checked in order to obtain a better fit with the results in LVTrans.

Model 6 and 7 should be studied in detail, varying the values of the turbine coefficients. These coefficients, which represent the nonlinear characteristic of the turbine, have to be extracted from the Hill Charts.

12.4 Comparison of the simulation results computed in SIMPOW and LVTrans

The following studies involve frequency response analysis to evaluate the effects to the stability analysis of hydraulic power generating system implemented in SIMPOW and LVTrans. The hydro turbine implemented in SIMPOW is modelled by

- the nonlinear model assuming Inelastic water columns in penstock and tunnel (Model 4)
- the nonlinear model assuming elastic water column in penstock (Model 5)
- the linear model assuming inelastic water columns in penstock and tunnel (Model 6)
- the linear model including elastic water column effects in the penstock (Model 7)

The frequency response of the hydraulic power system model has been simulated and analyzed with droop and without droop in the dynamic tool LVTrans version LVTrans8_1.1.2. The feedback from the gate opening position to the controller is included when the simulation is performed with droop. The droop is usually 4% to 8%.

In Figure 12-9 and Figure 12-10, the dynamic performance of the blue solid line represents the hydropower generating system without droop and with droop computed in LVTrans, respectively. The green dashed line represents the model 4, the red dash-dotted line represents the model 5, the turquoise dotted line represents the model 6, and the purple dashed line represents the model 7.

Figure 12-9 compares the magnitude and phase of the transfer function of water pressure and gate opening of a hydraulic power system represented by model 4, 5, 6 and 7, in SIMPOW, and the hydraulic power system model without droop in LVTrans. It is observed that both models in SIMPOW and model in LVTrans has a slightly difference in the magnitude at low frequencies. However, significant difference is observed in the phase.

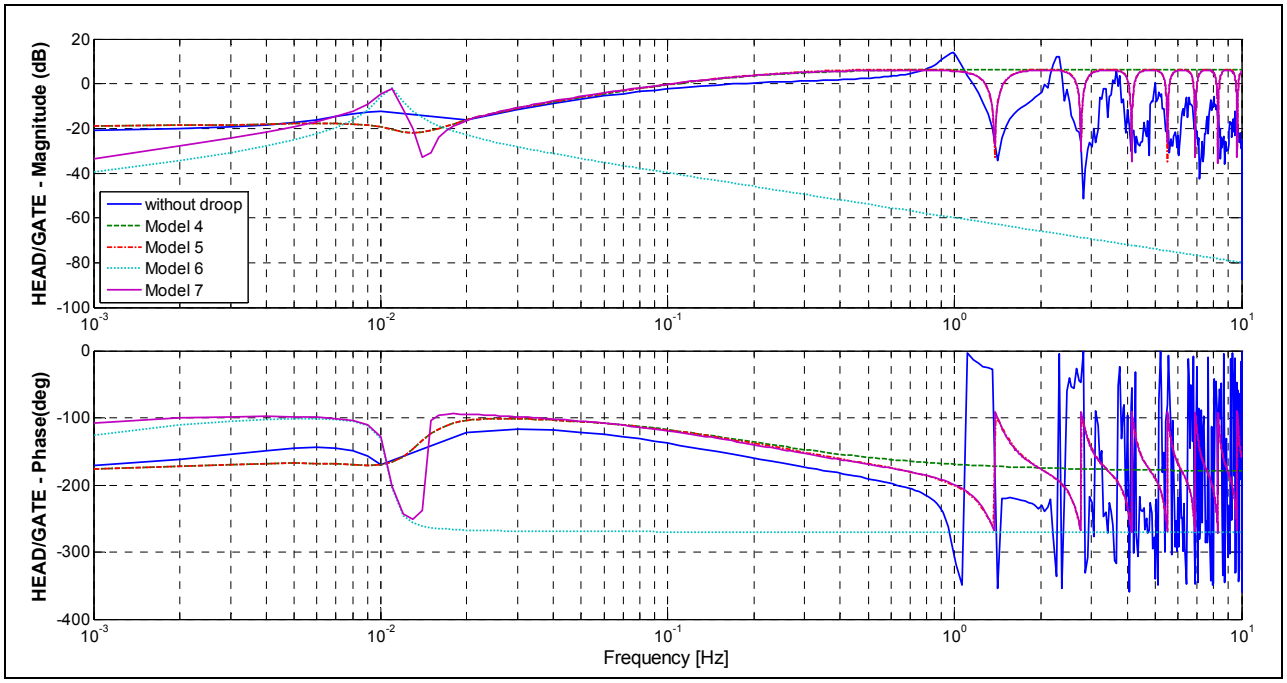

Figure 12-9: Frequency Responses of the transfer function of the conduit system of Hydraulic Power System Models implemented in SIMPOW and LVTrans (without droop)

Figure 12-10 compares the magnitude and phase of the transfer function of water pressure and gate opening of a hydraulic power system represented by model 4, 5, 6 and 7, in SIMPOW, and model with droop implemented in LVTrans. It is observed that both models in SIMPOW and model in LVTrans has a slightly difference in the magnitude at low frequencies. However, significant difference is observed in the phase. The oscillations at high frequency of the model 5 and 7, and the model computed in LVTrans are due to the elasticity of the conduit system.

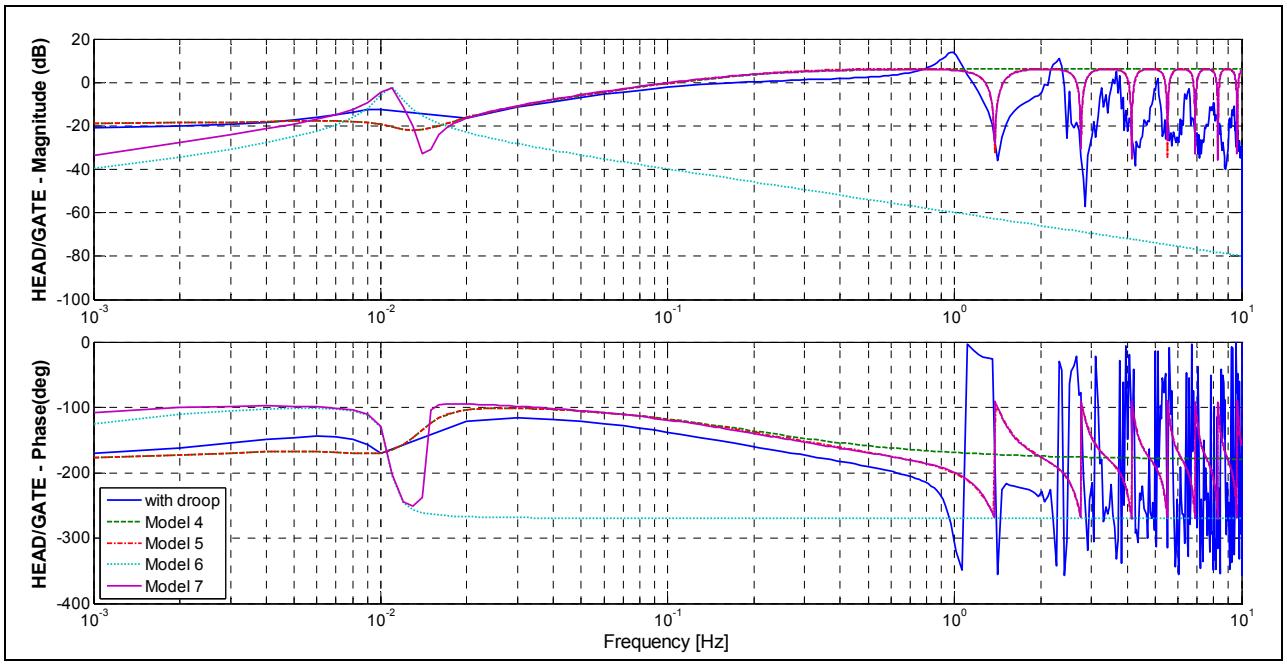

Figure 12-10: Frequency Responses of the transfer function of the conduit system of Hydraulic Power System Models implemented in SIMPOW and LVTrans (with droop)

From the models implemented in LVTrans, it can be concluded that the hydraulic system model without droop agrees well with the hydraulic system model with droop. The magnitude of both transfer functions shows two peaks at a resonance frequency of 0.01 Hz and 0.9 Hz. These frequencies correspond to the natural frequencies of the mass-oscillation and penstock, respectively. The effect of the droop has very little influence on the phase. The oscillations at higher frequencies are due to the elasticity of the conduit system.

The transfer functions of model 6, 7 in SIMPOW, and models in LVTrans feature a natural frequency with a high amplitude at 0.01 Hz. This frequency corresponds to the natural frequency of the mass-oscillation between the reservoir and the surge tank. The transfer functions of model 4, 5 and 7 in SIMPOW, and models in LVTrans, all of them, feature a high amplitude at 0.8 Hz that is the natural frequency of the penstock. For higher frequencies, the transfer functions of model 4 and 6 cannot represent the conduit dynamics with any acceptable degree of accuracy. This is evident when observing the frequency response between 1 and 10 Hz.

It is interesting to note that the magnitude of Model 7, which represents the most complete model until this stage, and model in LVTrans show a good fit. Model 7 features a lower peak in magnitude at 0.8 Hz. This could be due to the influence of the values of the turbine coefficients used in this model.

13 Conclusions

13.1 Conclusions

This Master's Thesis work deals with the development of improved hydro turbine models for the evaluation of a hydraulic power generating system performance in response to small disturbances in power system analysis tool. These improved models must be able to reflect the possible interaction between the hydraulic system and power system in the computer simulations of a power plant equipped with Francis turbines. Traditionally, mathematical models for hydraulic power generating systems, normally found in relevant literature and power system analysis tools, are simplified models. This implies that these models only reflect part of the real situations and as such could have a limited application.

The dynamics of hydraulic turbines have a considerable influence on the dynamic stability of the power system. The mathematical modelling of the flow and power output of a Francis turbine, and its transient behaviour is based on the characteristic curve of the hydraulic machine called *Hill Charts.* The turbine efficiency for any operating point given by runner speed, net head and gate position can be extracted from the Hill Charts. These values have to be measured precisely via field tests or taken from model tests. Although such curves are seldom used in specifications due to difficulties of measurement, the speed-torque characteristics of a wide variety of hydraulic turbines have the general form with the torque falling off roughly in proportion to speed over wide ranges of speed and gate opening position. The influence of the turbine coefficients on the model accuracy is critical.

The hydraulic power generating system model, which is developed in this Thesis work for the stability analysis, has been designed with a third-order synchronous generator model, a mechanical-hydraulic governing system model, and a hydraulic turbine. The hydraulic turbine is modelled with varying degrees of detail. The effect of the hydraulic power generating system is studied by means of analysis of the dynamic behaviour of the models of the hydraulic machine and conduit system about the steady-state operating condition following a small disturbance. The models of the hydraulic machine and conduit system developed as part of this study and implemented in SIMPOW, are listed below:

Model 1 Simplified Nonlinear Turbine Model
Model 2 Nonlinear Turbine Model without Surge Tank assuming Inelastic Water Column
Model 3 Nonlinear Turbine Model without Surge Tank including Elastic Water Column Effect
Model 4 Nonlinear Turbine Model with Surge Tank assuming Inelastic Water Columns
Model 5 Nonlinear Turbine Model with Surge Tank assuming Elastic Water Column in Penstock and Inelastic Water Column in Upstream Tunnel
Model 6 Linear Turbine Model with Surge Tank considering Inelastic Water Columns in Penstock and Tunnel, and turbine characteristics based in the turbine coefficients recommend by IEEE
Model 7 Linear Turbine Model with Surge Tank including Elastic Water Column in Penstock, and turbine characteristics based in the turbine coefficients recommend by IEEE

Frequency response analysis as well as transient analysis is performed to evaluate the effects of the detailed modelling of the turbine and conduit system to the stability analysis and the dynamic performance of the hydraulic power generating system. The hydraulic power generating system has also been implemented in the hydraulic system analysis tool LVTrans.

Eigenvalue analysis

The dynamic performance of the different Hydro Power System models connected to a power system has been investigated utilizing Eigenvalue analysis. The theoretical eigenvalues are determined via analytical approach for a classical simplified power system represented by the second-order synchronous machine model connected to an infinite busbar. Eigenvalues are also determined in Dynpow of the software SIMPOW. The error in the frequency of oscillation between the theoretical eigenvalues with K_D=0.50 and the computed eigenvalues of the different models is less that the 10% in all the representations.

Time-domain analysis

The dynamic behaviour of the hydraulic turbine represented by model 1, 2 and 3 are similar. It can be concluded that the simulation results of model 1 is slightly different. It means that the effect of different hydro turbine models on the power system transient stability simulation is comparatively small. The variables such as mechanical torque, flux rate and pressure head that are closely related to the conduit system have a little difference between model 1, and model 2 and 3. The changes in speed of the generator and gate position are almost the same for the three models.

The changes in speed of the generator is very similar for model 4, 5, 6 and 7; this means that the effect of different models of hydro turbine with surge tank on the power system transient stability simulation is comparatively small. The speed of the generator and the gate position are almost the same for the four models. The gate opening position in the test system changes slightly. The dynamic behaviour of the linear models, model 6 and 7, is very similar. It can be concluded that the simulation results of the nonlinear models are slightly different of the linear models.

Frequency Response Analysis

There is a good agreement between the frequency response of the three transfer functions of head pressure and gate position of a hydraulic turbine represented by model 1, 2 and 3. The transfer function features a natural frequency with a high amplitude at 0.8 Hz. This frequency corresponds to the first natural frequency of the penstock. For higher frequencies, the transfer functions of model 1 and 2 cannot represent the conduit dynamics with any acceptable degree of accuracy.

The frequency response of the transfer function of head pressure and gate position of a simple hydraulic turbine with surge tank represented by models 4, 5, 6 and 7 show differences at low frequencies. Transfer functions of model 4 and 5 shows an excellent fit at low frequencies up to 1 Hz. The transfer functions of model 6 and 7 feature a natural frequency with a high amplitude at 0.01 Hz. This frequency corresponds to the natural frequency of the mass-oscillation between the reservoir and the surge tank. The transfer functions of model 4, 5 and 7 feature the natural frequency of the penstock with a higher amplitude at 0.8 Hz. For higher frequencies, the transfer function of model 4 and 6 cannot represent the conduit dynamics with any acceptable degree of accuracy.

The dynamic behaviour of the Hydraulic Power System has been analyzed in the program LVTrans version LVTrans8_1.1.2 and version LVTrans86_1.3.1_T. LVTrans8_1.1.2 is a version created specifically for the detailed grid/waterway interaction. The frequency response of the hydraulic power generating system simulated in LVTrans8_1.1.2 is slightly different to that computed in LVTrans86_1.3.1_T. The frequency response of the hydraulic power generating system simulated in LVTrans86_1.3.1_T has more damping. Based on the simulation results from the models implemented in LVTrans, it can be concluded that the hydraulic system model without droop agrees well with the hydraulic system model with droop. The magnitude of both models show two peaks at a resonance frequency of 0.01 Hz and 0.9 Hz. These frequencies correspond to the natural frequencies of the mass-oscillation and penstock, respectively. The effect of the droop has very little influence on the phase. The oscillations at higher frequencies are due to the elasticity of the conduit system.

The transfer functions of model 6, 7 in SIMPOW, and models in LVTrans feature a natural frequency with a high amplitude at 0.01 Hz. This frequency corresponds to the natural frequency of the mass-oscillation between the reservoir and the surge tank. The transfer functions of model 4, 5 and 7 in SIMPOW, and models in LVTrans, all of them, feature a high amplitude at 0.8 Hz that is the natural frequency of the penstock. For higher frequencies, the transfer function of model 4 and 6 cannot represent the conduit dynamics with any acceptable degree of accuracy.

The simulation results of Model 4 and 5 do not show the natural frequency of the mass-oscillation between the reservoir and the surge tank. The implementation of Model 4 and 5 must be checked in order to obtain a better fit with the results in LVTrans.

Model 6 and 7 should be studied in detail, varying the values of the turbine coefficients. These coefficients, which represent the nonlinear characteristic of the turbine, have to be extracted from the Hill Charts.

It is interesting to note that the magnitude of Model 7, which represents the most complete model until this stage, and model in LVTrans show a good fit. Model 7 features a lower peak in magnitude at 0.8 Hz. This could be due to the influence of the values of the turbine coefficients used in this model.

13.2 Further Work

The implementation of Model 4 and 5 must be checked in order to obtain a better fit with the results in LVTrans. The effects of the surge tank must be better represented in the model to develop in SIMPOW. Additionally, these models could be improved, including the nonlinear characteristics of the turbine extracted from the Hill Charts.

Model 6 and 7 should be studied in detail, varying the nonlinear characteristics of the hydraulic turbine, in order to draw more accurate conclusions about the dynamic behaviour of the models. The influence of the turbine coefficients on the model accuracy is critical and these values should be extracted from the Hill Charts and linearized around an operating point.

Additionally, the hydroelectric power plant system may be modelled by the Structure Matrix Method, and be compared with the models implemented in SIMPOW and LVTrans.

14 Reference Bibliography

1. *Hydraulic turbine and turbine control models for system dynamic studies.* Power Systems, IEEE Transactions on, 1992. **7**(1): p. 167-179.
2. Kundur, P., N.J. Balu, and M.G. Lauby, *Power system stability and control*. 1994, New York ; London: McGraw-Hill. xxiii,1176p.
3. Parmakian, J., *Waterhammer analysis*. 1963, [S.l.]: Dover. 161 p.
4. Wood, D.J., *Waterhammer Analysis---Essential and Easy (and Efficient).* Journal of Environmental Engineering, 2005. **131**(8): p. 1123-1131.
5. Bergant, A., A.R. Simpson, and A.S. Tijsseling, *Water hammer with column separation: A historical review.* Journal of Fluids and Structures, 2006. **22**(2): p. 135-171.
6. Chaudhry, M.H., *Applied hydraulic transients*. 2nd ed. ed. 1987, New York ; Wokingham: Van Nostrand Reinhold. xvi,521p.
7. BOULOS, et al., *Hydraulic transient guidelines for protecting water distribution systems*. Vol. 97. 2005, Denver, CO, ETATS-UNIS: American Water Works Association. 14.
8. Almeida, A.B.d. and E. Koelle, *Fluid transients in pipe networks*. 1992, Southampton; Boston, Mass.; London; New York: Computational Mechanics Publications ; Elsevier Applied Science.
9. Zipparro, V.J., H. Hasen, and C.V. Davis, *Davis' handbook of applied hydraulics*. 4th ed. ed. 1993, New York: McGraw-Hill.
10. (TNSHP), T.N.o.S.h., *Guide on How to Develop a Small Hydropower Plant*, E.S.H.A.-. ESHA, Editor. 2004.
11. Konidaris, D.N. and J.A. Tegopoulos, *Investigation of oscillatory problems of hydraulic generating units equipped with Francis turbines.* Energy Conversion, IEEE Transactions on, 1997. **12**(4): p. 419-425.
12. Oldenburger, R. and J. Donelson, *Dynamic Response of a Hydroelectric Plant.* Power Apparatus and Systems, Part III. Transactions of the American Institute of Electrical Engineers, 1962. **81**(3): p. 403-418.
13. Romeo, E., C. Royo, and A. Monzón, *Improved explicit equations for estimation of the friction factor in rough and smooth pipes.* Chemical Engineering Journal, 2002. **86**(3): p. 369-374.
14. White, F.M., *Fluid mechanics*. 6th ed. ed. 2008, New York ; London: McGraw-Hill. xiii, 864 p.
15. Souza, O.H., Jr., N. Barbieri, and A.H.M. Santos, *Study of hydraulic transients in hydropower plants through simulation of nonlinear model of penstock and hydraulic turbine model.* Power Systems, IEEE Transactions on, 1999. **14**(4): p. 1269-1272.
16. Brekke, H., *A Stability Study on Hydro Power Plant Governing Including the influence from a Quasi nonlinear damping of oscillatory flow and from the turbine characteristics*. 1984, Norges Tekniske Høgskole: Trondheim.
17. Bakken, B.H., *Technical and economic aspects of operation of thermal and hydro power systems.* 1997, Trondheim: Norwegian University of Science and Technology. 222.
18. Hongqing, F., et al., *Basic Modeling and Simulation Tool for Analysis of Hydraulic Transients in Hydroelectric Power Plants.* Energy Conversion, IEEE Transactions on, 2008. **23**(3): p. 834-841.

19. Kishor, N., S.P. Singh, and A.S. Raghuvanshi, *Dynamic simulations of hydro turbine and its state estimation based LQ control.* Energy Conversion and Management, 2006. **47**(18-19): p. 3119-3137.
20. Nicolet, C., F. Avellan, and J.-J. Simond, *Hydroacoustic modelling and numerical simulation of unsteady operation of hydroelectric systems*, in *LMH, LME*. 2007, EPFL.
21. *IEEE Guide for the Application of Turbine Governing Systems for Hydroelectric Generating Units.* IEEE Std 1207-2004, 2004: p. 0_1-121.
22. Machowski, J., J. Bialek, and D.J. Bumby, *Power System Dynamics: Stability and Control*. 2nd ed. 2008: John Wiley & Sons, Ltd. .
23. Voros, N.G., C.T. Kiranoudis, and Z.B. Maroulis, *Short-cut design of small hydroelectric plants.* Renewable Energy, 2000. **19**(4): p. 545-563.
24. Undrill, J.M. and J.L. Woodward, *Nonlinear Hydro Governing Model and Improved Calculation for Determining Temporary Droop.* Power Apparatus and Systems, IEEE Transactions on, 1967. **PAS-86**(4): p. 443-453.
25. Haiyan, B., Y. Jiandong, and F. Liang. *Study on Nonlinear Dynamical Model and Control Strategy of Transient Process in Hydropower Station with Francis Turbine*. in *Power and Energy Engineering Conference, 2009. APPEEC 2009. Asia-Pacific*. 2009.
26. Fraile-Ardanuy, J., et al. *Speed Optimisation Module of a Hydraulic Francis turbine based on Artificial Neural Networks. Application to the Dynamic Analysis and Control of an Adjustable Speed Hydro Plant*. in *Neural Networks, 2006. IJCNN '06. International Joint Conference on*. 2006.
27. Pérez, J.I., J.R. Wilhelmi, and L. Maroto, *Adjustable speed operation of a hydropower plant associated to an irrigation reservoir.* Energy Conversion and Management, 2008. **49**(11): p. 2973-2978.
28. De Jaeger, E., et al., *Hydro turbine model for system dynamic studies.* Power Systems, IEEE Transactions on, 1994. **9**(4): p. 1709-1715.
29. Zhihuai, X., et al. *Identifying of Hydraulic Turbine Generating Unit Model Based on Neural Network*. in *Intelligent Systems Design and Applications, 2006. ISDA '06. Sixth International Conference on*. 2006.
30. Brekke, H. and X.-X. Li. *A new approach to the mathematic modelling of hydropower governing systems*. in *Control, 1988. CONTROL 88., International Conference on*. 1988.
31. Nicolet, C., et al., *New Tool for the Simulation of Transient Phenomena in Francis Turbine Power Plants.*, in *IAHR Symposium*. 2002, : .
32. Jiang, J., *Design of an optimal robust governor for hydraulic turbine generating units.* Energy Conversion, IEEE Transactions on, 1995. **10**(1): p. 188-194.
33. Hong-qing, F. and S. Zu-yi. *Modeling and Simulation of Hydraulic Transients for Hydropower Plants*. in *Transmission and Distribution Conference and Exhibition: Asia and Pacific, 2005 IEEE/PES*. 2005.
34. Thorne, D.H. and E.F. Hill, *Field Testing and Simulation of Hydraulic Turbine Governor Performance.* Power Apparatus and Systems, IEEE Transactions on, 1974. **PAS-93**(4): p. 1183-1191.
35. Izena, A., et al. *Practical hydraulic turbine model*. in *Power Engineering Society General Meeting, 2006. IEEE*. 2006.
36. Jadid, S. and A. Salami. *Accurate model of hydroelectric power plant for load pickup during power system restoration*. in *TENCON 2004. 2004 IEEE Region 10 Conference*. 2004.
37. Strah, B., O. Kuljaca, and Z. Vukic, *Speed and active power control of hydro turbine unit.* Energy Conversion, IEEE Transactions on, 2005. **20**(2): p. 424-434.

38. Zhijun, L. and C. Lijuan. *The building and analyzing of the fifth-order model of the synchronous generator in stand-alone infinite system*. in *Electrical Machines and Systems, 2008. ICEMS 2008. International Conference on*. 2008.
39. *IEEE Guide for Synchronous Generator Modeling Practices and Applications in Power System Stability Analyses.* IEEE Std 1110-2002 (Revision of IEEE Std 1110-1991), 2003: p. 0_1-72.
40. Kanjun, Z., et al. *Simulation Analysis of Dynamic Performance for Hydro-Generator Under Loss of Excitation Condition*. in *Universities Power Engineering Conference, 2006. UPEC '06. Proceedings of the 41st International*. 2006.
41. Mouni, E., S. Tnani, and G. Champenois. *Comparative study of three modelling methods of synchronous generator*. in *IEEE Industrial Electronics, IECON 2006 - 32nd Annual Conference on*. 2006.
42. Yongji, C. and Y. Jilai. *A long term dynamic simulation method of power system based on variables grouping and seceding grouping strategy*. in *Electric Utility Deregulation and Restructuring and Power Technologies, 2008. DRPT 2008. Third International Conference on*. 2008.
43. Saadat, H., *Power system analysis*. 2nd ed. ed. 2002, Boston ; London: McGraw-Hill Primis Custom Publishing. xix, 712 p.
44. Kazemi, A., M.R.J. Motlagh, and A.H. Naghshbandy, *Application of a new multi-variable feedback linearization method for improvement of power systems transient stability.* International Journal of Electrical Power & Energy Systems, 2007. **29**(4): p. 322-328.
45. Xianshan, L., et al. *The Effect of Hydro Turbines and Governors on Power System Low Frequency Oscillations*. in *Power System Technology, 2006. PowerCon 2006. International Conference on*. 2006.
46. Murty, M.S.R. and M.V. Hariharan, *Analysis and Improvement of the Stability of a Hydro-Turbine Generating Unit With Long Penstock.* Power Apparatus and Systems, IEEE Transactions on, 1984. **PAS-103**(2): p. 360-367.
47. Ramey, D.G. and J.W. Skooglund, *Detailed Hydrogovernor Representation for System Stability Studies.* Power Apparatus and Systems, IEEE Transactions on, 1970. **PAS-89**(1): p. 106-112.
48. Report, I.C., *Dynamic Models for Steam and Hydro Turbines in Power System Studies.* Power Apparatus and Systems, IEEE Transactions on, 1973. **PAS-92**(6): p. 1904-1915.
49. Culberg, J.L., M. Negnevitsky, and K.M. Muttaqi. *Hydro-turbine governor control: theory, techniques and limitations*. in *AUPEC'06*. 2006. Melbourne.
50. Kishor, N., R.P. Saini, and S.P. Singh, *A review on hydropower plant models and control.* Renewable and Sustainable Energy Reviews, 2007. **11**(5): p. 776-796.
51. Yin Chin, C., K.M. Muttaqi, and M. Negnevitsky. *Modelling of hydraulic turbine for dynamic studies and performance analysis*. in *Power Engineering Conference, 2007. AUPEC 2007. Australasian Universities*. 2007.
52. Sanathanan, C.K., *Accurate Low Order Model for Hydraulic Turbine-Penstock.* Energy Conversion, IEEE Transactions on, 1987. **EC-2**(2): p. 196-200.
53. Hagihara, S., et al., *Stability of a Hydraulic Turbine Generating Unit Controlled by P.I.D. Governor.* Power Apparatus and Systems, IEEE Transactions on, 1979. **PAS-98**(6): p. 2294-2298.
54. Smith, J.R., R. McLean, and J.F. Robbie, *Assessment of hydroturbine models for power-systems studies.* Generation, Transmission and Distribution, IEE Proceedings C, 1983. **130**(1): p. 1-7.

55. Kishor, N., R.P. Saini, and S.P. Singh. *Simulation of reduced order hydro turbine models to study its hydraulic transient characteristics*. in *9th International Multitopic Conference, IEEE INMIC 2005*. 2005.
56. Nicolet, C., et al., *High-Order Modeling of Hydraulic Power Plant in Islanded Power Network.* Power Systems, IEEE Transactions on, 2007. **22**(4): p. 1870-1880.
57. Vournas, C.D. and N. Daskalakis. *Governor tuning and regulating capacity of hydroelectric units*. in *WESCANEX 93. 'Communications, Computers and Power in the Modern Environment.' Conference Proceedings., IEEE*. 1993.
58. Nicolet, C., et al. *On the hydroelectric stability of an islanded power network*. in *Power Engineering Society General Meeting, 2006. IEEE*. 2006.
59. Wozniak, L. and T.L. Filbert, *Speed loop cancellation governor for hydrogenerators. I. Development.* Energy Conversion, IEEE Transactions on, 1988. **3**(1): p. 85-90.
60. Pannatier, Y., et al., *Dynamic Behavior of a 2 Variable Speed Pump-Turbine Power Plant*, in *ICEM'08XVIII 18th International Conference on Electrical Machines*. 2008, : Vilamoura, Algarve, Portugal.
61. Aguero, J.L., et al. *Hydraulic transients in hydropower plant impact on power system dynamic stability*. in *Power and Energy Society General Meeting - Conversion and Delivery of Electrical Energy in the 21st Century, 2008 IEEE*. 2008.
62. Huimin, G. and W. Chao. *Effect of Detailed Hydro Turbine Models on Power System Analysis*. in *Power Systems Conference and Exposition, 2006. PSCE '06. 2006 IEEE PES*. 2006.
63. Hannett, L.N., J.W. Feltes, and B. Fardanesh, *Field tests to validate hydro turbine-governor model structure and parameters.* Power Systems, IEEE Transactions on, 1994. **9**(4): p. 1744-1751.
64. Vournas, C.D., *Second order hydraulic turbine models for multimachine stability studies.* Energy Conversion, IEEE Transactions on, 1990. **5**(2): p. 239-244.
65. Slootweg, J.G., et al., *A Study of the Eigenvalue Analysis Capabilities of Power System Dynamics Simulation Software*, in *14th Power Systems Computation Conference, PSCC'02*. 2002: Sevilla, Spain. p. 8.
66. Persson, J., *Using Linear Analysis to find Eigenvalues and Eigenvectors in Power Systems*. 2002: Madrid, Spain.
67. Rogers, G., *Demystifying power system oscillations.* Computer Applications in Power, IEEE, 1996. **9**(3): p. 30-35.
68. Svingen, B., *Manual LVTrans for versjon 8_1.2.4*. 2007, SINTEF Energy Research: Trondheim. p. 66.